Supplementary Information

Materials design of perovskite solid solutions for thermochemical applications

Josua Vieten,[a, b] Brendan Bulfin,[c] Patrick Huck,[d] Matthew Horton,[d] Dorottya Guban,[a] Liya Zhu,[e] Youjun Lu,[e] Kristin A. Persson,[d] Martin Roeb,[a] and Christian Sattler[a, b]

a. Institute of Solar Research, Deutsches Zentrum für Luft- und Raumfahrt/German Aerospace Center, Linder Höhe, 51147 Köln, Germany.

b. Faculty of Mechanical Science and Engineering, Institute of Power Engineering, Professorship of Solar Fuel production, TU Dresden, 01062 Dresden, Germany.

c. Professorship for Renewable Energy Carriers, ETH Zurich, 8092 Zurich, Switzerland

d. Energy Technologies Area, Lawrence Berkeley National Laboratory, Berkeley, USA

e. State Key Laboratory of Multiphase Flow in Power Engineering (SKLMF), Xi'an Jiaotong University, Xi'an, Shaanxi 710049, China

1. DFT data on perovskite solid solutions and cross-references to *The Materials Project*

Table S 1. Theoretical data for the perovskite redox pairs investigated within this work. Solid solutions have the general composition $(A'_xA''_{1-x})^{(6-n)+}(M'_yM''_{1-y})^{(n-2\delta)+}O_{3-\delta}$ with n denoting the charge of the transition metal species M' and M'' in the fully oxidized state, and A' and A'' being two different alkali, alkali earth, or rare earth species. The tolerance factor of the perovskite is denoted by t and calculated with respect to the fully oxidized state as explained in the main manuscript. Values of $t < 0.9$ or $t > 1.1$ are marked in red, as they indicate that most likely other phases than the perovskite structure are more stable. The redox enthalpies ΔH are calculated using DFT (GGA and GGA+U as explained in the main manuscript) as per mol of oxygen O for the complete reduction from the perovskite to the brownmillerite phase ($\delta = 0$ and $\delta = 0.5$, respectively). Redox enthalpies below zero indicate highly unstable perovskite phases and are therefore marked in red. All materials are ranked according to their calculated redox enthalpies. More materials data including the energy above hull, the crystal structures, DFT calculation summaries, and simulated X-Ray diffractograms can be retrieved on *www.materialsproject.org* using the hyperlinks to the MP-IDs in each dataset.

Redox Material	*n*	*t*	ΔH (kJ/mol$_O$)	perovskite (oxidized phase)		brownmillerite (reduced phase)	
$MgCuO_{3-\delta}$	4	0.827	-337.87	$MgCuO_3$	mp-1076317	$Mg_2Cu_2O_5$	mp-1076527
$SmAgO_{3-\delta}$	3	0.864	-244.17	$SmAgO_3$	mp-1075933	$Sm_2Ag_2O_5$	mp-1076848
$CaCuO_{3-\delta}$	4	0.920	-154.45	$CaCuO_3$	mp-1099873	$Ca_2Cu_2O_5$	mp-772813
$EuAgO_{3-\delta}$	3	0.863	-102.97	$EuAgO_3$	mp-1077622	$Eu_2Ag_2O_5$	mp-1099927
$RbCrO_{3-\delta}$	5	1.163	-95.16	$RbCrO_3$	mp-1076360	$Rb_2Cr_2O_5$	mp-1076401
$Mg_{0.125}Ca_{0.875}CoO_{3-\delta}$	4	0.983	-81.80	$Ca_7Mg(CoO_3)_8$	mp-1076128	$Ca_7Mg(Co_2O_5)_4$	mp-1076526
$BaCuO_{3-\delta}$	4	1.012	-71.24	$BaCuO_3$	mp-1076800	$Ba_2Cu_2O_5$	mp-772788
$Mg_{0.125}Ca_{0.875}Fe_{0.125}Co_{0.875}O_{3-\delta}$	4	0.980	-65.13	$Ca_7MgFeCo_7O_{24}$	mp-1076139	$Ca_7MgFeCo_7O_{20}$	mp-1099907
$Mg_{0.125}Ca_{0.875}Co_{0.875}Cu_{0.125}O_{3-\delta}$	4	0.973	-56.05	$Ca_7MgCo_7CuO_{24}$	mp-1076132	$Ca_7MgCo_7CuO_{20}$	mp-1099952
$NaCrO_{3-\delta}$	5	1.033	-30.37	$NaCrO_3$	mp-1076642	$Na_2Cr_2O_5$	mp-1099683
$Ca_{0.5}Sr_{0.5}CoO_{3-\delta}$	4	1.015	-25.93	$SrCa(CoO_3)_2$	mp-1075928	$SrCaCo_2O_5$	mp-1099694
$Ca_{0.875}Sr_{0.125}Fe_{0.125}Co_{0.875}O_{3-\delta}$	4	0.997	-15.35	$SrCa_7FeCo_7O_{24}$	mp-1076861	$SrCa_7FeCo_7O_{20}$	mp-1099847
$Ca_{0.75}Sr_{0.25}CoO_{3-\delta}$	4	1.006	-14.17	$SrCa_3(CoO_3)_4$	mp-1076096	$SrCa_3(Co_2O_5)_2$	mp-1076675

Redox Material	*n*	*t*	ΔH (kJ/mol$_O$)	perovskite (oxidized phase)		brownmillerite (reduced phase)	
$SrCuO_{3-\delta}$	4	0.955	-7.35	$SrCuO_3$	mp-1076711	$Sr_2Cu_2O_5$	mp-21129
$Ca_{0.875}Sr_{0.125}Fe_{0.25}Co_{0.75}O_{3-\delta}$	4	0.994	-1.20	$SrCa_7Fe_2(CoO_4)_6$	mp-1076829	$SrCa_7Fe_2(Co_3O_{10})_2$	mp-1099745
$Ca_{0.75}Sr_{0.25}Co_{0.875}Cu_{0.125}O_{3-\delta}$	4	0.995	-0.57	$Sr_2Ca_6Co_7CuO_{24}$	mp-1099600	$Sr_2Ca_6Co_7CuO_{20}$	mp-1076470
$SrCoO_{3-\delta}$	4	1.035	0.82	$SrCoO_3$	mp-561952	$Sr_2Co_2O_5$	mp-556076
$Ca_{0.75}Sr_{0.25}Fe_{0.125}Co_{0.875}O_{3-\delta}$	4	1.002	6.06	$Sr_2Ca_6FeCo_7O_{24}$	mp-1076626	$Sr_2Ca_6FeCo_7O_{20}$	mp-1099653
$KCrO_{3-\delta}$	5	1.134	6.77	$KCrO_3$	mp-1076732	$K_2Cr_2O_5$	mp-1076696
$Ca_{0.625}Sr_{0.375}Fe_{0.125}Co_{0.875}O_{3-\delta}$	4	1.007	7.82	$Sr_3Ca_5FeCo_7O_{24}$	mp-1099827	$Sr_3Ca_5FeCo_7O_{20}$	mp-1076479
$Ca_{0.5}Sr_{0.5}Co_{0.875}Cu_{0.125}O_{3-\delta}$	4	1.005	13.73	$Sr_4Ca_4Co_7CuO_{24}$	mp-1099611	$Sr_4Ca_4Co_7CuO_{20}$	mp-1076175
$Ca_{0.5}Sr_{0.5}Co_{0.75}Cu_{0.25}O_{3-\delta}$	4	0.995	17.45	$Sr_2Ca_2Co_3CuO_{12}$	mp-1099844	$Sr_2Ca_2Co_3CuO_{10}$	mp-1076273
$Ca_{0.75}Sr_{0.25}Fe_{0.375}Co_{0.625}O_{3-\delta}$	4	0.995	19.14	$Sr_2Ca_6Fe_3Co_5O_{24}$	mp-1099890	$Sr_2Ca_6Fe_3(CoO_4)_5$	mp-1076198
$Sr_{0.125}Ba_{0.875}CuO_{3-\delta}$	4	1.005	20.46	$Ba_7Sr(CuO_3)_8$	mp-1099824	$Ba_7Sr(Cu_2O_5)_4$	mp-1099795
$Sr_{0.25}Ba_{0.75}CuO_{3-\delta}$	4	0.998	22.34	$Ba_3Sr(CuO_3)_4$	mp-1099602	$Ba_3Sr(Cu_2O_5)_2$	mp-1076189
$Sr_{0.25}Ba_{0.75}Co_{0.25}Cu_{0.75}O_{3-\delta}$	4	1.018	23.76	$Ba_3SrCo(CuO_4)_3$	mp-1099886	$Ba_3SrCoCu_3O_{10}$	mp-1100085
$Sr_{0.25}Ba_{0.75}Co_{0.125}Cu_{0.875}O_{3-\delta}$	4	1.008	23.79	$Ba_6Sr_2CoCu_7O_{24}$	mp-1076247	$Ba_6Sr_2CoCu_7O_{20}$	mp-1076296
$Ca_{0.5}Sr_{0.5}Fe_{0.125}Co_{0.875}O_{3-\delta}$	4	1.012	24.32	$Sr_4Ca_4FeCo_7O_{24}$	mp-1075997	$Sr_4Ca_4FeCo_7O_{20}$	mp-1100009
$Sm_{0.125}La_{0.875}Co_{0.75}Ag_{0.25}O_{3-\delta}$	3	0.943	26.19	$La_7SmCo_6(AgO_{12})_2$	mp-1076275	$La_7SmCo_6(AgO_{10})_2$	mp-1076866
$Ca_{0.25}Sr_{0.75}Co_{0.875}Cu_{0.125}O_{3-\delta}$	4	1.014	28.48	$Sr_6Ca_2Co_7CuO_{24}$	mp-1076741	$Sr_6Ca_2Co_7CuO_{20}$	mp-1076118
$Sm_{0.125}La_{0.875}Ag_{0.25}Ni_{0.75}O_{3-\delta}$	3	0.947	28.64	$La_7SmNi_6(AgO_{12})_2$	mp-1076723	$La_7SmNi_6(AgO_{10})_2$	mp-1099871
$Sr_{0.5}Ba_{0.5}Co_{0.25}Cu_{0.75}O_{3-\delta}$	4	1.003	30.08	$Ba_2Sr_2Co(CuO_4)_3$	mp-1099763	$Ba_2Sr_2CoCu_3O_{10}$	mp-1099812
$Sr_{0.5}Ba_{0.5}Co_{0.375}Cu_{0.625}O_{3-\delta}$	4	1.013	32.68	$Ba_4Sr_4Co_3Cu_5O_{24}$	mp-1076491	$Ba_4Sr_4Co_3(CuO_4)_5$	mp-1076896
$Ca_{0.5}Sr_{0.5}Fe_{0.25}Co_{0.75}O_{3-\delta}$	4	1.008	33.07	$Sr_2Ca_2Fe(CoO_4)_3$	mp-1099605	$Sr_2Ca_2FeCo_3O_{10}$	mp-1099665
$Sm_{0.5}La_{0.5}Co_{0.875}Ag_{0.125}O_{3-\delta}$	3	0.936	33.33	$La_4Sm_4Co_7AgO_{24}$	mp-1099698	$La_4Sm_4Co_7AgO_{20}$	mp-1076724
$Ca_{0.375}Sr_{0.625}Fe_{0.125}Co_{0.875}O_{3-\delta}$	4	1.016	34.36	$Sr_5Ca_3FeCo_7O_{24}$	mp-1076107	$Sr_5Ca_3FeCo_7O_{20}$	mp-1099816
$Ca_{0.625}Sr_{0.375}Fe_{0.625}Co_{0.375}O_{3-\delta}$	4	0.993	35.90	$Sr_3Ca_5Fe_5(CoO_8)_3$	mp-1076802	$Sr_3Ca_5Fe_5Co_3O_{20}$	mp-1076614

Redox Material	*n*	*t*	ΔH (kJ/mol$_O$)	perovskite (oxidized phase)		brownmillerite (reduced phase)	
$Ca_{0.25}Sr_{0.75}Co_{0.625}Cu_{0.375}O_{3-\delta}$	4	0.994	36.72	$Sr_6Ca_2Co_5(CuO_8)_3$	mp-1075901	$Sr_6Ca_2Co_5Cu_3O_{20}$	mp-1076678
$Sr_{0.75}Ba_{0.25}Co_{0.5}Cu_{0.5}O_{3-\delta}$	4	1.008	36.92	$BaSr_3Co_2(CuO_6)_2$	mp-1076528	$BaSr_3Co_2(CuO_5)_2$	mp-1100092
$Ca_{0.375}Sr_{0.625}Fe_{0.25}Co_{0.75}O_{3-\delta}$	4	1.013	37.34	$Sr_5Ca_3Fe_2(CoO_4)_6$	mp-1076260	$Sr_5Ca_3Fe_2(Co_3O_{10})_2$	mp-1099798
$Sr_{0.625}Ba_{0.375}Co_{0.375}Cu_{0.625}O_{3-\delta}$	4	1.006	37.84	$Ba_3Sr_5Co_3Cu_5O_{24}$	mp-1076600	$Ba_3Sr_5Co_3(CuO_4)_5$	mp-1076881
$Ca_{0.625}Sr_{0.375}Fe_{0.5}Co_{0.5}O_{3-\delta}$	4	0.996	39.01	$Sr_3Ca_5Fe_4(CoO_6)_4$	mp-1076602	$Sr_3Ca_5Fe_4(CoO_5)_4$	mp-1099708
$Sm_{0.25}La_{0.75}Co_{0.875}Ag_{0.125}O_{3-\delta}$	3	0.946	39.52	$La_6Sm_2Co_7AgO_{24}$	mp-1076287	$La_6Sm_2Co_7AgO_{20}$	mp-1076492
$Ca_{0.25}Sr_{0.75}Co_{0.75}Cu_{0.25}O_{3-\delta}$	4	1.004	40.17	$Sr_3CaCo_3CuO_{12}$	mp-1076688	$Sr_3CaCo_3CuO_{10}$	mp-1099678
$Sr_{0.75}Ba_{0.25}Co_{0.375}Cu_{0.625}O_{3-\delta}$	4	0.998	40.21	$Ba_2Sr_6Co_3Cu_5O_{24}$	mp-1076264	$Ba_2Sr_6Co_3(CuO_4)_5$	mp-1099742
$MgFeO_{3-\delta}$	4	0.871	40.85	$MgFeO_3$	mp-778717	$Mg_2Fe_2O_5$	mp-705864
$CaCoO_{3-\delta}$	4	0.996	41.41	$CaCoO_3$	mvc-3994	$Ca_2Co_2O_5$	mp-1099786
$Ca_{0.5}Sr_{0.5}Fe_{0.375}Co_{0.625}O_{3-\delta}$	4	1.004	41.82	$Sr_4Ca_4Fe_3Co_5O_{24}$	mp-1076674	$Sr_4Ca_4Fe_3(CoO_4)_5$	mp-1076502
$Ca_{0.5}Sr_{0.5}Fe_{0.75}Co_{0.25}O_{3-\delta}$	4	0.994	42.84	$Sr_2Ca_2Fe_3CoO_{12}$	mp-1075966	$Sr_2Ca_2Fe_3CoO_{10}$	mp-1076147
$Sr_{0.625}Ba_{0.375}Co_{0.5}Cu_{0.5}O_{3-\delta}$	4	1.016	47.17	$Ba_3Sr_5Co_4(CuO_6)_4$	mp-1075989	$Ba_3Sr_5Co_4(CuO_5)_4$	mp-1076683
$Sr_{0.75}Ba_{0.25}Co_{0.625}Cu_{0.375}O_{3-\delta}$	4	1.018	47.64	$Ba_2Sr_6Co_5(CuO_8)_3$	mp-1076429	$Ba_2Sr_6Co_5Cu_3O_{20}$	mp-1076893
$Sr_{0.875}Ba_{0.125}Co_{0.625}Cu_{0.375}O_{3-\delta}$	4	1.011	47.99	$BaSr_7Co_5(CuO_8)_3$	mp-1075982	$BaSr_7Co_5Cu_3O_{20}$	mp-1100068
$Sr_{0.875}Ba_{0.125}Co_{0.5}Cu_{0.5}O_{3-\delta}$	4	1.001	48.55	$BaSr_7Co_4(CuO_6)_4$	mp-1076054	$BaSr_7Co_4(CuO_5)_4$	mp-1099990
$EuCoO_{3-\delta}$	3	0.923	49.90	$EuCoO_3$	mp-1075975	$Eu_2Co_2O_5$	mp-1076123
$Sm_{0.375}La_{0.625}Ag_{0.125}Ni_{0.875}O_{3-\delta}$	3	0.945	52.78	$La_5Sm_3Ni_7AgO_{24}$	mp-1076249	$La_5Sm_3Ni_7AgO_{20}$	mp-1076656
$Ca_{0.25}Sr_{0.75}Fe_{0.375}Co_{0.625}O_{3-\delta}$	4	1.014	54.13	$Sr_6Ca_2Fe_3Co_5O_{24}$	mp-1076805	$Sr_6Ca_2Fe_3(CoO_4)_5$	mp-1076488
$CaFeO_{3-\delta}$	4	0.968	55.51	$CaFeO_3$	mvc-776	$Ca_2Fe_2O_5$	mp-25750
$Ca_{0.375}Sr_{0.625}Fe_{0.875}Co_{0.125}O_{3-\delta}$	4	0.995	56.98	$Sr_5Ca_3Fe_7CoO_{24}$	mp-1075955	$Sr_5Ca_3Fe_7CoO_{20}$	mp-1076516
$Mg_{0.125}Ca_{0.875}Mn_{0.875}Fe_{0.125}O_{3-\delta}$	4	0.980	57.56	$Ca_7MgMn_7FeO_{24}$	mp-1076214	$Ca_7MgMn_7FeO_{20}$	mp-1099831
$Mg_{0.125}Ca_{0.875}MnO_{3-\delta}$	4	0.983	61.05	$Ca_7MgMn_8O_{24}$	mp-1076485	$Ca_7MgMn_8O_{20}$	mp-1076897
$Ca_{0.25}Sr_{0.75}Fe_{0.625}Co_{0.375}O_{3-\delta}$	4	1.007	63.86	$Sr_6Ca_2Fe_5(CoO_8)_3$	mp-1076457	$Sr_6Ca_2Fe_5Co_3O_{20}$	mp-1076769

Redox Material	*n*	*t*	ΔH (kJ/mol$_O$)	perovskite (oxidized phase)		brownmillerite (reduced phase)	
$Ca_{0.25}Sr_{0.75}Fe_{0.875}Co_{0.125}O_{3-\delta}$	4	1.000	64.86	$Sr_6Ca_2Fe_7CoO_{24}$	mp-1076399	$Sr_6Ca_2Fe_7CoO_{20}$	mp-1100030
$Ca_{0.125}Sr_{0.875}Fe_{0.5}Co_{0.5}O_{3-\delta}$	4	1.015	65.92	$Sr_7CaFe_4(CoO_6)_4$	mp-1076747	$Sr_7CaFe_4(CoO_5)_4$	mp-1076159
$Ca_{0.25}Sr_{0.75}FeO_{3-\delta}$	4	0.997	68.03	$Sr_3Ca(FeO_3)_4$	mp-1094055	$Sr_3Ca(Fe_2O_5)_2$	mp-1076761
$Ca_{0.125}Sr_{0.875}Fe_{0.625}Co_{0.375}O_{3-\delta}$	4	1.012	68.95	$Sr_7CaFe_5(CoO_8)_3$	mp-1076062	$Sr_7CaFe_5Co_3O_{20}$	mp-1100087
$Ca_{0.125}Sr_{0.875}Fe_{0.875}Co_{0.125}O_{3-\delta}$	4	1.005	71.48	$Sr_7CaFe_7CoO_{24}$	mp-1076858	$Sr_7CaFe_7CoO_{20}$	mp-1099946
$Ca_{0.125}Sr_{0.875}Fe_{0.75}Co_{0.25}O_{3-\delta}$	4	1.008	72.40	$Sr_7CaFe_6(CoO_{12})_2$	mp-1076372	$Sr_7CaFe_6(CoO_{10})_2$	mp-1076631
$EuNiO_{3-\delta}$	3	0.928	73.85	$EuNiO_3$	mp-32341	$Eu_2Ni_2O_5$	mp-1076223
$Sm_{0.5}La_{0.5}NiO_{3-\delta}$	3	0.949	76.16	$LaSm(NiO_3)_2$	mp-1076325	$LaSmNi_2O_5$	mp-1076810
$Ca_{0.375}Sr_{0.625}Mn_{0.125}Fe_{0.875}O_{3-\delta}$	4	0.995	76.32	$Sr_5Ca_3MnFe_7O_{24}$	mp-1076079	$Sr_5Ca_3MnFe_7O_{20}$	mp-1076199
$SrFe_{0.875}Co_{0.125}O_{3-\delta}$	4	1.009	76.87	$Sr_8Fe_7CoO_{24}$	mp-1077660	$Sr_8Fe_7CoO_{20}$	mp-1076165
$Sr_{0.875}Ba_{0.125}Fe_{0.875}Co_{0.125}O_{3-\delta}$	4	1.017	78.02	$BaSr_7Fe_7CoO_{24}$	mp-1075935	$BaSr_7Fe_7CoO_{20}$	mp-1076892
$Mg_{0.125}Ca_{0.875}Ti_{0.125}Mn_{0.875}O_{3-\delta}$	4	0.979	79.23	$Ca_7MgTiMn_7O_{24}$	mp-1076543	$Ca_7MgTiMn_7O_{20}$	mp-1077701
$Sr_{0.875}Ba_{0.125}Fe_{0.75}Co_{0.25}O_{3-\delta}$	4	1.021	81.84	$BaSr_7Fe_6(CoO_{12})_2$	mp-1099936	$BaSr_7Fe_6(CoO_{10})_2$	mp-1099862
$Ca_{0.5}Sr_{0.5}Mn_{0.25}Fe_{0.75}O_{3-\delta}$	4	0.994	83.80	$Sr_2Ca_2Mn(FeO_4)_3$	mp-1076410	$Sr_2Ca_2MnFe_3O_{10}$	mp-1076444
$Ca_{0.25}Sr_{0.75}Mn_{0.125}Fe_{0.875}O_{3-\delta}$	4	1.000	85.26	$Sr_6Ca_2MnFe_7O_{24}$	mp-1075969	$Sr_6Ca_2MnFe_7O_{20}$	mp-1099974
$SrFeO_{3-\delta}$	4	1.006	87.77	$SrFeO_3$	mp-1076585	$Sr_2Fe_2O_5$	mp-561589
$Sr_{0.875}Ba_{0.125}FeO_{3-\delta}$	4	1.013	88.00	$BaSr_7(FeO_3)_8$	mp-1099685	$BaSr_7(Fe_2O_5)_4$	mp-1076090
$BaFeO_{3-\delta}$	4	1.066	94.77	$BaFeO_3$	mp-19035	$Ba_2Fe_2O_5$	mp-654312
$Sm_{0.5}La_{0.5}CoO_{3-\delta}$	3	0.944	94.88	$LaSm(CoO_3)_2$	mp-1075930	$LaSmCo_2O_5$	mp-1076759
$Ca_{0.125}Sr_{0.875}Mn_{0.125}Fe_{0.875}O_{3-\delta}$	4	1.005	95.92	$Sr_7CaMnFe_7O_{24}$	mp-1099701	$Sr_7CaMnFe_7O_{20}$	mp-1076487
$Ca_{0.625}Sr_{0.375}Mn_{0.375}Fe_{0.625}O_{3-\delta}$	4	0.993	96.08	$Sr_3Ca_5Mn_3Fe_5O_{24}$	mp-1076854	$Sr_3Ca_5Mn_3(FeO_4)_5$	mp-1076482
$Sm_{0.5}La_{0.5}Cu_{0.125}Co_{0.875}O_{3-\delta}$	3	0.938	98.69	$La_4Sm_4Co_7CuO_{24}$	mp-1076219	$La_4Sm_4Co_7CuO_{20}$	mp-1076483
$LaAgO_{3-\delta}$	3	0.902	99.65	$LaAgO_3$	mp-768308	$La_2Ag_2O_5$	mp-1076119
$Sr_{0.875}Ba_{0.125}Mn_{0.125}Fe_{0.875}O_{3-\delta}$	4	1.017	99.89	$BaSr_7MnFe_7O_{24}$	mp-1076592	$BaSr_7MnFe_7O_{20}$	mp-1076473

Redox Material	*n*	*t*	ΔH (kJ/mol$_O$)	perovskite (oxidized phase)		brownmillerite (reduced phase)	
$Ca_{0.875}Sr_{0.125}Mn_{0.75}Fe_{0.25}O_{3-\delta}$	4	0.994	101.07	$SrCa_7Mn_6(FeO_{12})_2$	mp-1077667	$SrCa_7Mn_6(FeO_{10})_2$	mp-1077691
$Ca_{0.875}Sr_{0.125}Mn_{0.875}Fe_{0.125}O_{3-\delta}$	4	0.997	102.62	$SrCa_7Mn_7FeO_{24}$	mp-1099696	$SrCa_7Mn_7FeO_{20}$	mp-1076449
$Na_{0.875}K_{0.125}V_{0.75}Cr_{0.25}O_{3-\delta}$	5	1.025	102.72	$KNa_7V_6Cr_2O_{24}$	mp-1099932	$KNa_7V_6Cr_2O_{20}$	mp-1099912
$EuCuO_{3-\delta}$	3	0.879	105.30	$EuCuO_3$	mp-1075902	$Eu_2Cu_2O_5$	mp-1099765
$Ca_{0.75}Sr_{0.25}Mn_{0.625}Fe_{0.375}O_{3-\delta}$	4	0.995	105.69	$Sr_2Ca_6Mn_5(FeO_8)_3$	mp-1076268	$Sr_2Ca_6Mn_5Fe_3O_{20}$	mp-1076862
$SrMn_{0.125}Fe_{0.875}O_{3-\delta}$	4	1.009	105.84	$Sr_8MnFe_7O_{24}$	mp-1076445	$Sr_8MnFe_7O_{20}$	mp-1076409
$Sm_{0.375}La_{0.625}Cu_{0.125}Co_{0.875}O_{3-\delta}$	3	0.943	106.73	$La_5Sm_3Co_7CuO_{24}$	mp-1076171	$La_5Sm_3Co_7CuO_{20}$	mp-1076874
$MgCoO_{3-\delta}$	4	0.895	110.14	$MgCoO_3$	mp-761524	$Mg_2Co_2O_5$	mp-1076088
$Ca_{0.125}Sr_{0.875}Mn_{0.25}Fe_{0.75}O_{3-\delta}$	4	1.008	110.29	$Sr_7CaMn_2(FeO_4)_6$	mp-1076597	$Sr_7CaMn_2(Fe_3O_{10})_2$	mp-1076092
$Ca_{0.75}Sr_{0.25}Mn_{0.875}Fe_{0.125}O_{3-\delta}$	4	1.002	110.63	$Sr_2Ca_6Mn_7FeO_{24}$	mp-1099788	$Sr_2Ca_6Mn_7FeO_{20}$	mp-1099810
$Ca_{0.625}Sr_{0.375}Mn_{0.5}Fe_{0.5}O_{3-\delta}$	4	0.996	114.92	$Sr_3Ca_5Mn_4(FeO_6)_4$	mp-1075968	$Sr_3Ca_5Mn_4(FeO_5)_4$	mp-1076450
$Ca_{0.25}Sr_{0.75}Mn_{0.375}Fe_{0.625}O_{3-\delta}$	4	1.007	116.98	$Sr_6Ca_2Mn_3Fe_5O_{24}$	mp-1077670	$Sr_6Ca_2Mn_3(FeO_4)_5$	mp-1076177
$Ca_{0.5}Sr_{0.5}Mn_{0.625}Fe_{0.375}O_{3-\delta}$	4	1.004	117.88	$Sr_4Ca_4Mn_5(FeO_8)_3$	mp-1076058	$Sr_4Ca_4Mn_5Fe_3O_{20}$	mp-1076190
$Ca_{0.5}Sr_{0.5}Mn_{0.75}Fe_{0.25}O_{3-\delta}$	4	1.008	119.85	$Sr_2Ca_2Mn_3FeO_{12}$	mp-1099674	$Sr_2Ca_2Mn_3FeO_{10}$	mp-1076197
$Sm_{0.125}La_{0.875}Cu_{0.25}Co_{0.75}O_{3-\delta}$	3	0.948	119.91	$La_7SmCo_6(CuO_{12})_2$	mp-1077605	$La_7SmCo_6(CuO_{10})_2$	mp-1076871
$Sr_{0.875}Ba_{0.125}Mn_{0.25}Fe_{0.75}O_{3-\delta}$	4	1.021	120.66	$BaSr_7Mn_2(FeO_4)_6$	mp-1076408	$BaSr_7Mn_2(Fe_3O_{10})_2$	mp-1076181
$Ca_{0.5}Sr_{0.5}MnO_{3-\delta}$	4	1.015	121.61	$SrCaMn_2O_6$	mp-1076213	$SrCaMn_2O_5$	mp-1076496
$Na_{0.875}K_{0.125}V_{0.875}Cr_{0.125}O_{3-\delta}$	5	1.022	121.67	$KNa_7V_7CrO_{24}$	mp-1076665	$KNa_7V_7CrO_{20}$	mp-1076821
$Ca_{0.5}Sr_{0.5}Mn_{0.875}Fe_{0.125}O_{3-\delta}$	4	1.012	123.20	$Sr_4Ca_4Mn_7FeO_{24}$	mp-1076359	$Sr_4Ca_4Mn_7FeO_{20}$	mp-1076163
$Sm_{0.125}La_{0.875}Cu_{0.375}Co_{0.625}O_{3-\delta}$	3	0.942	123.90	$La_7SmCo_5(CuO_8)_3$	mp-1075961	$La_7SmCo_5Cu_3O_{20}$	mp-1076880
$Ca_{0.375}Sr_{0.625}Mn_{0.75}Fe_{0.25}O_{3-\delta}$	4	1.013	125.87	$Sr_5Ca_3Mn_6(FeO_{12})_2$	mp-1099603	$Sr_5Ca_3Mn_6(FeO_{10})_2$	mp-1076601
$Ca_{0.125}Sr_{0.875}Mn_{0.375}Fe_{0.625}O_{3-\delta}$	4	1.012	126.36	$Sr_7CaMn_3Fe_5O_{24}$	mp-1076651	$Sr_7CaMn_3(FeO_4)_5$	mp-1099661
$Ca_{0.375}Sr_{0.625}Mn_{0.5}Fe_{0.5}O_{3-\delta}$	4	1.006	126.88	$Sr_5Ca_3Mn_4(FeO_6)_4$	mp-1076796	$Sr_5Ca_3Mn_4(FeO_5)_4$	mp-1076141
$Ca_{0.875}Sr_{0.125}Ti_{0.125}Mn_{0.875}O_{3-\delta}$	4	0.996	127.33	$SrCa_7TiMn_7O_{24}$	mp-1077663	$SrCa_7TiMn_7O_{20}$	mp-1077688

Redox Material	*n*	*t*	ΔH (kJ/mol$_O$)	perovskite (oxidized phase)		brownmillerite (reduced phase)	
$Ca_{0.375}Sr_{0.625}Mn_{0.875}Fe_{0.125}O_{3-\delta}$	4	1.016	130.00	$Sr_5Ca_3Mn_7FeO_{24}$	mp-1076080	$Sr_5Ca_3Mn_7FeO_{20}$	mp-1099672
$Ca_{0.25}Sr_{0.75}Mn_{0.625}Fe_{0.375}O_{3-\delta}$	4	1.014	130.54	$Sr_6Ca_2Mn_5(FeO_8)_3$	mp-1077671	$Sr_6Ca_2Mn_5Fe_3O_{20}$	mp-1076182
$Ca_{0.75}Sr_{0.25}Ti_{0.125}Mn_{0.875}O_{3-\delta}$	4	1.001	135.03	$Sr_2Ca_6TiMn_7O_{24}$	mp-1099702	$Sr_2Ca_6TiMn_7O_{20}$	mp-1076877
$Ca_{0.125}Sr_{0.875}Mn_{0.5}Fe_{0.5}O_{3-\delta}$	4	1.015	140.53	$Sr_7CaMn_4(FeO_6)_4$	mp-1099713	$Sr_7CaMn_4(FeO_5)_4$	mp-1099692
$LaNiO_{3-\delta}$	3	0.969	141.84	$LaNiO_3$	mp-19339	$La_2Ni_2O_5$	mp-1076121
$Na_{0.875}K_{0.125}VO_{3-\delta}$	5	1.018	142.67	$KNa_7V_8O_{24}$	mp-1099664	$KNa_7V_8O_{20}$	mp-1076630
$Ca_{0.625}Sr_{0.375}Ti_{0.125}Mn_{0.875}O_{3-\delta}$	4	1.005	143.35	$Sr_3Ca_5TiMn_7O_{24}$	mp-1076217	$Sr_3Ca_5TiMn_7O_{20}$	mp-1077695
$SmCuO_{3-\delta}$	3	0.880	147.50	$SmCuO_3$	mp-770767	$Sm_2Cu_2O_5$	mp-768866
$LaCuO_{3-\delta}$	3	0.919	149.59	$LaCuO_3$	mp-3474	$La_2Cu_2O_5$	mp-5696
$Ca_{0.5}Sr_{0.5}Ti_{0.125}Mn_{0.875}O_{3-\delta}$	4	1.010	149.66	$Sr_4Ca_4TiMn_7O_{24}$	mp-1076561	$Sr_4Ca_4TiMn_7O_{20}$	mp-1099799
$Ca_{0.75}Sr_{0.25}Ti_{0.25}Mn_{0.75}O_{3-\delta}$	4	0.996	152.20	$SrCa_3TiMn_3O_{12}$	mp-1076074	$SrCa_3TiMn_3O_{10}$	mp-1076776
$Ca_{0.375}Sr_{0.625}Ti_{0.125}Mn_{0.875}O_{3-\delta}$	4	1.015	155.01	$Sr_5Ca_3TiMn_7O_{24}$	mp-1075976	$Sr_5Ca_3TiMn_7O_{20}$	mp-1076192
$SmNiO_{3-\delta}$	3	0.928	162.20	$SmNiO_3$	mp-25588	$Sm_2Ni_2O_5$	mp-1099625
$Ca_{0.5}Sr_{0.5}Ti_{0.25}Mn_{0.75}O_{3-\delta}$	4	1.005	166.56	$Sr_2Ca_2TiMn_3O_{12}$	mp-1077669	$Sr_2Ca_2TiMn_3O_{10}$	mp-1076680
$Ca_{0.75}Sr_{0.25}MnO_{3-\delta}$	4	1.006	167.65	$SrCa_3Mn_4O_{12}$	mp-1094044	$SrCa_3Mn_4O_{10}$	mp-1076184
$Na_{0.875}K_{0.125}Mo_{0.125}V_{0.875}O_{3-\delta}$	5	1.014	170.32	$KNa_7V_7MoO_{24}$	mp-1076222	$KNa_7V_7MoO_{20}$	mp-1099669
$SrMnO_{3-\delta}$	4	1.035	170.33	$SrMnO_3$	mp-568977	$Sr_2Mn_2O_5$	mp-18798
$BaCoO_{3-\delta}$	4	1.096	172.09	$BaCoO_3$	mp-554938	$Ba_2Co_2O_5$	mp-1076439
$CaMnO_{3-\delta}$	4	0.996	173.13	$CaMnO_3$	mp-19201	$Ca_2Mn_2O_5$	mp-25008
$Ca_{0.625}Sr_{0.375}Ti_{0.375}Mn_{0.625}O_{3-\delta}$	4	0.996	173.40	$Sr_3Ca_5Ti_3Mn_5O_{24}$	mp-1076628	$Sr_3Ca_5Ti_3Mn_5O_{20}$	mp-1076134
$Na_{0.875}K_{0.125}Mo_{0.25}V_{0.75}O_{3-\delta}$	5	1.009	180.38	$KNa_7V_6(MoO_{12})_2$	mp-1076351	$KNa_7V_6(MoO_{10})_2$	mp-1099956
$Ca_{0.25}Sr_{0.75}Ti_{0.25}Mn_{0.75}O_{3-\delta}$	4	1.015	182.71	$Sr_3CaTiMn_3O_{12}$	mp-1099855	$Sr_3CaTiMn_3O_{10}$	mp-1076505
$Ca_{0.375}Sr_{0.625}Ti_{0.375}Mn_{0.625}O_{3-\delta}$	4	1.005	188.81	$Sr_5Ca_3Ti_3Mn_5O_{24}$	mp-1075962	$Sr_5Ca_3Ti_3Mn_5O_{20}$	mp-1099762
$Ca_{0.5}Sr_{0.5}Ti_{0.5}Mn_{0.5}O_{3-\delta}$	4	0.996	195.49	$SrCaTiMnO_6$	mp-1076384	$SrCaTiMnO_5$	mp-1099877

Redox Material	*n*	*t*	ΔH (kJ/mol$_O$)	perovskite (oxidized phase)		brownmillerite (reduced phase)	
$Na_{0.75}K_{0.25}Mo_{0.375}V_{0.625}O_{3-\delta}$	5	1.017	202.11	$K_2Na_6V_5(MoO_8)_3$	mp-1099629	$K_2Na_6V_5Mo_3O_{20}$	mp-1076545
$LaCoO_{3-\delta}$	3	0.965	202.55	$LaCoO_3$	mp-19051	$La_2Co_2O_5$	mp-1076438
$Ca_{0.125}Sr_{0.875}Ti_{0.375}Mn_{0.625}O_{3-\delta}$	4	1.015	206.19	$Sr_7CaTi_3Mn_5O_{24}$	mp-1076827	$Sr_7CaTi_3Mn_5O_{20}$	mp-1076183
$Sm_{0.125}La_{0.875}Fe_{0.375}Mn_{0.625}O_{3-\delta}$	3	0.943	215.02	$La_7SmMn_5(FeO_8)_3$	mp-1099887	$La_7SmMn_5Fe_3O_{20}$	mp-1099861
$Ca_{0.25}Sr_{0.75}Ti_{0.5}Mn_{0.5}O_{3-\delta}$	4	1.005	215.45	$Sr_3CaTi_2Mn_2O_{12}$	mp-1076138	$Sr_3CaTi_2Mn_2O_{10}$	mp-1076875
$Sm_{0.125}La_{0.875}Fe_{0.75}Mn_{0.25}O_{3-\delta}$	3	0.943	230.08	$La_7SmMn_2(FeO_4)_6$	mp-1076598	$La_7SmMn_2(Fe_3O_{10})_2$	mp-1076418
$Na_{0.75}K_{0.25}Mo_{0.5}V_{0.5}O_{3-\delta}$	5	1.012	231.24	$KNa_3V_2(MoO_6)_2$	mp-1099867	$KNa_3V_2(MoO_5)_2$	mp-1099868
$SmCoO_{3-\delta}$	3	0.924	232.71	$SmCoO_3$	mp-24877	$Sm_2Co_2O_5$	mp-1076063
$SrTi_{0.5}Mn_{0.5}O_{3-\delta}$	4	1.015	235.38	Sr_2TiMnO_6	mp-1099881	Sr_2TiMnO_5	mp-1076627
$Sm_{0.125}La_{0.875}Mn_{0.875}Cu_{0.125}O_{3-\delta}$	3	0.939	241.55	$La_7SmMn_7CuO_{24}$	mp-1099832	$La_7SmMn_7CuO_{20}$	mp-1076513
$Sm_{0.125}La_{0.875}Fe_{0.625}Mn_{0.375}O_{3-\delta}$	3	0.943	243.35	$La_7SmMn_3Fe_5O_{24}$	mp-1075984	$La_7SmMn_3(FeO_4)_5$	mp-1076455
$EuFeO_{3-\delta}$	3	0.907	244.26	$EuFeO_3$	mp-540832	$Eu_2Fe_2O_5$	mp-1077617
$Sm_{0.125}La_{0.875}Fe_{0.875}Mn_{0.125}O_{3-\delta}$	3	0.943	245.84	$La_7SmMnFe_7O_{24}$	mp-1076610	$La_7SmMnFe_7O_{20}$	mp-1099902
$MgMnO_{3-\delta}$	4	0.895	250.13	$MgMnO_3$	mp-770618	$Mg_2Mn_2O_5$	mp-1099805
$Sm_{0.125}La_{0.875}Fe_{0.5}Mn_{0.5}O_{3-\delta}$	3	0.943	251.41	$La_7SmMn_4(FeO_6)_4$	mp-1076671	$La_7SmMn_4(FeO_5)_4$	mp-1076172
$BaMnO_{3-\delta}$	4	1.096	252.31	$BaMnO_3$	mp-19267	$Ba_2Mn_2O_5$	mp-1099904
$Sm_{0.125}La_{0.875}Fe_{0.25}Mn_{0.75}O_{3-\delta}$	3	0.943	256.80	$La_7SmMn_6(FeO_{12})_2$	mp-1076669	$La_7SmMn_6(FeO_{10})_2$	mp-1076797
$Sm_{0.125}La_{0.875}Fe_1O_{3-\delta}$	3	0.943	258.54	$La_7Sm(FeO_3)_8$	mp-1076382	$La_7Sm(Fe_2O_5)_4$	mp-1076176
$EuMnO_{3-\delta}$	3	0.907	259.20	$EuMnO_3$	mp-25667	$Eu_2Mn_2O_5$	mp-1099747
$Sm_{0.125}La_{0.875}Fe_{0.125}Mn_{0.875}O_{3-\delta}$	3	0.943	260.34	$La_7SmMn_7FeO_{24}$	mp-1076792	$La_7SmMn_7FeO_{20}$	mp-1099704
$Sm_{0.125}La_{0.875}MnO_{3-\delta}$	3	0.943	265.38	$La_7SmMn_8O_{24}$	mp-1099923	$La_7SmMn_8O_{20}$	mp-1099865
$Na_{0.625}K_{0.375}Mo_{0.625}V_{0.375}O_{3-\delta}$	5	1.020	272.31	$K_3Na_5V_3Mo_5O_{24}$	mp-1099606	$K_3Na_5V_3(MoO_4)_5$	mp-1076888
$Ca_{0.375}Sr_{0.625}Ti_{0.625}Mn_{0.375}O_{3-\delta}$	4	0.996	285.80	$Sr_5Ca_3Ti_5Mn_3O_{24}$	mp-1077659	$Sr_5Ca_3Ti_5Mn_3O_{20}$	mp-1076557
$NaVO_{3-\delta}$	5	1.006	287.56	$NaVO_3$	mp-19083	$Na_2V_2O_5$	mp-1076048

Redox Material	*n*	*t*	ΔH (kJ/mol$_O$)	perovskite (oxidized phase)		brownmillerite (reduced phase)	
$EuCrO_{3-\delta}$	3	0.921	289.00	$EuCrO_3$	mp-771930	$Eu_2Cr_2O_5$	mp-1076286
$Sm_{0.125}La_{0.875}Cr_{0.125}Fe_{0.875}O_{3-\delta}$	3	0.945	289.65	$La_7SmCrFe_7O_{24}$	mp-1099808	$La_7SmCrFe_7O_{20}$	mp-1076459
$Na_{0.625}K_{0.375}Mo_{0.75}V_{0.25}O_{3-\delta}$	5	1.015	304.18	$K_3Na_5V_2(MoO_4)_6$	mp-1076484	$K_3Na_5V_2(Mo_3O_{10})_2$	mp-1076637
$Ca_{0.125}Sr_{0.875}Ti_{0.625}Mn_{0.375}O_{3-\delta}$	4	1.005	304.86	$Sr_7CaTi_5Mn_3O_{24}$	mp-1075948	$Sr_7CaTi_5Mn_3O_{20}$	mp-1076202
$Sr_{0.875}Ba_{0.125}Ti_{0.625}Mn_{0.375}O_{3-\delta}$	4	1.018	311.78	$BaSr_7Ti_5Mn_3O_{24}$	mp-1099624	$BaSr_7Ti_5Mn_3O_{20}$	mp-1100246
$NaMoO_{3-\delta}$	5	0.971	319.41	$NaMoO_3$	mp-1076843	$Na_2Mo_2O_5$	mp-1099875
$Sm_{0.125}La_{0.875}Cr_{0.25}Fe_{0.75}O_{3-\delta}$	3	0.947	319.75	$La_7SmCr_2(FeO_4)_6$	mp-1076431	$La_7SmCr_2(Fe_3O_{10})_2$	mp-1076204
$Sm_{0.25}La_{0.75}Cr_{0.375}Fe_{0.625}O_{3-\delta}$	3	0.943	325.74	$La_6Sm_2Cr_3Fe_5O_{24}$	mp-1076529	$La_6Sm_2Cr_3(FeO_4)_5$	mp-1099892
$Na_{0.625}K_{0.375}Mo_{0.875}V_{0.125}O_{3-\delta}$	5	1.011	342.40	$K_3Na_5VMo_7O_{24}$	mp-1099938	$K_3Na_5VMo_7O_{20}$	mp-1076540
$LaMnO_{3-\delta}$	3	0.948	353.27	$LaMnO_3$	mp-629046	$La_2Mn_2O_5$	mp-1099627
$Sm_{0.25}La_{0.75}Cr_{0.5}Fe_{0.5}O_{3-\delta}$	3	0.945	353.33	$La_3SmCr_2(FeO_6)_2$	mp-1076611	$La_3SmCr_2(FeO_5)_2$	mp-1076194
$Na_{0.5}K_{0.5}MoO_{3-\delta}$	5	1.018	362.81	$KNa(MoO_3)_2$	mp-1076831	$KNaMo_2O_5$	mp-1076606
$KVO_{3-\delta}$	5	1.104	374.19	KVO_3	mp-18815	$K_2V_2O_5$	mp-1099837
$LaFeO_{3-\delta}$	3	0.948	377.56	$LaFeO_3$	mp-542920	$La_2Fe_2O_5$	mp-1099626
$EuVO_{3-\delta}$	3	0.910	381.81	$EuVO_3$	mp-769926	$Eu_2V_2O_5$	mp-1099750
$SmVO_{3-\delta}$	3	0.910	382.21	$SmVO_3$	mp-1099803	$Sm_2V_2O_5$	mp-1076055
$SmMnO_{3-\delta}$	3	0.908	388.21	$SmMnO_3$	mp-25026	$Sm_2Mn_2O_5$	mp-1076289
$Sm_{0.25}La_{0.75}Cr_{0.625}Fe_{0.375}O_{3-\delta}$	3	0.947	390.31	$La_6Sm_2Cr_5(FeO_8)_3$	mp-1099896	$La_6Sm_2Cr_5Fe_3O_{20}$	mp-1099978
$Ca_{0.25}Sr_{0.75}Ti_{0.75}Mn_{0.25}O_{3-\delta}$	4	0.996	396.73	$Sr_3CaTi_3MnO_{12}$	mp-1099703	$Sr_3CaTi_3MnO_{10}$	mp-1076170
$RbMoO_{3-\delta}$	5	1.093	398.52	$RbMoO_3$	mp-975304	$Rb_2Mo_2O_5$	mp-1099822
$SmFeO_{3-\delta}$	3	0.908	401.32	$SmFeO_3$	mp-24989	$Sm_2Fe_2O_5$	mp-1076463
$KMoO_{3-\delta}$	5	1.066	405.11	$KMoO_3$	mp-1076474	$K_2Mo_2O_5$	mp-1075956
$Sr_{0.875}Ba_{0.125}Ti_{0.75}Mn_{0.25}O_{3-\delta}$	4	1.013	407.83	$BaSr_7Ti_6Mn_2O_{24}$	mp-1075988	$BaSr_7Ti_6Mn_2O_{20}$	mp-1076196
$Sm_{0.375}La_{0.625}Cr_{0.75}Fe_{0.25}O_{3-\delta}$	3	0.943	408.22	$La_5Sm_3Cr_6(FeO_{12})_2$	mp-1076580	$La_5Sm_3Cr_6(FeO_{10})_2$	mp-1076203

Redox Material	*n*	*t*	ΔH (kJ/mol$_O$)	perovskite (oxidized phase)		brownmillerite (reduced phase)	
$SmCrO_{3-\delta}$	3	0.922	415.04	$SmCrO_3$	mp-19257	$Sm_2Cr_2O_5$	mp-1099951
$RbVO_{3-\delta}$	5	1.133	422.16	$RbVO_3$	mp-19031	$Rb_2V_2O_5$	mp-1076354
$Na_{0.5}K_{0.5}W_{0.125}Mo_{0.875}O_{3-\delta}$	5	1.018	423.65	$K_4Na_4Mo_7WO_{24}$	mp-1076546	$K_4Na_4Mo_7WO_{20}$	mp-1076754
$Sm_{0.375}La_{0.625}Cr_{0.875}Fe_{0.125}O_{3-\delta}$	3	0.945	433.61	$La_5Sm_3Cr_7FeO_{24}$	mp-1075954	$La_5Sm_3Cr_7FeO_{20}$	mp-1100047
$NaWO_{3-\delta}$	5	0.966	434.58	$NaWO_3$	mp-1099918	$Na_2W_2O_5$	mp-1097724
$Sm_{0.125}La_{0.875}VO_{3-\delta}$	3	0.945	447.65	$La_7SmV_8O_{24}$	mp-1076131	$La_7SmV_8O_{20}$	mp-1076878
$Na_{0.5}K_{0.5}W_{0.25}Mo_{0.75}O_{3-\delta}$	5	1.017	451.70	$K_2Na_2Mo_3WO_{12}$	mp-1076836	$K_2Na_2Mo_3WO_{10}$	mp-1076891
$Sm_{0.375}La_{0.625}CrO_{3-\delta}$	3	0.947	455.88	$La_5Sm_3Cr_8O_{24}$	mp-1076603	$La_5Sm_3Cr_8O_{20}$	mp-1100028
$Sm_{0.375}La_{0.625}V_{0.25}Cr_{0.75}O_{3-\delta}$	3	0.944	468.90	$La_5Sm_3V_2Cr_6O_{24}$	mp-1099675	$La_5Sm_3V_2Cr_6O_{20}$	mp-1076879
$Sm_{0.375}La_{0.625}V_{0.125}Cr_{0.875}O_{3-\delta}$	3	0.945	469.00	$La_5Sm_3VCr_7O_{24}$	mp-1099724	$La_5Sm_3VCr_7O_{20}$	mp-1076766
$Na_{0.5}K_{0.5}W_{0.375}Mo_{0.625}O_{3-\delta}$	5	1.017	486.14	$K_4Na_4Mo_5(WO_8)_3$	mp-1099727	$K_4Na_4Mo_5W_3O_{20}$	mp-1076890
$Na_{0.5}K_{0.5}WO_{3-\delta}$	5	1.013	488.95	$KNa(WO_3)_2$	mp-1076224	$KNaW_2O_5$	mp-1099945
$Sm_{0.25}La_{0.75}V_{0.5}Cr_{0.5}O_{3-\delta}$	3	0.946	489.89	$La_3SmV_2Cr_2O_{12}$	mp-1076218	$La_3SmV_2Cr_2O_{10}$	mp-1099885
$Sm_{0.25}La_{0.75}V_{0.625}Cr_{0.375}O_{3-\delta}$	3	0.945	490.79	$La_6Sm_2V_5Cr_3O_{24}$	mp-1076253	$La_6Sm_2V_5Cr_3O_{20}$	mp-1099931
$Sm_{0.25}La_{0.75}V_{0.375}Cr_{0.625}O_{3-\delta}$	3	0.948	492.03	$La_6Sm_2V_3Cr_5O_{24}$	mp-1076584	$La_6Sm_2V_3Cr_5O_{20}$	mp-1076179
$Na_{0.375}K_{0.625}Nb_{0.5}W_{0.5}O_{3-\delta}$	5	1.020	494.87	$K_5Na_3Nb_4(WO_6)_4$	mp-1099943	$K_5Na_3Nb_4(WO_5)_4$	mp-1076208
$Sr_{0.625}Ba_{0.375}Ti_{0.875}Mn_{0.125}O_{3-\delta}$	4	1.023	495.35	$Ba_3Sr_5Ti_7MnO_{24}$	mp-1075974	$Ba_3Sr_5Ti_7MnO_{20}$	mp-1076186
$Na_{0.5}K_{0.5}Nb_{0.375}W_{0.625}O_{3-\delta}$	5	1.010	497.38	$K_4Na_4Nb_3W_5O_{24}$	mp-1099687	$K_4Na_4Nb_3(WO_4)_5$	mp-1076755
$Ca_{0.125}Sr_{0.875}Ti_{0.875}Mn_{0.125}O_{3-\delta}$	4	0.996	497.69	$Sr_7CaTi_7MnO_{24}$	mp-1076570	$Sr_7CaTi_7MnO_{20}$	mp-1099889
$Sr_{0.875}Ba_{0.125}Ti_{0.875}Mn_{0.125}O_{3-\delta}$	4	1.008	497.73	$BaSr_7Ti_7MnO_{24}$	mp-1076377	$BaSr_7Ti_7MnO_{20}$	mp-1076193
$Na_{0.5}K_{0.5}Nb_{0.25}W_{0.75}O_{3-\delta}$	5	1.011	500.92	$K_2Na_2Nb(WO_4)_3$	mp-1076812	$K_2Na_2NbW_3O_{10}$	mp-1076206
$Na_{0.375}K_{0.625}Nb_{0.625}W_{0.375}O_{3-\delta}$	5	1.019	504.46	$K_5Na_3Nb_5(WO_8)_3$	mp-1076481	$K_5Na_3Nb_5W_3O_{20}$	mp-1076886
$KWO_{3-\delta}$	5	1.061	508.05	KWO_3	mp-1099818	$K_2W_2O_5$	mp-1097834
$Sm_{0.25}La_{0.75}V_{0.75}Cr_{0.25}O_{3-\delta}$	3	0.943	509.16	$La_3SmV_3CrO_{12}$	mp-1076348	$La_3SmV_3CrO_{10}$	mp-1076191

Redox Material	*n*	*t*	ΔH (kJ/mol$_O$)	perovskite (oxidized phase)		brownmillerite (reduced phase)	
$Sm_{0.125}La_{0.875}V_{0.875}Cr_{0.125}O_{3-\delta}$	3	0.947	509.22	$La_7SmV_7CrO_{24}$	mp-1076679	$La_7SmV_7CrO_{20}$	mp-1076889
$Sm_{0.125}La_{0.875}Ti_{0.25}V_{0.75}O_{3-\delta}$	3	0.942	509.53	$La_7SmTi_2V_6O_{24}$	mp-1099746	$La_7SmTi_2V_6O_{20}$	mp-1076595
$Na_{0.375}K_{0.625}Nb_{0.75}W_{0.25}O_{3-\delta}$	5	1.018	510.96	$K_5Na_3Nb_6(WO_{12})_2$	mp-1076412	$K_5Na_3Nb_6(WO_{10})_2$	mp-1099913
$Sm_{0.125}La_{0.875}Ti_{0.125}V_{0.875}O_{3-\delta}$	3	0.944	511.97	$La_7SmTiV_7O_{24}$	mp-1075987	$La_7SmTiV_7O_{20}$	mp-1076664
$Sm_{0.125}La_{0.875}Ti_{0.375}V_{0.625}O_{3-\delta}$	3	0.940	514.30	$La_7SmTi_3V_5O_{24}$	mp-1076581	$La_7SmTi_3V_5O_{20}$	mp-1076885
$RbWO_{3-\delta}$	5	1.088	517.61	$RbWO_3$	mp-975156	$Rb_2W_2O_5$	mp-1075937
$Na_{0.5}K_{0.5}W_{0.5}Mo_{0.5}O_{3-\delta}$	5	1.016	519.41	$KNaMoWO_6$	mp-1076659	$KNaMoWO_5$	mp-1076195
$Na_{0.5}K_{0.5}W_{0.625}Mo_{0.375}O_{3-\delta}$	5	1.015	522.02	$K_4Na_4Mo_3W_5O_{24}$	mp-1099601	$K_4Na_4Mo_3(WO_4)_5$	mp-1076205
$Na_{0.5}K_{0.5}W_{0.75}Mo_{0.25}O_{3-\delta}$	5	1.015	522.72	$K_2Na_2Mo(WO_4)_3$	mp-1099821	$K_2Na_2MoW_3O_{10}$	mp-1099722
$Na_{0.375}K_{0.625}Nb_{0.875}W_{0.125}O_{3-\delta}$	5	1.016	523.02	$K_5Na_3Nb_7WO_{24}$	mp-1099622	$K_5Na_3Nb_7WO_{20}$	mp-1076894
$Na_{0.5}K_{0.5}Nb_{0.125}W_{0.875}O_{3-\delta}$	5	1.012	524.84	$K_4Na_4NbW_7O_{24}$	mp-1076751	$K_4Na_4NbW_7O_{20}$	mp-1099948
$Na_{0.5}K_{0.5}W_{0.875}Mo_{0.125}O_{3-\delta}$	5	1.014	526.37	$K_4Na_4MoW_7O_{24}$	mp-1076685	$K_4Na_4MoW_7O_{20}$	mp-1099972
$Na_{0.375}K_{0.625}NbO_{3-\delta}$	5	1.015	529.59	$K_5Na_3Nb_8O_{24}$	mp-1076335	$K_5Na_3Nb_8O_{20}$	mp-1076768
$Na_{0.375}K_{0.625}Ta_{0.125}Nb_{0.875}O_{3-\delta}$	5	1.015	538.93	$K_5Na_3TaNb_7O_{24}$	mp-1076363	$K_5Na_3TaNb_7O_{20}$	mp-1076887
$Na_{0.375}K_{0.625}Ta_{0.25}Nb_{0.75}O_{3-\delta}$	5	1.015	548.04	$K_5Na_3Ta_2Nb_6O_{24}$	mp-1099712	$K_5Na_3Ta_2Nb_6O_{20}$	mp-1076895
$Na_{0.375}K_{0.625}Ta_{0.375}Nb_{0.625}O_{3-\delta}$	5	1.015	558.23	$K_5Na_3Ta_3Nb_5O_{24}$	mp-1076512	$K_5Na_3Ta_3Nb_5O_{20}$	mp-1077704
$Na_{0.375}K_{0.625}Ta_{0.5}Nb_{0.5}O_{3-\delta}$	5	1.015	567.34	$K_5Na_3Ta_4Nb_4O_{24}$	mp-1076095	$K_5Na_3Ta_4Nb_4O_{20}$	mp-1099857
$LaCrO_{3-\delta}$	3	0.962	570.86	$LaCrO_3$	mp-19281	$La_2Cr_2O_5$	mp-1097715
$CaTiO_{3-\delta}$	4	0.959	578.97	$CaTiO_3$	mp-4019	$Ca_2Ti_2O_5$	mp-1096895
$Ca_{0.125}Sr_{0.875}TiO_{3-\delta}$	4	0.991	584.67	$Sr_7CaTi_8O_{24}$	mp-1075922	$Sr_7CaTi_8O_{20}$	mp-1076695
$Na_{0.375}K_{0.625}Ta_{0.625}Nb_{0.375}O_{3-\delta}$	5	1.015	585.41	$K_5Na_3Ta_5Nb_3O_{24}$	mp-1075953	$K_5Na_3Ta_5Nb_3O_{20}$	mp-1100247
$EuTiO_{3-\delta}$	3	0.896	586.90	$EuTiO_3$	mp-1079111	$Eu_2Ti_2O_5$	mp-1076037
$BaTiO_{3-\delta}$	4	1.055	588.75	$BaTiO_3$	mp-5020	$Ba_2Ti_2O_5$	mp-1076521
$Sr_{0.625}Ba_{0.375}TiO_{3-\delta}$	4	1.018	589.22	$Ba_3Sr_5Ti_8O_{24}$	mp-1075943	$Ba_3Sr_5Ti_8O_{20}$	mp-1099792

Redox Material	*n*	*t*	ΔH (kJ/mol$_O$)	perovskite (oxidized phase)		brownmillerite (reduced phase)	
$Sr_{0.875}Ba_{0.125}TiO_{3-\delta}$	4	1.003	589.44	$BaSr_7Ti_8O_{24}$	mp-1099778	$BaSr_7Ti_8O_{20}$	mp-1099682
$SrTiO_{3-\delta}$	4	0.996	589.85	$SrTiO_3$	mp-4651	$Sr_2Ti_2O_5$	mp-1097778
$KNbO_{3-\delta}$	5	1.050	594.00	$KNbO_3$	mp-7375	$K_2Nb_2O_5$	mp-1076215
$Na_{0.375}K_{0.625}Ta_{0.75}Nb_{0.25}O_{3-\delta}$	5	1.015	606.41	$K_5Na_3Ta_6Nb_2O_{24}$	mp-1099860	$K_5Na_3Ta_6Nb_2O_{20}$	mp-1099903
$RbNbO_{3-\delta}$	5	1.077	624.20	$RbNbO_3$	mp-3283	$Rb_2Nb_2O_5$	mp-1076323
$Na_{0.375}K_{0.625}Ta_{0.875}Nb_{0.125}O_{3-\delta}$	5	1.015	625.94	$K_5Na_3Ta_7NbO_{24}$	mp-1076413	$K_5Na_3Ta_7NbO_{20}$	mp-1100141
$LaTiO_{3-\delta}$	3	0.937	633.41	$LaTiO_3$	mp-22013	$La_2Ti_2O_5$	mp-1097763
$NaTaO_{3-\delta}$	5	0.957	646.24	$NaTaO_3$	mp-3858	$Na_2Ta_2O_5$	mp-1075952
$SmTiO_{3-\delta}$	3	0.897	654.10	$SmTiO_3$	mp-22416	$Sm_2Ti_2O_5$	mp-1099757
$KTaO_{3-\delta}$	5	1.050	660.41	$KTaO_3$	mp-3614	$K_2Ta_2O_5$	mp-1099764
$MgTiO_{3-\delta}$	4	0.862	696.82	$MgTiO_3$	mp-3771	$Mg_2Ti_2O_5$	mp-1076652
$RbTaO_{3-\delta}$	5	1.077	705.99	$RbTaO_3$	mp-3033	$Rb_2Ta_2O_5$	mp-1076737

2. DFT data on perovskite solid solution endmembers

Table S 2. Theoretical data for the perovskite redox pairs investigated within this work including the species and redox enthalpies of the endmembers. All redox enthalpies given per mol of oxygen O released (kJ/mol$_O$). ΔH_{DFT} corresponds to ΔH in table S1. The δ-dependent redox enthalpy of a perovskite solid solution with two different redox-active species on the M site is calculated using the redox enthalpies for the limiting cases of $\delta \rightarrow 0$ (ΔH_{min}) and $\delta \rightarrow 0$ (ΔH_{max}). These are derived from the DFT-calculated redox enthalpies of the solid solution endmembers (EM) as explained in the main manuscript. The redox enthalpy of materials with only one species on the *M* site is assumed to be independent of δ and the endmember redox enthalpies are only given for comparison, as $\Delta H_{min} = \Delta H_{max} = \Delta H_{DFT}$ in these cases (marked in red). If the mean redox enthalpy calculated using the solid solution endmembers differs by more than 30 kJ/mol from the DFT-calculated value for the solid solution (diff > 30), $\Delta H_{min} = \Delta H_{max} = \Delta H_{DFT}$ is used instead.

Redox Material	ΔH_{DFT}	ΔH_{min}	ΔH_{max}	diff>30	EM 1	ΔH_{EM1}	EM 2	ΔH_{EM2}	EM 3	ΔH_{EM3}	EM 4	ΔH_{EM4}
$MgCuO_{3-\delta}$	-337.87	-337.87	-337.87		$MgCuO_{3-\delta}$	-337.87						
$SmAgO_{3-\delta}$	-244.17	-244.17	-244.17		$SmAgO_{3-\delta}$	-244.17						
$CaCuO_{3-\delta}$	-154.45	-154.45	-154.45		$CaCuO_{3-\delta}$	-154.45						
$EuAgO_{3-\delta}$	-102.97	-102.97	-102.97		$EuAgO_{3-\delta}$	-102.97						
$RbCrO_{3-\delta}$	-95.16	-95.16	-95.16		$RbCrO_{3-\delta}$	-95.16						
$Mg_{0.125}Ca_{0.875}CoO_{3-\delta}$	-81.80	-81.80	-81.80		$MgCoO_{3-\delta}$	110.14	$CaCoO_{3-\delta}$	41.41				
$BaCuO_{3-\delta}$	-71.24	-71.24	-71.24		$BaCuO_{3-\delta}$	-71.24						
$Mg_{0.125}Ca_{0.875}Fe_{0.125}Co_{0.875}O_{3-\delta}$	-65.13	-65.13	-65.13	yes	$MgFeO_{3-\delta}$	40.85	$CaFeO_{3-\delta}$	55.51	$MgCoO_{3-\delta}$	110.14	$CaCoO_{3-\delta}$	41.41
$Mg_{0.125}Ca_{0.875}Co_{0.875}Cu_{0.125}O_{3-\delta}$	-56.05	-56.05	-56.05	yes	$MgCoO_{3-\delta}$	110.14	$CaCoO_{3-\delta}$	41.41	$MgCuO_{3-\delta}$	-337.87	$CaCuO_{3-\delta}$	-154.45
$NaCrO_{3-\delta}$	-30.37	-30.37	-30.37		$NaCrO_{3-\delta}$	-30.37						
$Ca_{0.5}Sr_{0.5}CoO_{3-\delta}$	-25.93	-25.93	-25.93		$CaCoO_{3-\delta}$	41.41	$SrCoO_{3-\delta}$	0.82				
$Ca_{0.875}Sr_{0.125}Fe_{0.125}Co_{0.875}O_{3-\delta}$	-15.35	-15.35	-15.35	yes	$CaFeO_{3-\delta}$	55.51	$SrFeO_{3-\delta}$	87.77	$CaCoO_{3-\delta}$	41.41	$SrCoO_{3-\delta}$	0.82
$Ca_{0.75}Sr_{0.25}CoO_{3-\delta}$	-14.17	-14.17	-14.17		$CaCoO_{3-\delta}$	41.41	$SrCoO_{3-\delta}$	0.82				
$SrCuO_{3-\delta}$	-7.35	-7.35	-7.35		$SrCuO_{3-\delta}$	-7.35						
$Ca_{0.875}Sr_{0.125}Fe_{0.25}Co_{0.75}O_{3-\delta}$	-1.20	-1.20	-1.20	yes	$CaFeO_{3-\delta}$	55.51	$SrFeO_{3-\delta}$	87.77	$CaCoO_{3-\delta}$	41.41	$SrCoO_{3-\delta}$	0.82

Redox Material	ΔH_{DFT}	ΔH_{min}	ΔH_{max}	diff>30	EM 1	ΔH_{EM1}	EM 2	ΔH_{EM2}	EM 3	ΔH_{EM3}	EM 4	ΔH_{EM4}
$Ca_{0.75}Sr_{0.25}Co_{0.875}Cu_{0.125}O_{3-\delta}$	-0.57	-163.07	22.64		$CaCoO_{3-\delta}$	41.41	$SrCoO_{3-\delta}$	0.82	$CaCuO_{3-\delta}$	-154.45	$SrCuO_{3-\delta}$	-7.35
$SrCoO_{3-\delta}$	0.82	0.82	0.82		$SrCoO_{3-\delta}$	0.82						
$Ca_{0.75}Sr_{0.25}Fe_{0.125}Co_{0.875}O_{3-\delta}$	6.06	6.06	6.06	yes	$CaFeO_{3-\delta}$	55.51	$SrFeO_{3-\delta}$	87.77	$CaCoO_{3-\delta}$	41.41	$SrCoO_{3-\delta}$	0.82
$KCrO_{3-\delta}$	6.77	6.77	6.77		$KCrO_{3-\delta}$	6.77						
$Ca_{0.625}Sr_{0.375}Fe_{0.125}Co_{0.875}O_{3-\delta}$	7.82	7.82	7.82	yes	$CaFeO_{3-\delta}$	55.51	$SrFeO_{3-\delta}$	87.77	$CaCoO_{3-\delta}$	41.41	$SrCoO_{3-\delta}$	0.82
$Ca_{0.5}Sr_{0.5}Co_{0.875}Cu_{0.125}O_{3-\delta}$	13.73	-139.89	35.68		$CaCoO_{3-\delta}$	41.41	$SrCoO_{3-\delta}$	0.82	$CaCuO_{3-\delta}$	-154.45	$SrCuO_{3-\delta}$	-7.35
$Ca_{0.5}Sr_{0.5}Co_{0.75}Cu_{0.25}O_{3-\delta}$	17.45	17.45	17.45	yes	$CaCoO_{3-\delta}$	41.41	$SrCoO_{3-\delta}$	0.82	$CaCuO_{3-\delta}$	-154.45	$SrCuO_{3-\delta}$	-7.35
$Ca_{0.75}Sr_{0.25}Fe_{0.375}Co_{0.625}O_{3-\delta}$	19.14	19.14	19.14	yes	$CaFeO_{3-\delta}$	55.51	$SrFeO_{3-\delta}$	87.77	$CaCoO_{3-\delta}$	41.41	$SrCoO_{3-\delta}$	0.82
$Sr_{0.125}Ba_{0.875}CuO_{3-\delta}$	20.46	20.46	20.46	yes	$SrCuO_{3-\delta}$	-7.35	$BaCuO_{3-\delta}$	-71.24				
$Sr_{0.25}Ba_{0.75}CuO_{3-\delta}$	22.34	22.34	22.34	yes	$SrCuO_{3-\delta}$	-7.35	$BaCuO_{3-\delta}$	-71.24				
$Sr_{0.25}Ba_{0.75}Co_{0.25}Cu_{0.75}O_{3-\delta}$	23.76	-10.40	126.22		$SrCoO_{3-\delta}$	0.82	$BaCoO_{3-\delta}$	172.09	$SrCuO_{3-\delta}$	-7.35	$BaCuO_{3-\delta}$	-71.24
$Sr_{0.25}Ba_{0.75}Co_{0.125}Cu_{0.875}O_{3-\delta}$	23.79	6.71	143.33		$SrCoO_{3-\delta}$	0.82	$BaCoO_{3-\delta}$	172.09	$SrCuO_{3-\delta}$	-7.35	$BaCuO_{3-\delta}$	-71.24
$Ca_{0.5}Sr_{0.5}Fe_{0.125}Co_{0.875}O_{3-\delta}$	24.32	20.54	50.77		$CaFeO_{3-\delta}$	55.51	$SrFeO_{3-\delta}$	87.77	$CaCoO_{3-\delta}$	41.41	$SrCoO_{3-\delta}$	0.82
$Sm_{0.125}La_{0.875}Co_{0.75}Ag_{0.25}O_{3-\delta}$	26.19	26.19	26.19	yes	$SmCoO_{3-\delta}$	232.71	$LaCoO_{3-\delta}$	202.55	$SmAgO_{3-\delta}$	-244.17	$LaAgO_{3-\delta}$	99.65
$Ca_{0.25}Sr_{0.75}Co_{0.875}Cu_{0.125}O_{3-\delta}$	28.48	28.48	28.48	yes	$CaCoO_{3-\delta}$	41.41	$SrCoO_{3-\delta}$	0.82	$CaCuO_{3-\delta}$	-154.45	$SrCuO_{3-\delta}$	-7.35
$Sm_{0.125}La_{0.875}Ag_{0.25}Ni_{0.75}O_{3-\delta}$	28.64	28.64	28.64	yes	$SmAgO_{3-\delta}$	-244.17	$LaAgO_{3-\delta}$	99.65	$SmNiO_{3-\delta}$	162.20	$LaNiO_{3-\delta}$	141.84
$Sr_{0.5}Ba_{0.5}Co_{0.25}Cu_{0.75}O_{3-\delta}$	30.08	6.63	100.44		$SrCoO_{3-\delta}$	0.82	$BaCoO_{3-\delta}$	172.09	$SrCuO_{3-\delta}$	-7.35	$BaCuO_{3-\delta}$	-71.24
$Sr_{0.5}Ba_{0.5}Co_{0.375}Cu_{0.625}O_{3-\delta}$	32.68	-2.50	91.30		$SrCoO_{3-\delta}$	0.82	$BaCoO_{3-\delta}$	172.09	$SrCuO_{3-\delta}$	-7.35	$BaCuO_{3-\delta}$	-71.24
$Ca_{0.5}Sr_{0.5}Fe_{0.25}Co_{0.75}O_{3-\delta}$	33.07	25.51	55.74		$CaFeO_{3-\delta}$	55.51	$SrFeO_{3-\delta}$	87.77	$CaCoO_{3-\delta}$	41.41	$SrCoO_{3-\delta}$	0.82
$Sm_{0.5}La_{0.5}Co_{0.875}Ag_{0.125}O_{3-\delta}$	33.33	33.33	33.33	yes	$SmCoO_{3-\delta}$	232.71	$LaCoO_{3-\delta}$	202.55	$SmAgO_{3-\delta}$	-244.17	$LaAgO_{3-\delta}$	99.65
$Ca_{0.375}Sr_{0.625}Fe_{0.125}Co_{0.875}O_{3-\delta}$	34.36	30.08	64.34		$CaFeO_{3-\delta}$	55.51	$SrFeO_{3-\delta}$	87.77	$CaCoO_{3-\delta}$	41.41	$SrCoO_{3-\delta}$	0.82
$Ca_{0.625}Sr_{0.375}Fe_{0.625}Co_{0.375}O_{3-\delta}$	35.90	19.52	45.72		$CaFeO_{3-\delta}$	55.51	$SrFeO_{3-\delta}$	87.77	$CaCoO_{3-\delta}$	41.41	$SrCoO_{3-\delta}$	0.82
$Ca_{0.25}Sr_{0.75}Co_{0.625}Cu_{0.375}O_{3-\delta}$	36.72	36.72	36.72	yes	$CaCoO_{3-\delta}$	41.41	$SrCoO_{3-\delta}$	0.82	$CaCuO_{3-\delta}$	-154.45	$SrCuO_{3-\delta}$	-7.35
$Sr_{0.75}Ba_{0.25}Co_{0.5}Cu_{0.5}O_{3-\delta}$	36.92	11.43	62.41		$SrCoO_{3-\delta}$	0.82	$BaCoO_{3-\delta}$	172.09	$SrCuO_{3-\delta}$	-7.35	$BaCuO_{3-\delta}$	-71.24

Redox Material	ΔH_{DFT}	ΔH_{min}	ΔH_{max}	diff>30	EM 1	ΔH_{EM1}	EM 2	ΔH_{EM2}	EM 3	ΔH_{EM3}	EM 4	ΔH_{EM4}
$Ca_{0.375}Sr_{0.625}Fe_{0.25}Co_{0.75}O_{3-\delta}$	37.34	28.77	63.04		$CaFeO_{3-\delta}$	55.51	$SrFeO_{3-\delta}$	87.77	$CaCoO_{3-\delta}$	41.41	$SrCoO_{3-\delta}$	0.82
$Sr_{0.625}Ba_{0.375}Co_{0.375}Cu_{0.625}O_{3-\delta}$	37.84	10.69	83.09		$SrCoO_{3-\delta}$	0.82	$BaCoO_{3-\delta}$	172.09	$SrCuO_{3-\delta}$	-7.35	$BaCuO_{3-\delta}$	-71.24
$Ca_{0.625}Sr_{0.375}Fe_{0.5}Co_{0.5}O_{3-\delta}$	39.01	25.91	52.11		$CaFeO_{3-\delta}$	55.51	$SrFeO_{3-\delta}$	87.77	$CaCoO_{3-\delta}$	41.41	$SrCoO_{3-\delta}$	0.82
$Sm_{0.25}La_{0.75}Co_{0.875}Ag_{0.125}O_{3-\delta}$	39.52	39.52	39.52	yes	$SmCoO_{3-\delta}$	232.71	$LaCoO_{3-\delta}$	202.55	$SmAgO_{3-\delta}$	-244.17	$LaAgO_{3-\delta}$	99.65
$Ca_{0.25}Sr_{0.75}Co_{0.75}Cu_{0.25}O_{3-\delta}$	40.17	40.17	40.17	yes	$CaCoO_{3-\delta}$	41.41	$SrCoO_{3-\delta}$	0.82	$CaCuO_{3-\delta}$	-154.45	$SrCuO_{3-\delta}$	-7.35
$Sr_{0.75}Ba_{0.25}Co_{0.375}Cu_{0.625}O_{3-\delta}$	40.21	21.09	72.08		$SrCoO_{3-\delta}$	0.82	$BaCoO_{3-\delta}$	172.09	$SrCuO_{3-\delta}$	-7.35	$BaCuO_{3-\delta}$	-71.24
$MgFeO_{3-\delta}$	40.85	40.85	40.85		$MgFeO_{3-\delta}$	40.85						
$CaCoO_{3-\delta}$	41.41	41.41	41.41		$CaCoO_{3-\delta}$	41.41						
$Ca_{0.5}Sr_{0.5}Fe_{0.375}Co_{0.625}O_{3-\delta}$	41.82	30.48	60.72		$CaFeO_{3-\delta}$	55.51	$SrFeO_{3-\delta}$	87.77	$CaCoO_{3-\delta}$	41.41	$SrCoO_{3-\delta}$	0.82
$Ca_{0.5}Sr_{0.5}Fe_{0.75}Co_{0.25}O_{3-\delta}$	42.84	20.16	50.40		$CaFeO_{3-\delta}$	55.51	$SrFeO_{3-\delta}$	87.77	$CaCoO_{3-\delta}$	41.41	$SrCoO_{3-\delta}$	0.82
$Sr_{0.625}Ba_{0.375}Co_{0.5}Cu_{0.5}O_{3-\delta}$	47.17	10.97	83.36		$SrCoO_{3-\delta}$	0.82	$BaCoO_{3-\delta}$	172.09	$SrCuO_{3-\delta}$	-7.35	$BaCuO_{3-\delta}$	-71.24
$Sr_{0.75}Ba_{0.25}Co_{0.625}Cu_{0.375}O_{3-\delta}$	47.64	15.78	66.76		$SrCoO_{3-\delta}$	0.82	$BaCoO_{3-\delta}$	172.09	$SrCuO_{3-\delta}$	-7.35	$BaCuO_{3-\delta}$	-71.24
$Sr_{0.875}Ba_{0.125}Co_{0.625}Cu_{0.375}O_{3-\delta}$	47.99	47.99	47.99	yes	$SrCoO_{3-\delta}$	0.82	$BaCoO_{3-\delta}$	172.09	$SrCuO_{3-\delta}$	-7.35	$BaCuO_{3-\delta}$	-71.24
$Sr_{0.875}Ba_{0.125}Co_{0.5}Cu_{0.5}O_{3-\delta}$	48.55	48.55	48.55	yes	$SrCoO_{3-\delta}$	0.82	$BaCoO_{3-\delta}$	172.09	$SrCuO_{3-\delta}$	-7.35	$BaCuO_{3-\delta}$	-71.24
$EuCoO_{3-\delta}$	49.90	49.90	49.90		$EuCoO_{3-\delta}$	49.90						
$Sm_{0.375}La_{0.625}Ag_{0.125}Ni_{0.875}O_{3-\delta}$	52.78	52.78	52.78	yes	$SmAgO_{3-\delta}$	-244.17	$LaAgO_{3-\delta}$	99.65	$SmNiO_{3-\delta}$	162.20	$LaNiO_{3-\delta}$	141.84
$Ca_{0.25}Sr_{0.75}Fe_{0.375}Co_{0.625}O_{3-\delta}$	54.13	39.77	78.06		$CaFeO_{3-\delta}$	55.51	$SrFeO_{3-\delta}$	87.77	$CaCoO_{3-\delta}$	41.41	$SrCoO_{3-\delta}$	0.82
$CaFeO_{3-\delta}$	55.51	55.51	55.51		$CaFeO_{3-\delta}$	55.51						
$Ca_{0.375}Sr_{0.625}Fe_{0.875}Co_{0.125}O_{3-\delta}$	56.98	27.00	61.26		$CaFeO_{3-\delta}$	55.51	$SrFeO_{3-\delta}$	87.77	$CaCoO_{3-\delta}$	41.41	$SrCoO_{3-\delta}$	0.82
$Mg_{0.125}Ca_{0.875}Mn_{0.875}Fe_{0.125}O_{3-\delta}$	57.56	57.56	57.56	yes	$MgMnO_{3-\delta}$	250.13	$CaMnO_{3-\delta}$	173.13	$MgFeO_{3-\delta}$	40.85	$CaFeO_{3-\delta}$	55.51
$Mg_{0.125}Ca_{0.875}MnO_{3-\delta}$	61.05	61.05	61.05		$MgMnO_{3-\delta}$	250.13	$CaMnO_{3-\delta}$	173.13				
$Ca_{0.25}Sr_{0.75}Fe_{0.625}Co_{0.375}O_{3-\delta}$	63.86	39.92	78.22		$CaFeO_{3-\delta}$	55.51	$SrFeO_{3-\delta}$	87.77	$CaCoO_{3-\delta}$	41.41	$SrCoO_{3-\delta}$	0.82
$Ca_{0.25}Sr_{0.75}Fe_{0.875}Co_{0.125}O_{3-\delta}$	64.86	31.35	69.65		$CaFeO_{3-\delta}$	55.51	$SrFeO_{3-\delta}$	87.77	$CaCoO_{3-\delta}$	41.41	$SrCoO_{3-\delta}$	0.82
$Ca_{0.125}Sr_{0.875}Fe_{0.5}Co_{0.5}O_{3-\delta}$	65.92	44.76	87.09		$CaFeO_{3-\delta}$	55.51	$SrFeO_{3-\delta}$	87.77	$CaCoO_{3-\delta}$	41.41	$SrCoO_{3-\delta}$	0.82

Redox Material	ΔH_{DFT}	ΔH_{min}	ΔH_{max}	diff>30	EM 1	ΔH_{EM1}	EM 2	ΔH_{EM2}	EM 3	ΔH_{EM3}	EM 4	ΔH_{EM4}
$Ca_{0.25}Sr_{0.75}FeO_{3-\delta}$	68.03	68.03	92.23		$CaFeO_{3-\delta}$	55.51	$SrFeO_{3-\delta}$	87.77				
$Ca_{0.125}Sr_{0.875}Fe_{0.625}Co_{0.375}O_{3-\delta}$	68.95	42.49	84.82		$CaFeO_{3-\delta}$	55.51	$SrFeO_{3-\delta}$	87.77	$CaCoO_{3-\delta}$	41.41	$SrCoO_{3-\delta}$	0.82
$Ca_{0.125}Sr_{0.875}Fe_{0.875}Co_{0.125}O_{3-\delta}$	71.48	34.45	76.78		$CaFeO_{3-\delta}$	55.51	$SrFeO_{3-\delta}$	87.77	$CaCoO_{3-\delta}$	41.41	$SrCoO_{3-\delta}$	0.82
$Ca_{0.125}Sr_{0.875}Fe_{0.75}Co_{0.25}O_{3-\delta}$	72.40	40.65	82.98		$CaFeO_{3-\delta}$	55.51	$SrFeO_{3-\delta}$	87.77	$CaCoO_{3-\delta}$	41.41	$SrCoO_{3-\delta}$	0.82
$EuNiO_{3-\delta}$	73.85	73.85	73.85		$EuNiO_{3-\delta}$	73.85						
$Sm_{0.5}La_{0.5}NiO_{3-\delta}$	76.16	76.16	76.16		$SmNiO_{3-\delta}$	162.20	$LaNiO_{3-\delta}$	141.84				
$Ca_{0.375}Sr_{0.625}Mn_{0.125}Fe_{0.875}O_{3-\delta}$	76.32	61.83	177.70		$CaMnO_{3-\delta}$	173.13	$SrMnO_{3-\delta}$	170.33	$CaFeO_{3-\delta}$	55.51	$SrFeO_{3-\delta}$	87.77
$SrFe_{0.875}Co_{0.125}O_{3-\delta}$	76.87	0.79	87.74		$SrFeO_{3-\delta}$	87.77	$SrFeO_{3-\delta}$	87.77	$SrCoO_{3-\delta}$	0.82	$SrCoO_{3-\delta}$	0.82
$Sr_{0.875}Ba_{0.125}Fe_{0.875}Co_{0.125}O_{3-\delta}$	78.02	1.17	89.00		$SrFeO_{3-\delta}$	87.77	$BaFeO_{3-\delta}$	94.77	$SrCoO_{3-\delta}$	0.82	$BaCoO_{3-\delta}$	172.09
$Mg_{0.125}Ca_{0.875}Ti_{0.125}Mn_{0.875}O_{3-\delta}$	79.23	79.23	79.23	yes	$MgTiO_{3-\delta}$	696.82	$CaTiO_{3-\delta}$	578.97	$MgMnO_{3-\delta}$	250.13	$CaMnO_{3-\delta}$	173.13
$Sr_{0.875}Ba_{0.125}Fe_{0.75}Co_{0.25}O_{3-\delta}$	81.84	15.97	103.79		$SrFeO_{3-\delta}$	87.77	$BaFeO_{3-\delta}$	94.77	$SrCoO_{3-\delta}$	0.82	$BaCoO_{3-\delta}$	172.09
$Ca_{0.5}Sr_{0.5}Mn_{0.25}Fe_{0.75}O_{3-\delta}$	83.80	54.74	170.96		$CaMnO_{3-\delta}$	173.13	$SrMnO_{3-\delta}$	170.33	$CaFeO_{3-\delta}$	55.51	$SrFeO_{3-\delta}$	87.77
$Ca_{0.25}Sr_{0.75}Mn_{0.125}Fe_{0.875}O_{3-\delta}$	85.26	70.82	186.34		$CaMnO_{3-\delta}$	173.13	$SrMnO_{3-\delta}$	170.33	$CaFeO_{3-\delta}$	55.51	$SrFeO_{3-\delta}$	87.77
$SrFeO_{3-\delta}$	87.77	87.77	87.77		$SrFeO_{3-\delta}$	87.77						
$Sr_{0.875}Ba_{0.125}FeO_{3-\delta}$	88.00	88.00	88.00		$SrFeO_{3-\delta}$	87.77	$BaFeO_{3-\delta}$	94.77				
$BaFeO_{3-\delta}$	94.77	94.77	94.77		$BaFeO_{3-\delta}$	94.77						
$Sm_{0.5}La_{0.5}CoO_{3-\delta}$	94.88	94.88	94.88		$SmCoO_{3-\delta}$	232.71	$LaCoO_{3-\delta}$	202.55				
$Ca_{0.125}Sr_{0.875}Mn_{0.125}Fe_{0.875}O_{3-\delta}$	95.92	81.53	196.70		$CaMnO_{3-\delta}$	173.13	$SrMnO_{3-\delta}$	170.33	$CaFeO_{3-\delta}$	55.51	$SrFeO_{3-\delta}$	87.77
$Ca_{0.625}Sr_{0.375}Mn_{0.375}Fe_{0.625}O_{3-\delta}$	96.08	52.37	168.94		$CaMnO_{3-\delta}$	173.13	$SrMnO_{3-\delta}$	170.33	$CaFeO_{3-\delta}$	55.51	$SrFeO_{3-\delta}$	87.77
$Sm_{0.5}La_{0.5}Cu_{0.125}Co_{0.875}O_{3-\delta}$	98.69	98.69	98.69	yes	$SmCuO_{3-\delta}$	147.50	$LaCuO_{3-\delta}$	149.59	$SmCoO_{3-\delta}$	232.71	$LaCoO_{3-\delta}$	202.55
$LaAgO_{3-\delta}$	99.65	99.65	99.65		$LaAgO_{3-\delta}$	99.65						
$Sr_{0.875}Ba_{0.125}Mn_{0.125}Fe_{0.875}O_{3-\delta}$	99.89	88.29	181.10		$SrMnO_{3-\delta}$	170.33	$BaMnO_{3-\delta}$	252.31	$SrFeO_{3-\delta}$	87.77	$BaFeO_{3-\delta}$	94.77
$Ca_{0.875}Sr_{0.125}Mn_{0.75}Fe_{0.25}O_{3-\delta}$	101.07	101.07	101.07	yes	$CaMnO_{3-\delta}$	173.13	$SrMnO_{3-\delta}$	170.33	$CaFeO_{3-\delta}$	55.51	$SrFeO_{3-\delta}$	87.77
$Ca_{0.875}Sr_{0.125}Mn_{0.875}Fe_{0.125}O_{3-\delta}$	102.62	102.62	102.62	yes	$CaMnO_{3-\delta}$	173.13	$SrMnO_{3-\delta}$	170.33	$CaFeO_{3-\delta}$	55.51	$SrFeO_{3-\delta}$	87.77

Redox Material	ΔH_{DFT}	ΔH_{min}	ΔH_{max}	diff>30	EM 1	ΔH_{EM1}	EM 2	ΔH_{EM2}	EM 3	ΔH_{EM3}	EM 4	ΔH_{EM4}
$Na_{0.875}K_{0.125}V_{0.75}Cr_{0.25}O_{3-\delta}$	102.72	102.72	102.72	yes	$NaVO_{3-\delta}$	287.56	$KVO_{3-\delta}$	374.19	$NaCrO_{3-\delta}$	-30.37	$KCrO_{3-\delta}$	6.77
$EuCuO_{3-\delta}$	105.30	105.30	105.30		$EuCuO_{3-\delta}$	105.30						
$Ca_{0.75}Sr_{0.25}Mn_{0.625}Fe_{0.375}O_{3-\delta}$	105.69	32.61	149.53		$CaMnO_{3-\delta}$	173.13	$SrMnO_{3-\delta}$	170.33	$CaFeO_{3-\delta}$	55.51	$SrFeO_{3-\delta}$	87.77
$SrMn_{0.125}Fe_{0.875}O_{3-\delta}$	105.84	95.52	178.08		$SrMnO_{3-\delta}$	170.33	$SrMnO_{3-\delta}$	170.33	$SrFeO_{3-\delta}$	87.77	$SrFeO_{3-\delta}$	87.77
$Sm_{0.375}La_{0.625}Cu_{0.125}Co_{0.875}O_{3-\delta}$	106.73	106.73	106.73	yes	$SmCuO_{3-\delta}$	147.50	$LaCuO_{3-\delta}$	149.59	$SmCoO_{3-\delta}$	232.71	$LaCoO_{3-\delta}$	202.55
$MgCoO_{3-\delta}$	110.14	110.14	110.14		$MgCoO_{3-\delta}$	110.14						
$Ca_{0.125}Sr_{0.875}Mn_{0.25}Fe_{0.75}O_{3-\delta}$	110.29	81.49	196.66		$CaMnO_{3-\delta}$	173.13	$SrMnO_{3-\delta}$	170.33	$CaFeO_{3-\delta}$	55.51	$SrFeO_{3-\delta}$	87.77
$Ca_{0.75}Sr_{0.25}Mn_{0.875}Fe_{0.125}O_{3-\delta}$	110.63	110.63	110.63	yes	$CaMnO_{3-\delta}$	173.13	$SrMnO_{3-\delta}$	170.33	$CaFeO_{3-\delta}$	55.51	$SrFeO_{3-\delta}$	87.77
$Ca_{0.625}Sr_{0.375}Mn_{0.5}Fe_{0.5}O_{3-\delta}$	114.92	56.63	173.20		$CaMnO_{3-\delta}$	173.13	$SrMnO_{3-\delta}$	170.33	$CaFeO_{3-\delta}$	55.51	$SrFeO_{3-\delta}$	87.77
$Ca_{0.25}Sr_{0.75}Mn_{0.375}Fe_{0.625}O_{3-\delta}$	116.98	73.66	189.18		$CaMnO_{3-\delta}$	173.13	$SrMnO_{3-\delta}$	170.33	$CaFeO_{3-\delta}$	55.51	$SrFeO_{3-\delta}$	87.77
$Ca_{0.5}Sr_{0.5}Mn_{0.625}Fe_{0.375}O_{3-\delta}$	117.88	45.24	161.46		$CaMnO_{3-\delta}$	173.13	$SrMnO_{3-\delta}$	170.33	$CaFeO_{3-\delta}$	55.51	$SrFeO_{3-\delta}$	87.77
$Ca_{0.5}Sr_{0.5}Mn_{0.75}Fe_{0.25}O_{3-\delta}$	119.85	32.69	148.91		$CaMnO_{3-\delta}$	173.13	$SrMnO_{3-\delta}$	170.33	$CaFeO_{3-\delta}$	55.51	$SrFeO_{3-\delta}$	87.77
$Sm_{0.125}La_{0.875}Cu_{0.25}Co_{0.75}O_{3-\delta}$	119.91	119.91	119.91	yes	$SmCuO_{3-\delta}$	147.50	$LaCuO_{3-\delta}$	149.59	$SmCoO_{3-\delta}$	232.71	$LaCoO_{3-\delta}$	202.55
$Sr_{0.875}Ba_{0.125}Mn_{0.25}Fe_{0.75}O_{3-\delta}$	120.66	97.46	190.27		$SrMnO_{3-\delta}$	170.33	$BaMnO_{3-\delta}$	252.31	$SrFeO_{3-\delta}$	87.77	$BaFeO_{3-\delta}$	94.77
$Ca_{0.5}Sr_{0.5}MnO_{3-\delta}$	121.61	121.61	121.61		$CaMnO_{3-\delta}$	173.13	$SrMnO_{3-\delta}$	170.33				
$Na_{0.875}K_{0.125}V_{0.875}Cr_{0.125}O_{3-\delta}$	121.67	121.67	121.67	yes	$NaVO_{3-\delta}$	287.56	$KVO_{3-\delta}$	374.19	$NaCrO_{3-\delta}$	-30.37	$KCrO_{3-\delta}$	6.77
$Ca_{0.5}Sr_{0.5}Mn_{0.875}Fe_{0.125}O_{3-\delta}$	123.20	123.20	123.20	yes	$CaMnO_{3-\delta}$	173.13	$SrMnO_{3-\delta}$	170.33	$CaFeO_{3-\delta}$	55.51	$SrFeO_{3-\delta}$	87.77
$Sm_{0.125}La_{0.875}Cu_{0.375}Co_{0.625}O_{3-\delta}$	123.90	123.90	123.90	yes	$SmCuO_{3-\delta}$	147.50	$LaCuO_{3-\delta}$	149.59	$SmCoO_{3-\delta}$	232.71	$LaCoO_{3-\delta}$	202.55
$Ca_{0.375}Sr_{0.625}Mn_{0.75}Fe_{0.25}O_{3-\delta}$	125.87	38.97	154.84		$CaMnO_{3-\delta}$	173.13	$SrMnO_{3-\delta}$	170.33	$CaFeO_{3-\delta}$	55.51	$SrFeO_{3-\delta}$	87.77
$Ca_{0.125}Sr_{0.875}Mn_{0.375}Fe_{0.625}O_{3-\delta}$	126.36	83.17	198.34		$CaMnO_{3-\delta}$	173.13	$SrMnO_{3-\delta}$	170.33	$CaFeO_{3-\delta}$	55.51	$SrFeO_{3-\delta}$	87.77
$Ca_{0.375}Sr_{0.625}Mn_{0.5}Fe_{0.5}O_{3-\delta}$	126.88	68.95	184.82		$CaMnO_{3-\delta}$	173.13	$SrMnO_{3-\delta}$	170.33	$CaFeO_{3-\delta}$	55.51	$SrFeO_{3-\delta}$	87.77
$Ca_{0.875}Sr_{0.125}Ti_{0.125}Mn_{0.875}O_{3-\delta}$	127.33	127.33	127.33	yes	$CaTiO_{3-\delta}$	578.97	$SrTiO_{3-\delta}$	589.85	$CaMnO_{3-\delta}$	173.13	$SrMnO_{3-\delta}$	170.33
$Ca_{0.375}Sr_{0.625}Mn_{0.875}Fe_{0.125}O_{3-\delta}$	130.00	28.61	144.48		$CaMnO_{3-\delta}$	173.13	$SrMnO_{3-\delta}$	170.33	$CaFeO_{3-\delta}$	55.51	$SrFeO_{3-\delta}$	87.77
$Ca_{0.25}Sr_{0.75}Mn_{0.625}Fe_{0.375}O_{3-\delta}$	130.54	58.34	173.86		$CaMnO_{3-\delta}$	173.13	$SrMnO_{3-\delta}$	170.33	$CaFeO_{3-\delta}$	55.51	$SrFeO_{3-\delta}$	87.77

Redox Material	ΔH_{DFT}	ΔH_{min}	ΔH_{max}	diff>30	EM 1	ΔH_{EM1}	EM 2	ΔH_{EM2}	EM 3	ΔH_{EM3}	EM 4	ΔH_{EM4}
$Ca_{0.75}Sr_{0.25}Ti_{0.125}Mn_{0.875}O_{3-\delta}$	135.03	135.03	135.03	yes	$CaTiO_{3-\delta}$	578.97	$SrTiO_{3-\delta}$	589.85	$CaMnO_{3-\delta}$	173.13	$SrMnO_{3-\delta}$	170.33
$Ca_{0.125}Sr_{0.875}Mn_{0.5}Fe_{0.5}O_{3-\delta}$	140.53	82.95	198.11		$CaMnO_{3-\delta}$	173.13	$SrMnO_{3-\delta}$	170.33	$CaFeO_{3-\delta}$	55.51	$SrFeO_{3-\delta}$	87.77
$LaNiO_{3-\delta}$	141.84	141.84	141.84		$LaNiO_{3-\delta}$	141.84						
$Na_{0.875}K_{0.125}VO_{3-\delta}$	142.67	142.67	142.67		$NaVO_{3-\delta}$	287.56	$KVO_{3-\delta}$	374.19				
$Ca_{0.625}Sr_{0.375}Ti_{0.125}Mn_{0.875}O_{3-\delta}$	143.35	143.35	143.35	yes	$CaTiO_{3-\delta}$	578.97	$SrTiO_{3-\delta}$	589.85	$CaMnO_{3-\delta}$	173.13	$SrMnO_{3-\delta}$	170.33
$SmCuO_{3-\delta}$	147.50	147.50	147.50		$SmCuO_{3-\delta}$	147.50						
$LaCuO_{3-\delta}$	149.59	149.59	149.59		$LaCuO_{3-\delta}$	149.59						
$Ca_{0.5}Sr_{0.5}Ti_{0.125}Mn_{0.875}O_{3-\delta}$	149.66	149.66	149.66	yes	$CaTiO_{3-\delta}$	578.97	$SrTiO_{3-\delta}$	589.85	$CaMnO_{3-\delta}$	173.13	$SrMnO_{3-\delta}$	170.33
$Ca_{0.75}Sr_{0.25}Ti_{0.25}Mn_{0.75}O_{3-\delta}$	152.20	152.20	152.20	yes	$CaTiO_{3-\delta}$	578.97	$SrTiO_{3-\delta}$	589.85	$CaMnO_{3-\delta}$	173.13	$SrMnO_{3-\delta}$	170.33
$Ca_{0.375}Sr_{0.625}Ti_{0.125}Mn_{0.875}O_{3-\delta}$	155.01	155.01	155.01	yes	$CaTiO_{3-\delta}$	578.97	$SrTiO_{3-\delta}$	589.85	$CaMnO_{3-\delta}$	173.13	$SrMnO_{3-\delta}$	170.33
$SmNiO_{3-\delta}$	162.20	162.20	162.20		$SmNiO_{3-\delta}$	162.20						
$Ca_{0.5}Sr_{0.5}Ti_{0.25}Mn_{0.75}O_{3-\delta}$	166.56	166.56	166.56	yes	$CaTiO_{3-\delta}$	578.97	$SrTiO_{3-\delta}$	589.85	$CaMnO_{3-\delta}$	173.13	$SrMnO_{3-\delta}$	170.33
$Ca_{0.75}Sr_{0.25}MnO_{3-\delta}$	167.65	167.65	168.35		$CaMnO_{3-\delta}$	173.13	$SrMnO_{3-\delta}$	170.33				
$Na_{0.875}K_{0.125}Mo_{0.125}V_{0.875}O_{3-\delta}$	170.32	170.32	170.32	yes	$NaMoO_{3-\delta}$	319.41	$KMoO_{3-\delta}$	405.11	$NaVO_{3-\delta}$	287.56	$KVO_{3-\delta}$	374.19
$SrMnO_{3-\delta}$	170.33	170.33	170.33		$SrMnO_{3-\delta}$	170.33						
$BaCoO_{3-\delta}$	172.09	172.09	172.09		$BaCoO_{3-\delta}$	172.09						
$CaMnO_{3-\delta}$	173.13	173.13	173.13		$CaMnO_{3-\delta}$	173.13						
$Ca_{0.625}Sr_{0.375}Ti_{0.375}Mn_{0.625}O_{3-\delta}$	173.40	173.40	173.40	yes	$CaTiO_{3-\delta}$	578.97	$SrTiO_{3-\delta}$	589.85	$CaMnO_{3-\delta}$	173.13	$SrMnO_{3-\delta}$	170.33
$Na_{0.875}K_{0.125}Mo_{0.25}V_{0.75}O_{3-\delta}$	180.38	180.38	180.38	yes	$NaMoO_{3-\delta}$	319.41	$KMoO_{3-\delta}$	405.11	$NaVO_{3-\delta}$	287.56	$KVO_{3-\delta}$	374.19
$Ca_{0.25}Sr_{0.75}Ti_{0.25}Mn_{0.75}O_{3-\delta}$	182.71	182.71	182.71	yes	$CaTiO_{3-\delta}$	578.97	$SrTiO_{3-\delta}$	589.85	$CaMnO_{3-\delta}$	173.13	$SrMnO_{3-\delta}$	170.33
$Ca_{0.375}Sr_{0.625}Ti_{0.375}Mn_{0.625}O_{3-\delta}$	188.81	188.81	188.81	yes	$CaTiO_{3-\delta}$	578.97	$SrTiO_{3-\delta}$	589.85	$CaMnO_{3-\delta}$	173.13	$SrMnO_{3-\delta}$	170.33
$Ca_{0.5}Sr_{0.5}Ti_{0.5}Mn_{0.5}O_{3-\delta}$	195.49	195.49	195.49	yes	$CaTiO_{3-\delta}$	578.97	$SrTiO_{3-\delta}$	589.85	$CaMnO_{3-\delta}$	173.13	$SrMnO_{3-\delta}$	170.33
$Na_{0.75}K_{0.25}Mo_{0.375}V_{0.625}O_{3-\delta}$	202.11	202.11	202.11	yes	$NaMoO_{3-\delta}$	319.41	$KMoO_{3-\delta}$	405.11	$NaVO_{3-\delta}$	287.56	$KVO_{3-\delta}$	374.19
$LaCoO_{3-\delta}$	202.55	202.55	202.55		$LaCoO_{3-\delta}$	202.55						

Redox Material	ΔH_{DFT}	ΔH_{min}	ΔH_{max}	diff>30	EM 1	ΔH_{EM1}	EM 2	ΔH_{EM2}	EM 3	ΔH_{EM3}	EM 4	ΔH_{EM4}
$Ca_{0.125}Sr_{0.875}Ti_{0.375}Mn_{0.625}O_{3-\delta}$	206.19	206.19	206.19	yes	$CaTiO_{3-\delta}$	578.97	$SrTiO_{3-\delta}$	589.85	$CaMnO_{3-\delta}$	173.13	$SrMnO_{3-\delta}$	170.33
$Sm_{0.125}La_{0.875}Fe_{0.375}Mn_{0.625}O_{3-\delta}$	215.02	215.02	215.02	yes	$SmFeO_{3-\delta}$	401.32	$LaFeO_{3-\delta}$	377.56	$SmMnO_{3-\delta}$	388.21	$LaMnO_{3-\delta}$	353.27
$Ca_{0.25}Sr_{0.75}Ti_{0.5}Mn_{0.5}O_{3-\delta}$	215.45	215.45	215.45	yes	$CaTiO_{3-\delta}$	578.97	$SrTiO_{3-\delta}$	589.85	$CaMnO_{3-\delta}$	173.13	$SrMnO_{3-\delta}$	170.33
$Sm_{0.125}La_{0.875}Fe_{0.75}Mn_{0.25}O_{3-\delta}$	230.08	230.08	230.08	yes	$SmFeO_{3-\delta}$	401.32	$LaFeO_{3-\delta}$	377.56	$SmMnO_{3-\delta}$	388.21	$LaMnO_{3-\delta}$	353.27
$Na_{0.75}K_{0.25}Mo_{0.5}V_{0.5}O_{3-\delta}$	231.24	231.24	231.24	yes	$NaMoO_{3-\delta}$	319.41	$KMoO_{3-\delta}$	405.11	$NaVO_{3-\delta}$	287.56	$KVO_{3-\delta}$	374.19
$SmCoO_{3-\delta}$	232.71	232.71	232.71		$SmCoO_{3-\delta}$	232.71						
$SrTi_{0.5}Mn_{0.5}O_{3-\delta}$	235.38	235.38	235.38	yes	$SrTiO_{3-\delta}$	589.85	$SrTiO_{3-\delta}$	589.85	$SrMnO_{3-\delta}$	170.33	$SrMnO_{3-\delta}$	170.33
$Sm_{0.125}La_{0.875}Mn_{0.875}Cu_{0.125}O_{3-\delta}$	241.55	241.55	241.55	yes	$SmMnO_{3-\delta}$	388.21	$LaMnO_{3-\delta}$	353.27	$SmCuO_{3-\delta}$	147.50	$LaCuO_{3-\delta}$	149.59
$Sm_{0.125}La_{0.875}Fe_{0.625}Mn_{0.375}O_{3-\delta}$	243.35	243.35	243.35	yes	$SmFeO_{3-\delta}$	401.32	$LaFeO_{3-\delta}$	377.56	$SmMnO_{3-\delta}$	388.21	$LaMnO_{3-\delta}$	353.27
$EuFeO_{3-\delta}$	244.26	244.26	244.26		$EuFeO_{3-\delta}$	244.26						
$Sm_{0.125}La_{0.875}Fe_{0.875}Mn_{0.125}O_{3-\delta}$	245.84	245.84	245.84	yes	$SmFeO_{3-\delta}$	401.32	$LaFeO_{3-\delta}$	377.56	$SmMnO_{3-\delta}$	388.21	$LaMnO_{3-\delta}$	353.27
$MgMnO_{3-\delta}$	250.13	250.13	250.13		$MgMnO_{3-\delta}$	250.13						
$Sm_{0.125}La_{0.875}Fe_{0.5}Mn_{0.5}O_{3-\delta}$	251.41	251.41	251.41	yes	$SmFeO_{3-\delta}$	401.32	$LaFeO_{3-\delta}$	377.56	$SmMnO_{3-\delta}$	388.21	$LaMnO_{3-\delta}$	353.27
$BaMnO_{3-\delta}$	252.31	252.31	252.31		$BaMnO_{3-\delta}$	252.31						
$Sm_{0.125}La_{0.875}Fe_{0.25}Mn_{0.75}O_{3-\delta}$	256.80	256.80	256.80	yes	$SmFeO_{3-\delta}$	401.32	$LaFeO_{3-\delta}$	377.56	$SmMnO_{3-\delta}$	388.21	$LaMnO_{3-\delta}$	353.27
$Sm_{0.125}La_{0.875}Fe_{1}O_{3-\delta}$	258.54	258.54	258.54		$SmFeO_{3-\delta}$	401.32	$LaFeO_{3-\delta}$	377.56				
$EuMnO_{3-\delta}$	259.20	259.20	259.20		$EuMnO_{3-\delta}$	259.20						
$Sm_{0.125}La_{0.875}Fe_{0.125}Mn_{0.875}O_{3-\delta}$	260.34	260.34	260.34	yes	$SmFeO_{3-\delta}$	401.32	$LaFeO_{3-\delta}$	377.56	$SmMnO_{3-\delta}$	388.21	$LaMnO_{3-\delta}$	353.27
$Sm_{0.125}La_{0.875}MnO_{3-\delta}$	265.38	265.38	265.38		$SmMnO_{3-\delta}$	388.21	$LaMnO_{3-\delta}$	353.27				
$Na_{0.625}K_{0.375}Mo_{0.625}V_{0.375}O_{3-\delta}$	272.31	272.31	272.31	yes	$NaMoO_{3-\delta}$	319.41	$KMoO_{3-\delta}$	405.11	$NaVO_{3-\delta}$	287.56	$KVO_{3-\delta}$	374.19
$Ca_{0.375}Sr_{0.625}Ti_{0.625}Mn_{0.375}O_{3-\delta}$	285.80	285.80	285.80	yes	$CaTiO_{3-\delta}$	578.97	$SrTiO_{3-\delta}$	589.85	$CaMnO_{3-\delta}$	173.13	$SrMnO_{3-\delta}$	170.33
$NaVO_{3-\delta}$	287.56	287.56	287.56		$NaVO_{3-\delta}$	287.56						
$EuCrO_{3-\delta}$	289.00	289.00	289.00		$EuCrO_{3-\delta}$	289.00						
$Sm_{0.125}La_{0.875}Cr_{0.125}Fe_{0.875}O_{3-\delta}$	289.65	289.65	289.65	yes	$SmCrO_{3-\delta}$	415.04	$LaCrO_{3-\delta}$	570.86	$SmFeO_{3-\delta}$	401.32	$LaFeO_{3-\delta}$	377.56

Redox Material	ΔH_{DFT}	ΔH_{min}	ΔH_{max}	diff>30	EM 1	ΔH_{EM1}	EM 2	ΔH_{EM2}	EM 3	ΔH_{EM3}	EM 4	ΔH_{EM4}
$Na_{0.625}K_{0.375}Mo_{0.75}V_{0.25}O_{3-\delta}$	304.18	304.18	304.18	yes	$NaMoO_{3-\delta}$	319.41	$KMoO_{3-\delta}$	405.11	$NaVO_{3-\delta}$	287.56	$KVO_{3-\delta}$	374.19
$Ca_{0.125}Sr_{0.875}Ti_{0.625}Mn_{0.375}O_{3-\delta}$	304.86	304.86	304.86	yes	$CaTiO_{3-\delta}$	578.97	$SrTiO_{3-\delta}$	589.85	$CaMnO_{3-\delta}$	173.13	$SrMnO_{3-\delta}$	170.33
$Sr_{0.875}Ba_{0.125}Ti_{0.625}Mn_{0.375}O_{3-\delta}$	311.78	311.78	311.78	yes	$SrTiO_{3-\delta}$	589.85	$BaTiO_{3-\delta}$	588.75	$SrMnO_{3-\delta}$	170.33	$BaMnO_{3-\delta}$	252.31
$NaMoO_{3-\delta}$	319.41	319.41	319.41		$NaMoO_{3-\delta}$	319.41						
$Sm_{0.125}La_{0.875}Cr_{0.25}Fe_{0.75}O_{3-\delta}$	319.75	319.75	319.75	yes	$SmCrO_{3-\delta}$	415.04	$LaCrO_{3-\delta}$	570.86	$SmFeO_{3-\delta}$	401.32	$LaFeO_{3-\delta}$	377.56
$Sm_{0.25}La_{0.75}Cr_{0.375}Fe_{0.625}O_{3-\delta}$	325.74	325.74	325.74	yes	$SmCrO_{3-\delta}$	415.04	$LaCrO_{3-\delta}$	570.86	$SmFeO_{3-\delta}$	401.32	$LaFeO_{3-\delta}$	377.56
$Na_{0.625}K_{0.375}Mo_{0.875}V_{0.125}O_{3-\delta}$	342.40	286.42	350.40		$NaMoO_{3-\delta}$	319.41	$KMoO_{3-\delta}$	405.11	$NaVO_{3-\delta}$	287.56	$KVO_{3-\delta}$	374.19
$LaMnO_{3-\delta}$	353.27	353.27	353.27		$LaMnO_{3-\delta}$	353.27						
$Sm_{0.25}La_{0.75}Cr_{0.5}Fe_{0.5}O_{3-\delta}$	353.33	353.33	353.33	yes	$SmCrO_{3-\delta}$	415.04	$LaCrO_{3-\delta}$	570.86	$SmFeO_{3-\delta}$	401.32	$LaFeO_{3-\delta}$	377.56
$Na_{0.5}K_{0.5}MoO_{3-\delta}$	362.81	362.81	362.81		$NaMoO_{3-\delta}$	319.41	$KMoO_{3-\delta}$	405.11				
$KVO_{3-\delta}$	374.19	374.19	374.19		$KVO_{3-\delta}$	374.19						
$LaFeO_{3-\delta}$	377.56	377.56	377.56		$LaFeO_{3-\delta}$	377.56						
$EuVO_{3-\delta}$	381.81	381.81	381.81		$EuVO_{3-\delta}$	381.81						
$SmVO_{3-\delta}$	382.21	382.21	382.21		$SmVO_{3-\delta}$	382.21						
$SmMnO_{3-\delta}$	388.21	388.21	388.21		$SmMnO_{3-\delta}$	388.21						
$Sm_{0.25}La_{0.75}Cr_{0.625}Fe_{0.375}O_{3-\delta}$	390.31	390.31	390.31	yes	$SmCrO_{3-\delta}$	415.04	$LaCrO_{3-\delta}$	570.86	$SmFeO_{3-\delta}$	401.32	$LaFeO_{3-\delta}$	377.56
$Ca_{0.25}Sr_{0.75}Ti_{0.75}Mn_{0.25}O_{3-\delta}$	396.73	396.73	396.73	yes	$CaTiO_{3-\delta}$	578.97	$SrTiO_{3-\delta}$	589.85	$CaMnO_{3-\delta}$	173.13	$SrMnO_{3-\delta}$	170.33
$RbMoO_{3-\delta}$	398.52	398.52	398.52		$RbMoO_{3-\delta}$	398.52						
$SmFeO_{3-\delta}$	401.32	401.32	401.32		$SmFeO_{3-\delta}$	401.32						
$KMoO_{3-\delta}$	405.11	405.11	405.11		$KMoO_{3-\delta}$	405.11						
$Sr_{0.875}Ba_{0.125}Ti_{0.75}Mn_{0.25}O_{3-\delta}$	407.83	407.83	407.83	yes	$SrTiO_{3-\delta}$	589.85	$BaTiO_{3-\delta}$	588.75	$SrMnO_{3-\delta}$	170.33	$BaMnO_{3-\delta}$	252.31
$Sm_{0.375}La_{0.625}Cr_{0.75}Fe_{0.25}O_{3-\delta}$	408.22	408.22	408.22	yes	$SmCrO_{3-\delta}$	415.04	$LaCrO_{3-\delta}$	570.86	$SmFeO_{3-\delta}$	401.32	$LaFeO_{3-\delta}$	377.56
$SmCrO_{3-\delta}$	415.04	415.04	415.04		$SmCrO_{3-\delta}$	415.04						
$RbVO_{3-\delta}$	422.16	422.16	422.16		$RbVO_{3-\delta}$	422.16						

Redox Material	ΔH_{DFT}	ΔH_{min}	ΔH_{max}	diff>30	EM 1	ΔH_{EM1}	EM 2	ΔH_{EM2}	EM 3	ΔH_{EM3}	EM 4	ΔH_{EM4}
$Na_{0.5}K_{0.5}W_{0.125}Mo_{0.875}O_{3-\delta}$	423.65	423.65	423.65	yes	$NaWO_{3-\delta}$	434.58	$KWO_{3-\delta}$	508.05	$NaMoO_{3-\delta}$	319.41	$KMoO_{3-\delta}$	405.11
$Sm_{0.375}La_{0.625}Cr_{0.875}Fe_{0.125}O_{3-\delta}$	433.61	433.61	433.61	yes	$SmCrO_{3-\delta}$	415.04	$LaCrO_{3-\delta}$	570.86	$SmFeO_{3-\delta}$	401.32	$LaFeO_{3-\delta}$	377.56
$NaWO_{3-\delta}$	434.58	434.58	434.58		$NaWO_{3-\delta}$	434.58						
$Sm_{0.125}La_{0.875}VO_{3-\delta}$	455.88	455.88	455.88		*missing data for $LaVO_{3-\delta}$*							
$Na_{0.5}K_{0.5}W_{0.25}Mo_{0.75}O_{3-\delta}$	451.70	451.70	451.70	yes	$NaWO_{3-\delta}$	434.58	$KWO_{3-\delta}$	508.05	$NaMoO_{3-\delta}$	319.41	$KMoO_{3-\delta}$	405.11
$Sm_{0.375}La_{0.625}CrO_{3-\delta}$	455.88	455.88	455.88	yes	$SmCrO_{3-\delta}$	415.04	$LaCrO_{3-\delta}$	570.86	$SmCrO_{3-\delta}$	415.04	$SmCrO_{3-\delta}$	415.04
$Sm_{0.375}La_{0.625}V_{0.25}Cr_{0.75}O_{3-\delta}$	468.90	468.90	468.90		*missing data for $LaVO_{3-\delta}$*							
$Sm_{0.375}La_{0.625}V_{0.125}Cr_{0.875}O_{3-\delta}$	469.00	469.00	469.00		*missing data for $LaVO_{3-\delta}$*							
$Na_{0.5}K_{0.5}W_{0.375}Mo_{0.625}O_{3-\delta}$	486.14	486.14	486.14	yes	$NaWO_{3-\delta}$	434.58	$KWO_{3-\delta}$	508.05	$NaMoO_{3-\delta}$	319.41	$KMoO_{3-\delta}$	405.11
$Na_{0.5}K_{0.5}WO_{3-\delta}$	488.95	488.95	488.95		$NaWO_{3-\delta}$	434.58	$KWO_{3-\delta}$	508.05				
$Sm_{0.25}La_{0.75}V_{0.5}Cr_{0.5}O_{3-\delta}$	489.89	489.89	489.89		*missing data for $LaVO_{3-\delta}$*							
$Sm_{0.25}La_{0.75}V_{0.625}Cr_{0.375}O_{3-\delta}$	490.79	490.79	490.79		*missing data for $LaVO_{3-\delta}$*							
$Sm_{0.25}La_{0.75}V_{0.375}Cr_{0.625}O_{3-\delta}$	492.03	492.03	492.03		*missing data for $LaVO_{3-\delta}$*							
$Na_{0.375}K_{0.625}Nb_{0.5}W_{0.5}O_{3-\delta}$	494.87	494.87	494.87		*missing data for $NaNbO_{3-\delta}$*							
$Sr_{0.625}Ba_{0.375}Ti_{0.875}Mn_{0.125}O_{3-\delta}$	495.35	495.35	495.35	yes	$SrTiO_{3-\delta}$	589.85	$BaTiO_{3-\delta}$	588.75	$SrMnO_{3-\delta}$	170.33	$BaMnO_{3-\delta}$	252.31
$Na_{0.5}K_{0.5}Nb_{0.375}W_{0.625}O_{3-\delta}$	497.38	497.38	497.38		*missing data for $NaNbO_{3-\delta}$*							
$Ca_{0.125}Sr_{0.875}Ti_{0.875}Mn_{0.125}O_{3-\delta}$	497.69	497.69	497.69	yes	$CaTiO_{3-\delta}$	578.97	$SrTiO_{3-\delta}$	589.85	$CaMnO_{3-\delta}$	173.13	$SrMnO_{3-\delta}$	170.33
$Sr_{0.875}Ba_{0.125}Ti_{0.875}Mn_{0.125}O_{3-\delta}$	497.73	497.73	497.73	yes	$SrTiO_{3-\delta}$	589.85	$BaTiO_{3-\delta}$	588.75	$SrMnO_{3-\delta}$	170.33	$BaMnO_{3-\delta}$	252.31
$Na_{0.5}K_{0.5}Nb_{0.25}W_{0.75}O_{3-\delta}$	500.92	500.92	500.92		*missing data for $NaNbO_{3-\delta}$*							
$Na_{0.375}K_{0.625}Nb_{0.625}W_{0.375}O_{3-\delta}$	504.46	504.46	504.46		*missing data for $NaNbO_{3-\delta}$*							
$KWO_{3-\delta}$	508.05	508.05	508.05		$KWO_{3-\delta}$	508.05						
$Sm_{0.25}La_{0.75}V_{0.75}Cr_{0.25}O_{3-\delta}$	509.16	509.16	509.16		*missing data for $LaVO_{3-\delta}$*							
$Sm_{0.125}La_{0.875}V_{0.875}Cr_{0.125}O_{3-\delta}$	509.22	509.22	509.22		*missing data for $LaVO_{3-\delta}$*							
$Sm_{0.125}La_{0.875}Ti_{0.25}V_{0.75}O_{3-\delta}$	509.53	509.53	509.53		*missing data for $LaVO_{3-\delta}$*							

Redox Material	ΔH_{DFT}	ΔH_{min}	ΔH_{max}	diff>30	EM 1	ΔH_{EM1}	EM 2	ΔH_{EM2}	EM 3	ΔH_{EM3}	EM 4	ΔH_{EM4}
$Na_{0.375}K_{0.625}Nb_{0.75}W_{0.25}O_{3-\delta}$	510.96	510.96	510.96		*missing data for $NaNbO_{3-\delta}$*							
$Sm_{0.125}La_{0.875}Ti_{0.125}V_{0.875}O_{3-\delta}$	511.97	511.97	511.97		*missing data for $LaVO_{3-\delta}$*							
$Sm_{0.125}La_{0.875}Ti_{0.375}V_{0.625}O_{3-\delta}$	514.30	514.30	514.30		*missing data for $LaVO_{3-\delta}$*							
$RbWO_{3-\delta}$	517.61	517.61	517.61		$RbWO_{3-\delta}$	517.61						
$Na_{0.5}K_{0.5}W_{0.5}Mo_{0.5}O_{3-\delta}$	519.41	519.41	519.41	yes	$NaWO_{3-\delta}$	434.58	$KWO_{3-\delta}$	508.05	$NaMoO_{3-\delta}$	319.41	$KMoO_{3-\delta}$	405.11
$Na_{0.5}K_{0.5}W_{0.625}Mo_{0.375}O_{3-\delta}$	522.02	522.02	522.02	yes	$NaWO_{3-\delta}$	434.58	$KWO_{3-\delta}$	508.05	$NaMoO_{3-\delta}$	319.41	$KMoO_{3-\delta}$	405.11
$Na_{0.5}K_{0.5}W_{0.75}Mo_{0.25}O_{3-\delta}$	522.72	522.72	522.72	yes	$NaWO_{3-\delta}$	434.58	$KWO_{3-\delta}$	508.05	$NaMoO_{3-\delta}$	319.41	$KMoO_{3-\delta}$	405.11
$Na_{0.375}K_{0.625}Nb_{0.875}W_{0.125}O_{3-\delta}$	523.02	523.02	523.02		*missing data for $NaNbO_{3-\delta}$*							
$Na_{0.5}K_{0.5}Nb_{0.125}W_{0.875}O_{3-\delta}$	524.84	524.84	524.84		*missing data for $NaNbO_{3-\delta}$*							
$Na_{0.5}K_{0.5}W_{0.875}Mo_{0.125}O_{3-\delta}$	526.37	526.37	526.37	yes	$NaWO_{3-\delta}$	434.58	$KWO_{3-\delta}$	508.05	$NaMoO_{3-\delta}$	319.41	$KMoO_{3-\delta}$	405.11
$Na_{0.375}K_{0.625}NbO_{3-\delta}$	529.59	529.59	529.59		*missing data for $NaNbO_{3-\delta}$*							
$Na_{0.375}K_{0.625}Ta_{0.125}Nb_{0.875}O_{3-\delta}$	538.93	538.93	538.93		*missing data for $NaNbO_{3-\delta}$*							
$Na_{0.375}K_{0.625}Ta_{0.25}Nb_{0.75}O_{3-\delta}$	548.04	548.04	548.04		*missing data for $NaNbO_{3-\delta}$*							
$Na_{0.375}K_{0.625}Ta_{0.375}Nb_{0.625}O_{3-\delta}$	558.23	558.23	558.23		*missing data for $NaNbO_{3-\delta}$*							
$Na_{0.375}K_{0.625}Ta_{0.5}Nb_{0.5}O_{3-\delta}$	567.34	567.34	567.34		*missing data for $NaNbO_{3-\delta}$*							
$LaCrO_{3-\delta}$	570.86	570.86	570.86		$LaCrO_{3-\delta}$	570.86						
$CaTiO_{3-\delta}$	578.97	578.97	578.97		$CaTiO_{3-\delta}$	578.97						
$Ca_{0.125}Sr_{0.875}TiO_{3-\delta}$	584.67	584.67	584.67		$CaTiO_{3-\delta}$	578.97	$SrTiO_{3-\delta}$	589.85				
$Na_{0.375}K_{0.625}Ta_{0.625}Nb_{0.375}O_{3-\delta}$	585.41	585.41	585.41		*missing data for $NaNbO_{3-\delta}$*							
$EuTiO_{3-\delta}$	586.90	586.90	586.90		$EuTiO_{3-\delta}$	586.90						
$BaTiO_{3-\delta}$	588.75	588.75	588.75		$BaTiO_{3-\delta}$	588.75						
$Sr_{0.625}Ba_{0.375}TiO_{3-\delta}$	589.22	589.22	589.22		$SrTiO_{3-\delta}$	589.85	$BaTiO_{3-\delta}$	588.75				
$Sr_{0.875}Ba_{0.125}TiO_{3-\delta}$	589.44	589.44	589.44		$SrTiO_{3-\delta}$	589.85	$BaTiO_{3-\delta}$	588.75				
$SrTiO_{3-\delta}$	589.85	589.85	589.85		$SrTiO_{3-\delta}$	589.85						

Redox Material	ΔH_{DFT}	ΔH_{min}	ΔH_{max}	diff>30	EM 1	ΔH_{EM1}	EM 2	ΔH_{EM2}	EM 3	ΔH_{EM3}	EM 4	ΔH_{EM4}
$KNbO_{3-\delta}$	594.00	594.00	594.00		$KNbO_{3-\delta}$	594.00						
$Na_{0.375}K_{0.625}Ta_{0.75}Nb_{0.25}O_{3-\delta}$	606.41	606.41	606.41		*missing data for $NaNbO_{3-\delta}$*							
$RbNbO_{3-\delta}$	624.20	624.20	624.20		$RbNbO_{3-\delta}$	624.20						
$Na_{0.375}K_{0.625}Ta_{0.875}Nb_{0.125}O_{3-\delta}$	625.94	625.94	625.94		*missing data for $NaNbO_{3-\delta}$*							
$LaTiO_{3-\delta}$	633.41	633.41	633.41		$LaTiO_{3-\delta}$	633.41						
$NaTaO_{3-\delta}$	646.24	646.24	646.24		$NaTaO_{3-\delta}$	646.24						
$SmTiO_{3-\delta}$	654.10	654.10	654.10		$SmTiO_{3-\delta}$	654.10						
$KTaO_{3-\delta}$	660.41	660.41	660.41		$KTaO_{3-\delta}$	660.41						
$MgTiO_{3-\delta}$	696.82	696.82	696.82		$MgTiO_{3-\delta}$	696.82						
$RbTaO_{3-\delta}$	705.99	705.99	705.99		$RbTaO_{3-\delta}$	705.99						

3. Empirical model to fit experimental data

As discussed in the main manuscript, we use the concept of limiting values for the minimum and maximum redox enthalpies to model the redox enthalpy of solid solutions. The minimum redox enthalpy represents the sub-lattice with more reducible species, whereas the upper limiting enthalpy value represents the species which are reduced less readily. To model the transition behavior, we empirically found that arctangent functions can be used to fit the data accurately. Similarly, an arctangent can be used to simulate two individual sub-lattices in terms of their entropic contributions in the solid solution. In the following, the equations used to fit this data are presented.

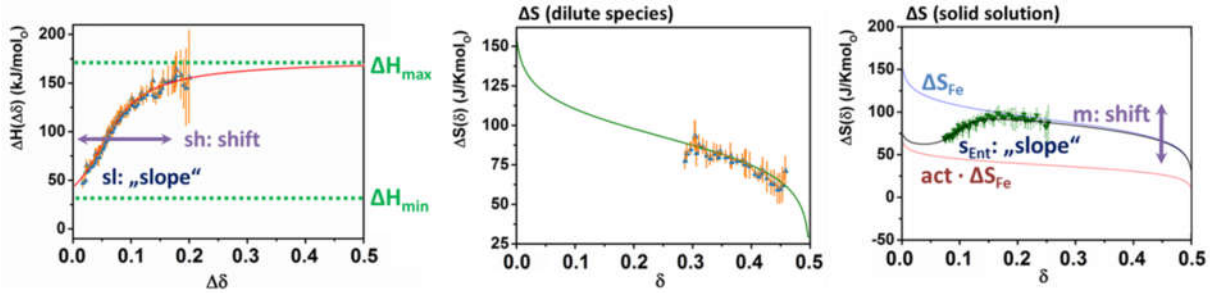

Figure S1. Empirical fits used for the experimental data. Left: Arctangent fit of ΔH data for perovskite solid solutions, defined by a minimum and maximum redox enthalpy and a transition area with slope s and shift h. Middle: Dilute species fit for ΔS of perovskites with only one species at the M site and Ti-Mn solid solutions, after Bulfin et. al. [1] Right: ΔS fit for Mn-Fe and Fe-Co solid solutions, composed of the entropy fit for $SrFeO_{3-\delta}$ obtained via the solid solution model, which is multiplied by the content in active species act to accurately represent the lower enthalpy for low values of δ, featuring a transition area with slope s_{Ent} and a shift in y direction $|m| < 15$ J/Kmol^{-1}. The reference non-stoichiometry δ_o can be obtained from the entropy fits to convert $\Delta\delta$ into the absolute δ according to $\Delta\delta = \delta - \delta_0$.

We call the limiting values for the redox enthalpy change ΔH_{min} and ΔH_{max}. $\Delta H(\Delta\delta)$ can be described using an arctangent function (see Fig. S1):

$$\Delta H(\Delta\delta) = \frac{\Delta H_{max} - \Delta H_{min}}{\pi} \cdot \left(\tan^{-1}\left((\Delta\delta - sh) \cdot sl\right) + \frac{\pi}{2}\right) + \Delta H_{min} \qquad \text{(S1)}$$

The variables sh and sl describe the transition between these extreme points, with sh referring to the shift of the transition point in δ direction, whereas sl describes the steepness or slope of the shift. That means that the transition is gradual for low values of sl, whereas in the extreme case of $sl \to \infty$, $\Delta H(\Delta\delta)$ turns into a step function with ΔH_{max} and dH_{min} as the only values. Eq. S1 can be fit using experimental data with ΔH_{max}, ΔH_{min}, sh, and sl as fit parameters. This purely empirical fit works very well for the 24 materials included in this work, but there are some important limitations. Firstly, the fit may reach unrealistic values when $\Delta\delta$ deviates strongly from the experimental data range. This happens especially if not the entire transition from dH_{min} to ΔH_{max} is covered experimentally. Therefore, it is important to consider the limited validity of the fit for data extrapolated far beyond the measured data range. Secondly, it is also possible to apply the fit for cases with only one species on the M site, however it results in rather small differences between ΔH_{min} and ΔH_{max}, which

are more related to temperature effects than the actual dependence of ΔH on $\Delta\delta$. For these two reasons, the parameter $\Delta H_{\min}$ is fixed for two cases with only one M species in order to stabilize the fit ($SrFeO_{3-\delta}$ and $Ca_{0.29}Sr_{0.71}FeO_{3-\delta}$). A constant redox enthalpy can also be used in these cases without introducing a large error.

As a first approximation, the entropy data can be fit using a dilute species model, as described by Bulfin et. al. (see Fig. S1): [1]

$$\Delta S(\delta) = \frac{1}{2}\cdot S_{O_2} + \Delta s_{\text{vib}} + 2\cdot a\cdot R\cdot\left(\ln\left(\frac{1}{2}-\delta\right) - \ln(\delta)\right) \qquad \text{(S2)}$$

With $\Delta\delta = \delta - \delta_0$, where δ_0 refers to the reference point at T = 400 °C and p_{O_2} = 0.18 bar, Eq. S2 is converted to yield the entropy change as a function of the relative change in the measured non-stoichiometry $\Delta\delta$ (see Fig. S1):

$$\Delta S(\Delta\delta) = \frac{1}{2}\cdot S_{O_2} + \Delta s_{vib} + 2\cdot a\cdot R\cdot\ln\left(\left(\frac{1}{2}-(\Delta\delta+\delta_0)\right) - ln\,(\Delta\delta+\delta_0)\right) \qquad \text{(S3)}$$

The resulting expression describes the change in entropy of non-stoichiometric redox reactions as the sum of the partial molar entropy of oxygen S_{O_2}, the vibrational entropy change Δs_{vib}, and the change in configurational entropy. R is the ideal gas constant, and a is a factor referring to the interaction of defects with a = 2 describing an ideal solid solution with no defect interaction. [1] The partial molar entropy of oxygen as a function of the temperature can be calculated using the Shomate equation and the NIST-JANAF thermochemical tables, [2] and it needs to be multiplied by the factor ½ to obtain the entropy change per mole of monatomic oxygen. For calculating S_{O_2}, the average temperature of the equilibrium TGA data points is used. The parameters Δs_{vib}, δ_0, and a are fit using the experimental data. To stabilize the fit, δ_0 is fixed by setting $\delta_0 = 0$ for all solid solutions containing only Mn and/or Ti, as no significant non-stoichiometry is expected at the reference point with T = 400 °C and p_{O_2} = 0.18 bar. [3, 4] This is necessary, as the $\Delta\delta$ range covered experimentally for Ti-Mn solid solutions is rather small. Using the δ_0 values for each material, $\Delta H(\Delta\delta)$ and $\Delta S(\Delta\delta)$ can be converted to functions of the absolute non-stoichiometry δ, yielding $\Delta H(\delta)$ and $\Delta S(\delta)$, respectively. Hence, a value for δ_0, i.e., δ at the reference point, is obtained from the entropy data only. While this approach performs well in the case of $SrFeO_{3-\delta}$ with a resulting value of δ_0 = 0.237 which is in very good agreement to literature data (see Fig. 1 in Takeda *et. al.* [5]), the results for other phases is not guaranteed.

For solid solutions, the model is adapted to allow for preferential reduction of one of the two species such that the entropy change is significantly reduced for low values of δ. We use the entropy change of $SrFeO_{3-\delta}$ denoted by ΔS_{Fe} as a reference, and an arctangent fit similar to Eq. S1 (see Fig. S1) to build an empirical function describing the entropy change based on ΔS_{Fe}:

$$\Delta S(\delta) = \underbrace{\frac{act\cdot\Delta S_{\text{Fe}}(\delta+\delta_0)}{\pi}}_{\text{active species}}\cdot\underbrace{\left(\tan^{-1}\left[(\delta-\delta_0)\cdot s_{\text{Ent}}\right]+\frac{\pi}{2}\right)}_{\text{transition}} + \underbrace{(1-act)\cdot\Delta S_{\text{Fe}}(\delta+\delta_0)}_{\text{less active species}} + \underbrace{m}_{\text{corr.}} \qquad \text{(S4)}$$

The material specific constant act refers to the content of the more redox active species in the solid solution (lower ΔH), i.e. $act = 0.4$ in $SrMn_{0.6}Fe_{0.4}O_{3-\delta}$. The upper limit of this function is the entropy of $SrFeO_{3-\delta}$, whereas its lower limit is the fraction of this entropy $act \cdot \Delta S_{\mathrm{Fe}}$, signifying that in $SrMn_{0.6}Fe_{0.4}O_{3-\delta}$, only the "$Sr_{0.4}Fe_{0.4}O_{1.2}$" sub-lattice is initially reduced, resulting in correspondingly lower the entropy change. The fit variable s_{Ent} refers to the "slope" of the transition, whereas δ_0 refers to the non-stoichiometry at the reference point with T = 400 °C and p_{O_2}= 0.18 bar. The variable m with $|m| < 15$ $JK^{-1}mol^{-1}$ refers to a shift in the y direction, accounting for slight changes in Δs_{vib} for different perovskite materials. If the condition $|m| < 15$ $J/Kmol^{-1}$ cannot be fulfilled, the fit is repeated with a fixed m = 0 to exclude any unphysical solutions. Despite the simplifying assumption that all perovskite redox materials act very similar to $SrFeO_{3-\delta}$ and the entropy change of any perovskite solid solution can be composed as a sum of two $SrFeO_{3-\delta}$ sub-lattices plus a constant shift in y direction, this expression performs very well for the Mn-Fe and Fe-Co solid solutions studied here. For Ti-Mn solid solutions and phases with only one species on the *M* site, the dilute species model according to Eq. S3 and S4 is employed instead. While Eq. S3 works well for an empirical representation of the ΔS values for Ti-Mn solid solutions, the physical meaning of the resulting a and s_{vib} values is doubtful due to the low $\Delta\delta$ range of experimental data. Again, it is crucial to point out that this is an empirical fit with the objective of accurately modelling our experimental data in the measured non-stoichiometry range, without requiring large generic polynomials with limited physical meaning. Using this approach, it is possible to interpolate accurately between the measured data points, and extrapolate in a small range beyond. We emphasize that the main objective of this fit is to interpolate between the measured data points in order to get an analytical function of $\Delta H(\delta)$ and $\Delta S(\delta)$ to plot isographs, and extrapolations based on these functions should always be regarded critically. Also, as previously mentioned, the δ_0 value may be inaccurate, which means that the change in non-stoichiometry $\Delta\delta$ is described accurately, but the absolute non-stoichiometry values δ may be imprecise.

4. Experimentally screened perovskites and fit parameters for thermodynamic data

The synthesized materials subjected to thermogravimetric analysis are listed in the following tables. Redox enthalpy and entropy changes have been determined using the van't Hoff method, and the data has been fit using the models described in the manuscript.
δ_0 values at the reference point T = 400 °C and p_{O_2} = 0.18 bar have been determined using the entropy fit. The data range covered experimentally is given as δ_{exp} min and δ_{exp} max. Extrapolations outside this data range are possible using the fit functions, but the accuracy decreases significantly with increasing extent of extrapolation. The resulting fit parameters are not always physically meaningful (for example: very high values for minimum and maximum enthalpies), but the fits can nevertheless be used for an accurate representation of ΔH and ΔS within the boundaries of δ_{exp} min and δ_{exp} max. Extrapolated values beyond these boundaries may be highly inaccurate.

Table S 3. Perovskites studied within the experimental materials screening.

Composition	δ_{exp} min	δ_{exp} max	δ_0 (from entropy fit[1])	tolerance factor (δ = 0)	molar_mass (δ = 0), g/mol
$Ca_{0.15}Sr_{0.85}Mn_{0.2}Fe_{0.8}O_{3-\delta}$	0.1080	0.2450	0.0690	1.006	184.1505
$Ca_{0.30}Sr_{0.70}Mn_{0.4}Fe_{0.6}O_{3-\delta}$	0.1103	0.2153	0.0973	1.006	176.8378
$Ca_{0.45}Sr_{0.55}Mn_{0.6}Fe_{0.4}O_{3-\delta}$	0.1316	0.3116	0.1056	1.006	169.5251
$Ca_{0.60}Sr_{0.40}Mn_{0.8}Fe_{0.2}O_{3-\delta}$	0.0768	0.3038	0.0638	1.006	162.2124
$Ca_{0.75}Sr_{0.25}MnO_{3-\delta}$	0.0130	0.2780	0	1.006	154.8997
$Ca_{0.54}Sr_{0.46}Ti_{0.2}Mn_{0.8}O_{3-\delta}$	0.0050	0.1870	0	1.006	163.4694
$Ca_{0.34}Sr_{0.66}Ti_{0.4}Mn_{0.6}O_{3-\delta}$	0.0150	0.1690	0	1.006	171.5635
$Ca_{0.13}Sr_{0.87}Ti_{0.6}Mn_{0.4}O_{3-\delta}$	0.0050	0.0920	0	1.006	180.1332
$SrFeO_{3-\delta}$	0.2885	0.4575	0.2365	1.006	191.4632
$Ca_{0.87}Sr_{0.13}Mn_{0.8}Fe_{0.2}O_{3-\delta}$	0.0720	0.3000	0.0520	0.995	149.3761
$Ca_{0.73}Sr_{0.27}Mn_{0.6}Fe_{0.4}O_{3-\delta}$	0.1337	0.1787	0.1247	0.995	156.2134
$Ca_{0.58}Sr_{0.42}Mn_{0.4}Fe_{0.6}O_{3-\delta}$	0.1034	0.1694	0.0894	0.995	163.5261
$Ca_{0.44}Sr_{0.56}Mn_{0.2}Fe_{0.8}O_{3-\delta}$	0.0971	0.1871	0.0761	0.995	170.3633
$Ca_{0.29}Sr_{0.71}FeO_{3-\delta}$	0.3026	0.4976	0.2606	0.995	177.6760
$Ca_{0.92}Sr_{0.08}Ti_{0.1}Mn_{0.9}O_{3-\delta}$	0.0070	0.2220	0	0.995	146.1105
$Ca_{0.82}Sr_{0.18}Ti_{0.2}Mn_{0.8}O_{3-\delta}$	0.0270	0.2420	0	0.995	150.1576
$Ca_{0.62}Sr_{0.38}Ti_{0.4}Mn_{0.6}O_{3-\delta}$	0.0120	0.1790	0	0.995	158.2518
$Ca_{0.42}Sr_{0.58}Ti_{0.6}Mn_{0.4}O_{3-\delta}$	0.0060	0.1000	0	0.995	166.3460
$Ca_{0.07}Sr_{0.93}Fe_{0.9}Co_{0.1}O_{3-\delta}$	0.3285	0.3655	0.3215	1.006	188.4441
$Ca_{0.30}Sr_{0.70}Fe_{0.6}Co_{0.4}O_{3-\delta}$	0.4580	0.4990	0.4530	1.006	178.4359
$Ca_{0.64}Sr_{0.36}Ti_{0.1}Mn_{0.9}O_{3-\delta}$	0.0060	0.1560	0	1.006	159.4223
$Ca_{0.21}Sr_{0.79}Mn_{0.6}Fe_{0.4}O_{3-\delta}$	0.0859	0.2659	0.0639	1.015	180.9352
$Ca_{0.51}Sr_{0.49}MnO_{3-\delta}$	0.0070	0.1860	0	1.015	166.3098
$Ca_{0.1}Sr_{0.9}Ti_{0.4}Mn_{0.6}O_{3-\delta}$	0.0110	0.1590	0	1.015	182.9736

[1] Set to zero for the Ti-Mn system due to negligible non-stoichiometry at 400 °C and p_{O_2} = 0.18 bar.

Table S 4. Enthalpy fit data for experimentally studied perovskites. Please refer to the main manuscript for an explanation of the fit functions and parameters.

Composition	dH_{max}	dH_{min}	sh	sl
$Ca_{0.15}Sr_{0.85}Mn_{0.2}Fe_{0.8}O_{3-\delta}$	24437.739	28.844	0.254	1772.649
$Ca_{0.30}Sr_{0.70}Mn_{0.4}Fe_{0.6}O_{3-\delta}$	20364.640	-20.095	0.200	602.646
$Ca_{0.45}Sr_{0.55}Mn_{0.6}Fe_{0.4}O_{3-\delta}$	202.021	-28183.726	-0.081	570.238
$Ca_{0.60}Sr_{0.40}Mn_{0.8}Fe_{0.2}O_{3-\delta}$	182.060	-28025.380	-0.114	652.266
$Ca_{0.75}Sr_{0.25}MnO_{3-\delta}$	199.639	115.776	0.265	15.148
$Ca_{0.54}Sr_{0.46}Ti_{0.2}Mn_{0.8}O_{3-\delta}$	173.523	-54594.202	-0.044	4652.384
$Ca_{0.34}Sr_{0.66}Ti_{0.4}Mn_{0.6}O_{3-\delta}$	190.733	141.082	0.063	35.227
$Ca_{0.13}Sr_{0.87}Ti_{0.6}Mn_{0.4}O_{3-\delta}$	199.827	-27222.407	-0.001	16954.431
$SrFeO_{3-\delta}$	87.441	63[2]	0.059	59.791
$Ca_{0.87}Sr_{0.13}Mn_{0.8}Fe_{0.2}O_{3-\delta}$	165.294	-17.616	0.020	33.042
$Ca_{0.73}Sr_{0.27}Mn_{0.6}Fe_{0.4}O_{3-\delta}$	144.528	-15054.692	-0.041	923.677
$Ca_{0.58}Sr_{0.42}Mn_{0.4}Fe_{0.6}O_{3-\delta}$	20685.743	-23.961	0.180	608.545
$Ca_{0.44}Sr_{0.56}Mn_{0.2}Fe_{0.8}O_{3-\delta}$	16532.294	25.542	0.206	998.139
$Ca_{0.29}Sr_{0.71}FeO_{3-\delta}$	32.521	22[†]	0.236	-293.341
$Ca_{0.92}Sr_{0.08}Ti_{0.1}Mn_{0.9}O_{3-\delta}$	166.550	108.510	0.019	373.552
$Ca_{0.82}Sr_{0.18}Ti_{0.2}Mn_{0.8}O_{3-\delta}$	304.780	-5753.333	-0.810	15.512
$Ca_{0.62}Sr_{0.38}Ti_{0.4}Mn_{0.6}O_{3-\delta}$	192.346	127.418	0.052	28.245
$Ca_{0.42}Sr_{0.58}Ti_{0.6}Mn_{0.4}O_{3-\delta}$	187.580	157.200	0.025	159.677
$Ca_{0.07}Sr_{0.93}Fe_{0.9}Co_{0.1}O_{3-\delta}$	74.133	-3273.552	-0.029	1281.024
$Ca_{0.30}Sr_{0.70}Fe_{0.6}Co_{0.4}O_{3-\delta}$	20.160	36.458	0.042	67702721.650
$Ca_{0.64}Sr_{0.36}Ti_{0.1}Mn_{0.9}O_{3-\delta}$	154.802	-234.439	0.001	174.027
$Ca_{0.21}Sr_{0.79}Mn_{0.6}Fe_{0.4}O_{3-\delta}$	171.225	-0.227	0.054	18.865
$Ca_{0.51}Sr_{0.49}MnO_{3-\delta}$	120.923	84.016	0.025	408.041
$Ca_{0.1}Sr_{0.9}Ti_{0.4}Mn_{0.6}O_{3-\delta}$	183.499	119.442	0.051	25.155

[2] dH_{min} fixed manually to stabilize the fit (see previous section of the supplementary information).

Table S 5. Entropy fit data for experimentally studied perovskites. Please refer to the main manuscript for an explanation of the fit functions and parameters.

Composition	Fit type	Δs_{vib}	a	s_{Ent}	m
$Ca_{0.15}Sr_{0.85}M_{n0.2}Fe_{0.8}O_{3-\delta}$	Solid Solution			3.2817	-13.8547
$Ca_{0.30}Sr_{0.70}Mn_{0.4}Fe_{0.6}O_{3-\delta}$	Solid Solution			31.0522	-6.7730
$Ca_{0.45}Sr_{0.55}Mn_{0.6}Fe_{0.4}O_{3-\delta}$	Solid Solution			41.5771	0
$Ca_{0.60}Sr_{0.40}Mn_{0.8}Fe_{0.2}O_{3-\delta}$	Solid Solution			76.0299	-12.8393
$Ca_{0.75}Sr_{0.25}MnO_{3-\delta}$	Dilute Species	-40.6063	0.4639		
$Ca_{0.54}Sr_{0.46}Ti_{0.2}Mn_{0.8}O_{3-\delta}$	Dilute Species	-26.2111	0.0125		
$Ca_{0.34}Sr_{0.66}Ti_{0.4}Mn_{0.6}O_{3-\delta}$	Dilute Species	-22.7249	0.2425		
$Ca_{0.13}Sr_{0.87}Ti_{0.6}Mn_{0.4}O_{3-\delta}$	Dilute Species	-8.4690	-0.0239		
$SrFeO_{3-\delta}$	Dilute Species	-28.0530	0.7567		
$Ca_{0.87}Sr_{0.13}Mn_{0.8}Fe_{0.2}O_{3-\delta}$	Solid Solution			319.9609	4.2984
$Ca_{0.73}Sr_{0.27}Mn_{0.6}Fe_{0.4}O_{3-\delta}$	Solid Solution			20.6839	0
$Ca_{0.58}Sr_{0.42}Mn_{0.4}Fe_{0.6}O_{3-\delta}$	Solid Solution			42.0604	0.9554
$Ca_{0.44}Sr_{0.56}Mn_{0.2}Fe_{0.8}O_{3-\delta}$	Solid Solution			1.6029	0.0000
$Ca_{0.29}Sr_{0.71}FeO_{3-\delta}$	Dilute Species	-79.3352	0.4334		
$Ca_{0.92}Sr_{0.08}Ti_{0.1}Mn_{0.9}O_{3-\delta}$	Dilute Species	-23.8004	0.6589		
$Ca_{0.82}Sr_{0.18}Ti_{0.2}Mn_{0.8}O_{3-\delta}$	Dilute Species	-24.9649	0.5865		
$Ca_{0.62}Sr_{0.38}Ti_{0.4}Mn_{0.6}O_{3-\delta}$	Dilute Species	-18.8441	0.1458		
$Ca_{0.42}Sr_{0.58}Ti_{0.6}Mn_{0.4}O_{3-\delta}$	Dilute Species	-27.7482	0.4430		
$Ca_{0.07}Sr_{0.93}Fe_{0.9}Co_{0.1}O_{3-\delta}$	Solid Solution			3748206.6430	0
$Ca_{0.30}Sr_{0.70}Fe_{0.6}Co_{0.4}O_{3-\delta}$	Solid Solution			21423185.5100	12.0446
$Ca_{0.64}Sr_{0.36}Ti_{0.1}Mn_{0.9}O_{3-\delta}$	Dilute Species	-7.6069	-0.3305		
$Ca_{0.21}Sr_{0.79}Mn_{0.6}Fe_{0.4}O_{3-\delta}$	Solid Solution			78.3719	-8.2539
$Ca_{0.51}Sr_{0.49}MnO_{3-\delta}$	Dilute Species	-51.1221	0.6084		
$Ca_{0.1}Sr_{0.9}Ti_{0.4}Mn_{0.6}O_{3-\delta}$	Dilute Species	-30.5018	0.1362		

Table S 6. Assignment of experimentally studied perovskite compositions to the sample numbers used within the *RedoxThermoCSP* code, the tolerance factors $\boldsymbol{t}$ of the experimentally studied phases for $\boldsymbol{\delta}$ = 0, and the composition of the corresponding phases in the DFT study.

Composition (exp)	Sample number	*t*	Composition (theo)
$Ca_{0.15}Sr_{0.85}Mn_{0.2}Fe_{0.8}O_{3-\delta}$	75	1.006	$Ca_{0.125}Sr_{0.875}Mn_{0.25}Fe_{0.75}O_{3-\delta}$
$Ca_{0.30}Sr_{0.70}Mn_{0.4}Fe_{0.6}O_{3-\delta}$	76	1.006	$Ca_{0.25}Sr_{0.75}Mn_{0.375}Fe_{0.625}O_{3-\delta}$
$Ca_{0.45}Sr_{0.55}Mn_{0.6}Fe_{0.4}O_{3-\delta}$	77	1.006	$Ca_{0.5}Sr_{0.5}Mn_{0.625}Fe_{0.375}O_{3-\delta}$
$Ca_{0.60}Sr_{0.40}Mn_{0.8}Fe_{0.2}O_{3-\delta}$	78	1.006	$Ca_{0.625}Sr_{0.375}Mn_{0.875}Fe_{0.125}O_{3-\delta}$
$Ca_{0.75}Sr_{0.25}MnO_{3-\delta}$	79	1.006	$Ca_{0.75}Sr_{0.25}MnO_{3-\delta}$
$Ca_{0.54}Sr_{0.46}Ti_{0.2}Mn_{0.8}O_{3-\delta}$	93	1.006	$Ca_{0.5}Sr_{0.5}Ti_{0.25}Mn_{0.75}O_{3-\delta}$
$Ca_{0.34}Sr_{0.66}Ti_{0.4}Mn_{0.6}O_{3-\delta}$	94	1.006	$Ca_{0.25}Sr_{0.75}Ti_{0.5}Mn_{0.5}O_{3-\delta}$
$Ca_{0.13}Sr_{0.87}Ti_{0.6}Mn_{0.4}O_{3-\delta}$	95	1.006	$Ca_{0.125}Sr_{0.875}Ti_{0.625}Mn_{0.375}O_{3-\delta}$
$SrFeO_{3-\delta}$	100	1.006	$SrFeO_{3-\delta}$
$Ca_{0.87}Sr_{0.13}Mn_{0.8}Fe_{0.2}O_{3-\delta}$	106	0.995	$Ca_{0.875}Sr_{0.125}Mn_{0.75}Fe_{0.25}O_{3-\delta}$
$Ca_{0.73}Sr_{0.27}Mn_{0.6}Fe_{0.4}O_{3-\delta}$	107	0.995	$Ca_{0.75}Sr_{0.25}Mn_{0.625}Fe_{0.375}O_{3-\delta}$
$Ca_{0.58}Sr_{0.42}Mn_{0.4}Fe_{0.6}O_{3-\delta}$	108	0.995	$Ca_{0.625}Sr_{0.375}Mn_{0.375}Fe_{0.625}O_{3-\delta}$
$Ca_{0.44}Sr_{0.56}Mn_{0.2}Fe_{0.8}O_{3-\delta}$	109	0.995	$Ca_{0.5}Sr_{0.5}Mn_{0.25}Fe_{0.75}O_{3-\delta}$
$Ca_{0.29}Sr_{0.71}FeO_{3-\delta}$	110	0.995	$Ca_{0.25}Sr_{0.75}FeO_{3-\delta}$
$Ca_{0.92}Sr_{0.08}Ti_{0.1}Mn_{0.9}O_{3-\delta}$	111	0.995	$Ca_{0.875}Sr_{0.125}Ti_{0.125}Mn_{0.875}O_{3-\delta}$
$Ca_{0.82}Sr_{0.18}Ti_{0.2}Mn_{0.8}O_{3-\delta}$	112	0.995	$Ca_{0.75}Sr_{0.25}Ti_{0.25}Mn_{0.75}O_{3-\delta}$
$Ca_{0.62}Sr_{0.38}Ti_{0.4}Mn_{0.6}O_{3-\delta}$	113	0.995	$Ca_{0.625}Sr_{0.375}Ti_{0.375}Mn_{0.625}O_{3-\delta}$
$Ca_{0.42}Sr_{0.58}Ti_{0.6}Mn_{0.4}O_{3-\delta}$	114	0.995	$Ca_{0.375}Sr_{0.625}Ti_{0.625}Mn_{0.375}O_{3-\delta}$
$Ca_{0.07}Sr_{0.93}Fe_{0.9}Co_{0.1}O_{3-\delta}$	116	1.006	$SrFe_{0.875}Co_{0.125}O_{3-\delta}$
$Ca_{0.30}Sr_{0.70}Fe_{0.6}Co_{0.4}O_{3-\delta}$	118	1.006	$Ca_{0.25}Sr_{0.75}Fe_{0.625}Co_{0.375}O_{3-\delta}$
$Ca_{0.64}Sr_{0.36}Ti_{0.1}Mn_{0.9}O_{3-\delta}$	122	1.006	$Ca_{0.625}Sr_{0.375}Ti_{0.125}Mn_{0.875}O_{3-\delta}$
$Ca_{0.21}Sr_{0.79}Mn_{0.6}Fe_{0.4}O_{3-\delta}$	128	1.015	$Ca_{0.25}Sr_{0.75}Mn_{0.625}Fe_{0.375}O_{3-\delta}$
$Ca_{0.51}Sr_{0.49}MnO_{3-\delta}$	129	1.015	$Sr_{0.5}Ca_{0.5}MnO_{3-\delta}$
$Ca_{0.1}Sr_{0.9}Ti_{0.4}Mn_{0.6}O_{3-\delta}$	130	1.015	$Ca_{0.125}Sr_{0.875}Ti_{0.375}Mn_{0.625}O_{3-\delta}$

5. Theoretical model for the redox thermodynamics

In the following we establish a model for the reduction process and determine $\Delta H(\delta, T)$. The total non-stoichiometry as a function of the temperature T and the oxygen partial pressure p_{O_2} in an ideal solid solution of two perovskites is the sum of the non-stochiometries induced in both individual sub-lattices. The non-stoichiometry in one sub-lattice δ_n is given by: [1]

$$\delta_{\mathrm{n}}(T, p_{\mathrm{O}_2}, \Delta H_{\mathrm{n}}) = \frac{\delta_{max,n} \cdot exp\left(\frac{1}{2} \cdot \frac{S_{0,\mathrm{O}_2}(T)}{R} \cdot \delta_{\mathrm{max,n}}\right) \cdot p_{O_2}^{\left(-\frac{1}{2}\delta_{\mathrm{max,n}}\right)} \cdot exp\left(-\Delta H_{\mathrm{n}} \cdot \frac{\delta_{\mathrm{max,n}}}{RT}\right)}{1 + exp\left(\frac{1}{2} \cdot \frac{S_{0,O_2}(T)}{R} \cdot \delta_{\mathrm{max,n}}\right) \cdot p_{\mathrm{O}_2}^{\left(-\frac{1}{2}\delta_{\mathrm{max,n}}\right)} \cdot exp\left(-\Delta H_{\mathrm{n}} \cdot \frac{\delta_{\mathrm{max,n}}}{RT}\right)} \tag{S5}$$

with $\delta_{\mathrm{max},1} = \mathrm{act}/2$, $\delta_{\mathrm{max},2} = (1 - act)/2$, $\Delta H_1 = \Delta H_{\mathrm{min,corr}}$, $\Delta H_2 = \Delta H_{\mathrm{max,corr}}$, $\delta_1 \geq \delta_2$, the ideal gas constant R, and the partial molar entropy of oxygen as a function of temperature $\mathrm{S}_{0,\mathrm{O}_2}(T)$. For a given set of T and δ, the oxygen partial pressure p_{O_2} can be calculated by finding where the sum of the oxygen vacancies induced in both sub-lattices (each described by Eq. S5) is equal to the actual value δ through finding zero points:

$$0 = \delta_1\left(T, p_{\mathrm{O}_2}, \Delta H_{\mathrm{min}}\right) + \delta_2\left(T, p_{\mathrm{O}_2}, dH_{\mathrm{max}}\right) - \delta \tag{S6}$$

This yields an expression for $p_{\mathrm{O}_2}(\delta, \Delta\mathrm{H}_{\mathrm{min}}, \Delta\mathrm{H}_{\mathrm{max}}, T)$ and $\Delta H(\delta, T)$ is then calculated as a numerical derivative of p_{O_2} with respect to the temperature:

$$\Delta H(\delta, T) = \frac{-\frac{1}{2} \cdot p_{\mathrm{O}_2}(\delta, \Delta H_{\mathrm{min}}, \Delta H_{\mathrm{max}}, T) - \frac{1}{2} \cdot p_{\mathrm{O}_2}(\delta, \Delta H_{\mathrm{min}}, \Delta H_{\mathrm{max}}, T + 0.01)}{\frac{1}{RT} - \frac{1}{R \cdot (T + 0.01)}} \tag{S7}$$

Within this model, the steepness of the increase from $\Delta\mathrm{H}_{\mathrm{min}}$ to $\Delta\mathrm{H}_{\mathrm{max}}$ is temperature dependent. At very low temperatures (i.e. 73 K), $\Delta H(\delta)$ resembles a step function, whereas at higher temperatures (i.e. 573 K), it is very similar to the arctangent function introduced earlier.

As previously discussed, the redox entropy change upon non-stoichiometric reduction of a perovskite can be calculated as the sum of the partial molar entropy of oxygen $S_{\mathrm{O}_2}(T)$, the vibrational entropy change $\Delta s_{\mathrm{vib}}(T)$, and the configurational entropy change $\Delta s_{\mathrm{conf}}(\delta, T)$: [1, 6, 7]

$$\Delta S(\delta, T) = \frac{1}{2} S_{\mathrm{O}_2}(T) + \Delta s_{\mathrm{vib}}(T) + \Delta s_{\mathrm{conf}}(\delta, T) \tag{S8}$$

$S_{\mathrm{O}_2}(T)$ can be calculated using the Shomate equation and the NIST-JANAF thermochemical tables. [2] The vibrational entropy change can be determined using the Debye model. The Debye temperatures of these phases are approximated using the corresponding elastic tensors and the *pymatgen* package. [8, 9] The elastic tensors for each of the phases studied here are available in the *Materials Project*, however, we include an option to use the tensors for $SrFeO_{3-\delta}$ as an approximation if no data for the

phase of interest is available. As the vibrational entropy change is usually the smallest out of the three contributions, the error introduced is correspondingly small. According to the Debye model, we obtain the absolute vibrational entropies $s_{\mathrm{vib},\delta}(T)$ for a given non-stoichiometry δ using the Debye temperatures $\Theta_{\mathrm{D},\delta}$ of these phases. [10] To obtain the change in vibrational entropy upon reduction or oxidation, we assume that the vibrational entropy and the Debye temperature $\Theta_{D,n}$ change linearly with decreasing δ. This is a valid assumption, as the number of vibrational modes scales with the atoms in the unit cell, and a change in non-stoichiometry is associated with a change in the amount of oxygen atoms in the lattice. We support this statement using data for partially reduced intermediate phases of $SrFeO_{3-\delta}$ (see section 11) showing a linear dependence between $\Theta_{D,n}$ and a decrease in δ. Under the assumption that the vibrational entropy correlates linearly with δ, the change in vibrational entropy Δs_{vib} is only dependent on the temperature, and can be calculated as the difference between the absolute vibrational entropies of the perovskite ($\delta = 0$) and the brownmillerite ($\delta = 0.5$):

$$\begin{aligned} \Delta s_{\mathrm{vib}} &= 2 \cdot s_{\mathrm{vib}}(\delta, T) \frac{\partial}{\partial T} \frac{\partial}{\partial \delta} \\ &= 2 \cdot (s_{\mathrm{vib},\delta=0}(T) - s_{\mathrm{vib},\delta=0.5}(T)) \end{aligned} \tag{S9}$$

The factor 2 is necessary as 2 mol of AMO_3 perovskite are required to release 1 mol of monatomic oxygen O. As the third component, the change in configurational entropy can be calculated. The change in configurational entropy of a solid solution with two individual sub-lattices is the sum of the entropy changes induced by each sub-lattice. The configurational entropy change of these can be calculated using the dilute species model with $\delta_{\mathrm{max},1} = act/2$, $\delta_{\mathrm{max},2} = (1 - act)/2$, $\delta_1 \geq \delta_2$, and Eq. S5 for $\delta_{\mathrm{n}}(T, p_{\mathrm{O}_2}, \Delta H_{\mathrm{n}})$ with $p_{\mathrm{O}_2}(\delta, \Delta H_{\mathrm{min}}, \Delta H_{\mathrm{max}}, T)$ derived using Eq. S6: [1]

$$\begin{aligned} \Delta s_{\mathrm{conf,n}}(\delta, \delta_{\mathrm{n}}, T, \Delta H_{\mathrm{n}}) &= \frac{1}{\delta_{\mathrm{max,n}}} \cdot \frac{a}{2} \cdot \mathrm{R} \\ \cdot \left[ln\left(\delta_{\mathrm{max,n}} - \delta_{\mathrm{n}}(T, p_{\mathrm{O}_2}, \Delta H_{\mathrm{n}})\right) - ln\, \delta_{\mathrm{n}}(T, p_{\mathrm{O}_2}, \Delta H_{\mathrm{n}}) \right] &\cdot \frac{\delta_{\mathrm{n}}(T, p_{\mathrm{O}_2}, \Delta H_{\mathrm{n}})}{\delta} \end{aligned} \tag{S10}$$

We assume a = 2, i.e. corresponding to an ideal solid solution. We note that the model may be improved by determining the interaction between the sub-lattices to adjust the value a. The configurational entropy is then given as the sum of the two contributions $\Delta s_{\mathrm{conf,n}}$ according to Eq. S10. This concludes the set of entropic contributions necessary to calculate the total entropy change according to Eq. S8.

6. Energy balance and modelling of the redox cycle energy demand

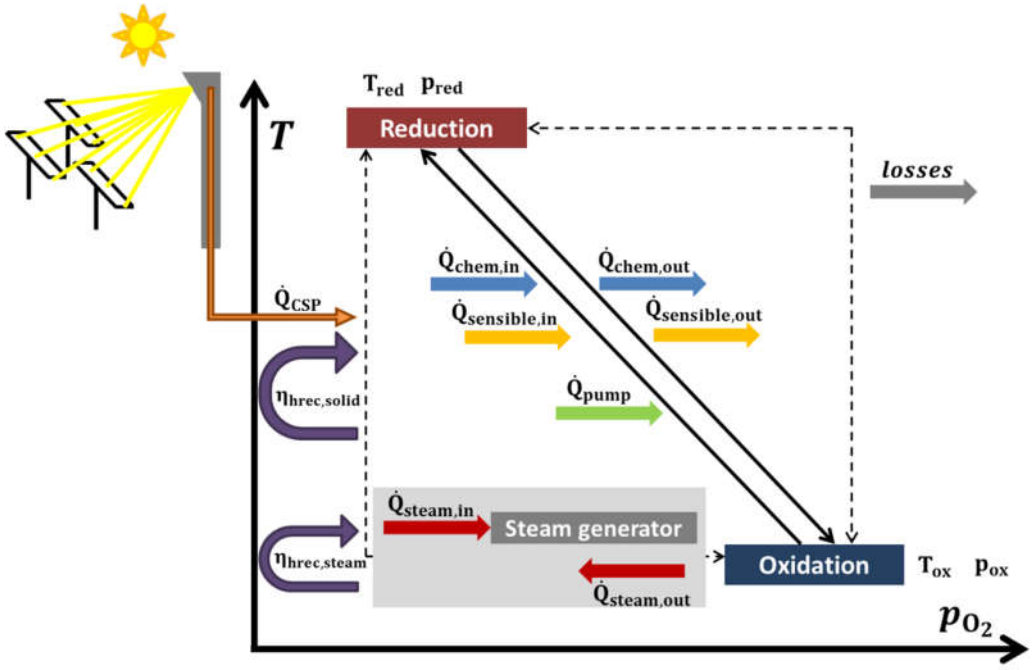

Figure S2. Process scheme of a two-step thermochemical redox cycle with CSP (concentrated solar power) as the heat source. The energy demand of the cycle can be split into chemical, sensible, and pumping energy. For thermochemical water splitting, the energy necessary to generate steam is added. The chemical and sensible energy can be partially recovered using solid–solid heat recovery at a heat recovery efficiency $\eta_{\mathrm{hrec,solid}}$, and a heat recovery efficiency from the remaining steam in the product stream $\eta_{\mathrm{hrec,steam}}$ is specified for water splitting. Because of thermal losses (grey), not all of the thermal energy supplied can be used for the thermochemical process; however, these losses are not further quantified within this work. The reduction and oxidation reaction are performed at the respective $T_{\mathrm{red}}/T_{\mathrm{ox}}$ and the partial pressures $p_{\mathrm{red}}/p_{\mathrm{ox}}$. T and $p_{\mathrm{O_2}}$ are changed gradually between the oxidation and reduction steps (solid arrows) but could also be changed one after another (dashed arrows).

Using the functions for $\delta(T, p_{\mathrm{O_2}})$, we can determine the molar amount of oxygen absorbed and released ($n_{\mathrm{O_2}}$) per mol of redox material for each of the materials in a redox cycle based on the oxidation and reduction oxygen partial pressure and temperature levels p_{ox}, T_{ox} and p_{red}, T_{red}:

$$n_{\mathrm{O_2}} = \frac{\delta(T_{\mathrm{red}}, p_{\mathrm{red}}) - \delta(T_{\mathrm{ox}}, p_{\mathrm{ox}})}{2} \tag{S11}$$

Conversely, the molar amount of redox material necessary to transfer one mole of oxygen is the reciprocal value. Throughout this work, the pressure values are considered to be oxygen partial pressures, and for brevity, we write for instance p_{red} instead of $p_{\mathrm{O_2,red}}$. Using the thermodynamic data for ΔH and ΔS, the energy consumption of the redox cycle can be determined. As a first step, we define the conditions for reduction and oxidation. We assume that the redox material is in equilibrium at the end of the redox reaction and that only this equilibrium position is relevant for the redox energetics. At the end of the reduction process, an oxygen partial

pressure p_{red} is reached at the temperature T_{red} as the released oxygen is removed from the reaction chamber. Conversely, the material is re-oxidized at T_{ox} at an equilibrium oxygen partial pressure p_{ox}. Instead of the oxygen partial pressure at oxidation, the $p_{\mathrm{H_2}}/p_{\mathrm{H_2O}}$ or $p_{\mathrm{CO}}/p_{\mathrm{CO_2}}$ partial pressure ratios can be specified if water or CO_2 are used as the respective oxidants. These ratios can be converted into equivalent oxygen partial pressures (see ESI section 15) assuming that the water or carbon-dioxide splitting reaction is in the equilibrium state for the given temperature and partial pressure ratio. We assume that no additional oxygen (for instance due to leakage) is present. Under these assumptions, we can define a generic process scheme for the complete thermochemical cycle (see Fig. S2). The type of heat source used to drive the process is irrelevant for our calculations. In Fig. S2, we assume that the thermal energy is supplied by CSP ($\dot{Q}_{\mathrm{CSP}}$); however, we do not account for inherent losses in CSP, such as the limited efficiency of the heliostat field or re-radiation. The total input heat flow rate is denoted here by $\dot{Q}_{\mathrm{in}}$, which corresponds to $\dot{Q}_{\mathrm{CSP}}$ in our simplified case. The energy balance can then be written as

$$\dot{Q}_{\mathrm{in}} = \underbrace{\dot{Q}_{\mathrm{chem}} + \dot{Q}_{\mathrm{sensible}} + \dot{Q}_{\mathrm{pump}} \left(+ \dot{Q}_{\mathrm{steam}} \right)}_{\dot{Q}_{\mathrm{total}}} + \mathrm{losses} \tag{S12}$$

The total energy flow used for operating the redox cycle is denoted by $\dot{Q}_{\mathrm{total}}$. Heat losses due to heat-transfer processes are summarized as "losses". These are not further considered in the following, meaning that heat losses due to radiation, conduction, and convection are neglected in our model. This is a necessary limitation, as these factors are dependent on the reactor design and operational parameters, which cannot be generalized. We therefore only consider the total thermal energy that can be used in the redox cycle Q_{total}. Instead of the heat flow $\dot{Q}_{\mathrm{total}}$, we use the absolute amount of thermal energy used in the process, as the exact flow rates depend on the reaction kinetics and heating rates. The individual terms contributing to our energy balance are discussed in the following sections.

Chemical Energy (Q_{chem})

The amount of energy required to drive the chemical reaction, i.e., the reduction and re-oxidation of the redox material, is referred to as chemical energy in the following text. The chemical energy depends on the heat effect of the reaction, which is defined by the change in the redox enthalpy ΔH. To partially reduce the redox material from an initial oxygen non-stoichiometry δ_{ox} to a final oxygen non-stoichiometry δ_{red} (with $\delta_{\mathrm{red}} > \delta_{\mathrm{ox}}$ by definition), the thermal energy $Q_{\mathrm{chem,red}}$ must be supplied:

$$Q_{\mathrm{chem,red}} = \int_{\delta_{\mathrm{ox}}}^{\delta_{\mathrm{red}}} \Delta H(\delta, T)\, \mathrm{d}\delta \tag{S13}$$

One peculiarity of non-stoichiometric reactions is that the reduction reaction does not only occur at T_{red} but gradually over the entire temperature range. Any change in the temperature or oxygen partial pressure induces a change in the state of the chemical equilibrium and an uptake or release of oxygen. Therefore, under ideal conditions, T_{red} does not need to be maintained to reach the full reduction extent; however, the reduction reaction is already completed as soon as the reduction conditions are reached. In practice, one must account for the reduction kinetics limiting the reduction rate as well the rate at which the evolved oxygen is removed from the reaction chamber. However, the time needed to complete the reaction is irrelevant in our case, as absolute amounts of energy are considered, independent of the time required to reach chemical equilibrium. Nevertheless, the result of Eq. S13 may slightly differ depending on the operating procedure because of the temperature dependence of thermodynamic properties. One can distinguish the following three cases for the reduction process:

a) the pressure is first changed isothermally from p_{ox} to p_{red}, and the temperature is then changed from T_{ox} to T_{red} (lower-left dashed arrow in Fig. S2) *or*

b) the reverse of (a), i.e., the temperature is changed from T_{ox} to T_{red}, and the pressure is then changed from p_{ox} to p_{red} (upper-right dashed arrow in Fig. S2) *or*

c) both the temperature and pressure are changed simultaneously (solid diagonal arrows in Fig. S2).

In case (c), the heat is supplied and released continuously, whereas cases (a) and (b) require intermittent heat flows. Therefore, only case (c) is considered within this work, as it allows for the most efficient use of the incoming heat and can generally be applied in all cases. Nevertheless, determining the most efficient option overall depends on the specific process conditions and the type of oxidant used. For instance, the hydrogen yield in water-splitting reactions should be higher if the material is only oxidized at T_{ox} instead of using case (c) with gradual oxidation.

The amount of energy released during re-oxidation of the material is equivalent to the heat required for the reduction process as long as the material is re-oxidized using only molecular oxygen. For water splitting or CO_2 splitting, however, the chemical energy is partially stored in the reaction products. The chemical energy released during oxidation of the redox material is then defined as

$$Q_{\mathrm{chem,ox}} = -\left(\int_{\delta_{\mathrm{ox}}}^{\delta_{\mathrm{red}}} \Delta H(\delta, T)\, \mathrm{d}\delta - \Delta H_{\mathrm{stored}}(T) \right) \tag{S14}$$

$\Delta H_{\mathrm{stored}}$ is zero for air-separation processes. For water splitting or carbon-dioxide splitting, we can derive $\Delta H_{\mathrm{stored}}$ from the redox enthalpy change of the water-splitting and carbon-dioxide-splitting reaction, respectively. For water splitting, $\Delta H_{\mathrm{stored}}$ per mole of O transferred is equivalent to the heat of formation of water at a given temperature. The heat of formation of water is calculated using the Shomate equation and the respective constants from the NIST–JANAF thermochemical tables, assuming

that water is only present in the gas phase. [2] For $\Delta H_{\mathrm{stored}}$ per mole of O for carbon-dioxide splitting, Hess's law is used to determine the difference in the formation enthalpies of CO_2 and CO. The temperature used for calculating $\Delta H_{\mathrm{stored}}$ is approximated using $T = 0.5\,(T_{\mathrm{ox}} + T_{\mathrm{red}})$ under the assumption that the temperature increases linearly during the reduction process. The heat released during the re-oxidation process can be partially re-used to drive the reduction reaction using solid–solid heat recovery. [11] We use a temperature-independent heat-recovery efficiency $\eta_{\mathrm{hrec,solid}}$ within this work, which can be regarded as the average heat-recovery efficiency between T_{ox} and T_{red}. To operate a full redox cycle, the chemical energy contribution to the total energy demand is then given as

$$Q_{\mathrm{chem}} = (1 - \eta_{\mathrm{hrec,solid}}) \cdot \int_{\delta_{\mathrm{ox}}}^{\delta_{\mathrm{red}}} \Delta H(\delta, T)\,\mathrm{d}\delta \; - \; \Delta H_{\mathrm{stored}}(T) \tag{S15}$$

$$\eta_{\mathrm{hrec,solid}} = 0 \ldots 1$$

A significant increase in the solid–solid heat recovery allows the overall process efficiency to be significantly improved irrespective of the redox material used. Eqn. S13–S15 specify the energy per mole of oxygen but can be converted to yield the energy needed per mole of redox material using Eq. S11.

Sensible Energy (Q_{sensible})

The sensible energy is dependent on the latent heat stored in the material based on its heat capacity, which can be calculated using the Debye model. Using DFT and *pymatgen*, the Debye temperatures of the perovskite ($\delta = 0$) and brownmillerite phases ($\delta = 0.5$) can be determined using their elastic tensors. [8, 9, 12] The heat capacity per mole of redox material is then given using the factor $\mathrm{y}_\delta = \mathrm{T}/\Theta_{\mathrm{D},\delta}$, where $\Theta_{D,\delta}$ denotes the Debye temperature as a function of the non-stoichiometry δ and the ideal gas constant R: [10, 13]

$$C(y_\delta) \approx C_v(y_\delta) = 9 \cdot R \cdot \; y_\delta^3 \cdot \int_0^{\frac{1}{y_\delta}} \frac{y_\delta^4 \cdot \; e^{y_\delta}}{(e^{y_\delta} - 1)^2}\, dy_\delta \; \cdot \; n_a. \tag{S16}$$

We assume that $C_v = C_p$, as we are only considering solid oxides, and generally denote the heat capacity by C. In fact, there are small differences between isochoric and isobaric heat capacity values depending on the non-stoichiometry, which we do not consider in this approximation. [14] Moreover, the Debye model does not account for second-order phase transitions, which could further affect the heat capacity. [15] The oxygen stoichiometry number n_a is given as $n_a = 4.5 + \delta$ for perovskites with oxygen non-stoichiometry $\delta = 0 \ldots 0.5$. $\Theta_{D,\delta}$ can be approximated using a linear interpolation between $\Theta_{\mathrm{D},\delta=0}$ (the Debye temperature of the perovskite) and $\Theta_{\mathrm{D},\delta=0.5}$ (the Debye temperature of the brownmillerite), as demonstrated by the authors. [12] Using this approximation, the specific molar heat capacity as a function of the temperature T and the non-stoichiometry δ is given as

$$C(T,\delta) = C\left(T,\delta=0,\Theta_{D,\delta=0}\right)\cdot\frac{0.5-\delta}{0.5} + C\left(T,\delta=0.5,\Theta_{D,\delta=0.5}\right)\cdot\frac{\delta}{0.5} \tag{S17}$$

The change in heat capacity between the oxidation and reduction step is typically rather small (< 5%–10%, see the ESI section 16). At high temperatures ($T \gg \Theta_{D,\delta}$), the heat capacity of a non-stoichiometric perovskite oxide depends only on n_a as long as the crystal structure remains intact, and only 10% of all atoms in the lattice can be removed or added ($n_a = 4.5 \ldots 5.0$). A good approximation of $C(T,\delta)$ for values between δ_{ox} and δ_{red} can therefore be determined using a linear interpolation of the δ values between T_{ox} and T_{red}. C is then only dependent on the temperature T and δ_{ox} and δ_{red}. The contribution of the sensible energy to the total energy demand per mole of redox material can then be determined by integration over the heat capacity between T_{ox} and T_{red}:

$$Q_{sensible} = \int_{T_{\mathrm{ox}}}^{T_{\mathrm{red}}} C(T,\delta_{\mathrm{ox}},\delta_{\mathrm{red}})\,\mathrm{d}T \cdot \left(1-\eta_{\mathrm{hrec,solid}}\right) \tag{S18}$$

In analogy to the chemical energy input, the sensible energy input per redox cycle can be lowered if the heat released during cool down is recovered, which is expressed by the heat recovery efficiency $\eta_{\mathrm{hrec,solid}}$. As both the chemical and sensible energy are transferred at the same time in our process, we use one value for the heat recovery efficiency for both processes.

Pumping Energy (Q_{pump})

The third component of the energy input, the pumping energy, describes the energy required to lower the oxygen partial pressure during the reduction step. We assume that this energy cannot be recovered and is always supplied as thermal energy, which is converted into electrical energy for mechanical pumps at an efficiency of 40%. One can use a function to estimate the pumping energy if mechanical pumps are used. Brendelberger *et al.* developed an envelope function describing the minimum energy input necessary for mechanical pumping, which is used within this work (see ESI section 17). [16] To use this function, we assume a constant temperature of the pumped gas at the pump and that all the gas is pumped at p_{red}. This assumption may lead to an overestimation of the required energy, and the process may be further optimized to minimize the pumping energy (compare cases (a), (b), and (c) in the section on chemical energy). The exact amount of pumping energy required depends on many factors, such as the type of pump used and the reactor volume and design. Within our *RedoxThermoCSP* app, we therefore allow users to specify the amount of pumping energy required within a specific reactor setup as an alternative to the envelope function. Instead of mechanical pumps, one could apply thermochemical pump systems with a redox material to transfer the oxygen. These pumps may be a viable and

efficient option in the range of low oxygen partial pressures (sub-millibar range) as long as the redox material used for pumping requires less energy per mole of oxygen pumped than the redox cycle itself. [16-18] Moreover, instead of pumping, a sweep gas could be used to remove the evolved oxygen. This sweep gas, however, would have to be recovered by separating the oxygen from the sweep gas. If thermochemical oxygen pumps are used, this process is very similar to directly using a thermochemical pump. We do not consider sweep gas operation any further, as sweep gas operation typically leads to lower overall process efficiencies than vacuum pumping. [19]

Steam-Generation Energy (Q_{steam})

For water-splitting cycles, the energy required to generate steam as an oxidant should not be neglected. Some materials may split water at a low energy input but also at low conversion rates. Thus, a large amount of water would have to be heated and evaporated to obtain a reasonable amount of hydrogen. Especially for oxidation at low $p_{\mathrm{H_2}}/p_{\mathrm{H_2O}}$ ratios, the amount of steam that must be prepared to generate one mole of hydrogen is very high. This factor significantly decreases the efficiency of solar-thermochemical water-splitting cycles when materials are used that only split water under the condition that a large excess of water with respect to hydrogen is present at all times. [20, 21] Similar to the calculation of $\Delta H_{\mathrm{stored}}(T)$, we use the mean temperature of the oxidation process $T = 0.5(T_{\mathrm{ox}} + T_{\mathrm{red}})$ to determine the average temperature to which the steam must be heated. The heat capacities of liquid water and steam can be calculated using the NIST–JANAF thermochemical tables, [2] and the heat of vaporization of water at 100 °C is taken from the literature (40.79 kJ/mol). [22] Under the assumption that the steam is at ambient pressure and that the temperature-dependent change in heat capacity is near-linear such that the heat capacity at T can be used as an approximation for the heat capacity between T_{ox} and T_{red}, we determine the steam generation energy:

$$Q_{steam}{}' = \left(\int_{T_{\mathrm{feed}}}^{373.15\ K} C_{\mathrm{p,water}}\,\mathrm{d}T + \Delta H_{\mathrm{vap}} + \int_{373.15\ K}^{0.5\,(T_{\mathrm{ox}}+T_{\mathrm{red}})} C_{\mathrm{p,steam}}\,dT\right) \cdot (1 - \eta_{\mathrm{hrec,steam}}) \qquad \text{(S19)}$$

Part of the energy supplied may be recovered from the steam/gas mixture leaving the reactor using a heat exchanger at a heat-recovery efficiency $\eta_{\mathrm{hrec,steam}}$. The calculated energy demand is given per mole of water. To determine the energy demand per mole of hydrogen produced, we need to divide the resulting value by the target partial pressure ratio of hydrogen vs. water $p(\mathrm{H_2})/p(\mathrm{H_2O})$:

$$Q_{\mathrm{steam}} = \frac{Q'_{\mathrm{steam}}}{p(\mathrm{H_2})/p(\mathrm{H_2O})}. \qquad \text{(S20)}$$

This concludes the list of material- and process-specific energy penalties required in order to account for in a two-step (solar) thermochemical redox cycle. For water splitting, we also define the total heat-to-fuel efficiency. This efficiency can be seen as an upper limit of the real process efficiency, as losses (related to re-radiation or the efficiency of the solar field for example) are not taken into account. Using the higher

heating value of hydrogen (HHV) and Q_{total}, both in terms of per mole of hydrogen produced, [23] the heat-to-fuel efficiency $\eta_{\text{heat/fuel}}$ is calculated as $\eta_{\text{heat/fuel}} = \frac{\text{HHV}}{Q_{\text{total}}}$.

7. Accuracy of the applied models and potential improvement

To gain insight into the accuracy of our models, we compared the predicted change in non-stoichiometry ($\Delta\delta$) for the theoretical and experimental datasets. The $\Delta\delta$ value describes the amount of oxygen released during the reduction reaction and is a measure of the material-specific oxygen storage capacity.

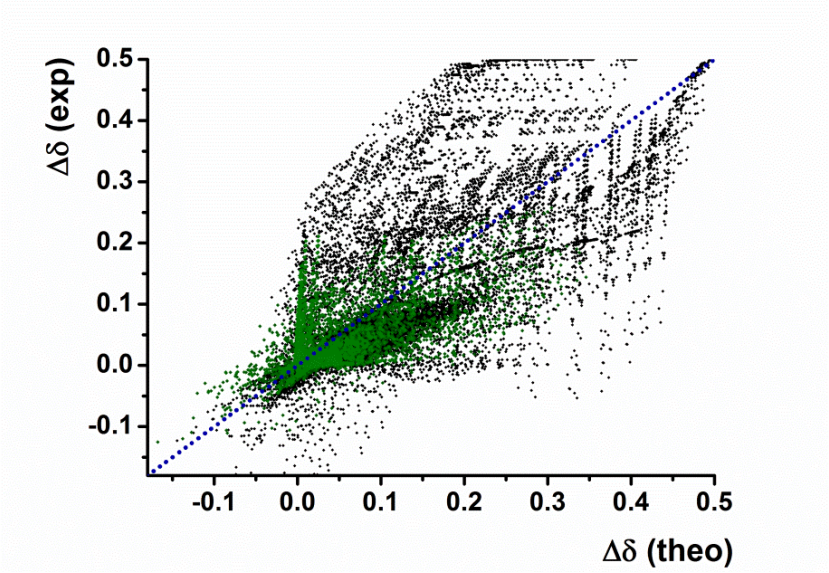

Figure S3. Comparison of change in non-stoichiometry $\Delta\delta$ predicted using our theoretical model (theo) and experimental model (exp). Each data point corresponds to one set of redox parameters (oxidation and reduction temperatures and oxygen partial pressures) and one material. The data points marked in black (>27,500 data points) indicate the complete data set, whereas the green data points (>4,500) are based on non-extrapolated δ values only, leading to a significant improvement in the accuracy of the experimental data. The dashed blue line indicates where the theoretical and experimental data match.

A comparison for the case of air-separation processes is shown in Fig. S3 for all of the parameter sets (oxidation and reduction temperatures and oxygen partial pressures) studied in this work and all the materials with experimental and theoretical data. The agreement between the theoretical and experimental data can be significantly improved by only considering data for which the δ_{ox} and δ_{red} values predicted by the experimental model are within the range of the measured data. The empirical fit functions may lead to highly inaccurate extrapolations for conditions strongly deviating from the experimentally covered data range. [12] The range of simulated conditions spans temperatures between 350 °C and 1400 °C and oxygen partial pressures between 10^{-20} and 1 bar, which is far beyond the range we covered experimentally. We are not comparing a model to experimental data but two different models, one based on experimental data and the other based on DFT data. Nevertheless, the amount of oxygen released is of the right order of magnitude for the vast majority of cases, indicating that the experimental and theoretical data are in

reasonable agreement. However, there is great room for improvement of our models in future studies, as the thermodynamics of perovskite solid solutions is a complex issue.

In many cases, the oxygen release predicted in the theoretical model is slightly higher than that experimentally observed, as our model overestimates the change in entropy ΔS for many perovskites. Because of oxygen vacancy ordering, the configurational entropy change in a real perovskite system may be reduced with respect to that of the ideal dilute species model. [12, 24] Moreover, the generalized crystal structures we used as a starting point for all the calculations may not be those with the lowest total energy in all cases. Minor discrepancies can also be attributed to the discretization of occupancies in our solid solutions necessary for DFT screening; however, these differences should not have a large impact. Another potential source of errors is the simplification used for calculating the vibrational entropy using the Debye model only (in many cases using data for $SrFeO_{3-\delta}$ as an approximation). The accuracy of these calculations, however, is constantly being improved as elastic tensors for increasingly more materials are calculated in the Materials Project and *RedoxThermoCSP* is updated regularly. Additionally, more accurate models for the redox enthalpy change ΔH during the reduction of perovskite phases, including DFT calculations for superstructures with long-range ordering and intermediate phases between perovskites and brownmillerites, could lead to further improvement of the theoretical description of the thermodynamics.

To improve the accuracy of the experimental data, it is necessary to measure data for these materials over a larger range of T and p_{O_2}. Moreover, we did not measure potential δ-independent temperature-dependent changes in ΔH and ΔS, which are considered in the theoretical models only. [12] Despite all the efforts to improve the experimental thermodynamic data, there are inherent limitations in measuring thermodynamic data using the van't Hoff method such as enthalpy–entropy compensation [25] and uncertainties in determining the mass change of the redox materials. Additionally, second-order phase transitions or disproportionation reactions may limit the practical applicability of a redox material. [6, 15, 26] Therefore, knowledge about the thermodynamic properties can be used to predict the expected mass change of a material with reasonable accuracy. Theoretical studies cannot currently entirely replace an experimental test of the material under real operational conditions. Improvements in terms of the thermodynamic models and representation of the solid solutions using DFT can be made; nevertheless, our data can be used to predict the redox properties of a large set of perovskite materials well enough to significantly narrow down the list of potential materials.

Our theoretical and experimental modelling approaches are compared in Table S7, including ideas on a potential improvement of these models.

Table S 7. Comparison of the experimental and theoretical models used within this work. Taken from J. Vieten (Dissertation). [27]

Model		Strengths/Weaknesses and potential improvements
Experimental model	+	Based on experimentally measured thermogravimetric data
	+	Fit accurately describes $\Delta H(\delta)$ and $\Delta S(\delta)$ within the measured data range
	+	Relatively simple analytical fit functions allow fast equilibrium calculations
	+	Broad experimental screening of 24 materials with a standardized procedure
	−	Inaccurate extrapolations outside the measured data range **Improvement:** measurement over a larger data range for materials of interest (increases experimental effort, may require reaching very low and very high oxygen partial pressures in the thermobalance)
	−	Temperature dependence of ΔH and ΔS not covered **Improvement:** measurement of significantly more data points and evaluation of different temperature ranges to evaluate temperature effects (disadvantage: measurement time per material increases by one order of magnitude)
	−	Non-stoichiometry at the reference point (400 °C, oxygen partial pressure 0.18 bar) δ_0 only determined from fit, often not very accurate **Improvement:** measurement of δ_0 through experimental methods such as iodometry or thermogravimetric reduction in hydrogen
Theoretical model	−	Relies purely on theoretical considerations, may be biased by model
	+	Thermodynamic models describe $\Delta H(\delta, T)$ and $\Delta S(\delta, T)$ for any $\delta = 0 \ldots 0.5$ and are based on well-estabilished fundamental properties and physical models
	−	Complex thermodynamic functions which are solved numerically and DFT calculations require long computation times
	+	Includes a large set of materials (over 240 perovskite-brownmillerite pairs)
	+	Does not depend on limited experimental data ranges
	+	Temperature dependence of ΔH and ΔS is covered
	+	Absolute δ values are determined instead of relative $\Delta\delta$ values, no δ_0 values required
	−	Metal species occupancies normalized to 1/8 to allow integer occupancy values in a 2x2x2 supercell as required by DFT, this may lead to aliasing effects (step-wise change of properties which are changing gradually in nature) **Improvement:** use larger supercells (longer computation times) or virtual crystal approximation (VCA, potentially lower accuracy)
	−	Discretized supercells do not necessarily represent a solid solution with random site occupancy **Improvement:** use virtual crystal approximation (VCA) or averaging of more than one ordered structure (increases computational time), potentially use special quasirandom structures (SQS) to find representative ordered structures
	−	Potential ordering of solid solutions not considered (for instance: complex stacking variants in some perovskites along one or more crystal axes) **Improvement:** increase the size of the supercells and simulate more than one ordered structure (limited due to exponential increase in computational times)
	−	Oxygen vacancy ordering not considered **Improvement:** simulate oxygen vacancy ordered structures through DFT and select those with lowest total energy (limited due significant increase in computational times)
	−	DFT only yields results for 0K, accuracy of $\Delta H(T)$ and $\Delta S(T)$ may be limited **Improvement:** further experimental studies of temperature effects, calculation of energetic barriers between different similar structures

8. Discussion of the redox energetics of H_2O and CO_2 splitting processes

Because of the high formation enthalpy of water, the thermodynamics of water splitting differ strongly from that of air separation. Our *RedoxThermoCSP* tool indicates that perovskites suitable for water splitting include lanthanum ferrites and manganates, which is in good agreement with literature reports on similar materials. [28-30] A large number of perovskite phases suggested by our tool have been previously identified as promising materials for thermochemical water splitting in earlier studies on materials that are not solid-solution phases. [31, 32] We can extend the range of possible materials by using solid-solution formation. Many of the perovskites reported in the literature require a large excess of steam to produce appreciable amounts of hydrogen, and our study helps elucidate the effect of this excess steam on the total process efficiency. A larger excess of steam results in a higher amount of steam-generation energy. However, these small conversion rates correspond to a higher equivalent oxygen partial pressure during oxidation, indicating that materials with lower oxygen affinity can be used. Therefore, the reduction temperature of such materials at a given oxygen partial pressure is lower than that for a material with high hydrogen yield. Both effects are counteracting, and we demonstrate the advantages of the low hydrogen yield of these materials compared with that of the state-of-the-art redox material ceria. Fig. S4 shows the redox materials with relatively high overall process efficiency predicted using our online tool assuming reduction at 1300 °C under an oxygen partial pressure $p_{\mathrm{red}} = 10^{-6}$ bar and oxidation at 700 °C at an equivalent oxygen partial pressure corresponding to a hydrogen conversion rate of 1%. The heat-to-fuel efficiency reached 2.7% at a solid–solid heat-recovery efficiency of 60% and a steam heat-recovery efficiency of 80%. This heat-to-fuel efficiency appears to be low compared with the values reported in some previous studies; however, it is crucial to stress that many of these reports did not account for the vacuum pumping energy (or recycling of sweep gas) or steam generation. [19, 33, 34] If we perform our evaluation using literature data for ceria (see ESI section 19), we reach a heat-to-fuel efficiency of only 1.83% under the same conditions. Therefore, perovskites offer the chance to increase the heat-to-fuel efficiency by approximately 50% under these conditions according to our calculations. Ceria-based redox cycles are more efficient at higher conversion rates involving higher reduction temperatures. Under the assumptions of the heat-recovery efficiencies made here, the heat-to-fuel efficiency of ceria-based cycles peaks at approximately 3%–3.5% in our model (which is not optimized in terms of minimizing the pumping energy or in terms of the oxidation temperature). Similar but slightly lower maximum efficiencies can be reached with perovskite-based cycles. Because of the very high entropy change of ceria during reduction and oxidation, the maximum heat-to-fuel efficiency of ceria-based cycles is slightly higher than that achieved using perovskites. [35, 36] However, we do not account for thermal losses due to re-radiation or other effects. These losses are significantly higher at higher temperatures.

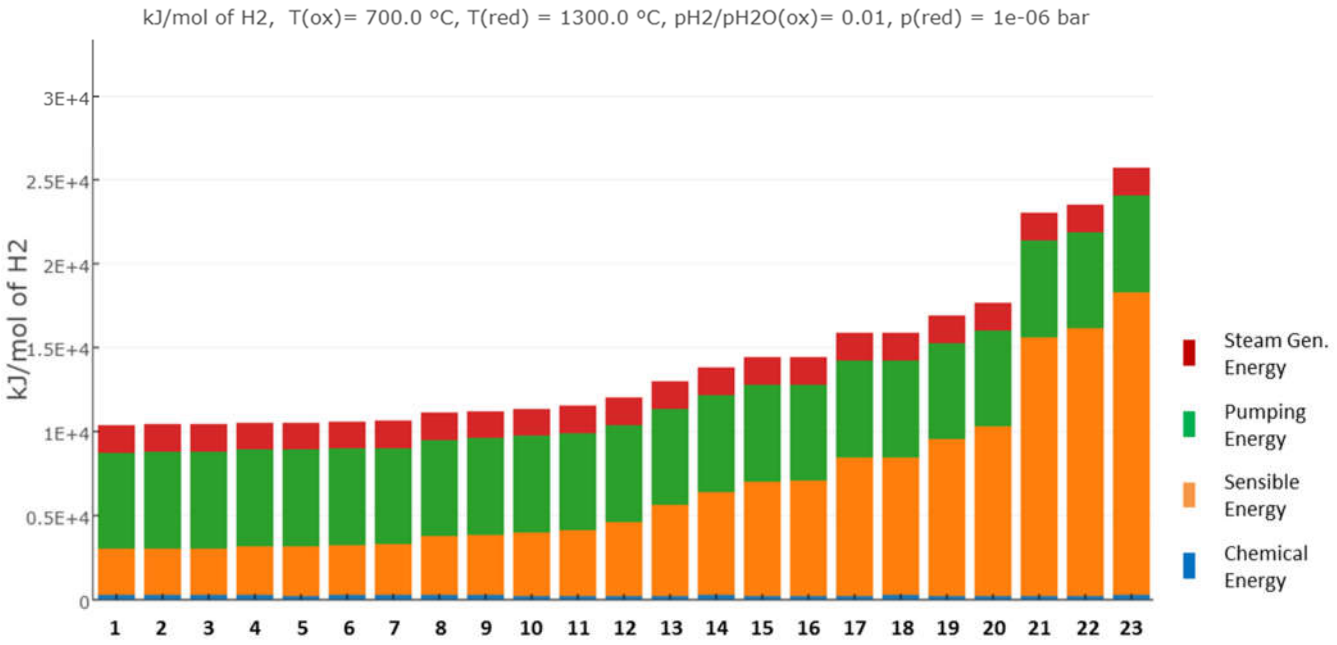

Figure S4. Plot from *RedoxThermoCSP* showing perovskite materials for water splitting as a ranked list of the thermal energy demand to operate a redox cycle with a hydrogen conversion rate of 1% ($p(\mathrm{H_2})/p(\mathrm{H_2O})$ = 0.01), reduction at 1300 °C under an oxygen partial pressure $p_{red} = 10^{-6}$ bar, and oxidation at 700 °C. $\eta_{\mathrm{hrec,solid}}$ = 0.6 and $\eta_{\mathrm{hrec,steam}}$ = 0.8 at a water feed temperature of 25 °C. The material compositions are replaced by indexes for clarity; see the notes section for the corresponding compositions.

Therefore, using perovskites at reduction temperatures of 1300 °C may lead to an increased overall efficiency depending on the type of reactor, despite the low conversion rates assuming that an oxygen partial pressure of $p_{\mathrm{red}} = 10^{-6}$ can be reached and maintained in practice. An even more significant factor could be the reduction of capital costs for building the reactors, as the challenges facing refractory materials engineering for application at 1300 °C are significantly reduced compared with those at 1500 °C.

The efficiency of both ceria- and perovskite-based redox cycles increases significantly if the solid–solid heat-recovery efficiency is improved. Additionally, by improving the steam heat-recovery efficiency, further increases in the overall heat-to-fuel efficiency can be achieved, especially for low conversion rates requiring a large excess of steam. Another appealing option could be to continuously remove the produced hydrogen from the reaction chamber while leaving the steam. This process would lower the steam generation energy at low conversion rates and shift the chemical equilibrium by constantly removing the gaseous reaction product. Moreover, by using thermochemical pumps, the amount of pumping energy can be reduced at low reduction pressures. [16-18] Nevertheless, using current technology, it appears very difficult for two-step thermochemical cycles to compete with other means of hydrogen production such as electrolysis in terms of efficiency. According to our data, the keys to reaching competitiveness are to increase the heat-recovery efficiencies and to make advances in hydrogen/steam separation techniques, potentially combined with thermochemically assisted reduction using redox materials for air separation. Under the most efficient operating conditions for these preconditions, it would then be possible to find an ideal perovskite redox material tailored for precisely these conditions.

Thermochemical splitting of carbon dioxide is thermodynamically similar to water splitting; however, the equivalent oxygen partial pressure differs slightly. The most significant difference is the lack of steam-generation energy. However, the separation of gaseous carbon monoxide from carbon dioxide in the product stream is challenging, and we do not account for the energy penalties potentially involved in our model. [37, 38] We also do not account for the energy demand of heating large amounts of carbon dioxide to the reduction temperature level. Despite these issues, the potentially greatest challenge for a sustainable fuel production process (such as using syngas in a Fischer–Tropsch plant) is capturing carbon dioxide from air. This process is possible in terms of technology but still expensive. [39] A carbon-neutral fuel can only be produced if the same amount of carbon dioxide released during its combustion is removed from the air when it is produced. Artificial fuels are currently the only carbon-neutral option for applications requiring high energy densities, such as those in intercontinental aviation. Using renewable heat sources such as CSP, thermochemical cycles remain an appealing option for the production of solar fuels if the technological challenges can be addressed.

Index – Materials in Fig. S4:

1 $Ca_{0.125}Sr_{0.875}Ti_{0.625}Mn_{0.375}O_{3-\delta}$
2 $EuCrO_{3-\delta}$
3 $Sr_{0.875}Ba_{0.125}Ti_{0.625}Mn_{0.375}O_{3-\delta}$
4 $Sm_{0.125}La_{0.875}Cr_{0.125}Fe_{0.875}O_{3-\delta}$
5 $Sm_{0.125}La_{0.875}MnO_{3-\delta}$
6 $Ca_{0.375}Sr_{0.625}Ti_{0.625}Mn_{0.375}O_{3-\delta}$
7 $Sm_{0.25}La_{0.75}Cr_{0.375}Fe_{0.625}O_{3-\delta}$
8 $Sm_{0.125}La_{0.875}Cr_{0.25}Fe_{0.75}O_{3-\delta}$
9 $Sm_{0.25}La_{0.75}Cr_{0.5}Fe_{0.5}O_{3-\delta}$
10 $EuMnO_{3-\delta}$
11 $Sm_{0.125}La_{0.875}FeO_{3-\delta}$
12 $Sm_{0.125}La_{0.875}Fe_{0.125}Mn_{0.875}O_{3-\delta}$
13 $Ca_{0.125}Sr_{0.875}Mn_{0.5}Fe_{0.5}O_{3-\delta}$
14 $Sm_{0.25}La_{0.75}Cr_{0.625}Fe_{0.375}O_{3-\delta}$
15 $Sm_{0.125}La_{0.875}Fe_{0.25}Mn_{0.75}O_{3-\delta}$
16 $BaMnO_{3-\delta}$
17 $Ca_{0.325}Sr_{0.625}Mn_{0.5}Fe_{0.5}O_{3-\delta}$
18 $Ca_{0.25}Sr_{0.75}Ti_{0.75}Mn_{0.25}O_{3-\delta}$
19 $Ca_{0.125}Sr_{0.875}Mn_{0.375}Fe_{0.625}O_{3-\delta}$
20 $Ca_{0.25}Sr_{0.75}Mn_{0.375}Fe_{0.625}O_{3-\delta}$
21 $Sm_{0.125}La_{0.875}Fe_{0.5}Mn_{0.5}O_{3-\delta}$
22 $Ca_{0.625}Sr_{0.375}Mn_{0.375}Fe_{0.625}O_{3-\delta}$
23 $LaMnO_{3-\delta}$

9. Details on materials synthesis and analysis

All materials are synthesized using the citric acid auto-combustion route, which is also referred to as Pechini method. Our version of this method is based on

1. Mixing 0.1 M aqueous metal nitrate solutions (or a titanium peroxo complex[40]) in the appropriate ratios according to the intended stoichiometries
2. Adding citric acid (4 mL 2.5 M solution)
3. Evaporation of most of the water on a hot plate while stirring
   ⇨ Formation of a gel
4. Drying this gel at gradually increased temperatures of up to 300 °C
5. Self-ignition of the dried gels at up to 500 °C
6. Pestling and mixing of the resulting dried oxide powder
7. Perovskite synthesis in alumina crucibles in a muffle furnace using two consecutive cycles at 800 °C for 10 h followed by one cycle at 1300 °C for 20 h (1100 °C for 20 h for Co containing samples).

5 mmol of each perovskite material are synthesized. The synthesis method is described in detail in an earlier publication.[40] The phase formation is analyzed using a Bruker D8 Advance diffractometer featuring an area detector in an angular range of 10-90 ° 2ϑ. The range is scanned in steps of 0.03° with 2.5 seconds acquisition time per step.
The equilibrium thermodynamic data is gathered using an STA 449 F3 Jupiter thermobalance manufactured by NETZSCH. Powdered samples (typically 100-250 mg) are placed on flat ceramic sample holders. The surface of these sample holders is covered with platinum foil. Different temperature and oxygen partial pressure levels are set, and the oxygen evolution is determined. The oxygen partial pressures are controlled by using different inlet gas mixtures of argon (purity 5.0, Linde), synthetic air (80:20 mol% mixture of nitrogen and oxygen, Linde), and oxygen (purity 4.5, Linde) at different flow rates of 2-200 mL/min. The oxygen partial pressures are monitored using an oxygen sensor by SETNAG. To correct for the different buoyancy of different gas mixtures and systematic errors, blank scans without samples are subtracted in each case. The measurements are conducted at different temperature and oxygen partial pressure levels according to the expected reducibility of the samples. Mass change data is retrieved under equilibrium conditions only (i.e. no mass change while temperature and oxygen partial pressure are maintained). To reach equilibrium conditions faster under low partial pressure conditions, the samples are briefly heated to a higher temperature above the intended equilibrium temperature.
Equilibrium mass change data is converted to the equilibrium change in non-stoichiometry $\Delta\delta$, where $\Delta\delta = 0$ is defined at a temperature T = 400 °C under an oxygen partial pressure p_{O_2}= 0.18 bar. A dataset of T and p_{O_2} values for constant $\Delta\delta$ values is retrieved. The data is plot as $-10^3/RT$ vs. $0.5 \ln p_{O_2}$ (van't Hoff plot) and linear fits are retrieved for constant $\Delta\delta$ values. The y intercept of these fits is proportional to the change in entropy ΔS, whereas the change in enthalpy ΔH can be retrieved from the slope of the linear fits. Measurement uncertainties refer to the confidence intervals of these linear fits as square roots of the covariance matrices.

The measurement and analysis methodology for the extraction of thermodynamic data has been partially previously described in the literature, and is summarized in the following using $Ca_{0.60}Sr_{0.40}Mn_{0.8}Fe_{0.2}O_{3-\delta}$ as an example. [6, 41]

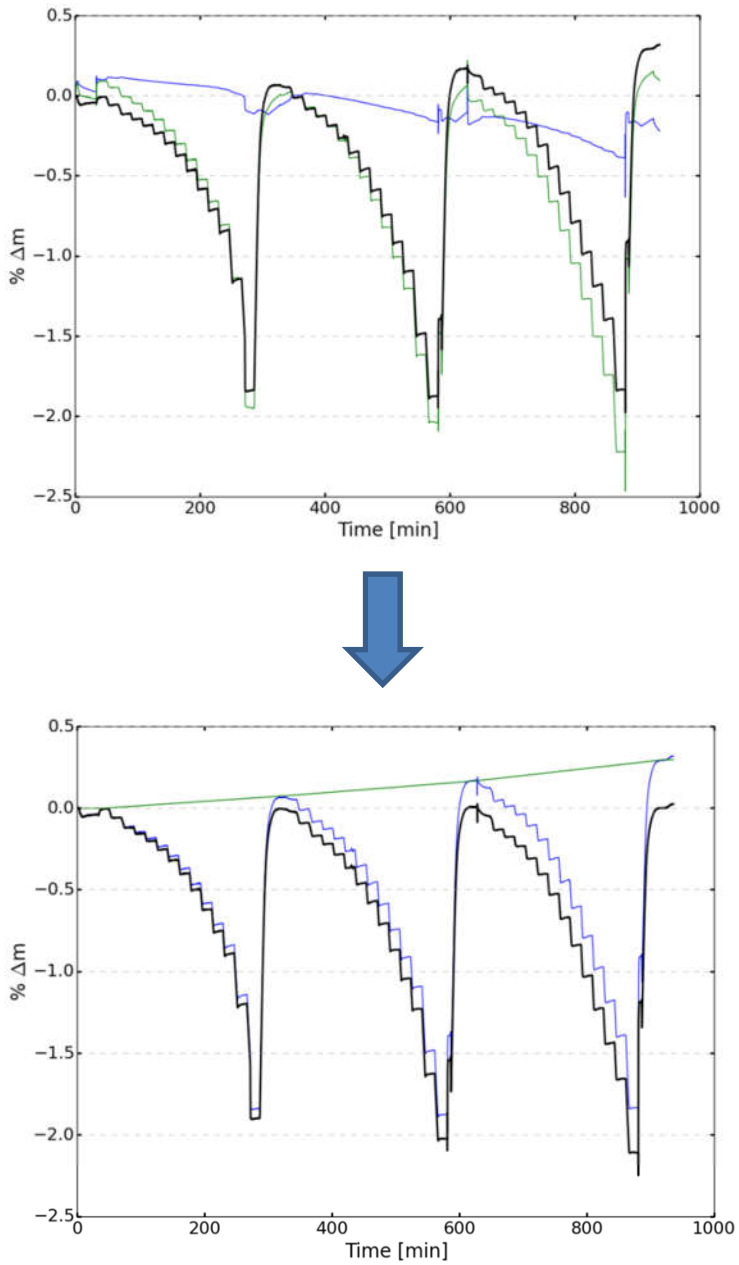

a) The mass change of the redox material is measured in the thermobalance using different temperatures and oxygen partial pressures. Different temperature and pressure programs are chosen to match the expected conditions in which the redox material is most active. One of these measurements is shown here, but up to three measurements per material are combined to get one thermodynamic dataset.

To correct for buoyancy effects of the sample holder, an empty measurement (blue) without sample is substracted from the measured data (green) to yield a corrected dataset (black).

b) In many cases, a constant drift of the measured mass signal is observed. It appears that this drift depends on the time of the day and it may be related to pressure variations in the laboratory. This drift is present despite the fact that a constant temperature of 27 °C of the thermobalance is maintained using a water circuit and a heating/cooling unit.

To correct for this drift, after each high temperature cycle a reference point at 400 °C and p_{O_2} = 0.18 bar is reached, which is defined as reference point where the mass change is zero. Using these reference points, the drift (green) is corrected, yielding the new dataset shown in black.

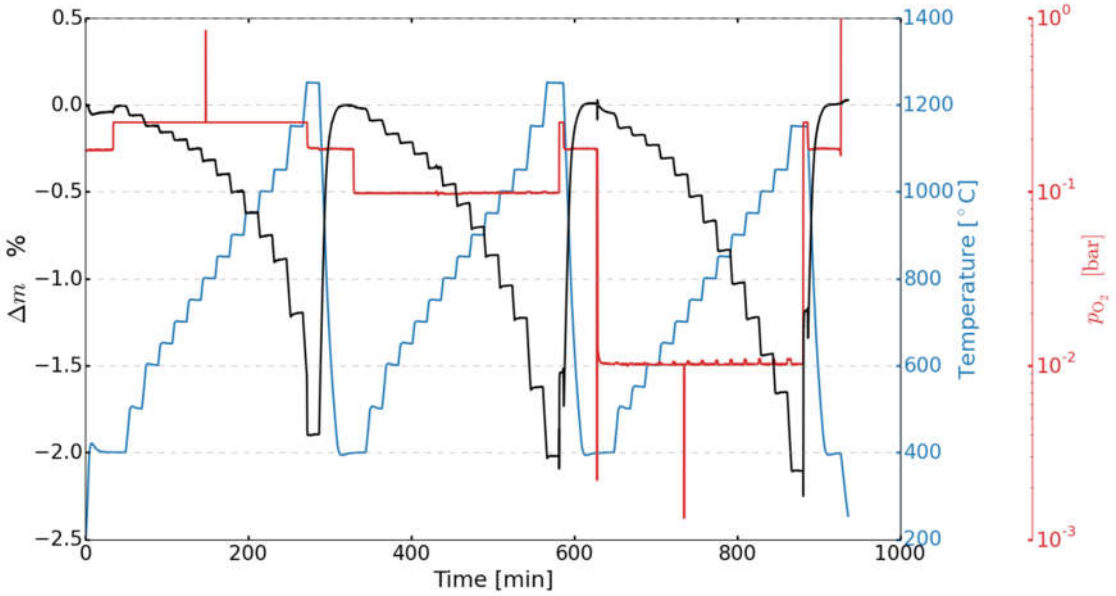

c) The corrected data (black) can then be shown together with the pressure data (red) from the lambda sensor. Short-term spikes in pressure are artefacts of the sensor which are ignored. Please note that the pressure sensor can only measure partial pressures up to 0.25 bar O_2.

At the equilibrium points where $\Delta T, \Delta p_{O_2}$, and Δm are zero, the mass change with respect to the reference state is extracted together with p_{O_2} and converted to a change in non-stoichiometry $\Delta\delta$ according to $\Delta\delta = \frac{\Delta m}{M_O} \cdot \frac{M_P}{m_s}$ with the molar mass of oxygen M_O, the molar mass of the perovskite in the oxidized state M_P, and the initial mass of the perovskite m_s.

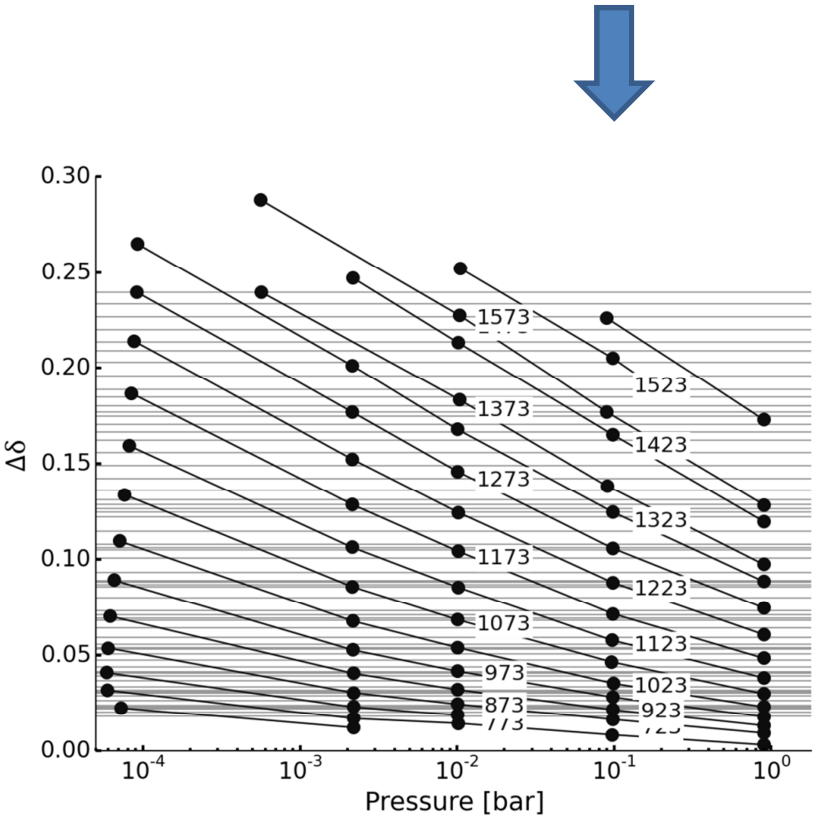

d) The equilibrium data (black dots) is then plotted for constant temperature values (in K) as the oxygen partial pressure in bar vs. $\Delta\delta$, and a linear interpolation is used to fill the gaps between the data points on the isothermal lines. Parallels to the x-axis are drawn indicating constant $\Delta\delta$ values. A new parallel is drawn for each set of consecutive $\Delta\delta$ values $\Delta\delta_n$ and $\Delta\delta_{n+1}$ in the measured data set at $1/2\,(\Delta\delta_n + \Delta\delta_{n+1})$. By this means, the density of these lines with constant $\Delta\delta$ is proportional to the density of data points in the original datasets. Furthermore, these lines of constant $\Delta\delta$ are only drawn if they intersect at least five isothermal lines.

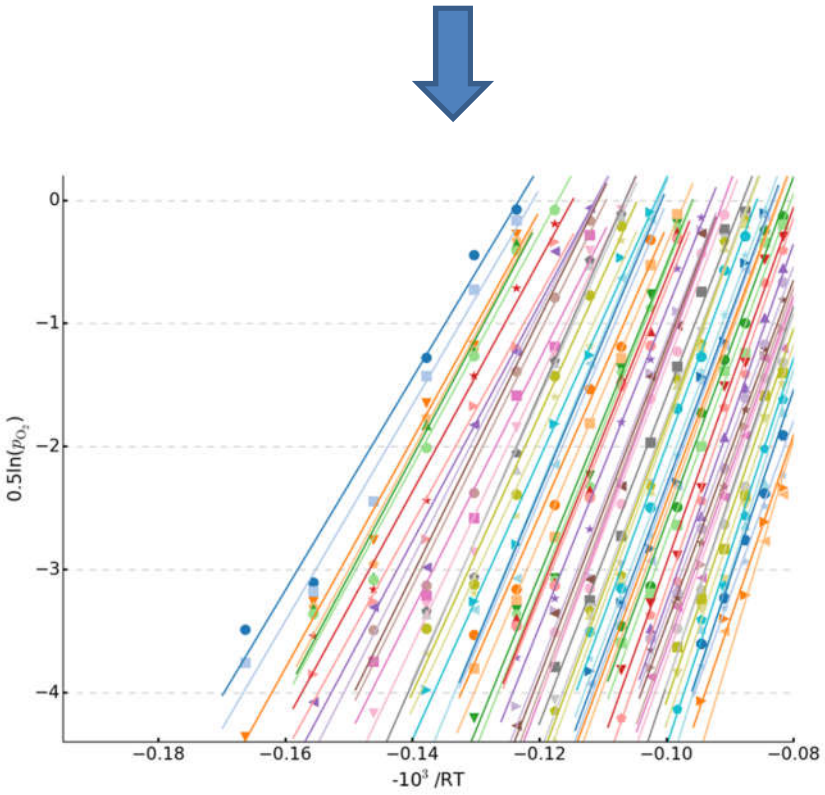

e) From the plot above, datasets of constant Δδ with corresponding values of T and p_{O_2} can be extracted as intersects between the isothermal and the iso"redox" lines (lines with constant Δδ) As mentioned before, for each value Δδ, at least five pairs of T and p_{O_2} values exist, meaning that at least five different conditions are known which lead to the same change in non-stoichiometry with respect to the reference state where Δδ = 0. Each of this datasets can be shown in a plot of $-10^3/RT$ vs. 0.5 $\ln(p_{O_2})$, which is also known as van't Hoff plot. Each color in the plot on the left represents a different Δδ value. Using a version of the Arrhenius equation, the enthalpy change ΔH(Δδ) can be extracted from the slopes of the linear fits for constant Δδ, whereas the entropy change ΔS(Δδ) is proportional to the y intercept of these linear fits.

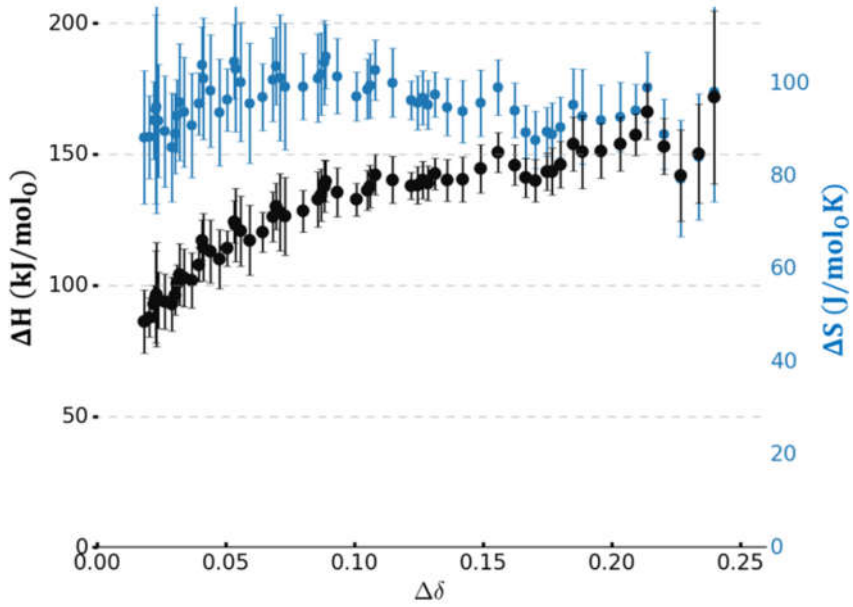

f) The enthalpy and entropy change as a function of Δδ per mol of oxygen O can then be shown in a new plot. The measurement uncertainties are derived as the square roots of the covariance matrices of the linear fits in the previous plot.

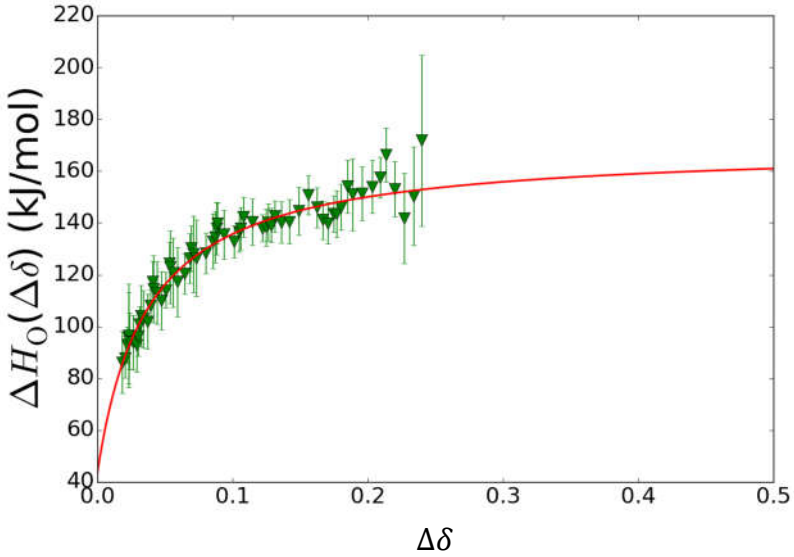

g) Using the fit method introduced in the main manuscript, an analytical expression for the redox enthalpy change $\Delta H(\Delta\delta)$ can be found.

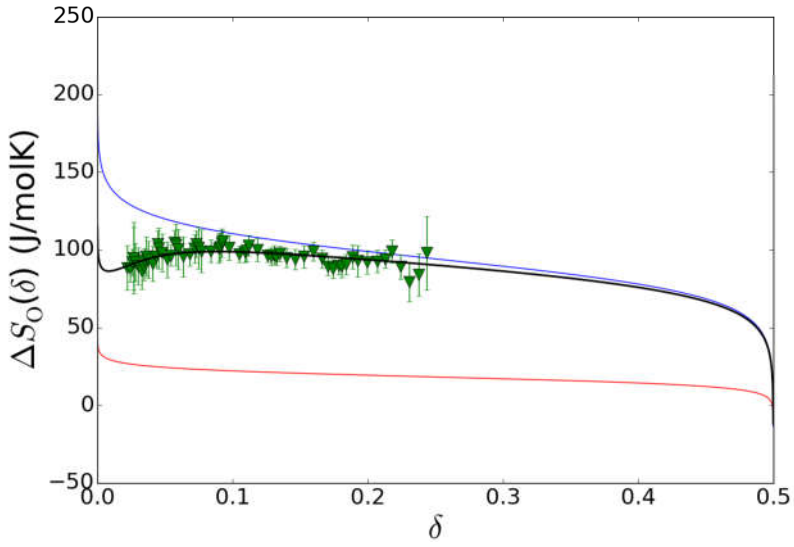

h) The same holds true for the entropy change ΔS(Δδ), which in this case is calculated using data for $SrFeO_{3-\delta}$ (blue) and the redox entropy change assuming that only one sub-lattice is redox active (red). This yields an analytical expression for ΔS(δ).

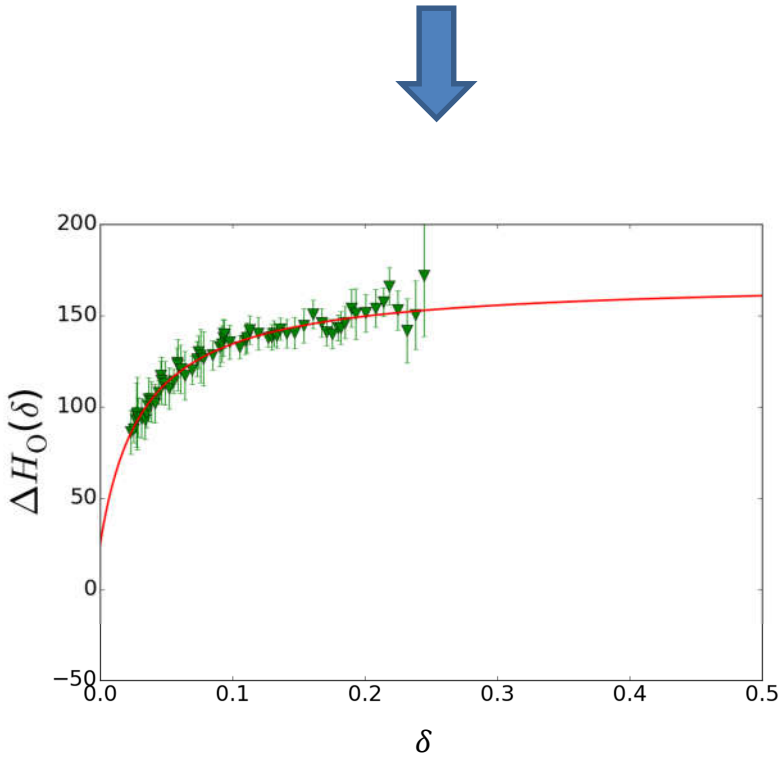

i) The redox entropy fit above also yields a value for δ_0, which is the non-stoichiometry at the reference point where $\Delta\delta = 0$ by definition (400 °C, $p_{O_2} = 0.18$ bar). Using this δ_0, the enthalpy data can also be corrected, as $\delta = \Delta\delta + \delta_0$. This yields an analytical expression for $\Delta H(\delta)$. Please note that an extrapolation of these values beyond the range of the measured data (with $\delta_{exp\ min}$ as the minimum and $\delta_{exp\ max}$ as the maximum recorded δ values) may be highly inaccurate. Moreover, our method of determining δ_0 is not reliable in all cases, therefore, expressions for the change in non-stoichiometry are typically more accurate than expressions giving absolute δ values.

Plots (d) and (f) are given for all screened materials in section 12.

The used starting materials for perovskite synthesis are listed in the following table.

Table S 8. Starting materials for synthesis of perovskites within our experimental perovskite screening. Nitrates are dissolved in water to yield 0.1 M solutions.

Purpose	Material
Fe source	Iron(III)-nitrate nonahydrate, MERCK, ACS, for analysis
Mn source	Manganese(III)-nitrate tetrahydrate, Acros Organics, for analysis
Co source	Cobalt(III)-nitrate hexahydrate, Acros Organics, 99 %
Ti source	Titanium(II)-oxide, Alfa Aesar, 99.5%, -325 mesh powder, dissolved in a 3:1 mixture (vol) of 30 % H_2O_2 (Merck, stabilized) and 28-30 % NH_3 (Merck, reagent grade)
Cu source (for tolerance factor reference measurement)	Copper(II)-nitrate hemipentahydrate, powder, Sigma Aldrich, 98%
Ca source	Calcium nitrate tetrahydrate, Alfa Aesar, 99 %
Sr source	Strontium nitrate, Alfa Aesar, 99 % min, ACS
Citric acid (complexant, fuel for auto-combustion)	anhydrous, Merck, 99 %

10. Estimation of unknown ionic radii

Shannon's table of ionic radii does not contain values for highly coordinated Mg, Eu, and Sm, as well as for Cu with coordination number (CN) 6 and the valences +3 (high spin) and +4. [42] However, based on the known ionic radii and using the Pauling bond strengths, the expected ionic radii can be estimated: [43]

$$r = a - b \cdot \log_{10}(z/CN) \qquad (S21)$$

where z is the charge and a and b are parameters fitted from existing z/CN pairs.

Table S 8. Ionic radii for Mg, Eu, Sm, and Cu in different environments / with different charges, [42] complemented by calculated ionic radii for cases with no literature data.

Mg, a = 0.24298, b = 1.05058		
z	**CN**	**r(Å)**
2	4	0.57
2	5	0.66
2	6	0.72
2	8	0.89
2	10	**0.98 (calc.)**
2	12	**1.06 (calc.)**
Eu, a = 0.65086, b = 0.97932		
z	**CN**	**r(Å)**
3	6	0.947
3	7	1.01
3	8	1.066
3	9	1.12
3	10	**1.16 (calc.)**
3	12	**1.24 (calc.)**
Sm, a = 0.67517, b = 0.94435		
z	**CN**	**r(Å)**
3	6	0.958
3	7	1.02
3	8	1.079
3	9	1.132
3	10	**1.17 (calc.)**
3	12	1.24
Cu, a = 0.66666, b = 0.13288		
z	**CN**	**r(Å)**
1	6	0.77
2	6	0.73
3	6	**0.71 (calc.)**
4	6	**0.69 (calc.)**

11. Calculated Debye temperatures as a function of the non-stoichiometry δ

For $SrFeO_{3-\delta}$, we calculated the elastic tensors for several intermediate phases using *The Materials Project*, and derived the Debye temperatures from these using Pymatgen (see manuscript). [8, 9] We found a near-linear relationship between the non-stoichiometry δ and the Debye temperatures (see Figure S S5).

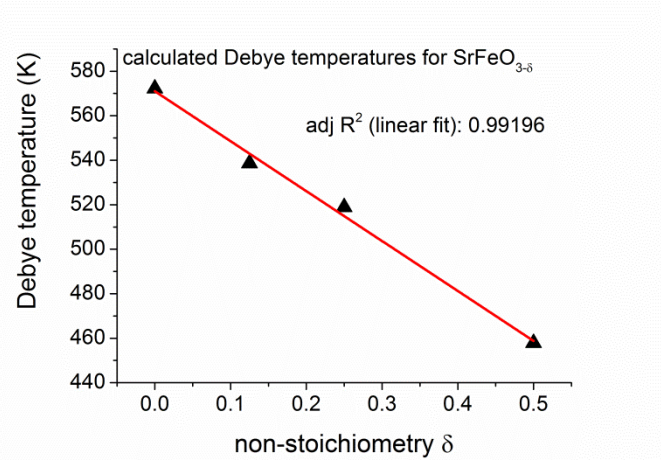

Figure S 5. Relationship between calculated Debye temperatures for $SrFeO_{3-\delta}$ and the non-stoichimetry δ, with the adjusted R^2 of the linear fit indicated.

12. Experimental thermodynamic data

The thermodynamic data is extracted experimentally as explained in section 9. For all materials, we show plots of $\Delta\delta$ vs. p_{O_2} at constant pressure in the following, together with the resulting $\Delta H(\Delta\delta)$ and $\Delta S(\Delta\delta)$. The data is grouped using the materials composition and sample numbers from Table S 6.
For interactive plots including the fits of thermodynamic data, please refer to https://contribs.materialsproject.org/.

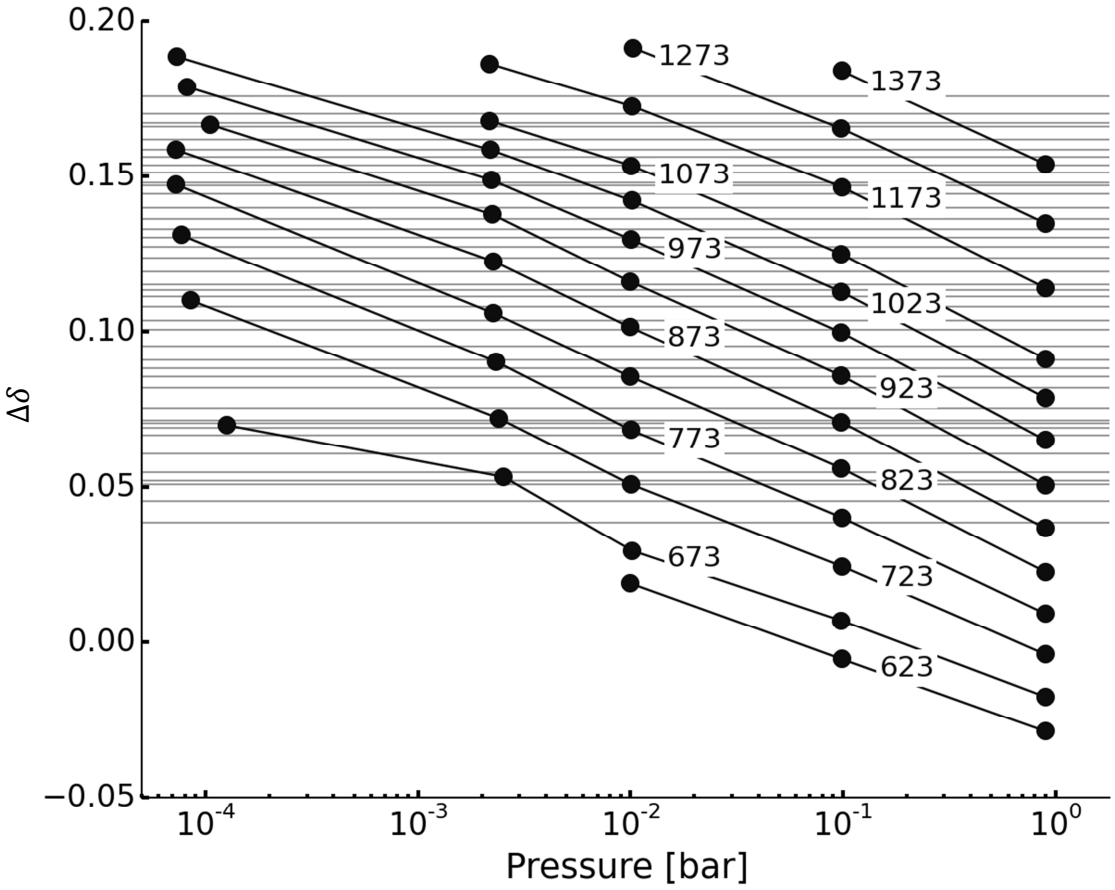
0.20
0.15
0.10
0.05
0.00
−0.05
Δδ
1273
1373
1073
1173
973
1023
873
923
773
823
673
723
623
10^{-4}
10^{-3}
10^{-2}
10^{-1}
10^{0}
Pressure [bar]

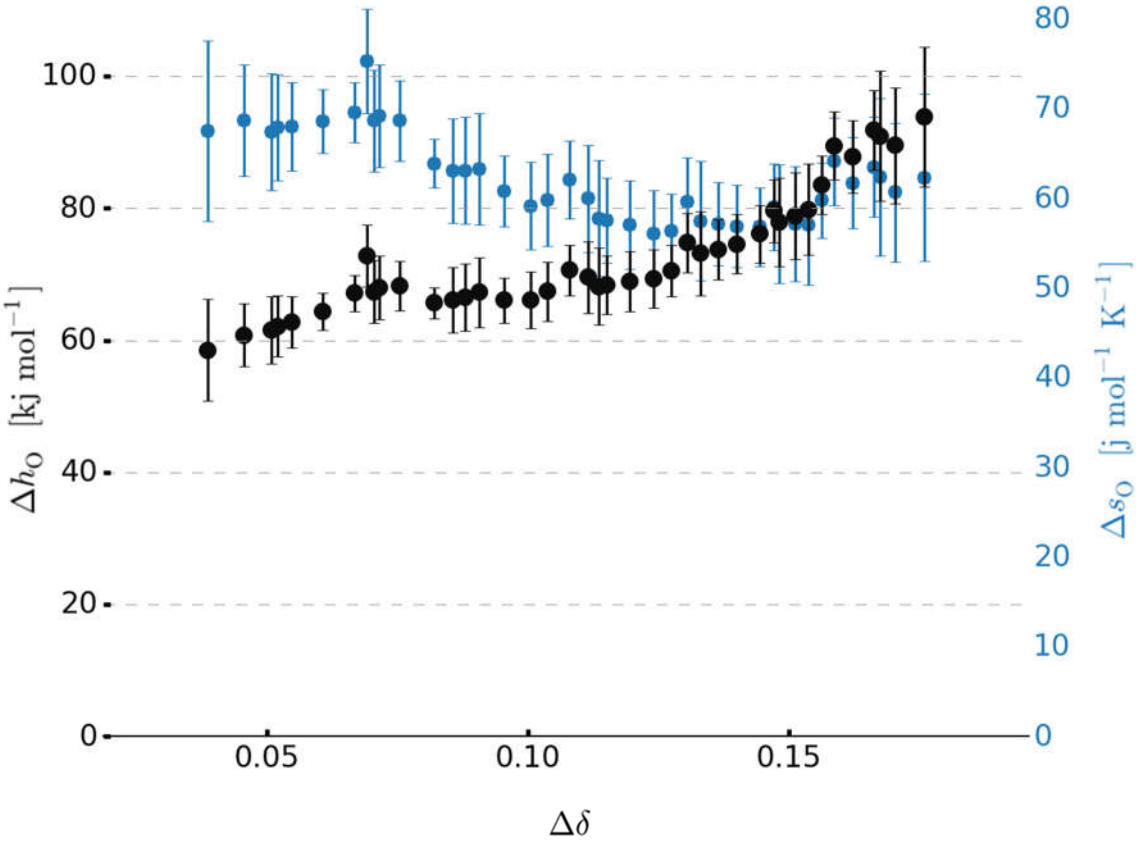
100
80
60
40
20
0
Δh_O [kj mol^{-1}]
80
70
60
50
40
30
20
10
0
Δs_O [j mol^{-1} K^{-1}]
0.05
0.10
0.15
$\Delta\delta$

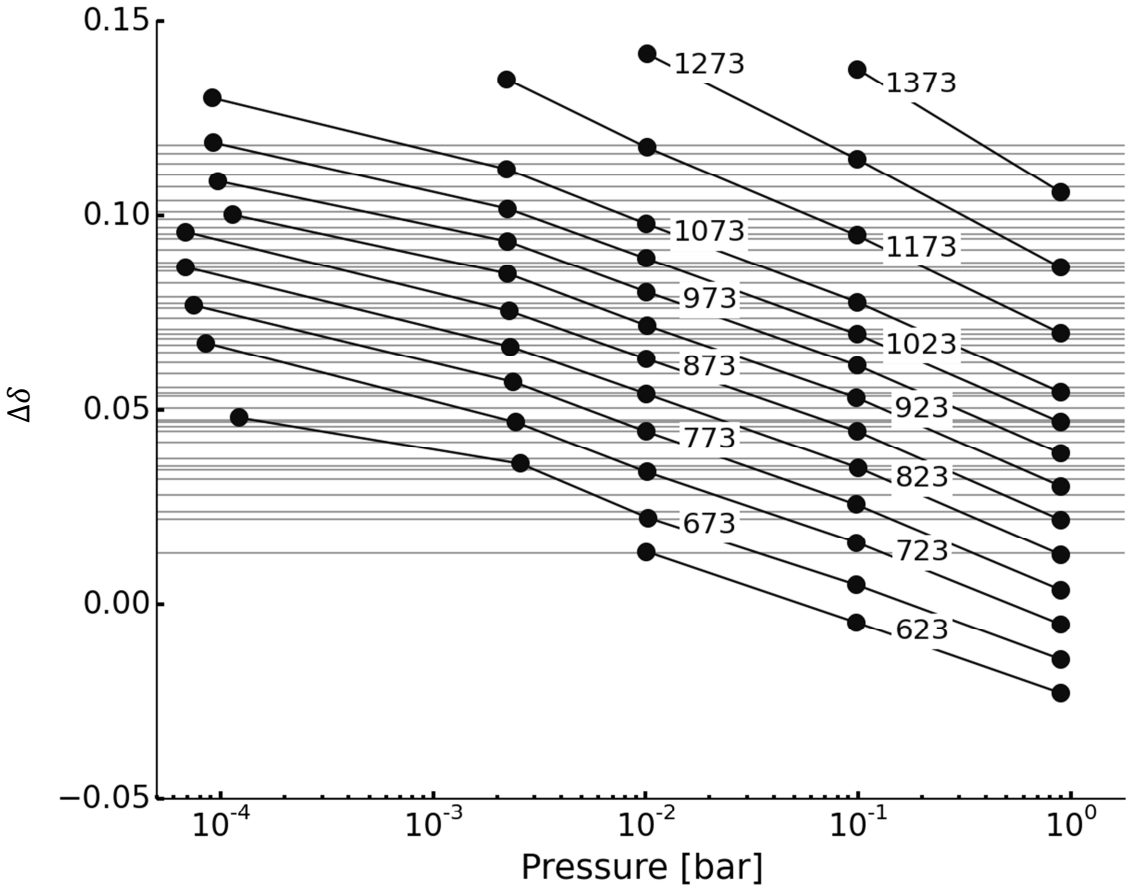
0.15
0.10
0.05
0.00
−0.05
Δδ
1273
1373
1073
1173
973
1023
873
923
773
823
673
723
623
10^{-4}
10^{-3}
10^{-2}
10^{-1}
10^{0}
Pressure [bar]

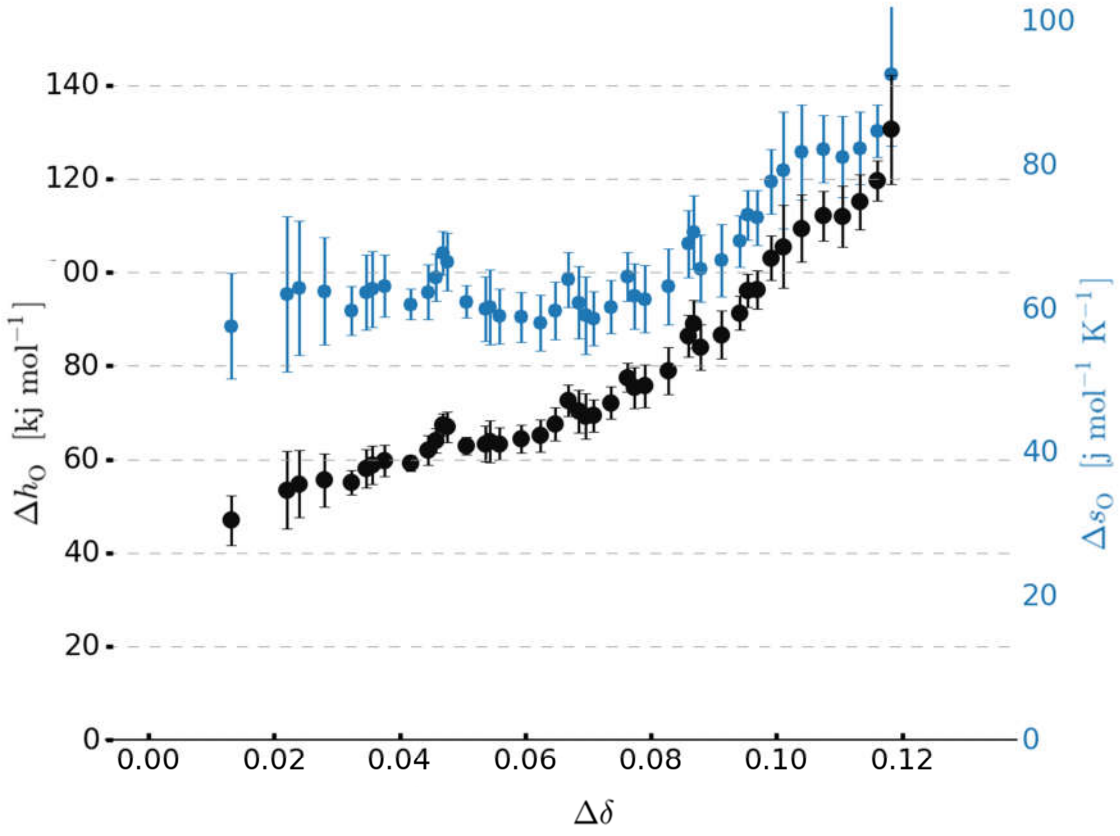
140
120
100
80
60
40
20
0
Δh_O [kj mol^{-1}]
100
80
60
40
20
0
Δs_O [j mol^{-1} K^{-1}]
0.00
0.02
0.04
0.06
0.08
0.10
0.12
$\Delta\delta$

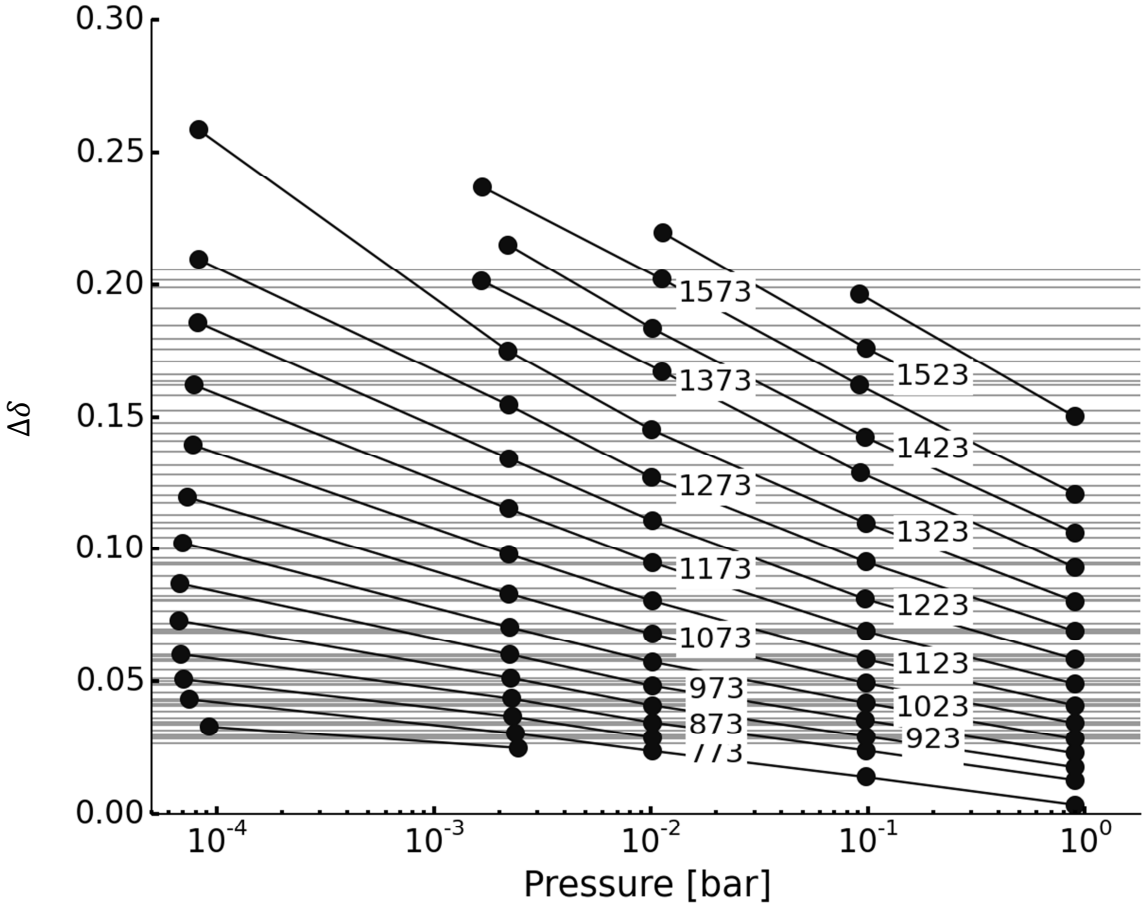
0.30
0.25
0.20
0.15
0.10
0.05
0.00
Δδ
1573
1523
1373
1423
1273
1323
1173
1223
1073
1123
973
1023
873
923
773
10^{-4}
10^{-3}
10^{-2}
10^{-1}
10^{0}
Pressure [bar]

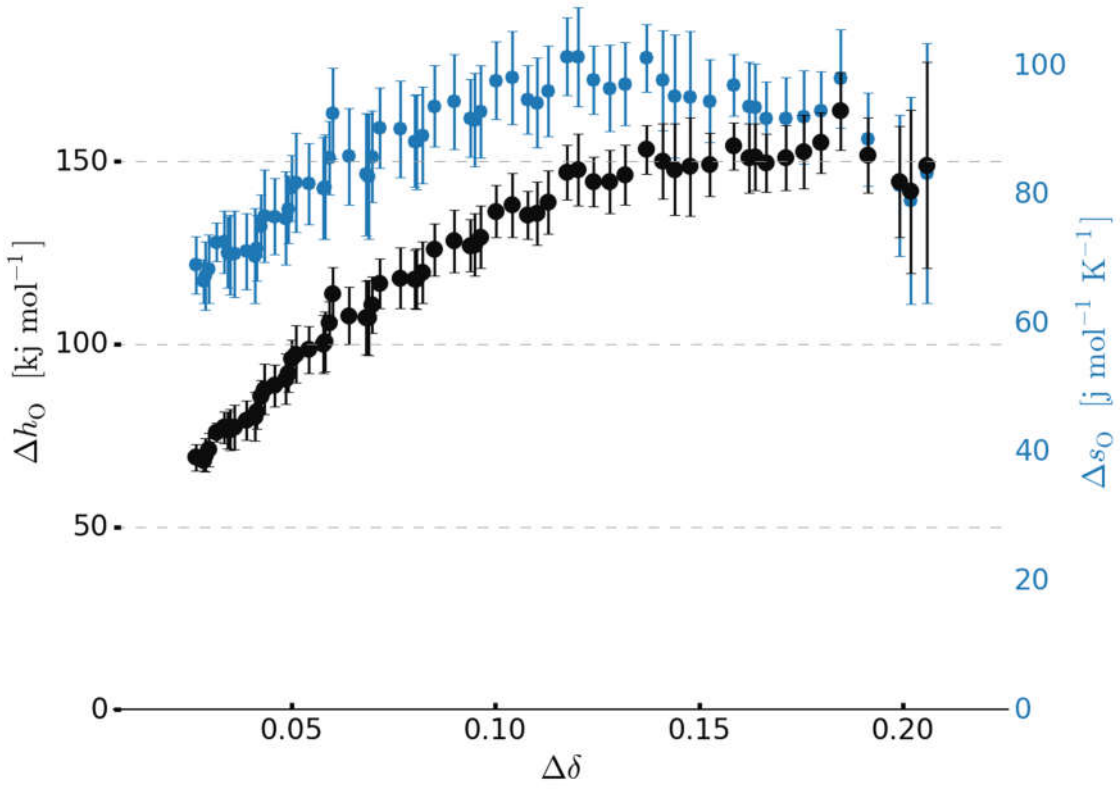
150
100
50
0
Δh_O [kj mol^{-1}]
100
80
60
40
20
0
Δs_O [j mol^{-1} K^{-1}]
0.05
0.10
0.15
0.20
Δδ

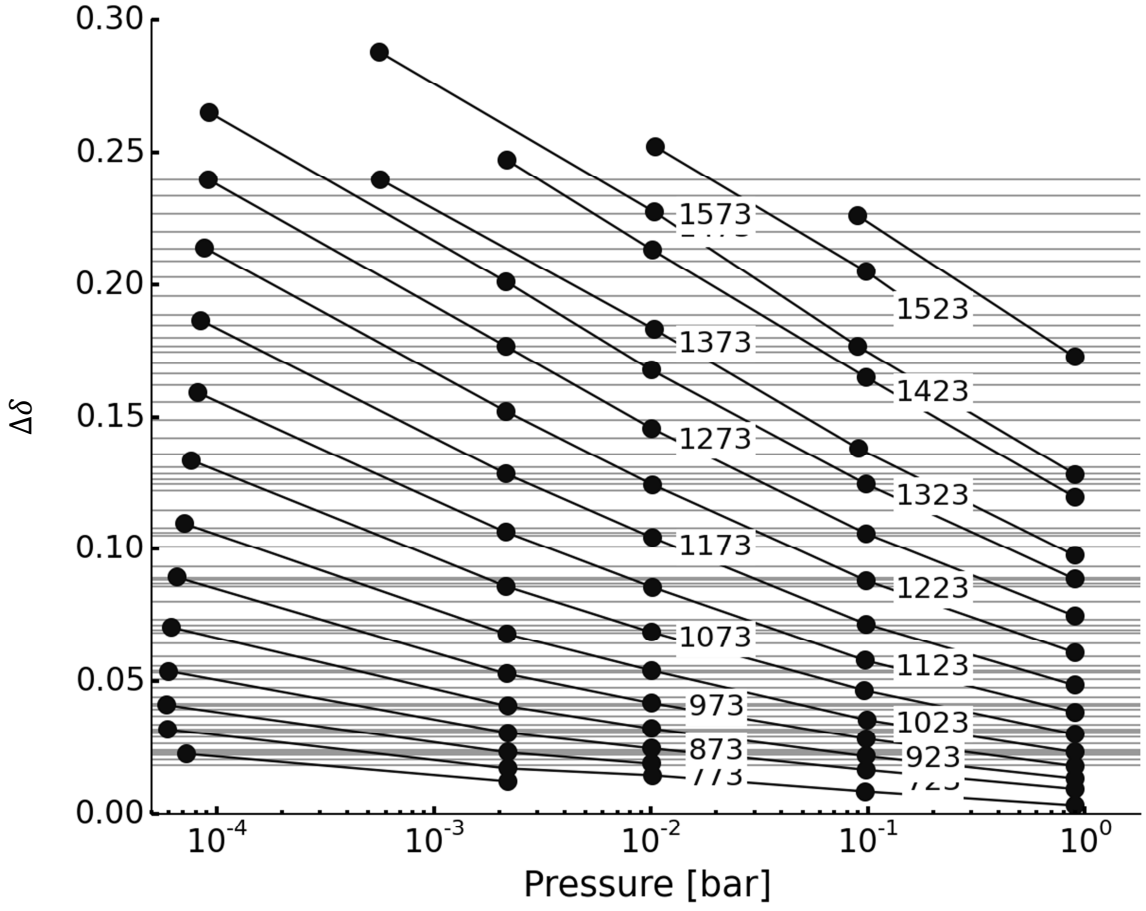
0.30
0.25
0.20
0.15
0.10
0.05
0.00
Δδ
1573
1523
1373
1423
1273
1323
1173
1223
1073
1123
973
1023
873
923
10^{-4}
10^{-3}
10^{-2}
10^{-1}
10^{0}
Pressure [bar]

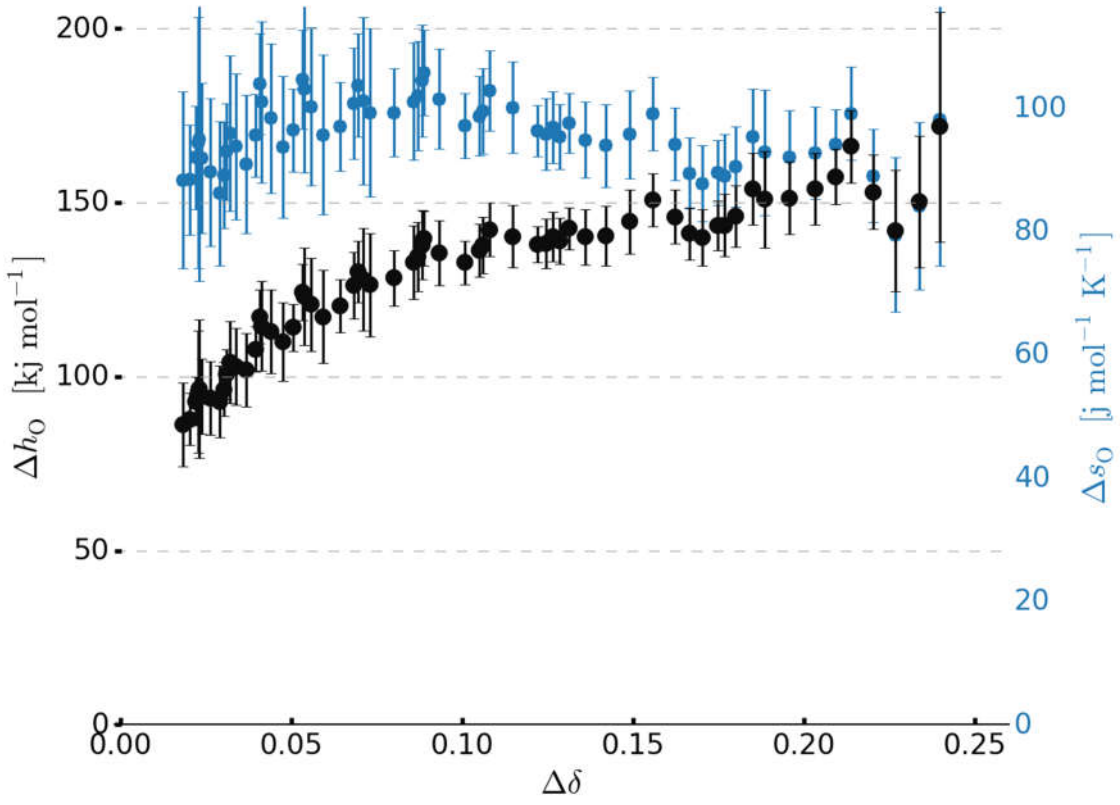
200
150
100
50
0
Δh_O [kj mol^{-1}]
100
80
60
40
20
0
Δs_O [j mol^{-1} K^{-1}]
0.00
0.05
0.10
0.15
0.20
0.25
Δδ

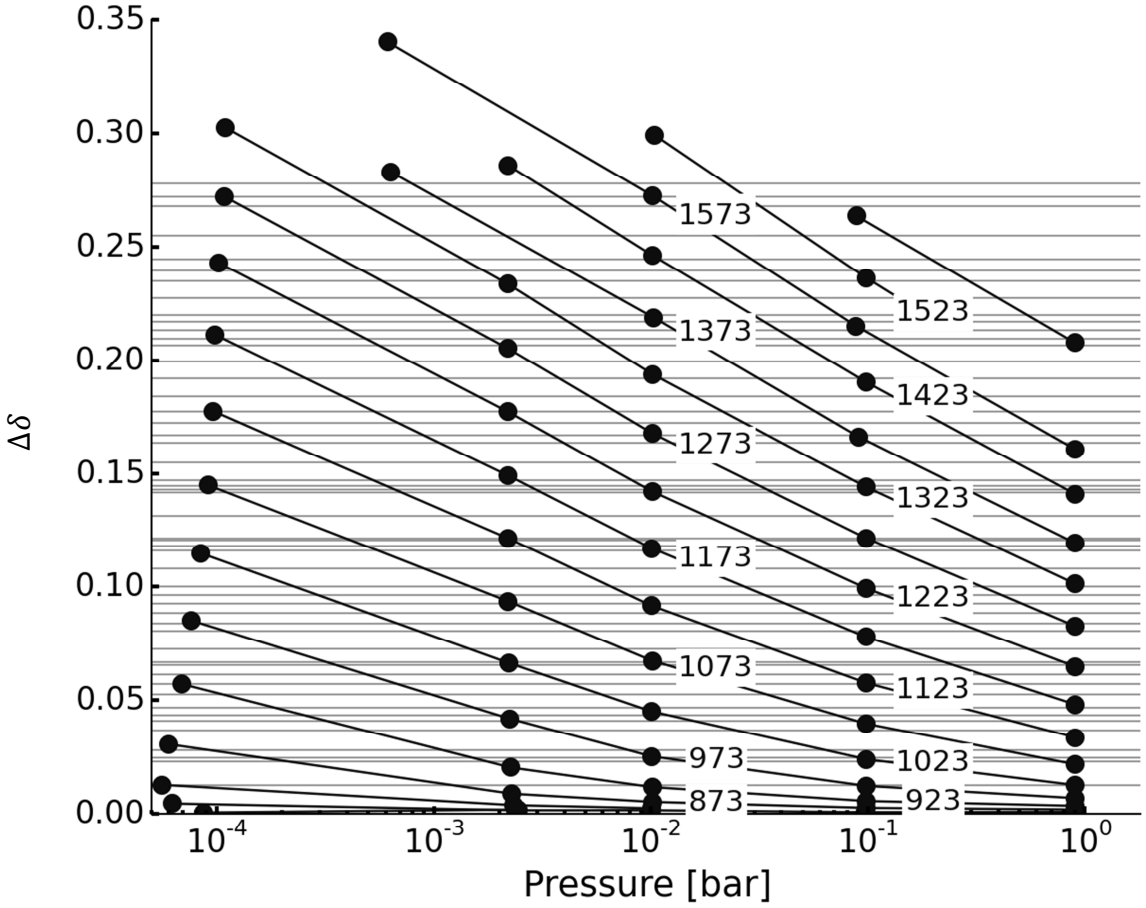
0.35
0.30
0.25
0.20
0.15
0.10
0.05
0.00
$\Delta\delta$
1573
1523
1373
1423
1273
1323
1173
1223
1073
1123
973
1023
873
923
10^{-4}
10^{-3}
10^{-2}
10^{-1}
10^{0}
Pressure [bar]

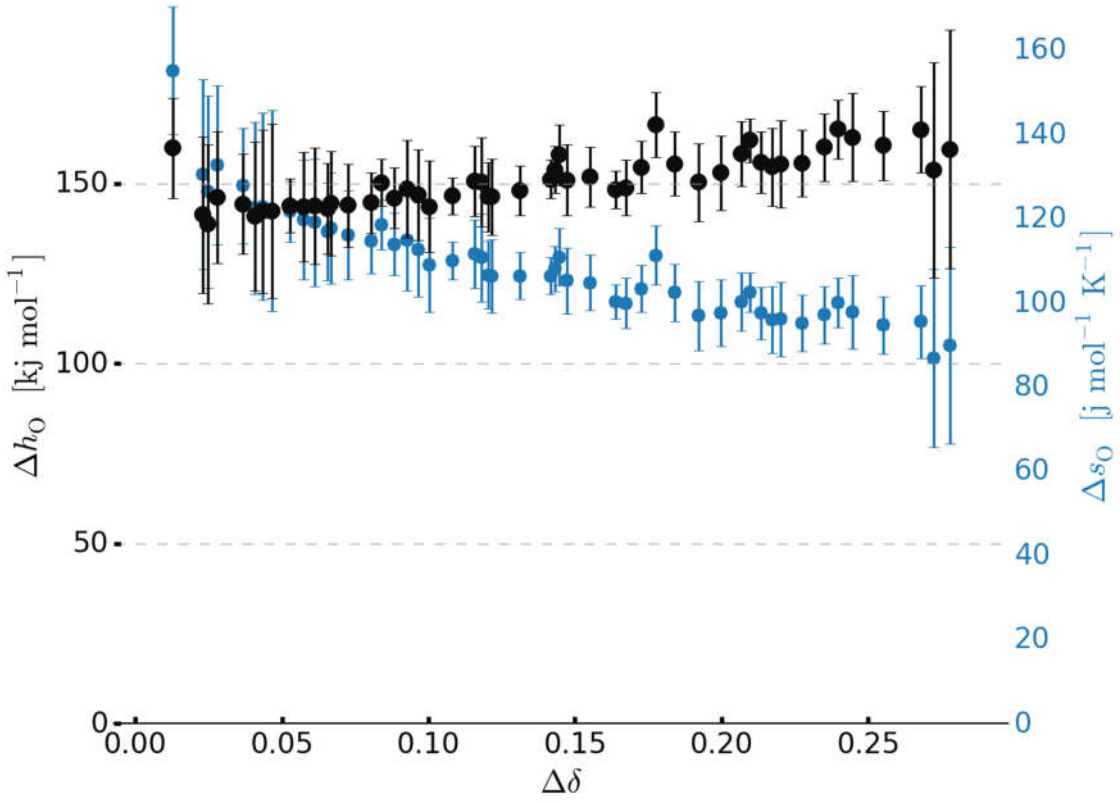
150
100
50
0
Δh_O [kj mol^{-1}]
160
140
120
100
80
60
40
20
0
Δs_O [j mol^{-1} K^{-1}]
0.00
0.05
0.10
0.15
0.20
0.25
$\Delta\delta$

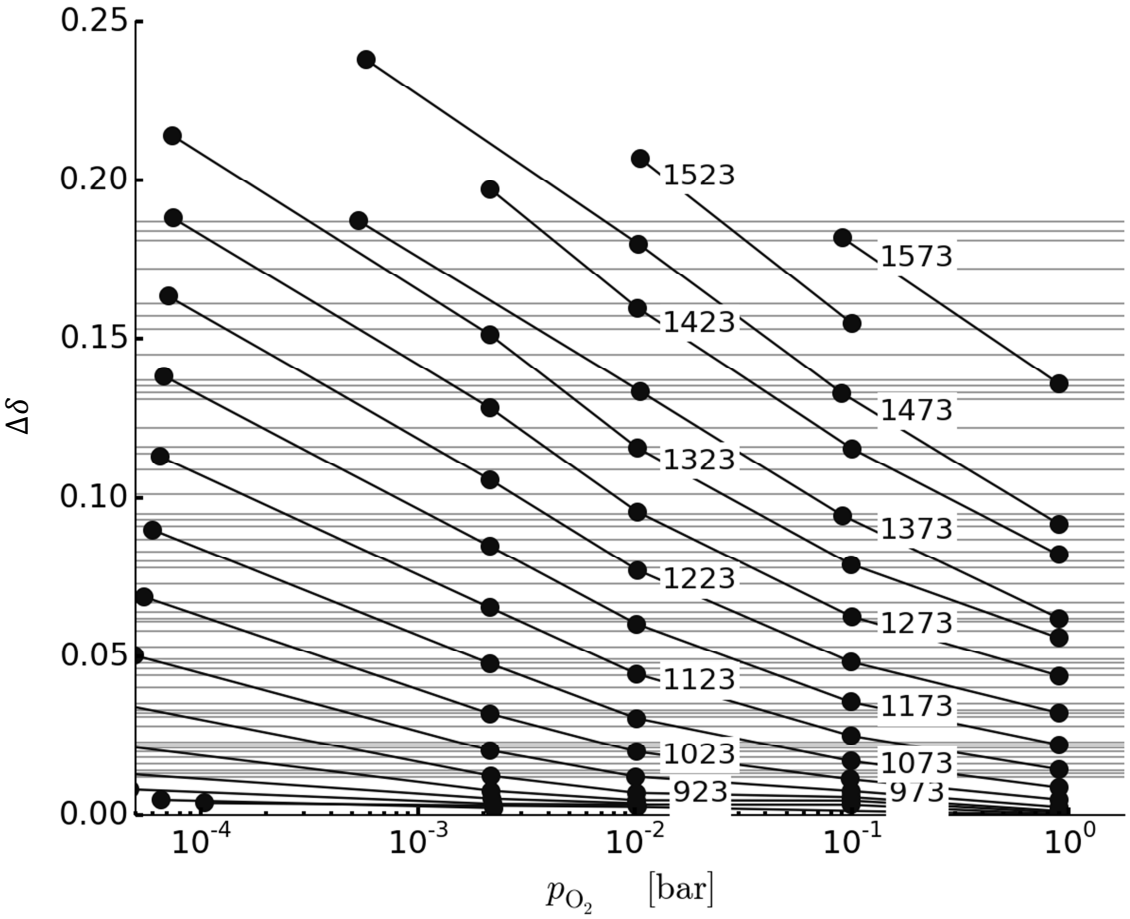
0.25
0.20
0.15
0.10
0.05
0.00
$\Delta\delta$
1523
1573
1423
1473
1323
1373
1223
1273
1123
1173
1023
1073
923
973
10^{-4}
10^{-3}
10^{-2}
10^{-1}
10^{0}
p_{O_2} [bar]

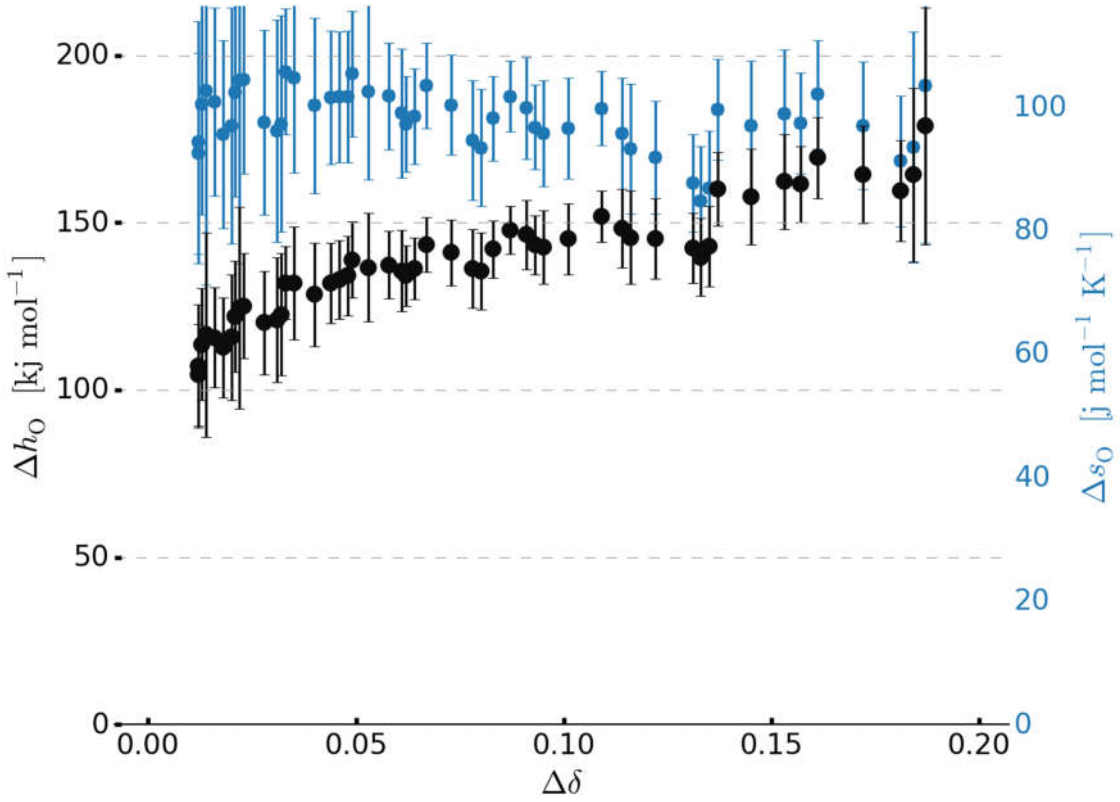
200
150
100
50
0
Δh_O [kj mol^{-1}]
100
80
60
40
20
0
Δs_O [j mol^{-1} K^{-1}]
0.00
0.05
0.10
0.15
0.20
$\Delta\delta$

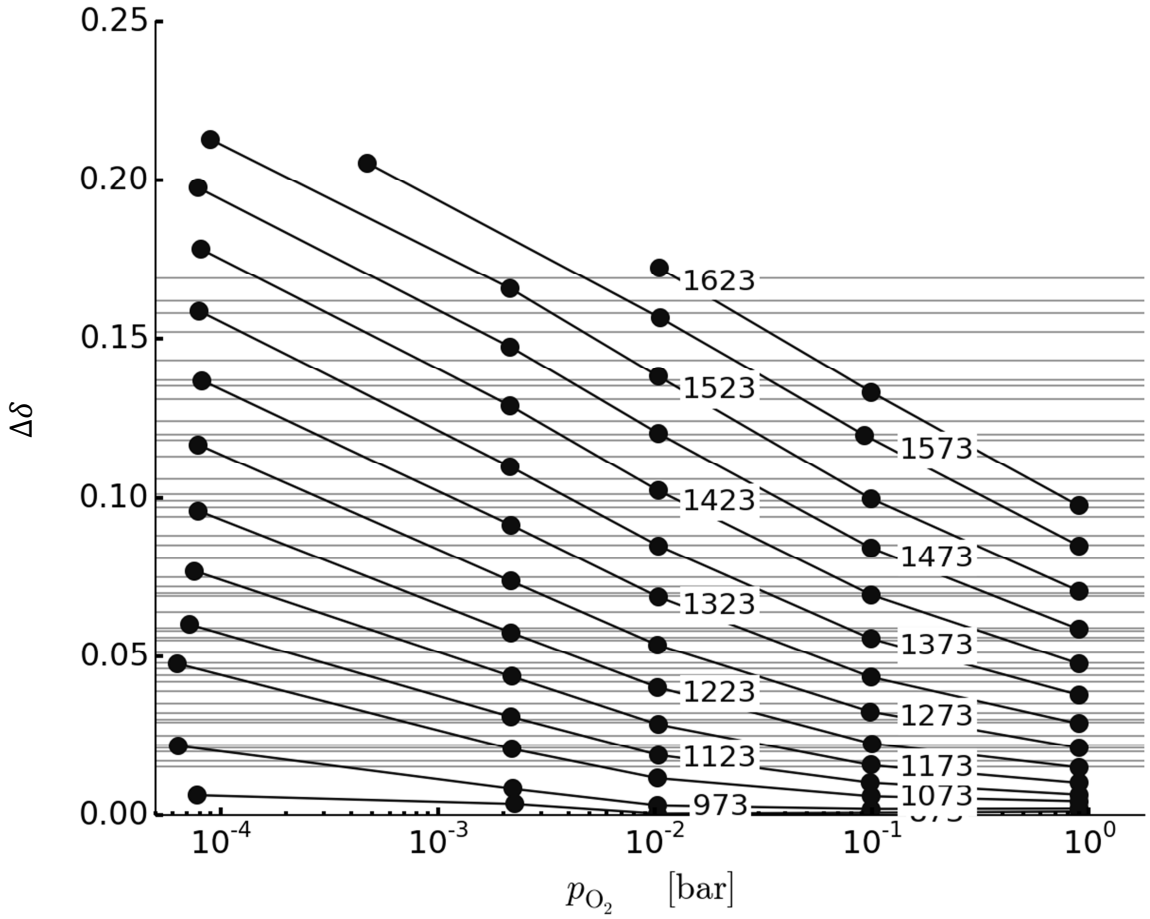
0.25
0.20
0.15
0.10
0.05
0.00
$\Delta\delta$
1623
1523
1573
1423
1473
1323
1373
1223
1273
1123
1173
973
1073
10^{-4}
10^{-3}
10^{-2}
10^{-1}
10^{0}
p_{O_2} [bar]

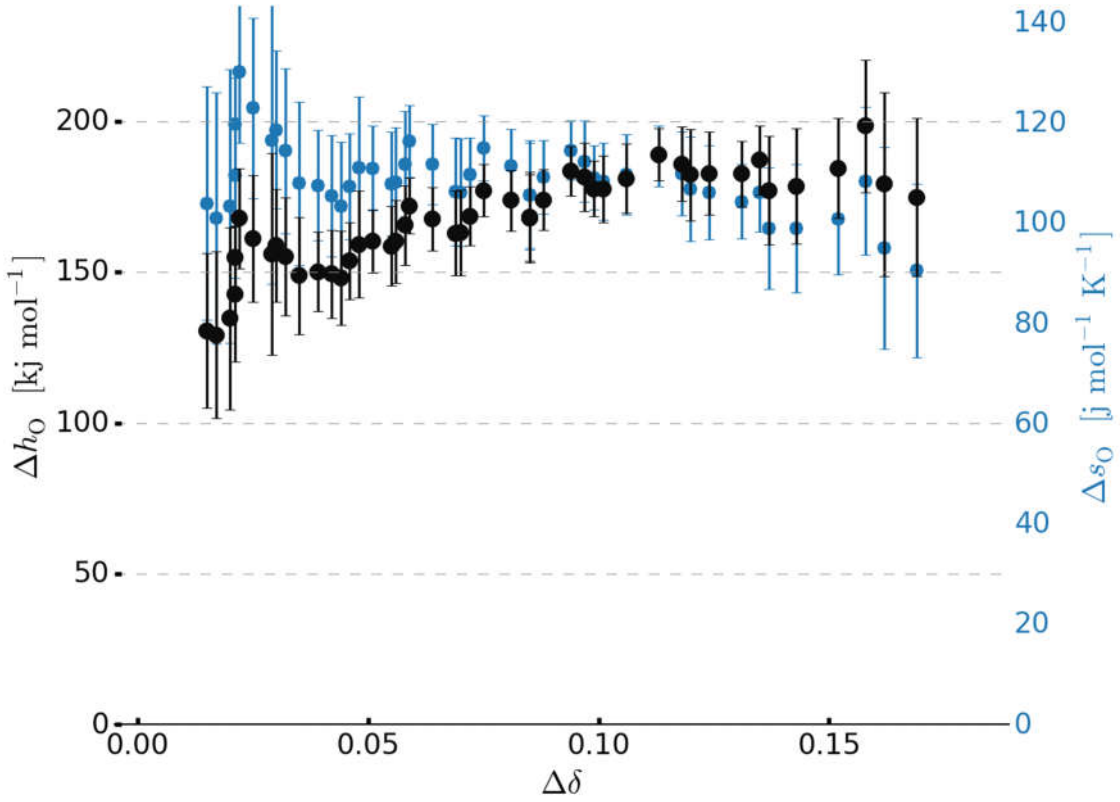
200
150
100
50
0
Δh_O [kj mol^{-1}]
140
120
100
80
60
40
20
0
Δs_O [j mol^{-1} K^{-1}]
0.00
0.05
0.10
0.15
$\Delta\delta$

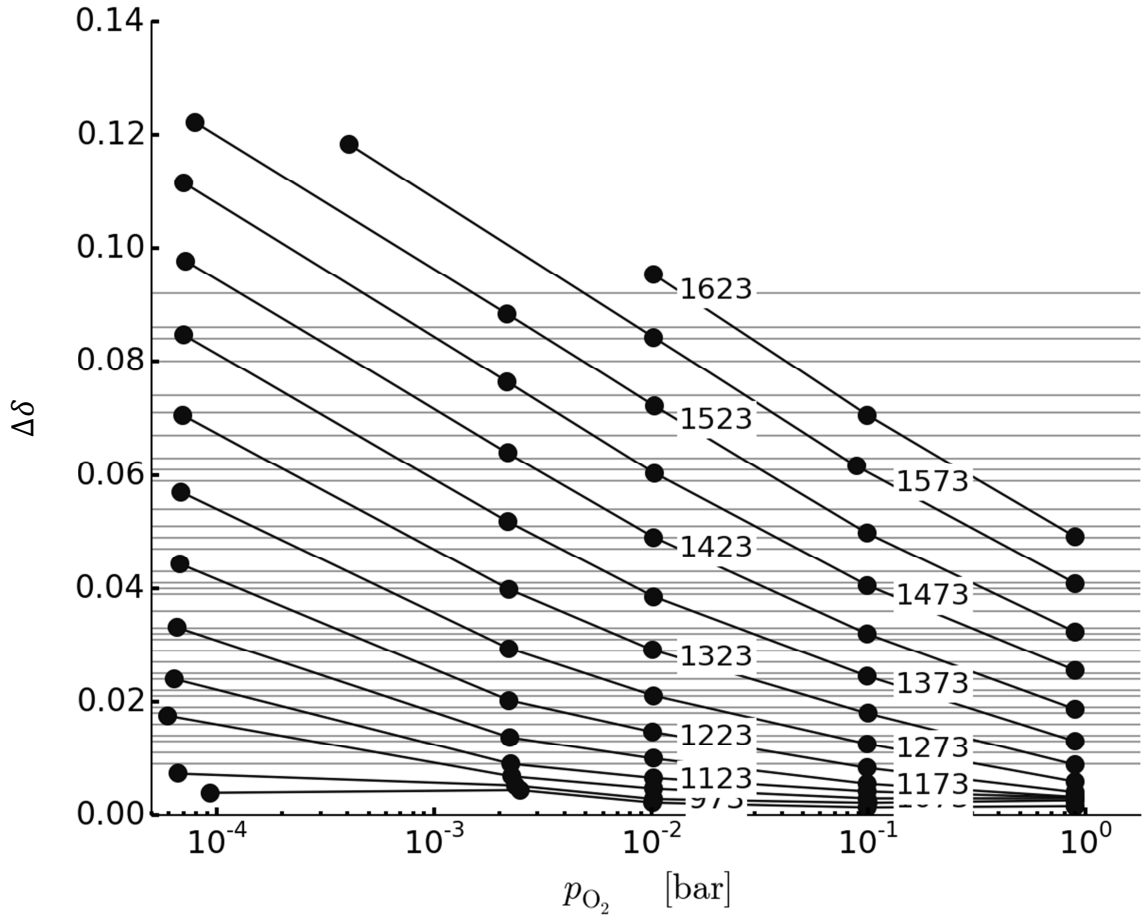
0.14
0.12
0.10
0.08
0.06
0.04
0.02
0.00
$\Delta\delta$
1623
1523
1573
1423
1473
1323
1373
1223
1273
1123
1173
10^{-4}
10^{-3}
10^{-2}
10^{-1}
10^{0}
p_{O_2} [bar]

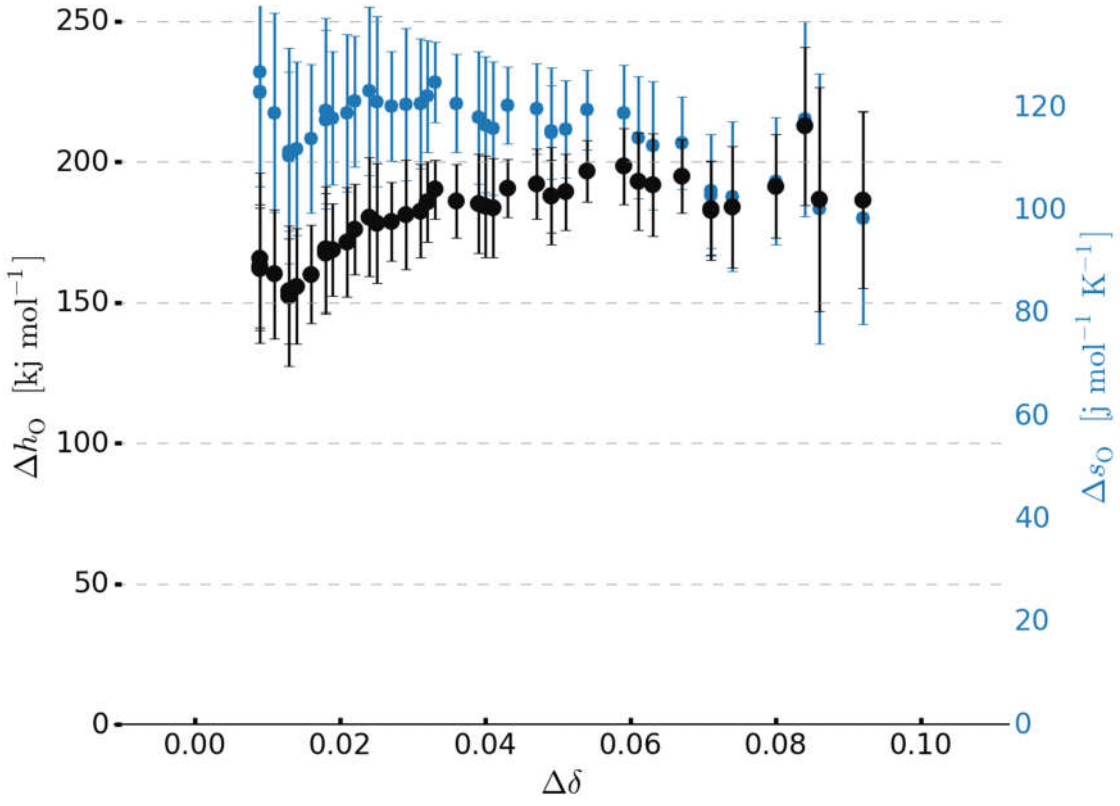
250
200
150
100
50
0
Δh_O [kj mol^{-1}]
120
100
80
60
40
20
0
Δs_O [j mol^{-1} K^{-1}]
0.00
0.02
0.04
0.06
0.08
0.10
$\Delta\delta$

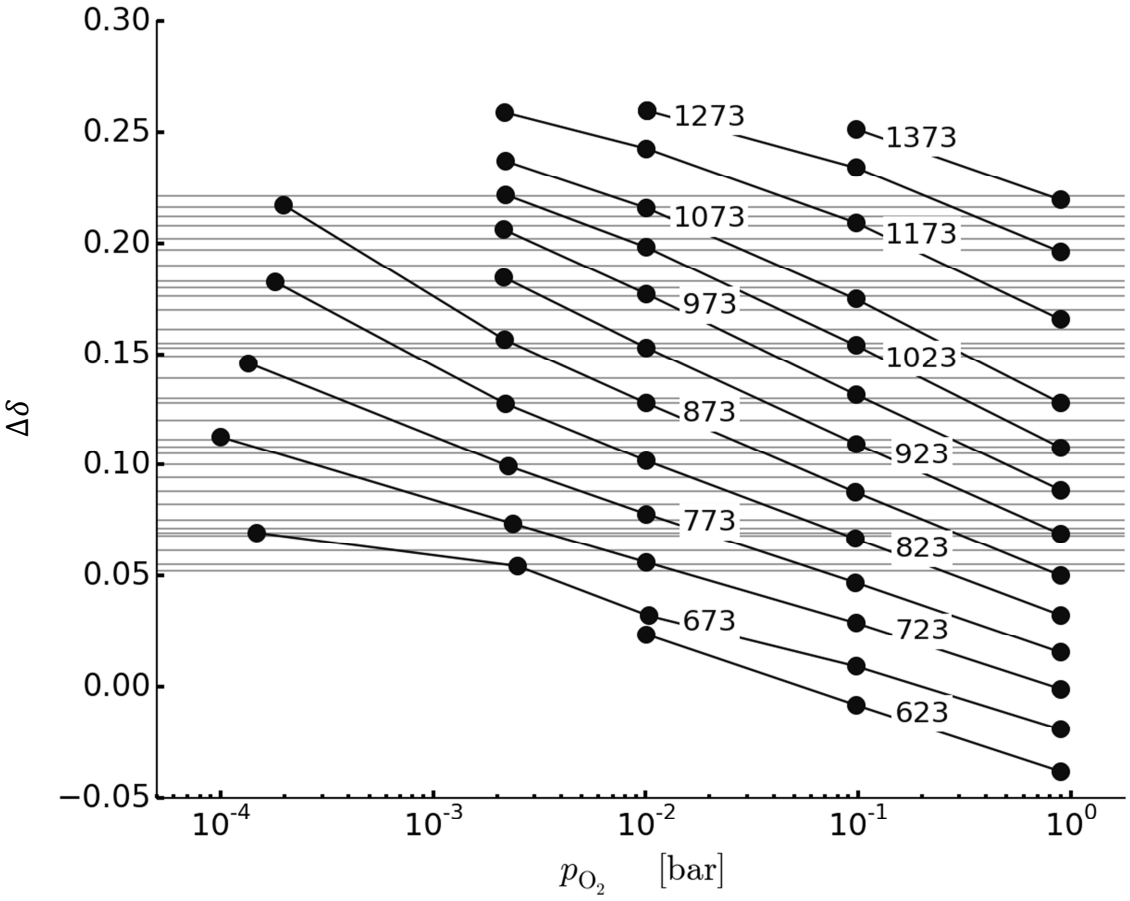
0.30
0.25
0.20
0.15
0.10
0.05
0.00
−0.05
Δδ
1273
1373
1073
1173
973
1023
873
923
773
823
673
723
623
10-4
10-3
10-2
10-1
100
pO2 [bar]

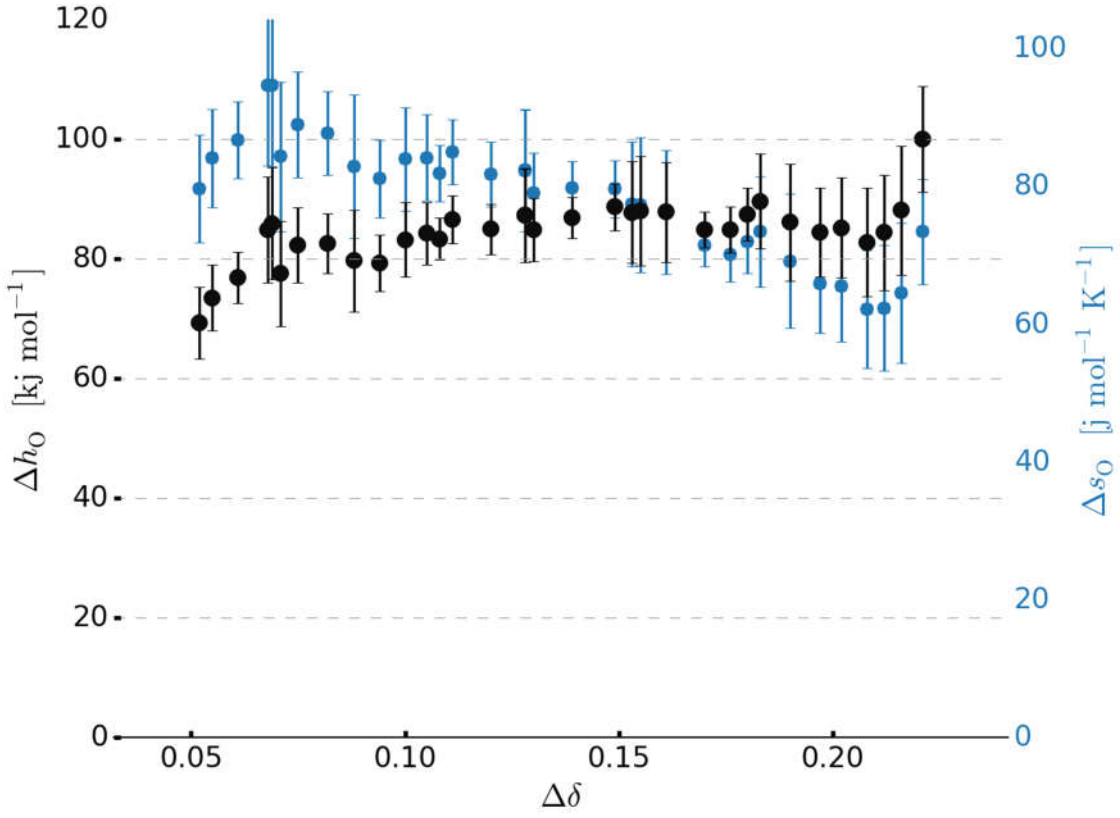
120
100
80
60
40
20
0
100
80
60
40
20
0
ΔhO [kj mol−1]
ΔsO [j mol−1 K−1]
0.05
0.10
0.15
0.20
Δδ

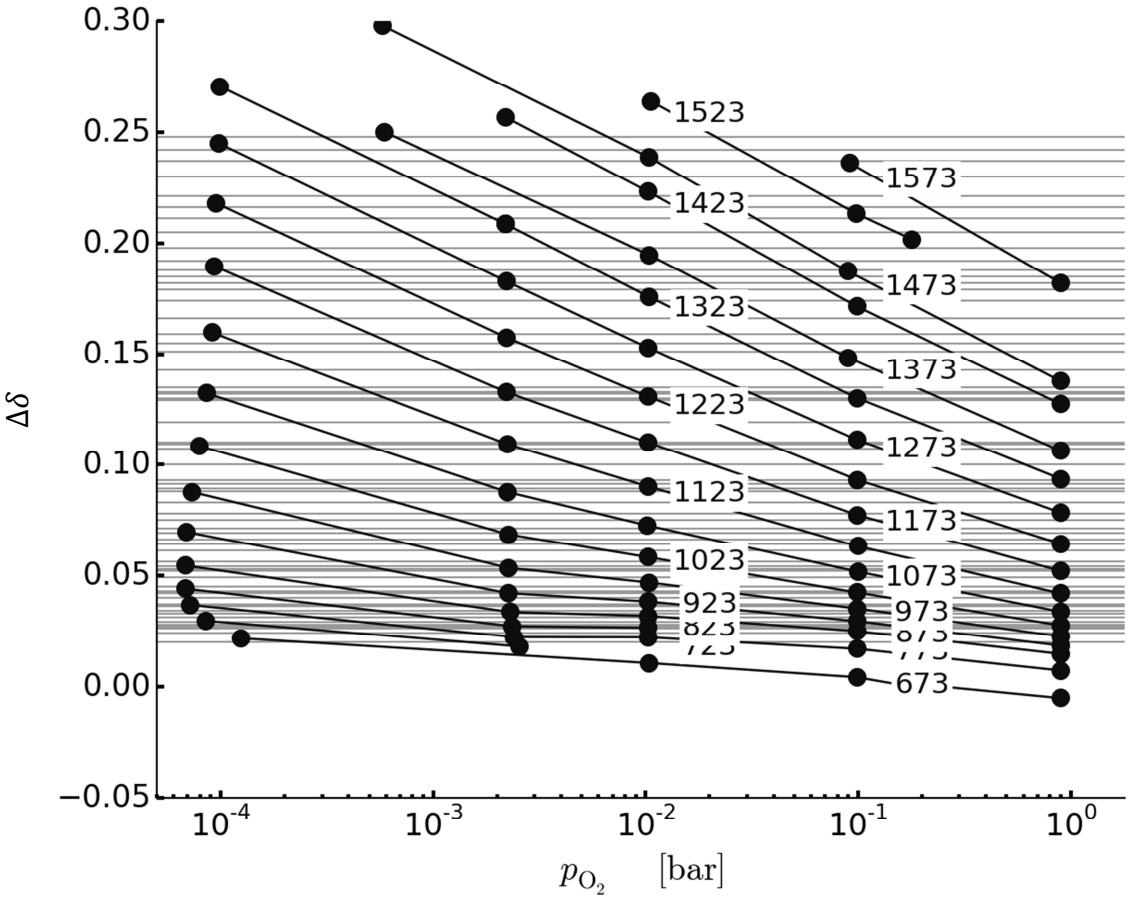
0.30
0.25
0.20
0.15
0.10
0.05
0.00
−0.05
Δδ
1523
1573
1423
1473
1323
1373
1223
1273
1123
1173
1023
1073
923
973
673
10-4
10-3
10-2
10-1
100
p_{O_2} [bar]

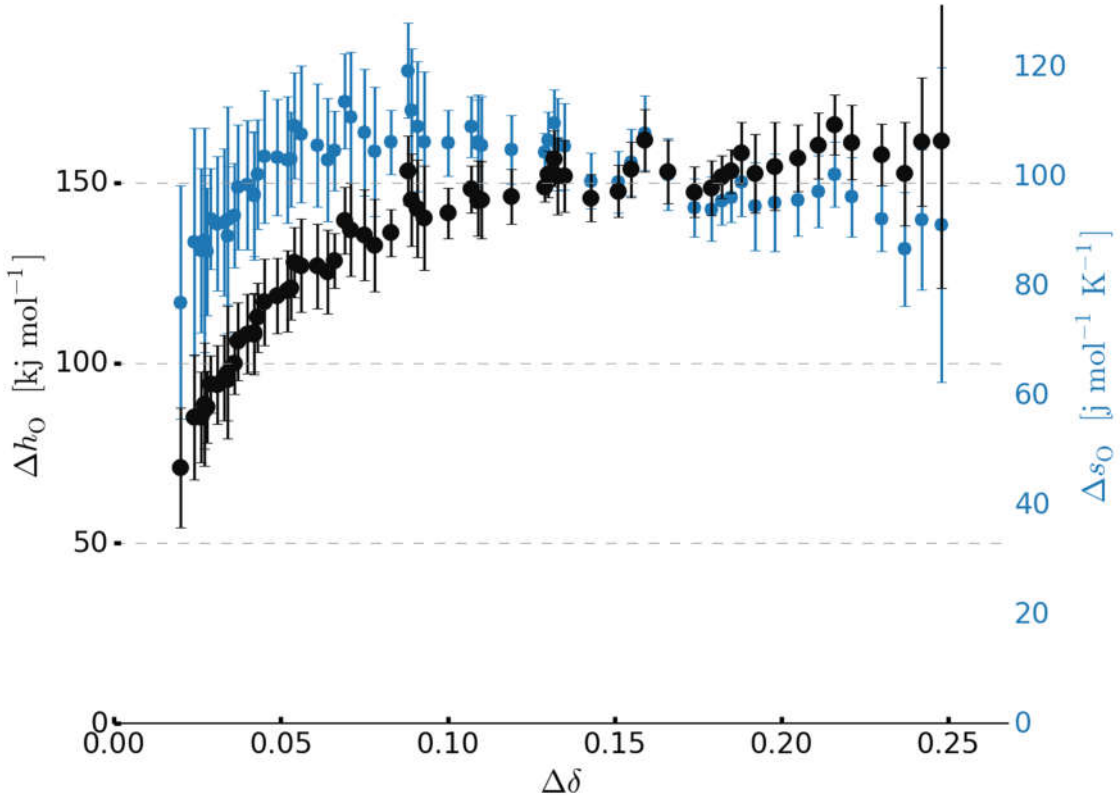
150
100
50
0
Δh_O [kj mol^{-1}]
120
100
80
60
40
20
0
Δs_O [j mol^{-1} K^{-1}]
0.00
0.05
0.10
0.15
0.20
0.25
Δδ

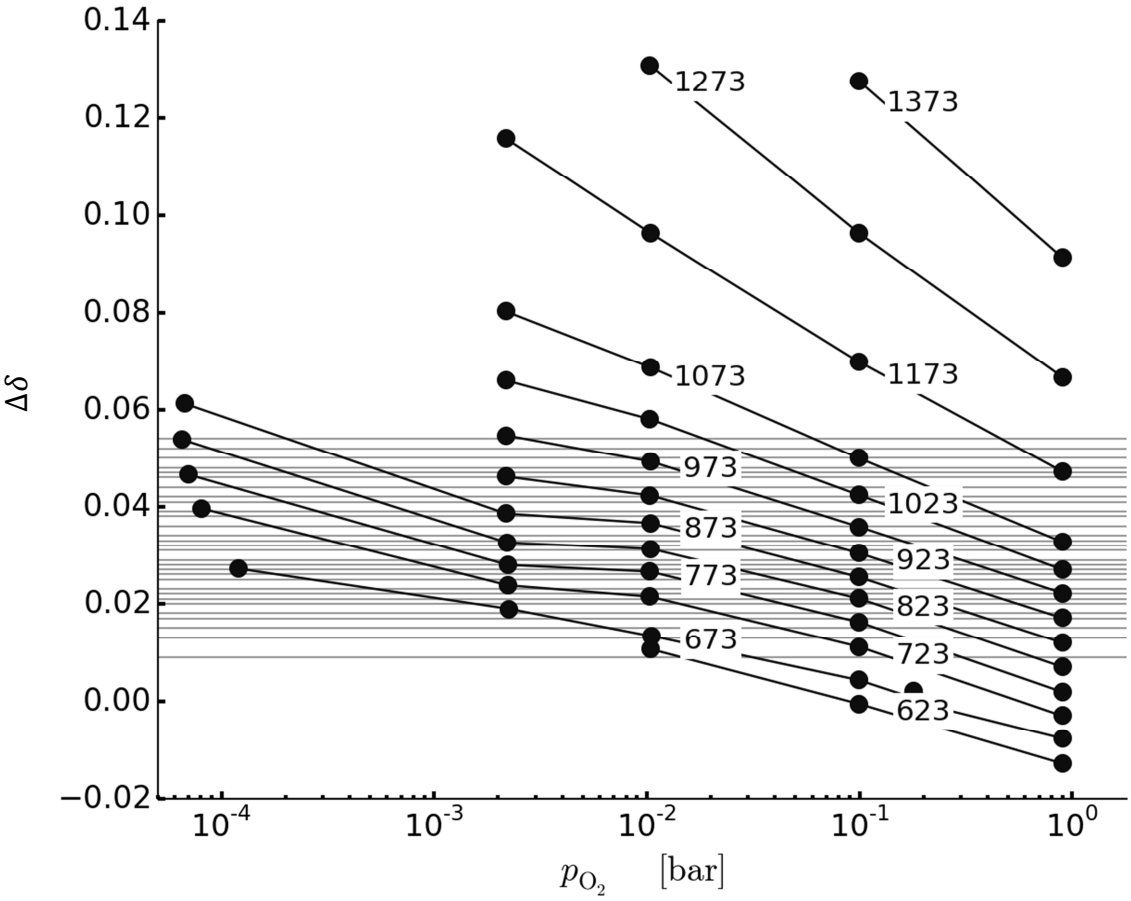
0.14
0.12
0.10
0.08
0.06
0.04
0.02
0.00
−0.02
Δδ
1273
1373
1073
1173
973
1023
873
923
773
823
673
723
623
10^{-4}
10^{-3}
10^{-2}
10^{-1}
10^{0}
p_{O_2} [bar]

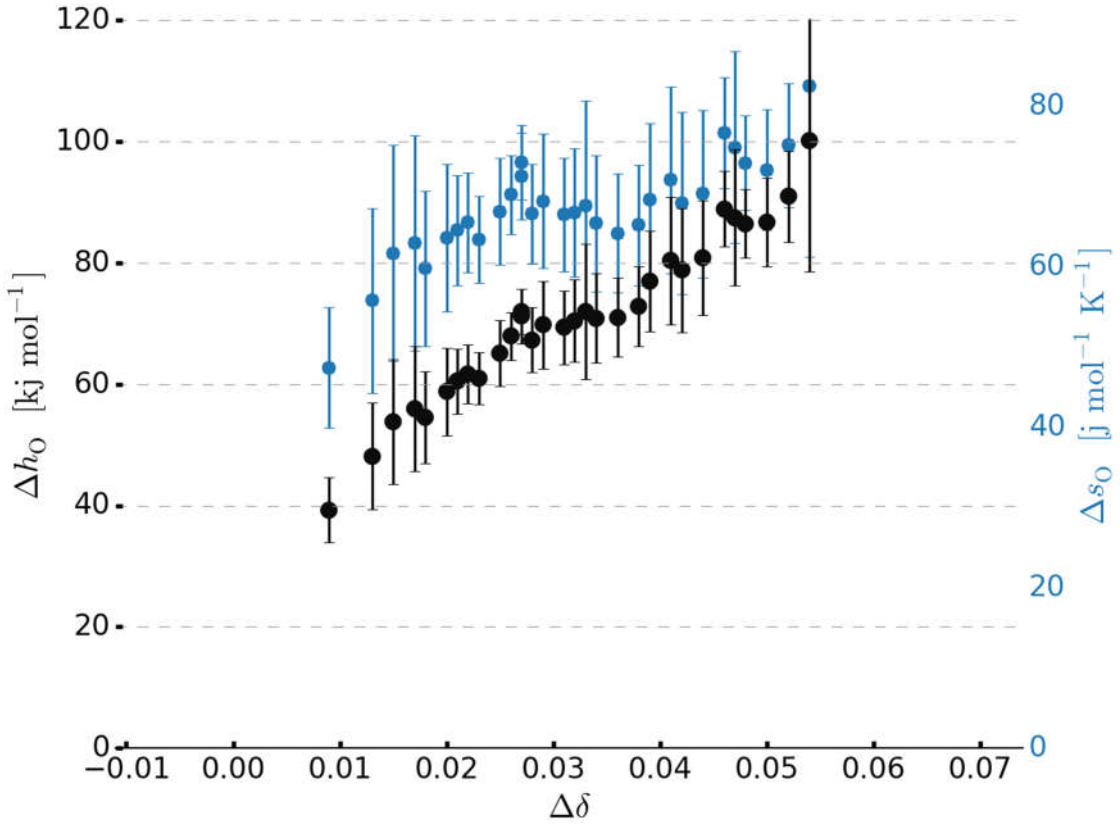
120
100
80
60
40
20
0
Δh_O [kj mol^{-1}]
80
60
40
20
0
Δs_O [j mol^{-1} K^{-1}]
−0.01
0.00
0.01
0.02
0.03
0.04
0.05
0.06
0.07
Δδ

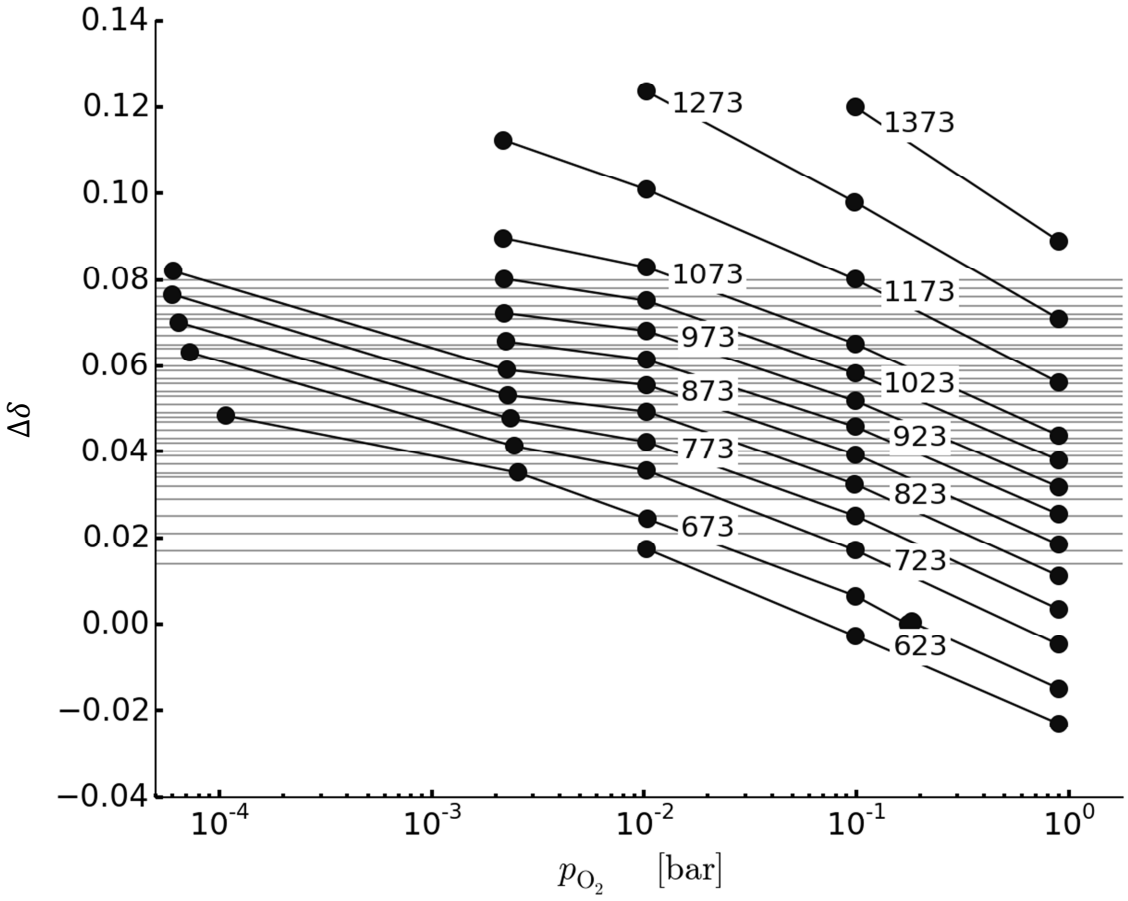
0.14
0.12
0.10
0.08
0.06
0.04
0.02
0.00
−0.02
−0.04
Δδ
1273
1373
1073
1173
973
1023
873
923
773
823
673
723
623
10-4
10-3
10-2
10-1
10^0
p_{O_2} [bar]

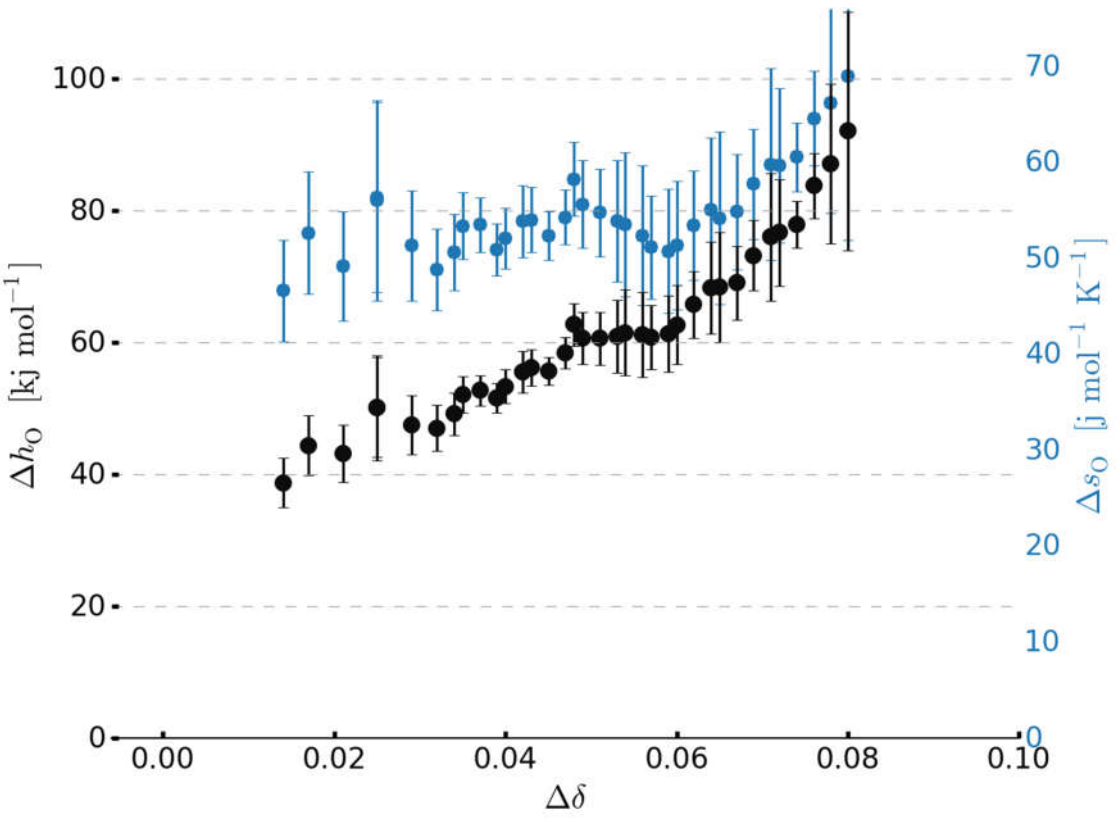
100
80
60
40
20
0
Δh_O [kj mol^{-1}]
70
60
50
40
30
20
10
0
Δs_O [j mol^{-1} K^{-1}]
0.00
0.02
0.04
0.06
0.08
0.10
Δδ

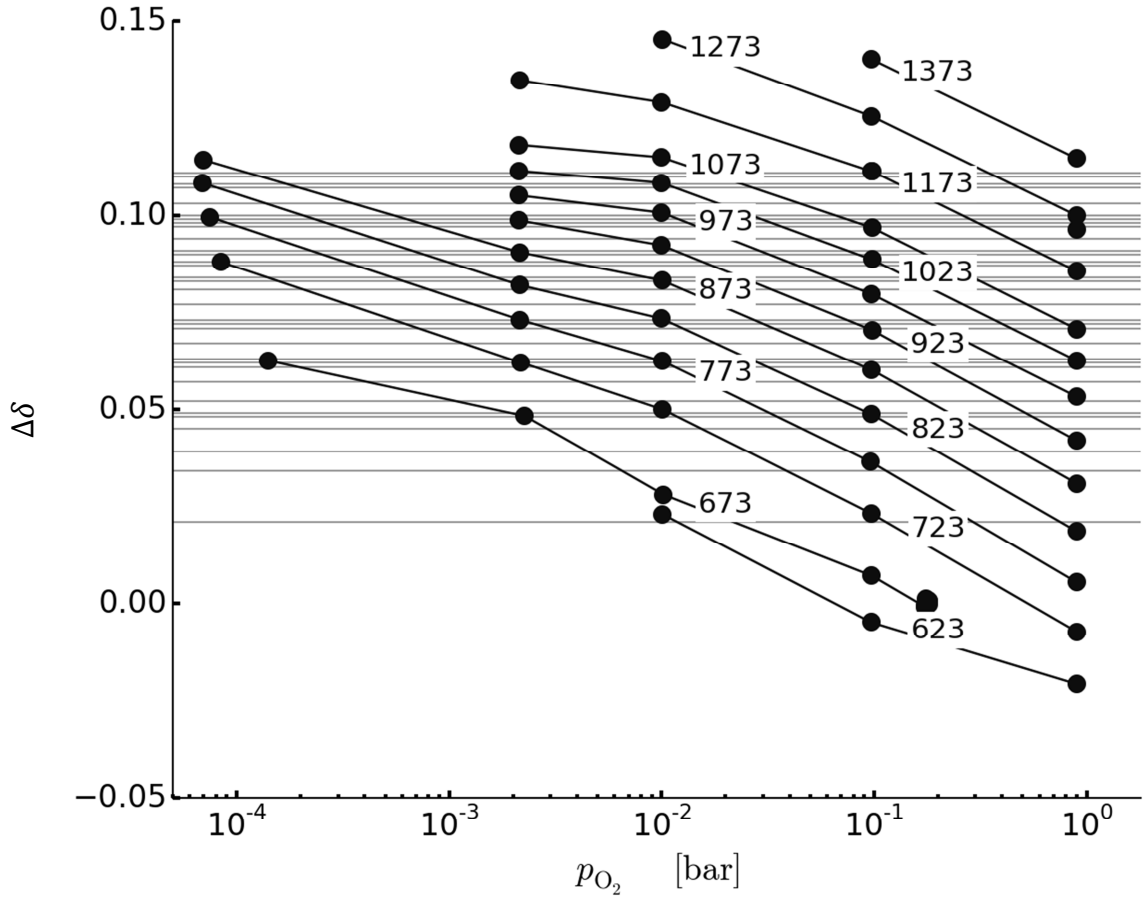
0.15
0.10
0.05
0.00
−0.05
Δδ
1273
1373
1073
1173
973
1023
873
923
773
823
673
723
623
10^-4
10^-3
10^-2
10^-1
10^0
p_O2 [bar]

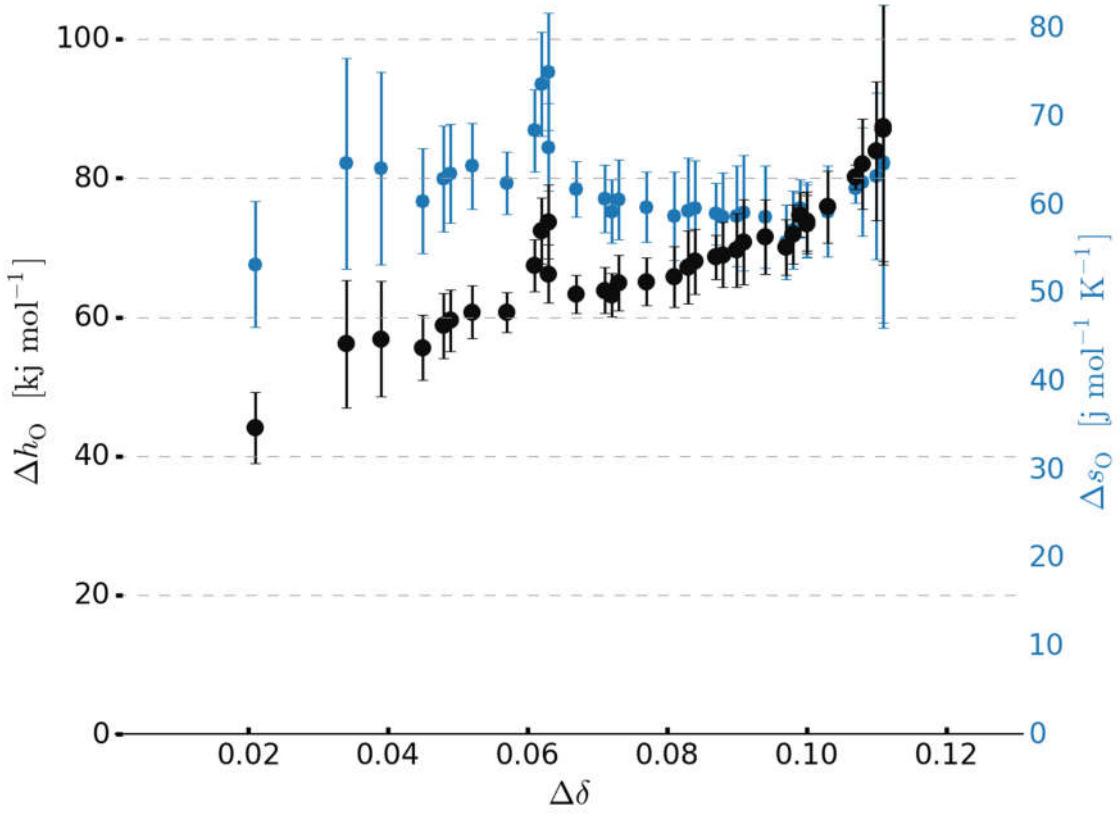
100
80
60
40
20
0
Δh_O [kj mol^-1]
80
70
60
50
40
30
20
10
0
Δs_O [j mol^-1 K^-1]
0.02
0.04
0.06
0.08
0.10
0.12
Δδ

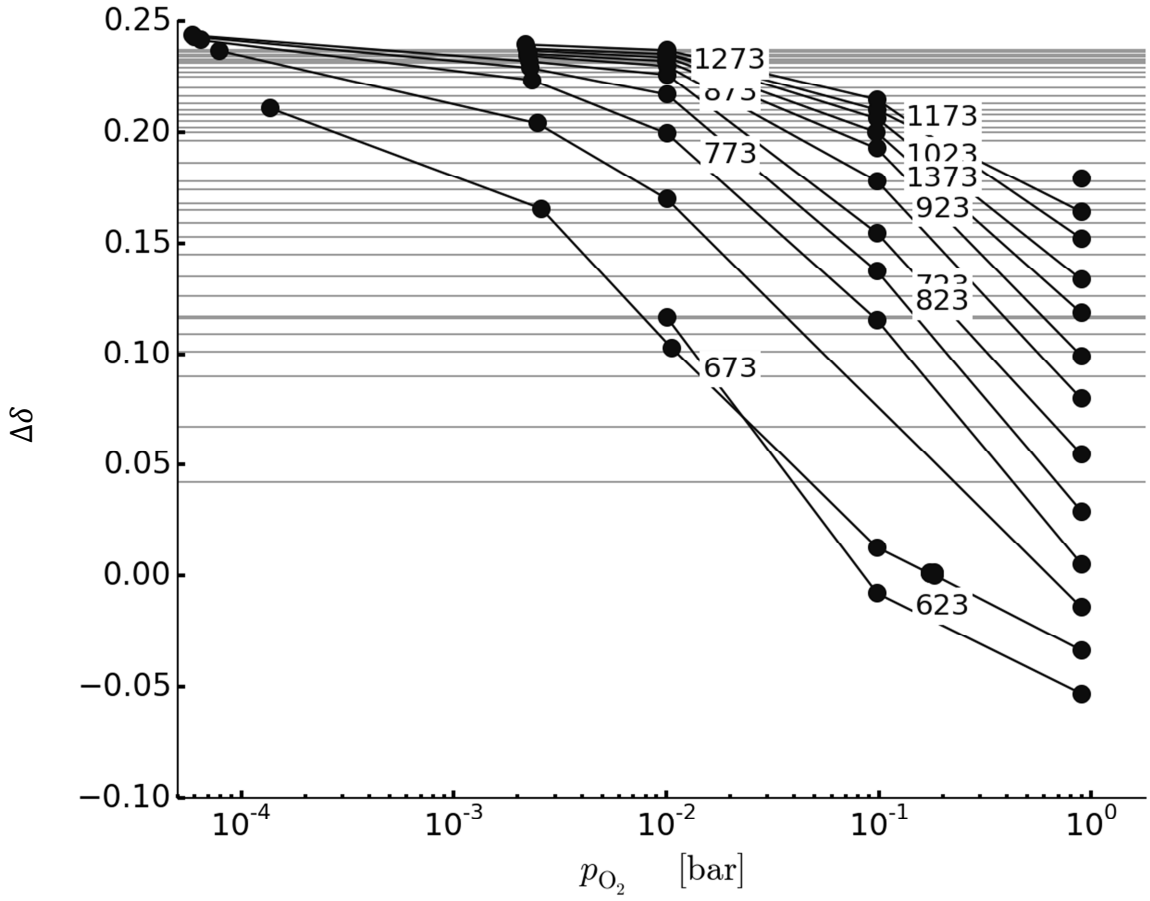
0.25
0.20
0.15
0.10
0.05
0.00
−0.05
−0.10
Δδ
1273
1173
773
1373
923
823
673
623
10^-4
10^-3
10^-2
10^-1
10^0
p_O2 [bar]

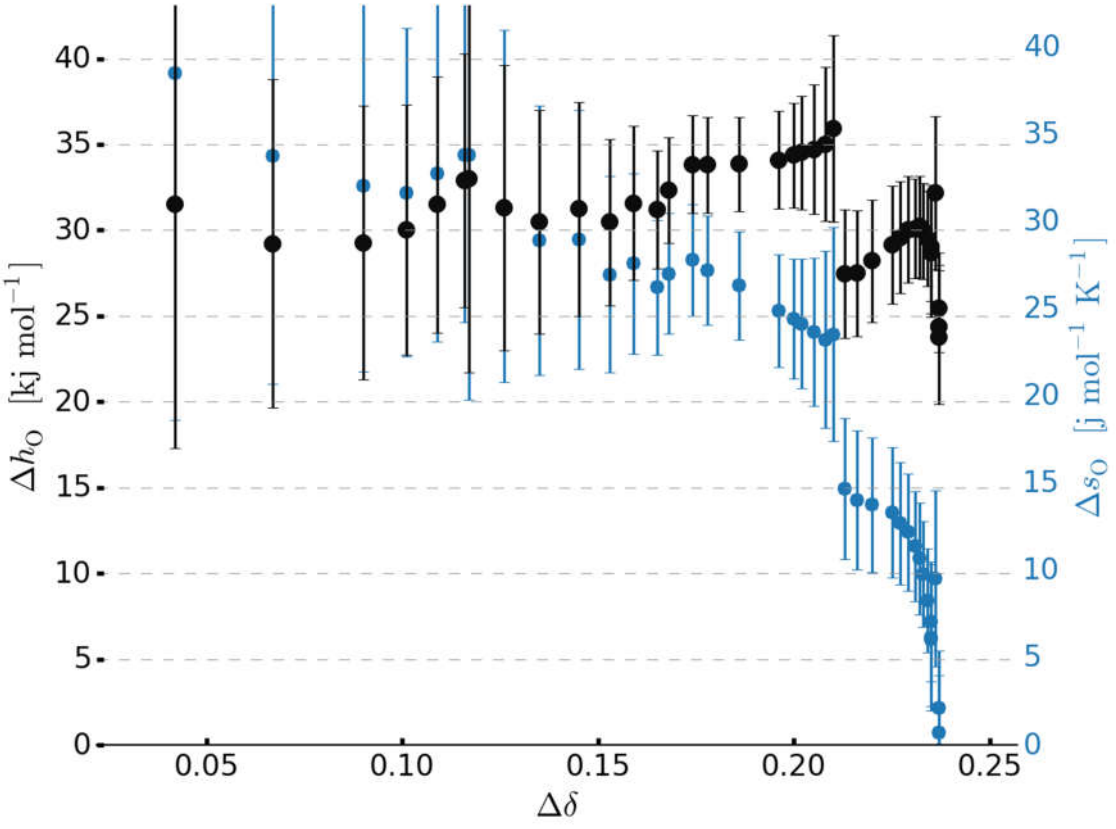
40
35
30
25
20
15
10
5
0
Δh_O [kj mol^-1]
Δs_O [j mol^-1 K^-1]
0.05
0.10
0.15
0.20
0.25
Δδ

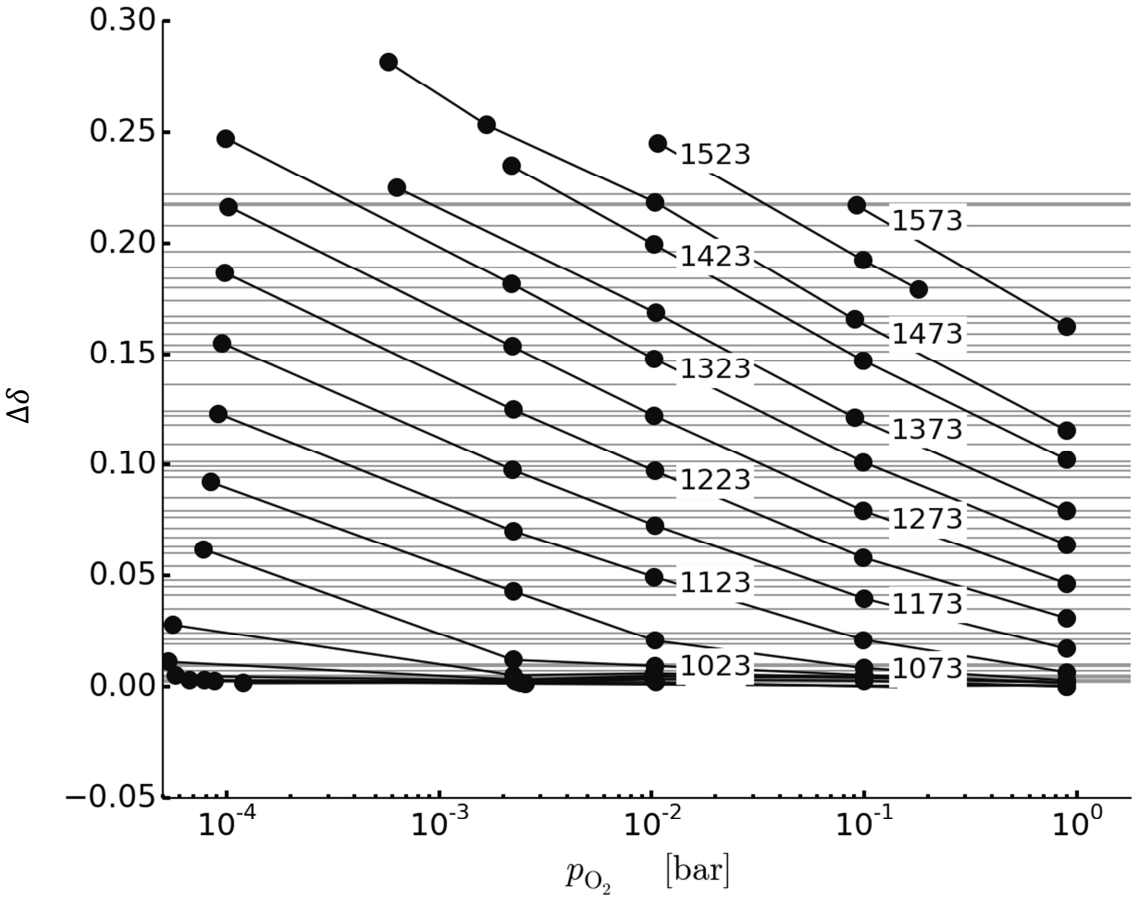
0.30
0.25
0.20
0.15
0.10
0.05
0.00
−0.05
Δδ
1523
1573
1423
1473
1323
1373
1223
1273
1123
1173
1023
1073
10-4
10-3
10-2
10-1
100
p_{O_2} [bar]

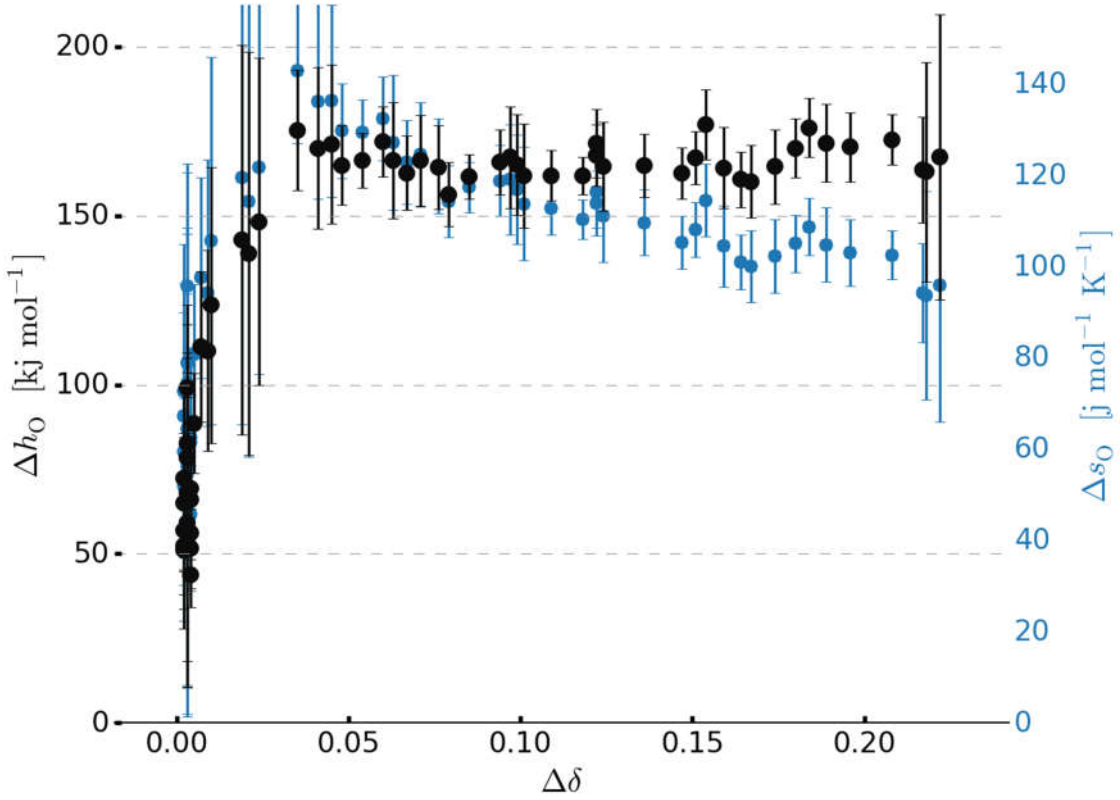
200
150
100
50
0
Δh_O [kj mol^{-1}]
140
120
100
80
60
40
20
0
Δs_O [j mol^{-1} K^{-1}]
0.00
0.05
0.10
0.15
0.20
Δδ

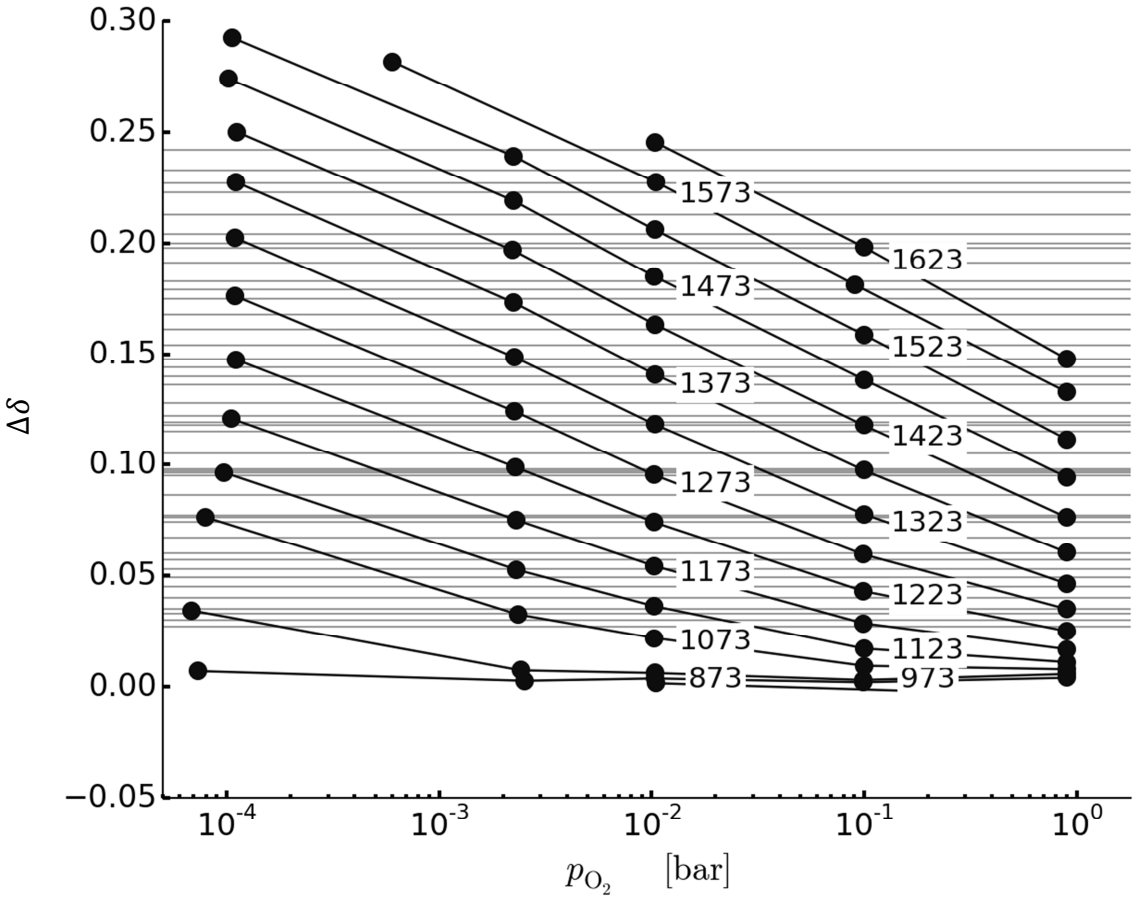
0.30
0.25
0.20
0.15
0.10
0.05
0.00
−0.05
Δδ
1573
1623
1473
1523
1373
1423
1273
1323
1173
1223
1073
1123
873
973
10-4
10-3
10-2
10-1
100
pO2 [bar]

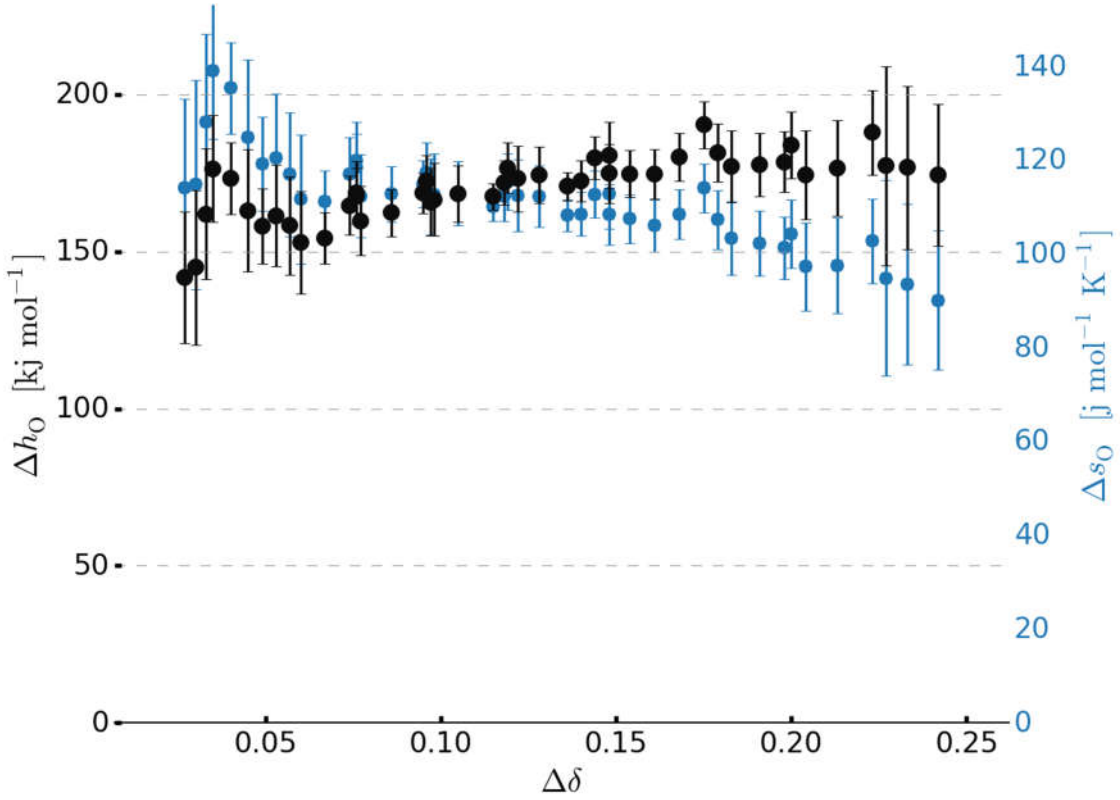
200
150
100
50
0
ΔhO [kj mol−1]
140
120
100
80
60
40
20
0
ΔsO [j mol−1 K−1]
0.05
0.10
0.15
0.20
0.25
Δδ

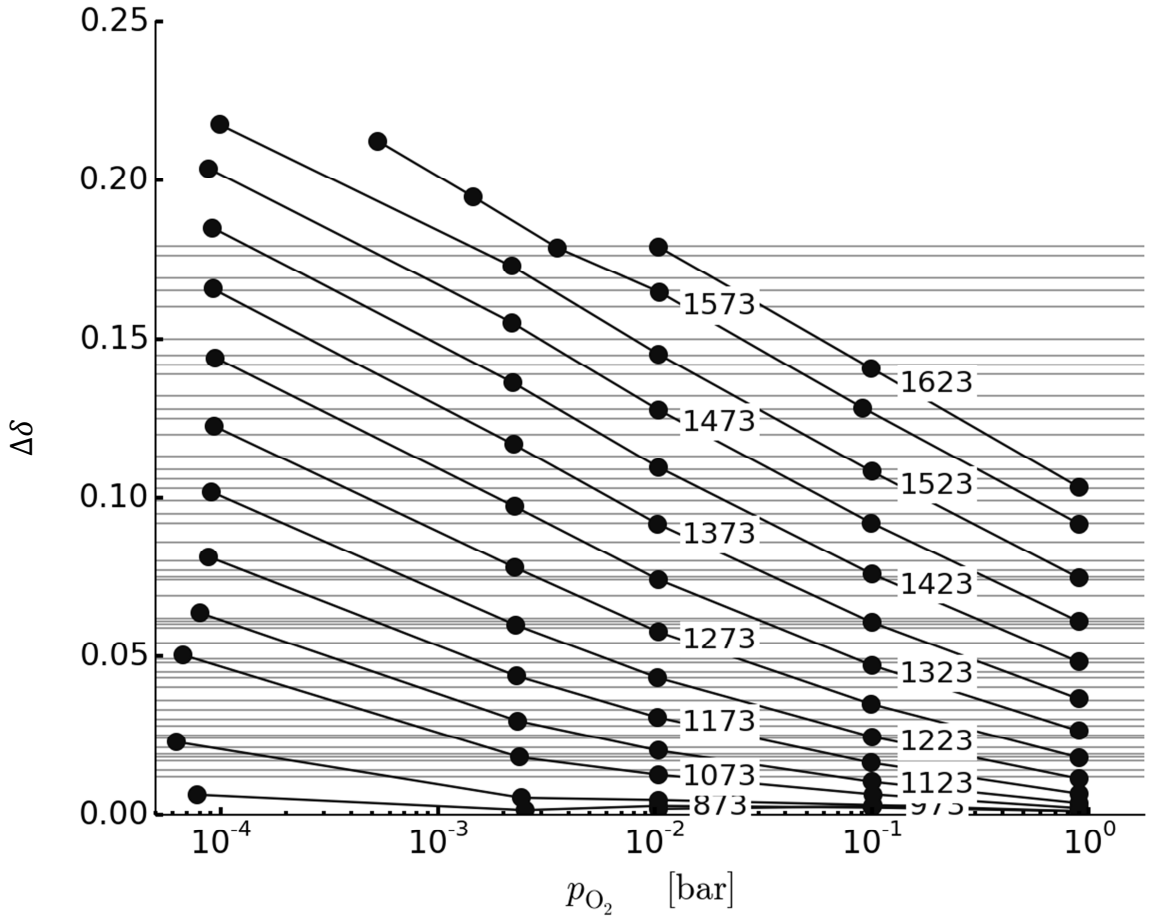
0.25
0.20
0.15
0.10
0.05
0.00
$\Delta\delta$
1573
1623
1473
1523
1373
1423
1273
1323
1173
1223
1073
1123
873
10^{-4}
10^{-3}
10^{-2}
10^{-1}
10^{0}
p_{O_2} [bar]

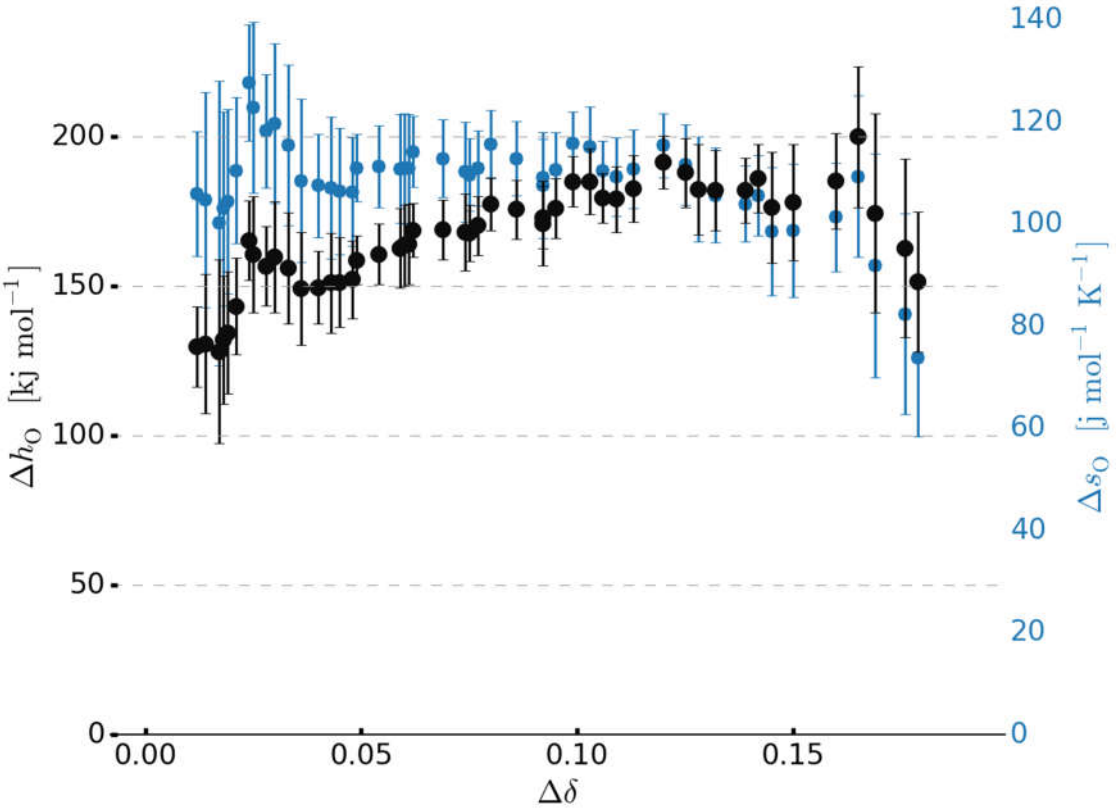
200
150
100
50
0
Δh_O [kj mol^{-1}]
140
120
100
80
60
40
20
0
Δs_O [j mol^{-1} K^{-1}]
0.00
0.05
0.10
0.15
$\Delta\delta$

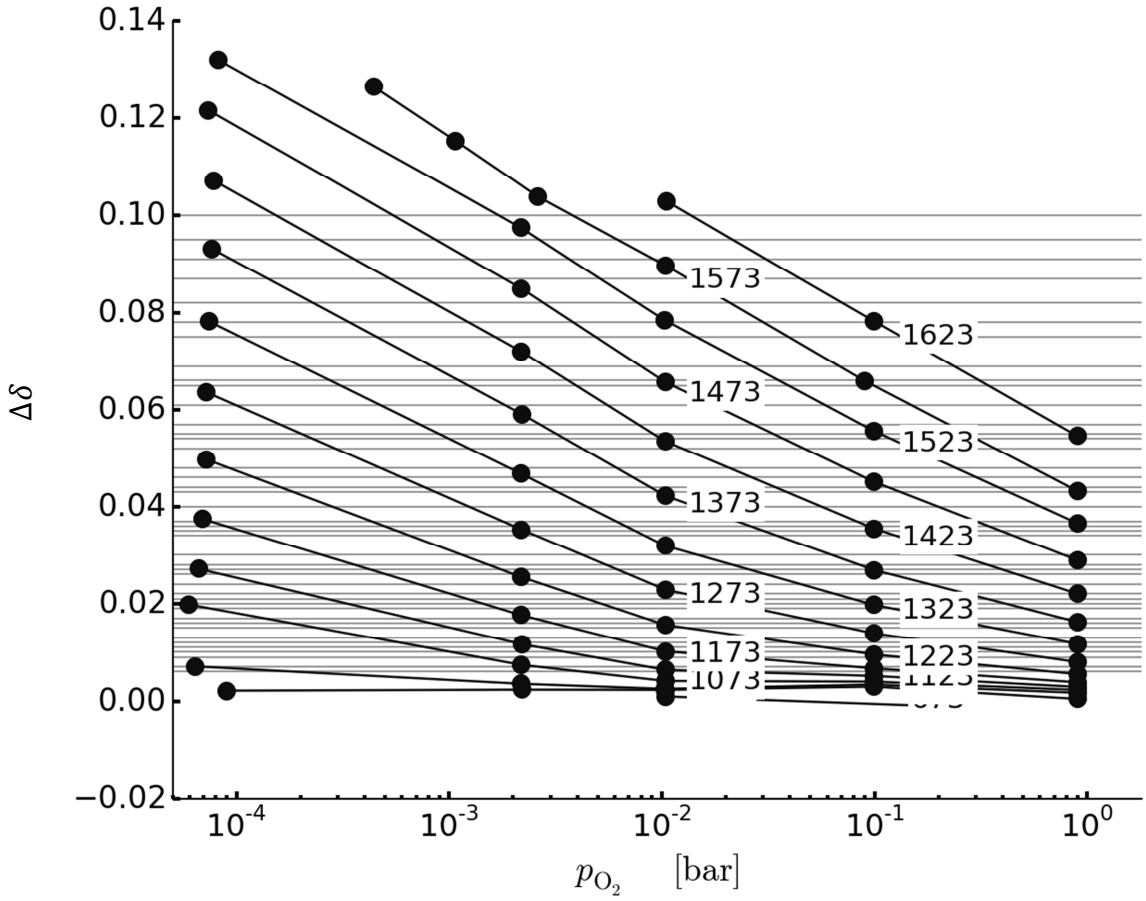
0.14
0.12
0.10
0.08
0.06
0.04
0.02
0.00
−0.02
Δδ
1573
1623
1473
1523
1373
1423
1273
1323
1173
1223
10^{-4}
10^{-3}
10^{-2}
10^{-1}
10^{0}
p_{O_2} [bar]

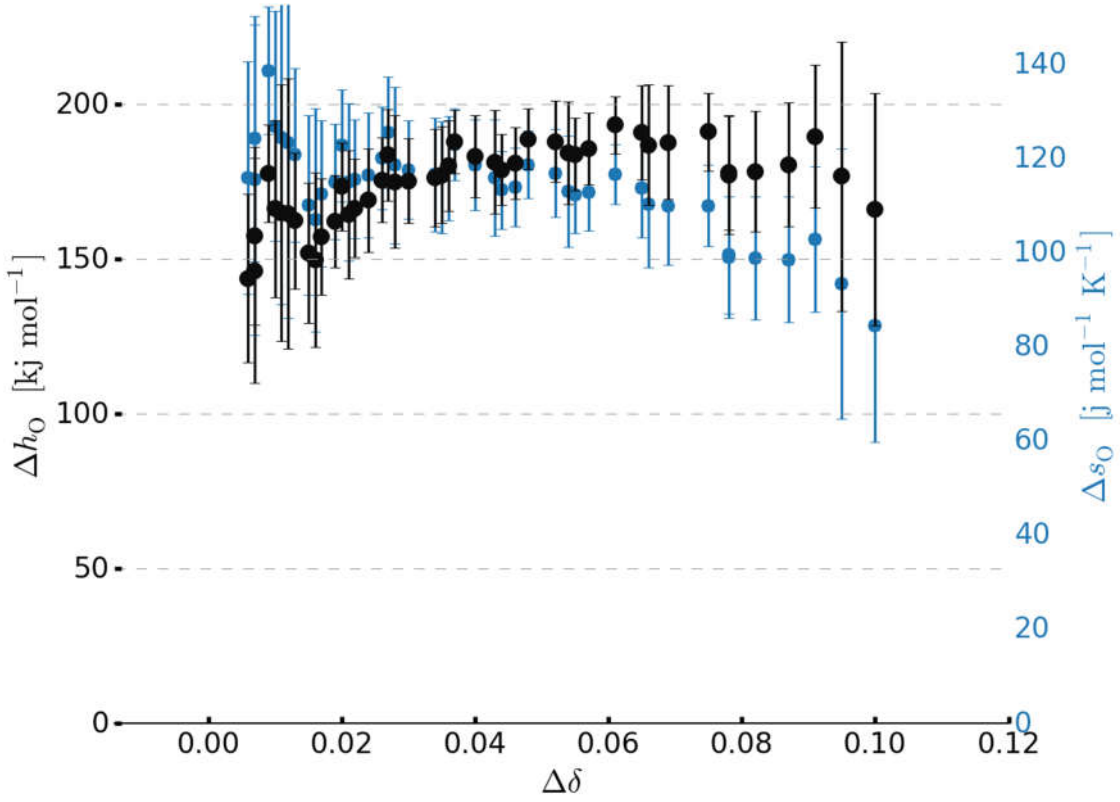
200
150
100
50
0
Δh_O [kj mol^{-1}]
140
120
100
80
60
40
20
0
Δs_O [j mol^{-1} K^{-1}]
0.00
0.02
0.04
0.06
0.08
0.10
0.12
Δδ

116

$Ca_{0.07}Sr_{0.93}Fe_{0.9}Co_{0.1}O_{3-\delta}$

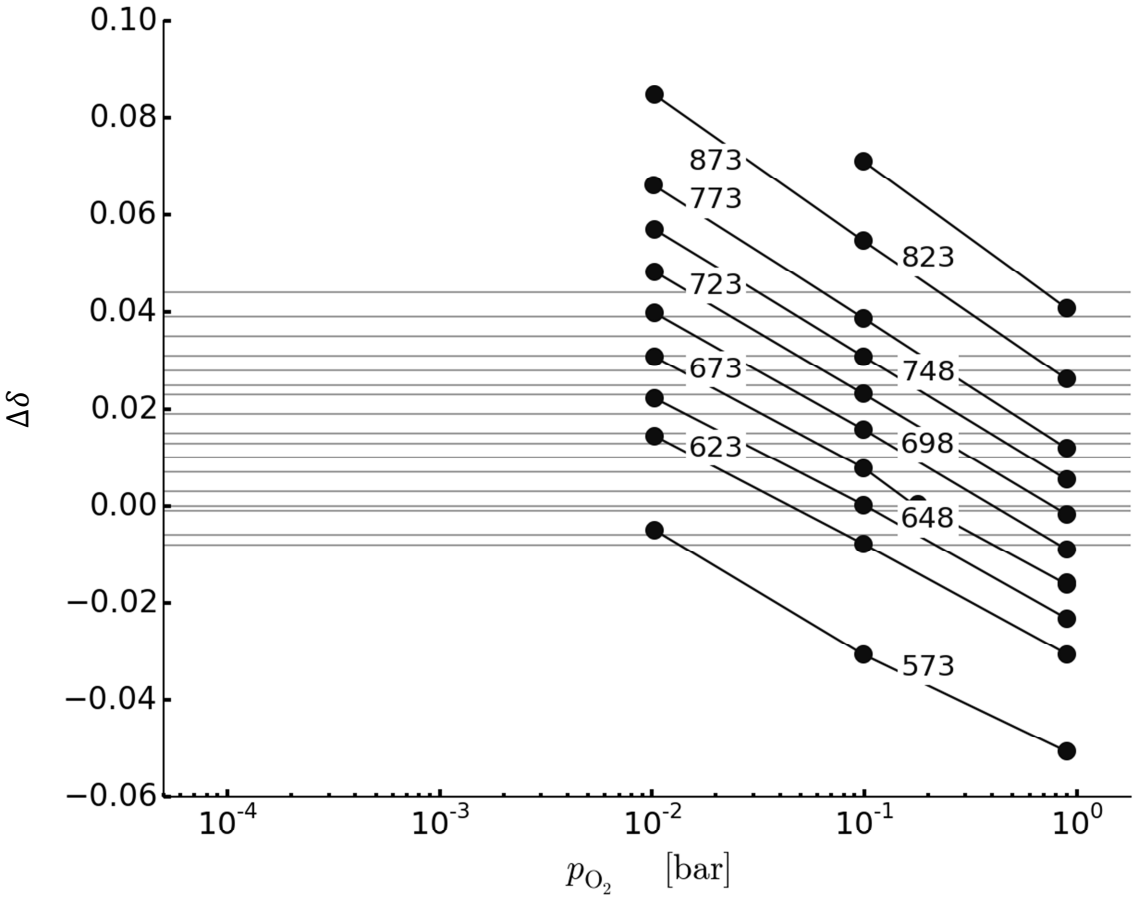

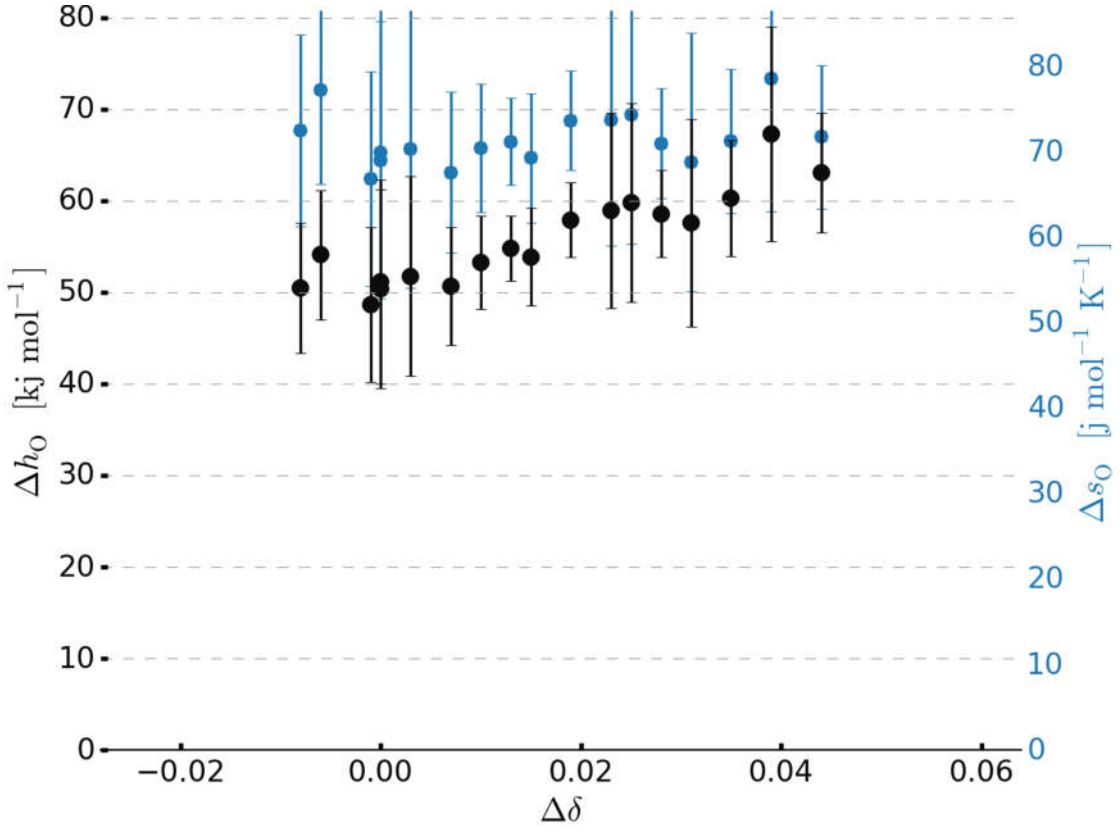

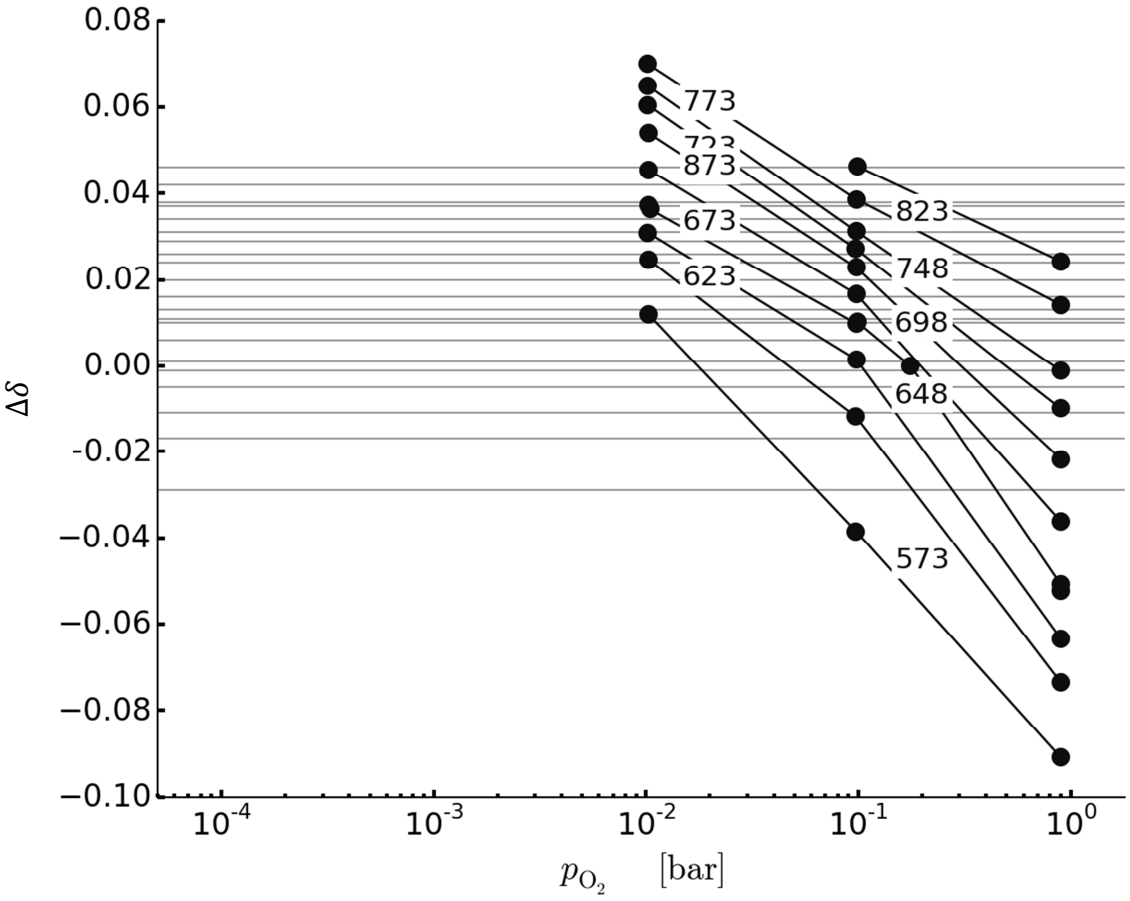
0.08
0.06
0.04
0.02
0.00
-0.02
−0.04
−0.06
−0.08
−0.10
Δδ
773
873
673
623
823
748
698
648
573
10^-4
10^-3
10^-2
10^-1
10^0
p_O2 [bar]

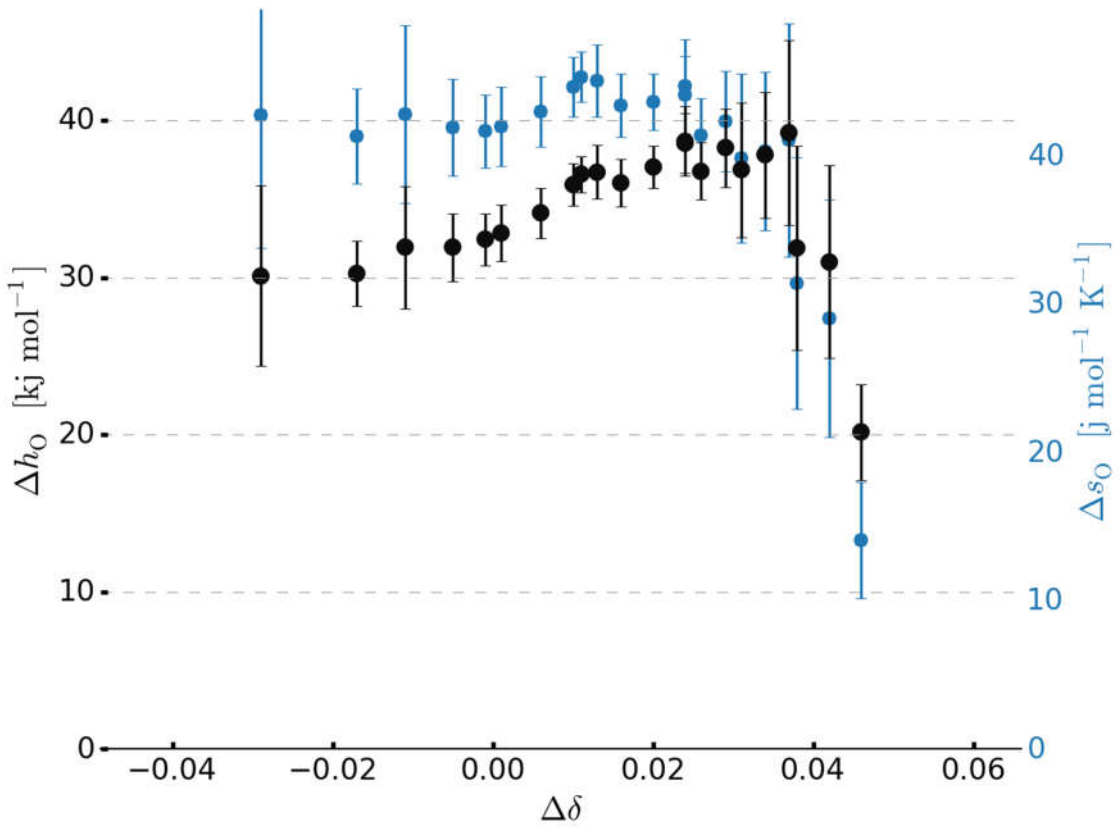
40
30
20
10
0
Δh_O [kj mol^-1]
Δs_O [j mol^-1 K^-1]
−0.04
−0.02
0.00
0.02
0.04
0.06
Δδ

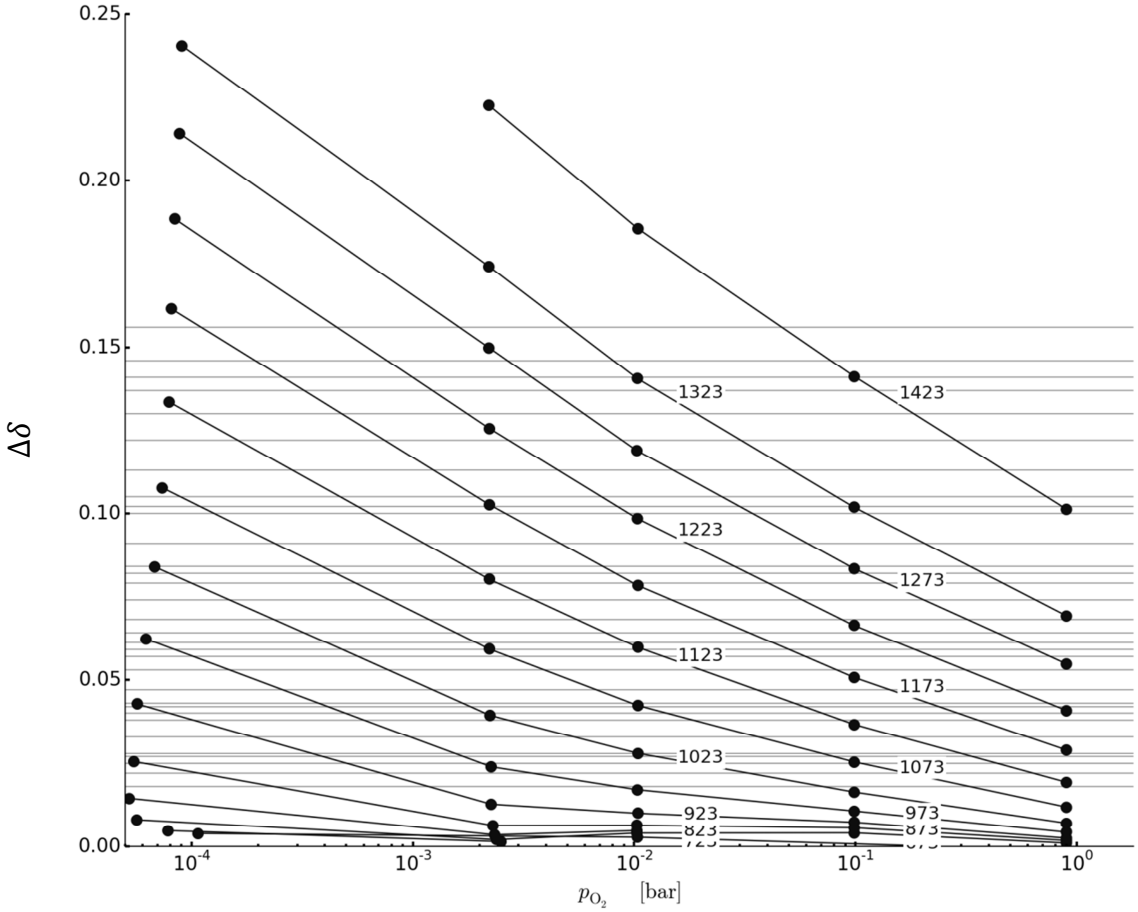
0.25
0.20
0.15
0.10
0.05
0.00
$\Delta\delta$
1423
1323
1223
1273
1123
1173
1023
1073
923
973
10^{-4}
10^{-3}
10^{-2}
10^{-1}
10^{0}
p_{O_2} [bar]

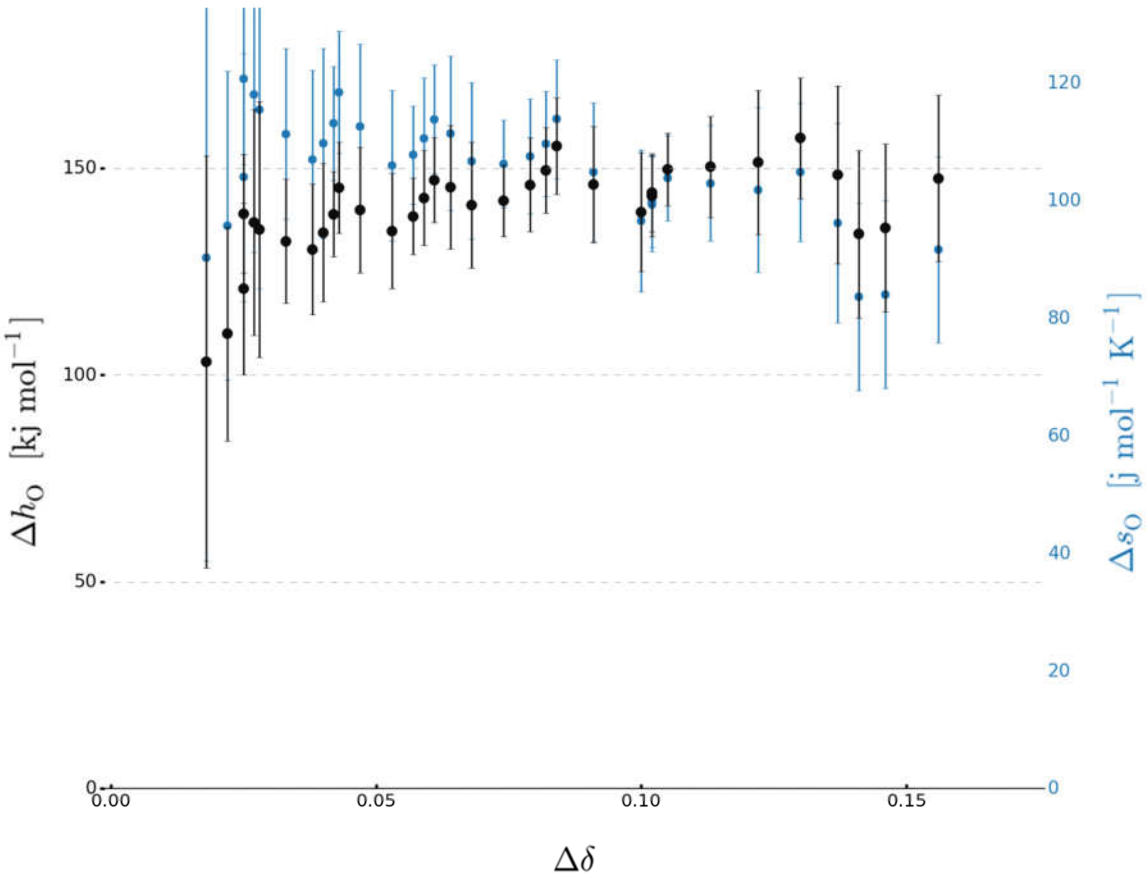
150
100
50
0
120
100
80
60
40
20
0
Δh_O [kj mol^{-1}]
Δs_O [j mol^{-1} K^{-1}]
0.00
0.05
0.10
0.15
$\Delta\delta$

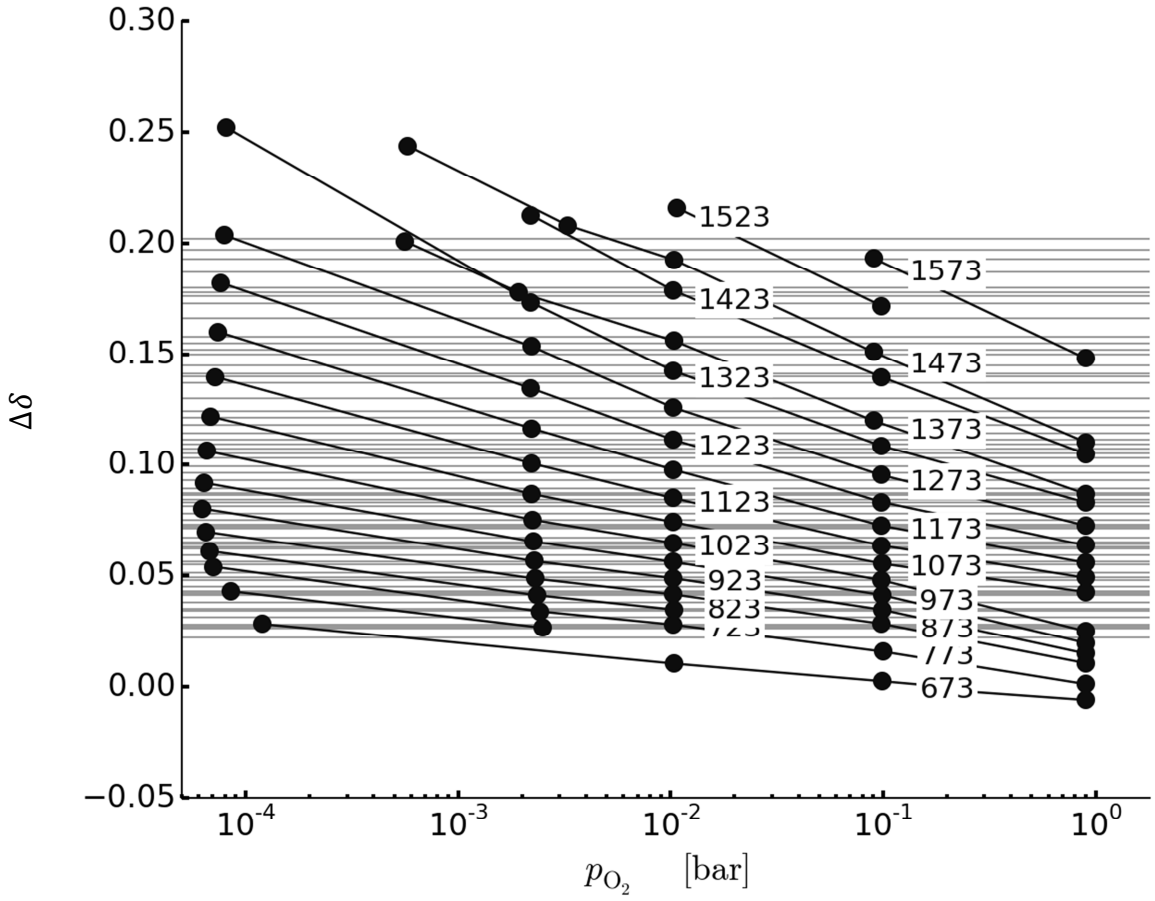
0.30
0.25
0.20
0.15
0.10
0.05
0.00
−0.05
Δδ
1523
1573
1423
1473
1323
1373
1223
1273
1123
1173
1023
1073
923
973
823
673
10-4
10-3
10-2
10-1
100
pO2 [bar]

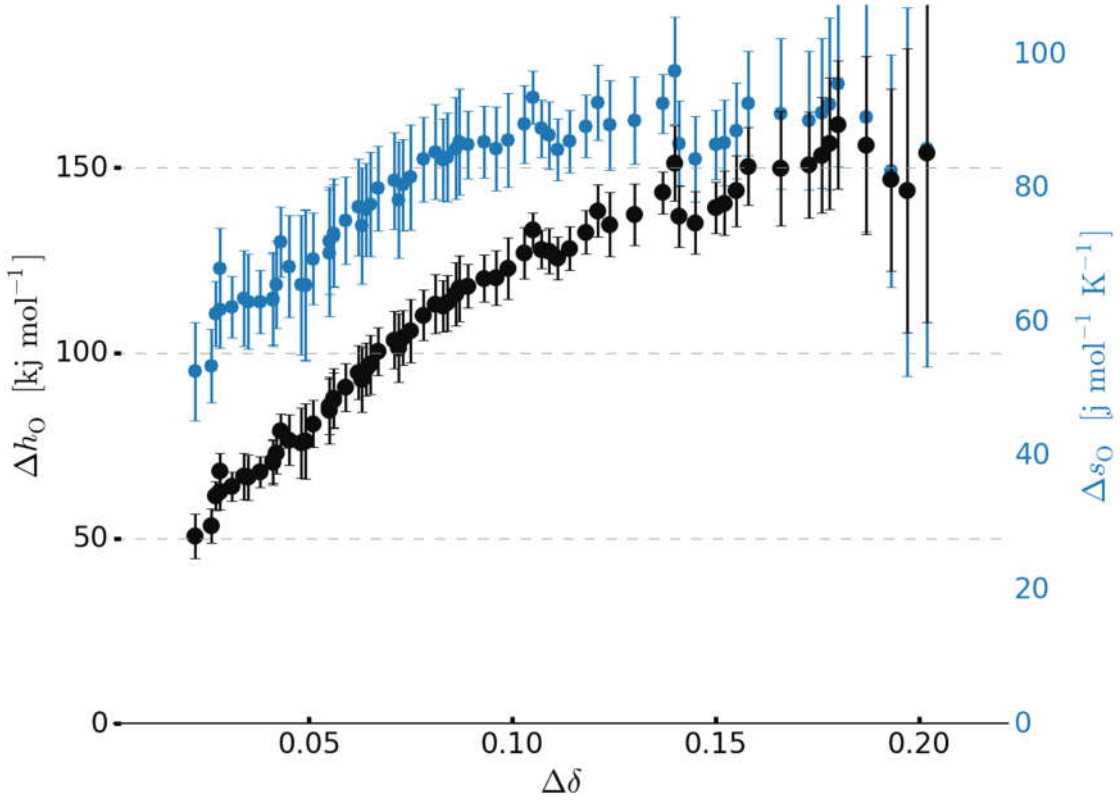
150
100
50
0
ΔhO [kj mol−1]
100
80
60
40
20
0
ΔsO [j mol−1 K−1]
0.05
0.10
0.15
0.20
Δδ

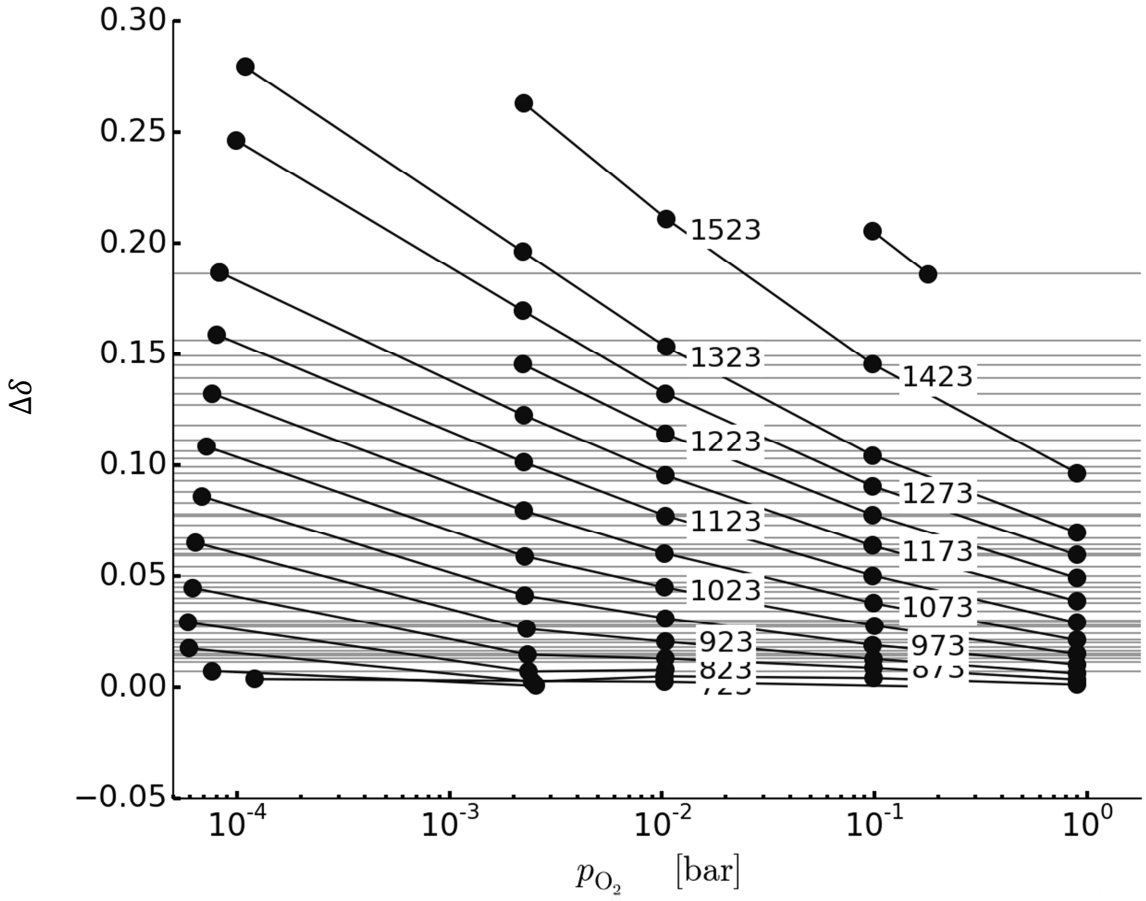
0.30
0.25
0.20
0.15
0.10
0.05
0.00
−0.05
Δδ
1523
1323
1423
1223
1273
1123
1173
1023
1073
923
973
10^{-4}
10^{-3}
10^{-2}
10^{-1}
10^{0}
p_{O_2} [bar]

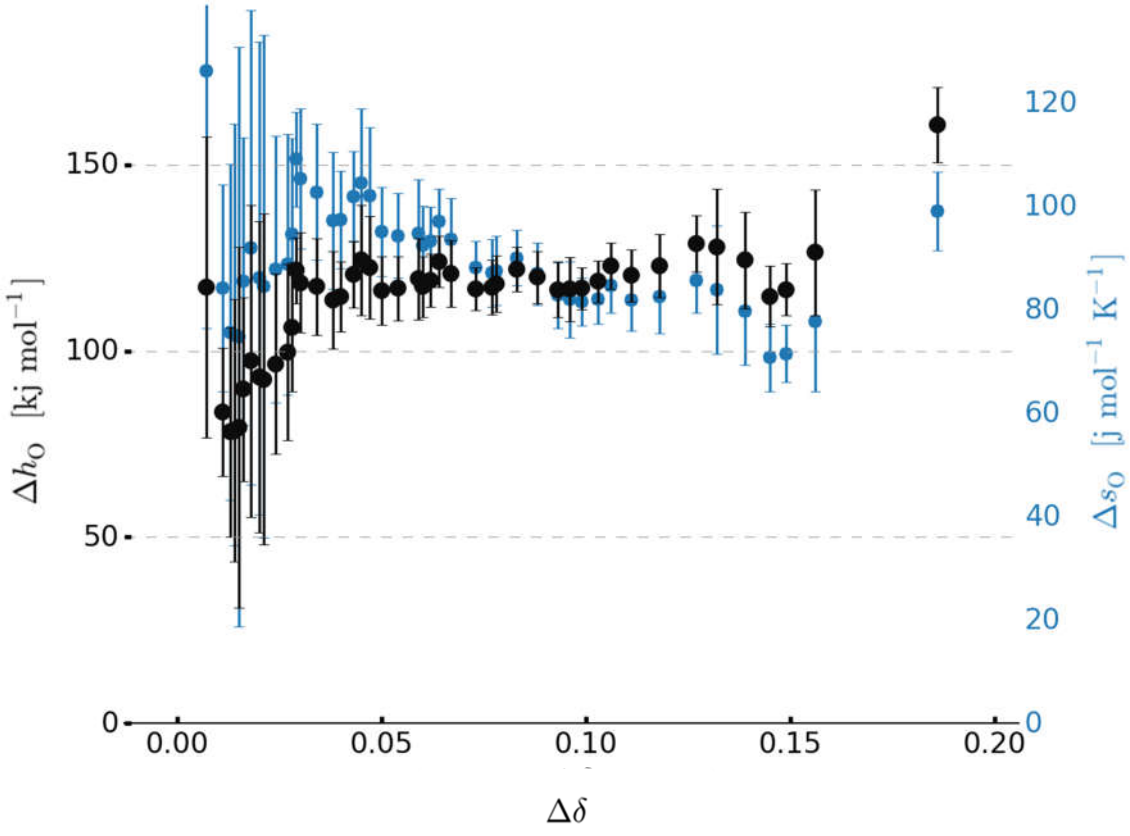
150
100
50
0
Δh_O [kj mol^{-1}]
120
100
80
60
40
20
0
Δs_O [j mol^{-1} K^{-1}]
0.00
0.05
0.10
0.15
0.20
Δδ

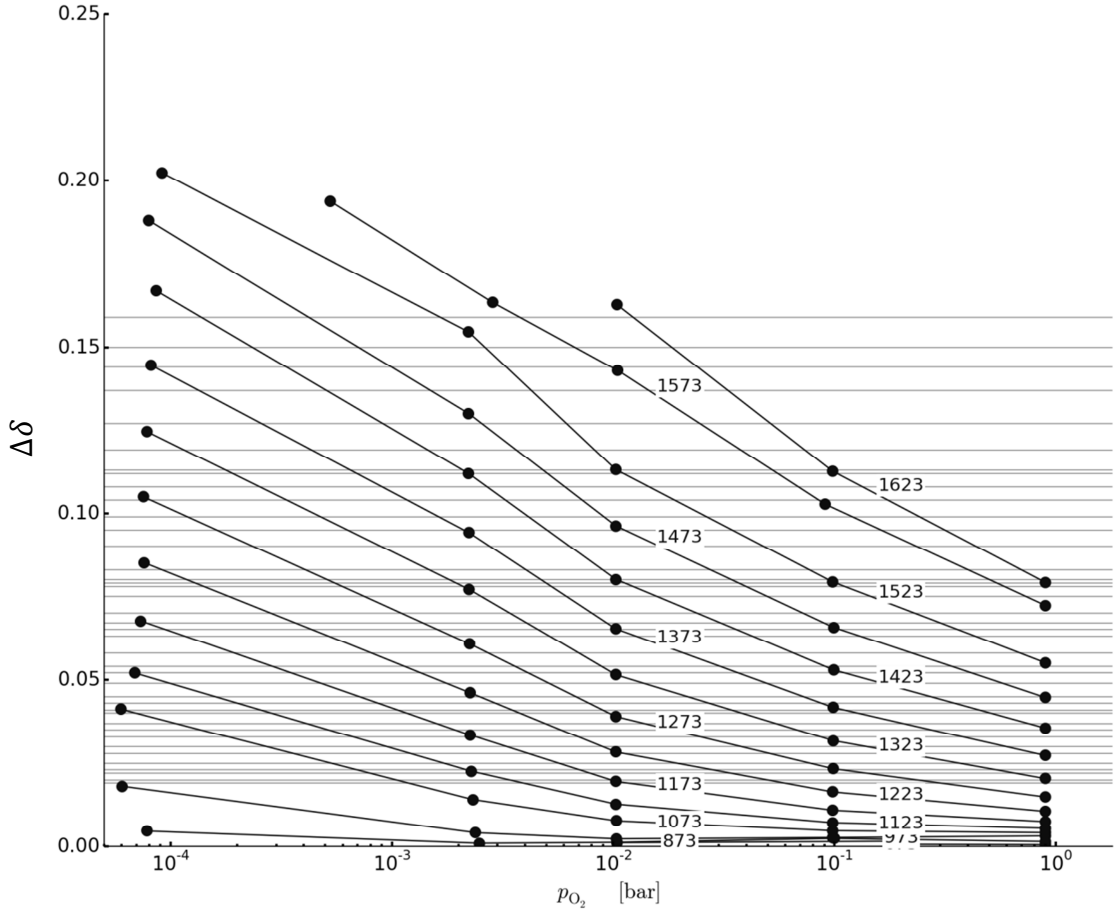
0.25
0.20
0.15
0.10
0.05
0.00
$\Delta\delta$
1573
1623
1473
1523
1373
1423
1273
1323
1173
1223
1073
1123
873
10^{-4}
10^{-3}
10^{-2}
10^{-1}
10^{0}
p_{O_2} [bar]

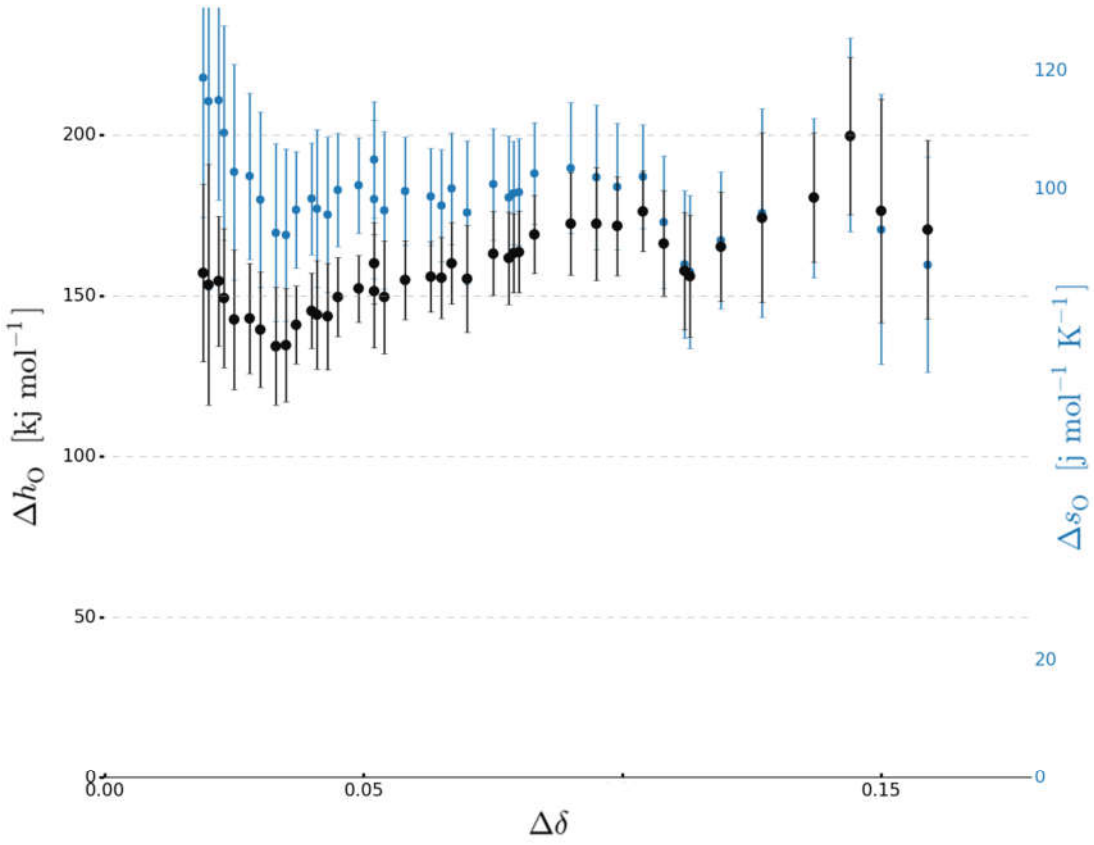
200
150
100
50
0
Δh_O [kj mol^{-1}]
120
100
20
0
Δs_O [j mol^{-1} K^{-1}]
0.00
0.05
0.15
$\Delta\delta$

13. X-Ray diffractograms

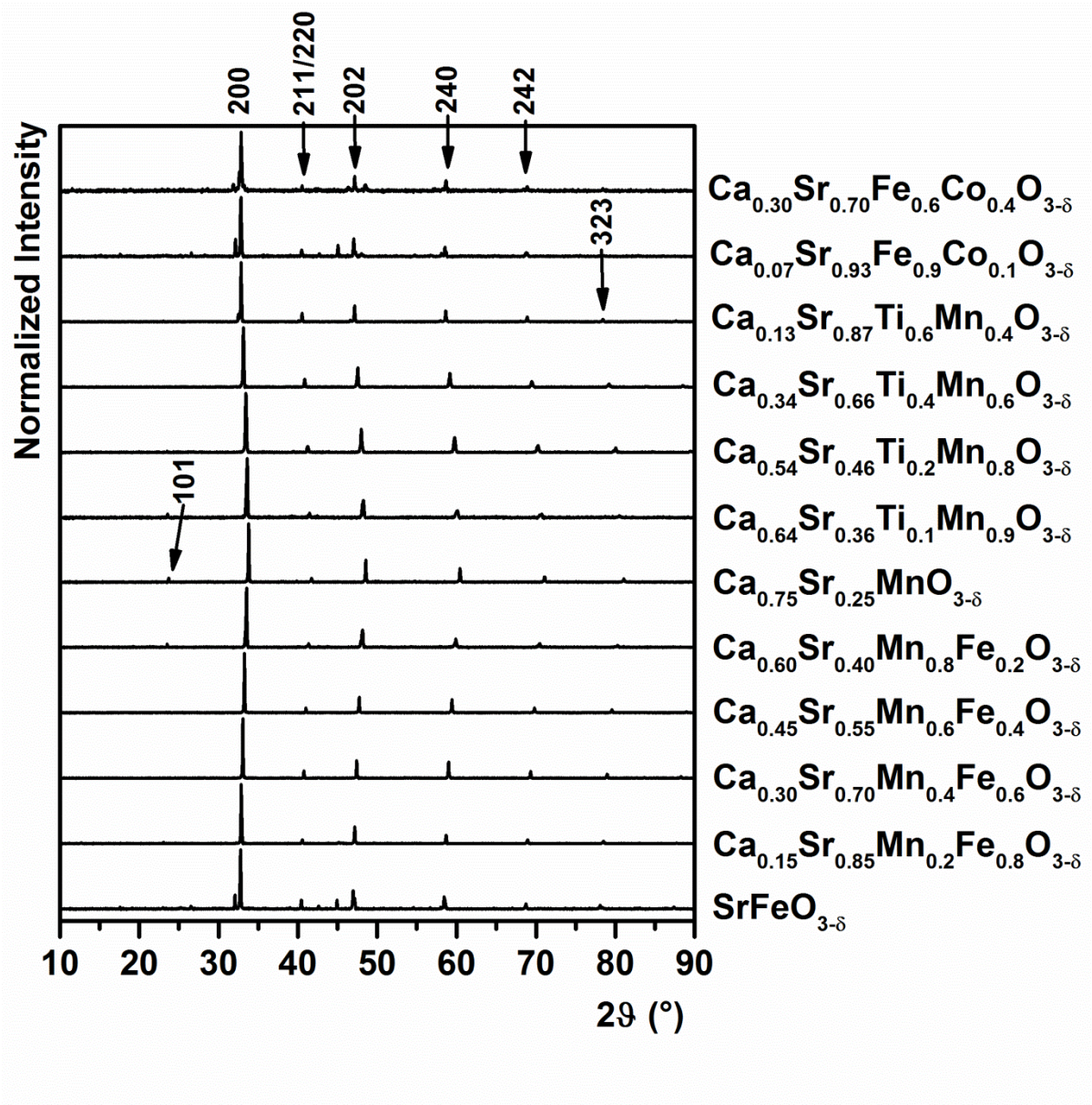

Figure S 6. X-Ray diffractograms at room temperature for perovskite solid solutions studied experimentally with t = 1.006. All phases are cubic perovskites, potentially with minor distortions due to partial reduction in equilibrium at room temperature. Not all reflections are clearly visible in all cases. Positions of the reflections shift according to Vegard's law, depending on the average ionic radii – large calcium and manganese contents lead to shifts towards higher 2ϑ values due to the decrease of the unit cell size. Reflection indexing: compare Bulfin et. al (supplementary information). [2]

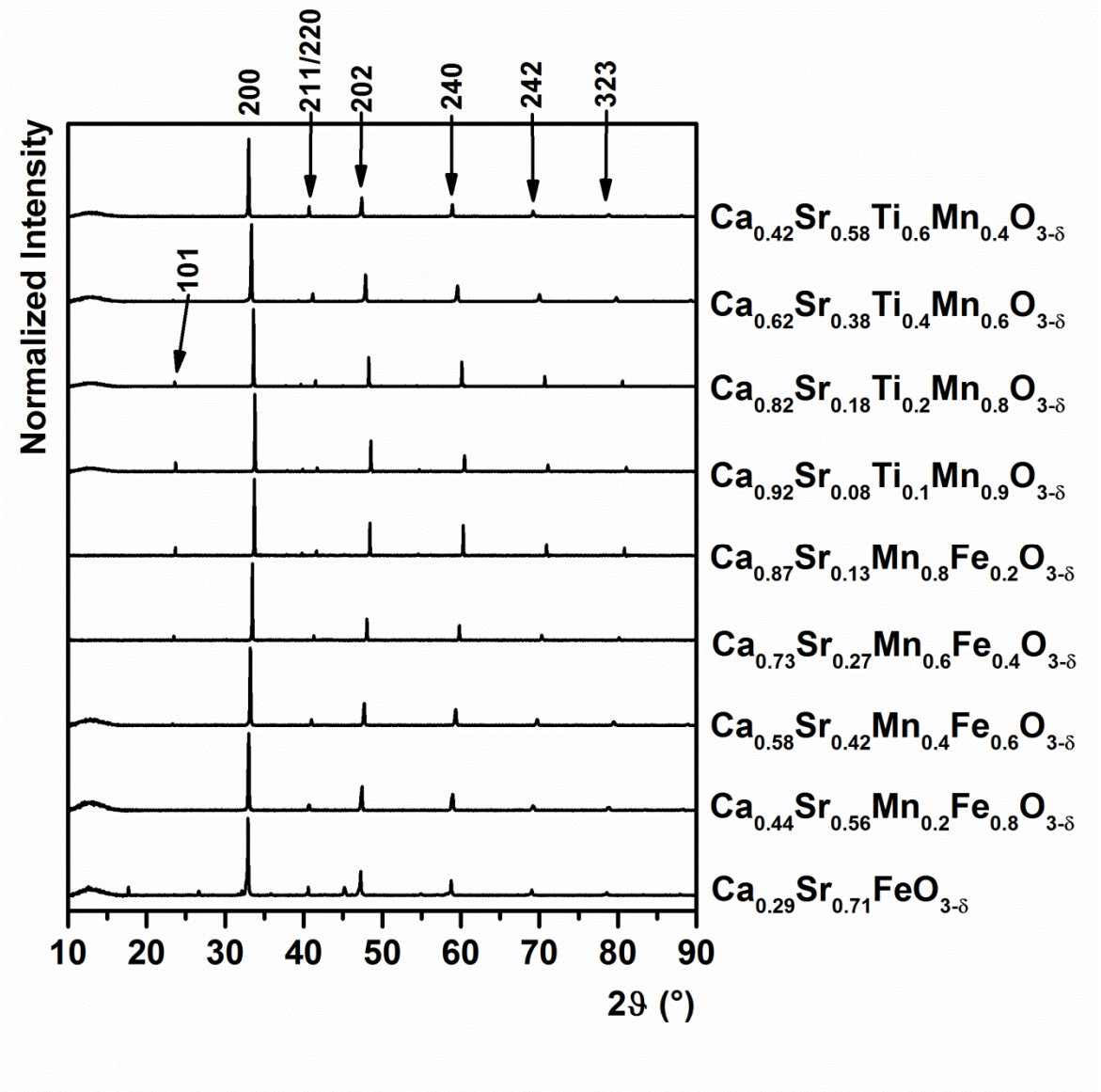

Figure S 7. X-Ray diffractograms at room temperature for perovskite solid solutions studied experimentally with t = 0.995. All phases are cubic perovskites, potentially with orthorhombic or tetragonal distortions. The relatively higher intensity of small reflections with respect to the samples at t = 1.006 might indicate a stronger distortion according to the decreased tolerance factor. [2] Not all reflections are clearly visible in all cases. Positions of the reflections shift according to Vegard's law. Reflection indexing: compare Bulfin et. al (supplementary information). [2]

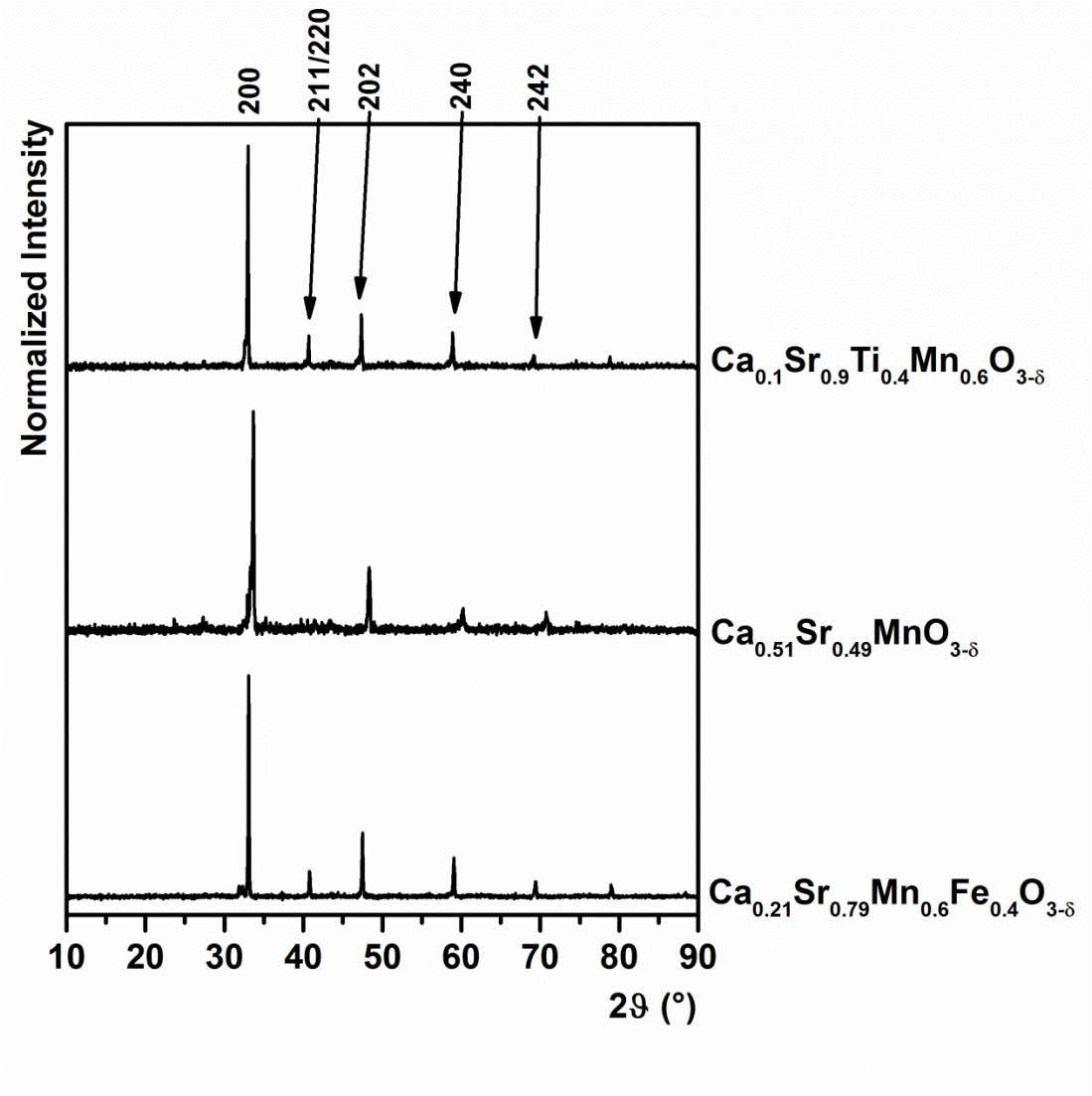

Figure S 8. X-Ray diffractograms at room temperature for perovskite solid solutions studied experimentally with t = 1.015. All phases are cubic perovskites. The relatively lower intensity of small reflections with respect to the samples at t = 1.006 and t = 0.995 might indicate a lower distortion according to the increased tolerance factor, i.e., the formation of ideal cubic perovskites. [2] Not all reflections are clearly visible in all cases. Positions of the reflections shift according to Vegard's law. Reflection indexing: compare Bulfin et. al (supplementary information). [2]

14. Vegard's law and DFT results

To check the validity of our DFT results, we analyzed the lattice parameters of one solid solution phase space exemplarily: (Ca-Sr)(Mn-Fe)$O_{3-\delta}$ for t = 1.006 ± 0.002 (see Fig. S9 below). All lattice parameters are normalized to represent 2x2x2 supercells. The lattice parameters are generally in good agreement with Vegard's law, with exceptions attributed to the discretization of partial occupancies.

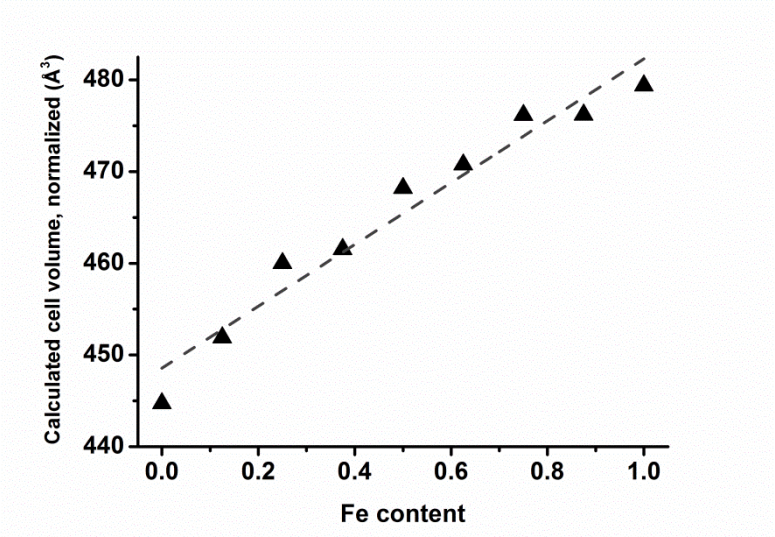

Figure S9. Normalized cell volume calculated for DFT-based unit cells of (Ca-Sr)(Mn-Fe)$O_{3-\delta}$ for t = 1.006 ± 0.002. A linear fit is indicated by the dashed line. The lattice constants follow Vegard's law, with deviations due to the discretization applied.

Composition	Normalized Cell volume (Å^3)	Tolerance factor
$Ca_{0.75}Sr_{0.25}MnO_{3-\delta}$	444.730	1.006
$Ca_{0.75}Sr_{0.25}Mn_{0.875}Fe_{0.125}O_{3-\delta}$	451.908	1.002
$Ca_{0.5}Sr_{0.5}Mn_{0.75}Fe_{0.25}O_{3-\delta}$	460.019	1.008
$Ca_{0.5}Sr_{0.5}Mn_{0.625}Fe_{0.375}O_{3-\delta}$	461.554	1.004
$Ca_{0.375}Sr_{0.625}Mn_{0.5}Fe_{0.5}O_{3-\delta}$	468.205	1.006
$Ca_{0.25}Sr_{0.75}Mn_{0.375}Fe_{0.625}O_{3-\delta}$	470.768	1.007
$Ca_{0.125}Sr_{0.875}Mn_{0.25}Fe_{0.75}O_{3-\delta}$	476.163	1.008
$Ca_{0.125}Sr_{0.875}Mn_{0.125}Fe_{0.875}O_{3-\delta}$	476.207	1.005
$SrFeO_{3-\delta}$	479.384	1.006

15. Conversion of product gas partial pressure ratios to an equivalent oxygen partial pressure for water and carbon dioxide splitting

To calculate equilibria for water splitting and CO_2 splitting cycles, we convert the partial pressure ratios of the splitting products vs. the educts to an equivalent oxygen partial pressure. For this purpose, we use the ΔG^0 of the splitting reactions to calculate the equilibrium constants K_{eq}:

$$K_{eq}(T) = e^{-\left(\frac{\Delta G^0(T)}{R \cdot T}\right)} \tag{S22}$$

where R is the ideal gas constant and T is the temperature in K. Using the equilibrium constants, we can determine the equivalent oxygen partial pressures $p_{O_2\,eq}$ for the for the water splitting (ws) and CO_2 splitting (cs) reactions at a given partial pressure ratio of p_{H_2}/p_{H_2O} or p_{CO}/p_{CO_2}: [44]

$$p_{O_2\,eq.ws}\left(T, \frac{p_{H_2}}{p_{H_2O}}\right) = \left(\frac{K_{eq.ws}(T)}{\frac{p_{H_2}}{p_{H_2O}}}\right)^2 \tag{S23}$$

$$p_{O_2\,eq.cs}\left(T, \frac{p_{CO}}{p_{CO_2}}\right) = \left(\frac{K_{eq.cs}(T)}{\frac{p_{CO}}{p_{CO_2}}}\right)^2 \tag{S24}$$

The ΔG^0 for the two reactions is derived from the respective values given in Barin. [45] For water splitting, the values given for ΔG_f^0 of water at T = 298.15 – 2000 K are fit using a linear function, resulting in:

$$\Delta G_{ws}^0(T) = \Delta G_{f\,H_2O}^0(T) = (-0.052489 \cdot T + 245.039) \cdot 1000\ \mathrm{Jmol^{-1}} \tag{S25}$$

These values are only valid if water in the gas phase (steam) is used as an oxidant, which is the case for all thermochemical water splitting cycles. For CO_2 splitting, $\Delta G^0_{cs}(T)$ can be calculated from the Gibbs free energies of formation for CO_2 and CO:

$$\Delta G^0_{cs}(T) = -\Delta G^0_{f\,CO_2}(T) + \Delta G^0_{f\,CO}(T) \quad (S26)$$

$\Delta G^0_{f\,CO_2}(T)$ can be fit using a second order polynomial, again using data from Barin at T = 298.15 – 2000 K: [45]

$$\Delta G^0_{f\,CO_2}(T) = (9.44 \cdot 10^{-7} \cdot T^2 - 0.0032113 \cdot T - 393.523) \cdot 1000\ \mathrm{Jmol^{-1}} \quad (S27)$$

$\Delta G^0_{f\,CO}(T)$ in the same temperature range can be fit using a linear function:

$$\Delta G^0_{f\,CO}(T) = (-0.0876385 \cdot T - 111.908) \cdot 1000\ \mathrm{Jmol^{-1}} \quad (S28)$$

16. Heat capacities of different perovskite phases according to the Debye model

The Debye model is used to calculate the heat capacities of perovskite phases according to the main manuscript. At high temperatures (significantly higher than the Debye temperature), the molar heat capacity only depends on the amount of atoms in the unit cell n_a. The change in heat capacity upon oxygen vacancy formation is below 5-10 %. This is demonstrated in Fig. S10 using data for different $SrFeO_{3-\delta}$ phases exemplarily, which has been calculated using *pymatgen* and elastic tensor data from DFT (The Materials Project). [8, 9, 46]

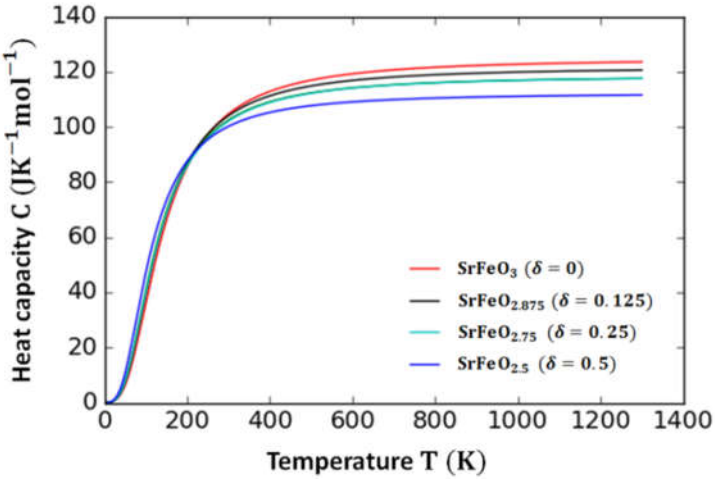

Figure S10. Specific molar heat capacity of different $SrFeO_{3-\delta}$ phases according to the Debye model using Materials Project database and elastic tensors calculated therein.

17. Mechanical envelope function used for calculating the pumping energy

We use a mechanical envelope function describing the energy demand of mechanical pumps according to Brendelberger *et al.* [16] The envelope function is defined as follows and only valid in the pressure range $10^{-6} < p_{red} < 0.7$ bar, and the pressures are converted using $p_0 = 10^5$ and $p = p_{\mathrm{red}} \cdot p_0$:

$$\mathrm{q_{iso}} = \mathrm{R} \cdot \mathrm{T} \cdot \ln(\mathrm{p_0/p}) \tag{S29}$$

$$\begin{aligned}\mathrm{eff} = 0.30557 \; - \; 0.17808 \cdot \ln\left(\frac{\mathrm{p}}{\mathrm{p_0}}\right) - 0.15514 \cdot \left[\ln\left(\frac{\mathrm{p}}{\mathrm{p_0}}\right)\right]^2 \\ -0.03173 \cdot \left[\ln\left(\frac{\mathrm{p}}{\mathrm{p_0}}\right)\right]^3 - 0.00203 \cdot \left[\ln\left(\frac{\mathrm{p}}{\mathrm{p_0}}\right)\right]^4\end{aligned} \tag{S30}$$

$$\mathrm{q_{pump}}\left[\frac{\mathrm{kJ}}{\mathrm{mol_O}}\right] = \frac{\mathrm{q_{iso}}}{\mathrm{eff} \cdot 0.4 \cdot 2000} \tag{S31}$$

The operating temperature of the pump is assumed to be T = 473 K. *eff* is an empirical function for the efficiency of the pump and q_{iso} refers to the work of isothermal compression of an ideal gas. The factor 0.4 originates from an assumed conversion efficiency from thermal to electrical energy of 40 %. [16] The factor 2000 is needed to convert J/mol$_{O2}$ to kJ/mol$_O$. The resulting value in kJ/mol$_O$ is converted to kJ/mol of material by multiplying it with the amount of oxygen released per mol of redox material, which is known according to the non-stoichiometry change between oxidation and reduction. Please note that the pumping energy is not zero at ambient pressure, as pumping is required to remove the oxygen produced during the reduction reaction in order to maintain a constant oxygen partial pressure.

18. Conversion of Q_{total} values in the energy and process analysis

The total energy necessary to drive a redox cycle can be calculated based on experimental or theoretical data as explained in the manuscript. The result Q_{total} is given in terms of kJ/mol of redox material. For the practical application, different figures may be necessary, which can be calculated according to the table below.

Table S 9. Conversion of the resulting energy values for analysis of different redox cycles.

	Air Separation	Water Splitting	CO_2 Splitting
kJ/mol of redox material	Q_{total}	Q_{total}	Q_{total}
kJ/kg of (oxidized) redox material	$\frac{Q_{total} \cdot 1000 \frac{kg}{g}}{n_{ox}\ (g/mol)}$	$\frac{Q_{total} \cdot 1000 \frac{kg}{g}}{n_{ox}\ (g/mol)}$	$\frac{Q_{total} \cdot 1000 \frac{kg}{g}}{n_{ox}\ (g/mol)}$
Wh/kg of (oxidized) redox material	$\frac{Q_{total} \cdot 1000 \frac{kg}{g}}{n_{ox} \cdot 3.6 \frac{kJ}{Wh}}$	$\frac{Q_{total} \cdot 1000 \frac{kg}{g}}{n_{ox} \cdot 3.6 \frac{kJ}{Wh}}$	$\frac{Q_{total} \cdot 1000 \frac{kg}{g}}{n_{ox} \cdot 3.6 \frac{kJ}{Wh}}$
kJ/mol of product	$\frac{Q_{total}}{\delta_{red} - \delta_{ox}}$ **(kJ/mol O)**	$\frac{Q_{total}}{\delta_{red} - \delta_{ox}}$ **(kJ/mol H_2)**	$\frac{Q_{total}}{\delta_{red} - \delta_{ox}}$ **(kJ/mol CO)**
kJ/L of product (ideal gas at SATP)	$\frac{2 \cdot Q_{total}}{(\delta_{red} - \delta_{ox}) \cdot 24.465 \frac{L}{mol}}$ **(kJ/L O_2)**	$\frac{Q_{total}}{(\delta_{red} - \delta_{ox}) \cdot 24.465 \frac{L}{mol}}$ **(kJ/L H_2)**	$\frac{Q_{total}}{(\delta_{red} - \delta_{ox}) \cdot 24.465 \frac{L}{mol}}$ **(kJ/L CO)**
Wh/L of product (ideal gas at SATP)	$\frac{2 \cdot Q_{total}}{(\delta_{red} - \delta_{ox}) \cdot 24.465 \frac{L}{mol} \cdot 3.6 \frac{kJ}{Wh}}$ **(Wh/L O_2)**	$\frac{Q_{total}}{(\delta_{red} - \delta_{ox}) \cdot 24.465 \frac{L}{mol} \cdot 3.6 \frac{kJ}{Wh}}$ **(Wh/L H_2)**	$\frac{Q_{total}}{(\delta_{red} - \delta_{ox}) \cdot 24.465 \frac{L}{mol} \cdot 3.6 \frac{kJ}{Wh}}$ **(Wh/L CO)**

Abbreviations and Units in Table S 9:

Q_{total}: Energy in kJ/mol of redox material

δ_{ox}: Oxygen non-stoichiometry of the perovskite in the oxidized state

δ_{red}: Oxygen non-stoichiometry of the perovskite in the reduced state

$\delta_{red} - \delta_{ox} = \Delta\delta$ Change in oxygen non-stoichiometry during the redox cycle operation; can also be interpreted as mol_O / $mol_{redox\ material}$

n_{ox}: Molar mass of the redox material in its oxidized state (at δ_{ox}) in g/mol

19. Reference values using literature data for ceria

In order to compare our data for perovskites with ceria as state-of-the-art reference material, we use our model and combine it with existing literature data.

As a function to calculate $\delta(T, p_{O_2})$, we can use the following analytical expression derived by Bulfin *et al.* and find its zero points and using the ideal gas constant R: [47]

$$0 = 8700 \cdot \mathrm{p}_{\mathrm{O}_2}^{-0.217} \cdot e^{-\frac{195600\,\frac{\mathrm{J}}{\mathrm{mol}}}{RT}} - \frac{\delta}{0.35 - \delta} \tag{S32}$$

To calculate the chemical energy demand, we use a constant ΔH value of 381 $\mathrm{kJ/mol_O}$ according to experimental data in the literature for the reduction of CeO_2 to Ce_2O_3. [46, 48] The sensible energy is calculated using the Debye model and elastic tensors for CeO_2 from The Materials Project. [8] Due to lack of data, elastic tensors for reduced phases are not used, and the heat capacity is assumed to be independent of δ as an approximation. The pumping energy and steam generation energy are calculated in analogy to the perovskite phases.

20. References

1. Bulfin, B.; Hoffmann, L.; de Oliveira, L.; Knoblauch, N.; Call, F.; Roeb, M.; Sattler, C.; Schmucker, M. Statistical thermodynamics of non-stoichiometric ceria and ceria zirconia solid solutions. *Physical Chemistry Chemical Physics* **2016,** 18 (33), 23147-23154 DOI: 10.1039/c6cp03158g.

2. Chase, M. W.; National Institute of, S.; Technology. *NIST-JANAF thermochemical tables*. American Chemical Society ; American Institute of Physics for the National Institute of Standards and Technology: [Washington, D.C.]; Woodbury, N.Y., 1998.

3. Rørmark, L.; Mørch, A. B.; Wiik, K.; Stølen, S.; Grande, T. Enthalpies of Oxidation of CaMnO3-δ, Ca2MnO4-δ and SrMnO3-δ Deduced Redox Properties. *Chemistry of Materials* **2001,** 13 (11), 4005-4013 DOI: 10.1021/cm011050l.

4. Balachandran, U.; Eror, N. G. Oxygen non-stoichiometry of tantalum-doped SrTiO3. *Journal of the Less Common Metals* **1982,** 85, 11-19 DOI: https://doi.org/10.1016/0022-5088(82)90053-4.

5. Takeda, Y.; Kanno, K.; Takada, T.; Yamamoto, O.; Takano, M.; Nakayama, N.; Bando, Y. Phase relation in the oxygen nonstoichiometric system, SrFeOx ($2.5 \leq x \leq 3.0$). *Journal of Solid State Chemistry* **1986,** 63 (2), 237-249 DOI: http://dx.doi.org/10.1016/0022-4596(86)90174-X.

6. Bulfin, B.; Vieten, J.; Starr, D. E.; Azarpira, A.; Zachäus, C.; Haevecker, M.; Skorupska, K.; Schmuecker, M.; Roeb, M.; Sattler, C. Redox chemistry of CaMnO3 and Ca0.8Sr0.2MnO3 oxygen storage perovskites. *Journal of Materials Chemistry A* **2017**, DOI: 10.1039/c7ta00822h.

7. Vieten, J.; Brendelberger, S.; Roeb, M.; Sattler, C. Thermochemical Oxygen Pumping for Improved Hydrogen Production in Solar Redox Cycles. *Submitted to International Journal of Hydrogen Energy* **2018**.

8. de Jong, M.; Chen, W.; Angsten, T.; Jain, A.; Notestine, R.; Gamst, A.; Sluiter, M.; Krishna Ande, C.; van der Zwaag, S.; Plata, J. J.; Toher, C.; Curtarolo, S.; Ceder, G.; Persson, K. A.; Asta, M. Charting the complete elastic properties of inorganic crystalline compounds. *Scientific Data* **2015,** 2, 150009 DOI: 10.1038/sdata.2015.9.

9. Ong, S. P.; Richards, W. D.; Jain, A.; Hautier, G.; Kocher, M.; Cholia, S.; Gunter, D.; Chevrier, V. L.; Persson, K. A.; Ceder, G. Python Materials Genomics (pymatgen): A robust, open-source python library for materials analysis. *Computational Materials Science* **2013,** 68, 314-319 DOI: https://doi.org/10.1016/j.commatsci.2012.10.028.

10. Fultz, B. Vibrational thermodynamics of materials. *Progress in Materials Science* **2010,** 55 (4), 247-352 DOI: https://doi.org/10.1016/j.pmatsci.2009.05.002.

11. Felinks, J.; Brendelberger, S.; Roeb, M.; Sattler, C.; Pitz-Paal, R. Heat recovery concept for thermochemical processes using a solid heat transfer medium. *Applied Thermal Engineering* **2014,** 73 (1), 1006-1013 DOI: https://doi.org/10.1016/j.applthermaleng.2014.08.036.

12. Vieten, J.; Bulfin, B.; Huck, P.; Horton, M.; Guban, D.; Zhu, L.; Persson, K.; Roeb, M.; Sattler, C. Materials design of perovskite solid solutions for thermochemical applications. *prepared* **2018**.

13. Grimvall, G. *Thermophysical Properties of Materials*. Elsevier Science: 1999.

14. Sedmidubský, D.; Holba, P. Material properties of nonstoichiometric solids. *Journal of Thermal Analysis and Calorimetry* **2015,** 120 (1), 183-188 DOI: 10.1007/s10973-015-4466-7.

15. Haavik, C.; Atake, T.; Kawaji, H.; Stolen, S. On the entropic contribution to the redox energetics of SrFeO3-[small delta]. *Physical Chemistry Chemical Physics* **2001,** 3 (17), 3863-3870 DOI: 10.1039/b104401j.

16. Brendelberger, S.; von Storch, H.; Bulfin, B.; Sattler, C. Vacuum pumping options for application in solar thermochemical redox cycles – Assessment of mechanical-, jet- and thermochemical pumping systems. *Solar Energy* **2017,** 141 (Supplement C), 91-102 DOI: https://doi.org/10.1016/j.solener.2016.11.023.

17. Brendelberger, S.; Vieten, J.; Vidyasagar, M. J.; Roeb, M.; Sattler, C. Demonstration of thermochemical oxygen pumping for atmosphere control in reduction reactions. *Solar Energy* **2018,** 170, 273-279 DOI: https://doi.org/10.1016/j.solener.2018.05.063.

18. Vieten, J.; Brendelberger, S.; Roeb, M.; Sattler, C., THERMOCCHEMICAL OXYGEN PUMPING FOR IMPROVED HYDROGEN PRODUCTION IN SOLAR REDOX CYCLES. In *9th International Conference on Hydrogen Production (ICH2P-2018)*, Zagreb, Croatia, 2018.

19. Brendelberger, S.; Roeb, M.; Lange, M.; Sattler, C. Counter flow sweep gas demand for the ceria redox cycle. *Solar Energy* **2015,** 122, 1011-1022 DOI: https://doi.org/10.1016/j.solener.2015.10.036.

20. McDaniel, A. H.; Debora R. Barcellos, C. S. o. M.; Michael Sanders, C. S. o. M.; Jianhua Tong, C. U.; Ryan O?Hayre, C. S. o. M. *A novel solar thermochemical water splitting material BaCe0.25Mn0.75O3 for hydrogen production*. ; Sandia National Lab. (SNL-CA), Livermore, CA (United States): 2017; p Medium: ED; Size: 16 p.

21. Romero Barcellos, D.; Sanders, M. D.; Tong, J.; McDaniel, A. H.; O'Hayre, R. BaCe0.25Mn0.75O3-δ — A promising perovskite-type oxide for solar thermochemical hydrogen production. *Energy & Environmental Science* **2018**, DOI: 10.1039/c8ee01989d.

22. Barghouthi, S.; Tullis, K. Determination of the Vapor Pressure Curve of a Liquid in the Presence of a Nonvolatile Solute. *The Chemical Educator* **2000,** 5 (4), 183-186 DOI: 10.1007/s00897000396a.

23. Pacific Northwest National Laboratory, Lower and Higher Heating Values of Fuels. www.h2tools.org/hyarc/calculator-tools/lower-and-higher-heating-values-fuels (accessed May 8th 2018),

24. Schmidt, M.; Campbell, S. J. In situ neutron diffraction study (300–1273 K) of non-stoichiometric strontium ferrite SrFeOx. *Journal of Physics and Chemistry of Solids* **2002,** 63 (11), 2085-2092 DOI: http://dx.doi.org/10.1016/S0022-3697(02)00198-1.

25. Krug, R. R.; Hunter, W. G.; Grieger, R. A. Statistical interpretation of enthalpy–entropy compensation. *Nature* **1976,** 261, 566 DOI: 10.1038/261566a0.

26. Haavik, C.; Bakken, E.; Norby, T.; Stolen, S.; Atake, T.; Tojo, T. Heat capacity of SrFeO3-[small delta]; [small delta][space]= 0.50, 0.25 and 0.15 - configurational entropy of structural entities in grossly non-stoichiometric oxides. *Dalton Transactions* **2003,** (3), 361-368 DOI: 10.1039/b209236k.

27. Vieten, J. Perovskite Materials Design for Two-Step Solar-Thermochemical Redox Cycles - Doctoral Thesis, TU Dresden (under review), 2019.

28. Nalbandian, L.; Evdou, A.; Zaspalis, V. La1−xSrxMO3 (M = Mn, Fe) perovskites as materials for thermochemical hydrogen production in conventional and membrane reactors. *International Journal of Hydrogen Energy* **2009,** 34 (17), 7162-7172 DOI: https://doi.org/10.1016/j.ijhydene.2009.06.076.

29. Rao, C. N. R.; Dey, S. Solar thermochemical splitting of water to generate hydrogen. *Proceedings of the National Academy of Sciences of the United States of America* **2017,** 114 (51), 13385-13393 DOI: 10.1073/pnas.1700104114.

30. Scheffe, J. R.; Weibel, D.; Steinfeld, A. Lanthanum–Strontium–Manganese Perovskites as Redox Materials for Solar Thermochemical Splitting of H2O and CO2. *Energy & Fuels* **2013,** 27 (8), 4250-4257 DOI: 10.1021/ef301923h.

31. Emery, A. A.; Wolverton, C. High-throughput DFT calculations of formation energy, stability and oxygen vacancy formation energy of ABO(3) perovskites. *Scientific Data* **2017,** 4, 170153 DOI: 10.1038/sdata.2017.153.

32. Emery, A. A.; Saal, J. E.; Kirklin, S.; Hegde, V. I.; Wolverton, C. High-Throughput Computational Screening of Perovskites for Thermochemical Water Splitting Applications. *Chemistry of Materials* **2016,** 28 (16), 5621-5634 DOI: 10.1021/acs.chemmater.6b01182.

33. Krenzke, P. T.; Davidson, J. H. On the Efficiency of Solar H2 and CO Production via the Thermochemical Cerium Oxide Redox Cycle: The Option of Inert-Swept Reduction. *Energy & Fuels* **2015,** 29 (2), 1045-1054 DOI: 10.1021/ef502601f.

34. Rager, T. Re-evaluation of the efficiency of a ceria-based thermochemical cycle for solar fuel generation. *Chemical Communications* **2012,** 48 (85), 10520-10522 DOI: 10.1039/c2cc34617f.

35. Bulfin, B.; Vieten, J.; Agrafiotis, C.; Roeb, M.; Sattler, C. Applications and limitations of two step metal oxide thermochemical redox cycles; a review. *Journal of Materials Chemistry A* **2017,** 5 (36), 18951-18966 DOI: 10.1039/c7ta05025a.

36. Naghavi, S. S.; Emery, A. A.; Hansen, H. A.; Zhou, F.; Ozolins, V.; Wolverton, C. Giant onsite electronic entropy enhances the performance of ceria for water splitting. *Nature Communications* **2017,** 8 (1), 285 DOI: 10.1038/s41467-017-00381-2.

37. Dutta, N. N.; Patil, G. S. Developments in CO separation. *Gas Separation & Purification* **1995,** 9 (4), 277-283 DOI: https://doi.org/10.1016/0950-4214(95)00011-Y.

38. Zhu, L.-q.; Tu, J.-l.; Shi, Y.-j. Separation of CO□CO2□N2 gas mixture for high-purity CO by pressure swing adsorption. *Gas Separation & Purification* **1991,** 5 (3), 173-176 DOI: https://doi.org/10.1016/0950-4214(91)80015-W.

39. Lackner, K. S. Capture of carbon dioxide from ambient air. *The European Physical Journal Special Topics* **2009,** 176 (1), 93-106 DOI: 10.1140/epjst/e2009-01150-3.

40. Vieten, J.; Bulfin, B.; Roeb, M.; Sattler, C. Citric acid auto-combustion synthesis of Ti-containing perovskites via aqueous precursors. *Solid State Ionics* **2018,** 315, 92-97 DOI: https://doi.org/10.1016/j.ssi.2017.12.010.

41. Vieten, J.; Bulfin, B.; Senholdt, M.; Roeb, M.; Sattler, C.; Schmücker, M. Redox thermodynamics and phase composition in the system SrFeO3 − δ — SrMnO3 − δ. *Solid State Ionics* **2017,** 308, 149-155 DOI: https://doi.org/10.1016/j.ssi.2017.06.014.

42. Shannon, R. Revised effective ionic radii and systematic studies of interatomic distances in halides and chalcogenides. *Acta Crystallographica Section A* **1976,** 32 (5), 751-767 DOI: doi:10.1107/S0567739476001551.

43. Kudoh, Y.; Prewitt, C. T.; Finger, L. W.; Ito, E. *Ionic Radius-Bond Strength Systematics, Ionic Compressibilities, and an Application to (Mg, Fe)SiO3 Perovskites*. 2013.

44. Körner, R. Untersuchung am System Cer-Sauerstoff, Thermische Ausdehnung im Bereich CeO2 bis CeO1,777 (German). Dissertation, Georg August Universität zu Göttingen, 1985.

45. Barin, I. *Thermochemical Data of Pure Substances, Third Edition*. 2008.

46. Jain, A.; Ong, S. P.; Hautier, G.; Chen, W.; Richards, W. D.; Dacek, S.; Cholia, S.; Gunter, D.; Skinner, D.; Ceder, G.; Persson, K. A. Commentary: The Materials Project: A materials genome approach to accelerating materials innovation. *APL Materials* **2013,** 1 (1), 011002 DOI: doi:http://dx.doi.org/10.1063/1.4812323.

47. Bulfin, B.; Call, F.; Lange, M.; Lübben, O.; Sattler, C.; Pitz-Paal, R.; Shvets, I. V. Thermodynamics of CeO2 Thermochemical Fuel Production. *Energy & Fuels* **2015,** 29 (2), 1001-1009 DOI: 10.1021/ef5019912.

48. Kubaschewski, O.; Alcock, C. B.; Spencer, P. J. *Materials thermochemistry*. Pergamon Press: 1993.